UNIVERSITY OF SOUTHAMPTON

FACULTY OF NATURAL AND ENVIRONMENTAL SCIENCES

Biological Sciences

Mouse Embryonic Stem Cells as a Model System for Periconceptional Developmental Programming

by

Pooja Khurana, M.Sc.

Thesis for the degree of Doctor of Philosophy

July 2018

UNIVERSITY OF SOUTHAMPTON

ABSTRACT

FACULTY OF NATURAL AND ENVIRONMENTAL SCIENCES

Biological Sciences

Thesis for the degree of Doctor of Philosophy

MOUSE EMBRYONIC STEM CELLS AS A MODEL SYSTEM FOR PERICONCEPTIONAL DEVELOPMENTAL PROGRAMMING

Pooja Khurana

The Developmental Origins of Health and Disease (DOHaD) hypothesis proposes that maternal environment during pregnancy induces changes in early development, and influences adult offspring health and chronic disease risk. Such developmental programming may occur within the preimplantation embryo. In rodents, adverse maternal environments such as advanced reproductive age and undernutrition have been shown to induce permanent and irreversible changes in the preimplantation embryo which, following implantation and term delivery, subsequently predisposes offspring to late onset non-communicable diseases such as cardiometabolic dysfunction. Disease probability in adult offspring has been correlated with perturbations in lineage specification and metabolism in preimplantation embryos. However, limited cell numbers and the inaccessibility of post-implantation embryos have restricted our ability to explore the underlying mechanisms that predispose to adult disease. To overcome these issues, the current study utilised mouse embryonic stem cells (mESCs) derived from inbred C57BL/6 mice as a model system. This presented the opportunity to overcome the aforementioned limitations and to characterise the pluripotent population of cells within the embryo (at E3.5) in order to investigate the effects of advanced maternal age (AMA) and maternal low protein diet (LPD, 9% casein). Furthermore, with this model it was possible to consider the effects of LPD on the efficiency of neural induction (NI).

Embryos retrieved from Old (7-8 months) dams exhibited developmental delay (i.e. an increased proportion of morulae and a reduced proportion of blastocysts) compared to those recovered from Young (7-8 weeks) dams. Mouse ESCs derived from blastocysts of Old and Young dams (i) showed no differences in mESC derivation efficiency, (ii) displayed dominance towards male sex and (iii)

generally displayed a similar pattern of gene expression for pluripotency (except *Sox2*), differentiation, early apoptosis and Dnmt (except *Dnmt3b*) markers. However, aneuploidy was greater in Old male mESCs, which were less proliferative and viable compared to Young male mESC lines. Old mESC lines were sexually dimorphic with respect to viability. Aneuploidy and apoptosis was greater in Old Female than Old Male mESC lines.

Global metabolomics of derived male LPD (9% casein) and normal protein diet, NPD (18% casein) mESC lines (undertaken in collaboration with Metabolon Inc.) showed evidence of altered glucose and fatty acid (FA) metabolism, while amino acid levels generally remained similar between the two dietary groups. Within the glycolytic pathway, LPD mESC lines exhibited increased levels of glucose 6-phosphate (G-6-P) and fructose 6-phosphate (F-6-P), and reduced downstream metabolites including fructose-1,6-bisphosphate (F-1,6-bP). Further analysis suggested reduced activity of phosphofructokinase (PFK), a key glycolytic enzyme that is allosterically regulated of LPD mESC lines. Interestingly, unlike previously reported *in vivo* data, LPD mESC lines displayed increased levels of n-3 and n-6 polyunsaturated FAs (PUFAs).

In separate experiments, derived male LPD and NPD mESC lines were expanded in serum-free (KO/SR) mESC medium and differentiated towards neural lineages (with Biotalentum Ltd.) using an optimised 14-day neural induction (NI) protocol, under standard NI medium (S-NIM) conditions. Preliminary results suggest increased NI efficiency of LPD mESC lines compared to NPD mESC lines. This was illustrated by precocious morphological appearance of rosettes and neurites, increased and protracted gene, and qualitative protein, expression for neural stem cell (NSC) and mature neuronal markers of differentiating LPD lines; all during the 14-day NI protocol.

Collectively, these data indicate that advanced maternal age and maternal diet can determine pluripotent mESC phenotype. Despite protracted periods of culture, the effects of adverse maternal environment on the developmental programming of blastocysts could be observed in derived mESC lines and cell populations derived following NI. These findings encourage further investigation of AMA and LPD on mechanistic adaptations in neural and other cell lineages to provide greater mechanistic insights into the induction of later disease using mESC as an *in vitro* model system, thereby reducing animal use.

Table of Contents

Table of Contents ..... **i**

Table of Tables ..... **vii**

Table of Figures ..... **ix**

Academic Thesis: Declaration Of Authorship ..... **xv**

Acknowledgements ..... **xvii**

Abbreviations ..... **xix**

Introduction ..... **xxiii**

Chapter 1 Literature review **1**

1.1 The DOHaD Hypothesis 1

1.1.1 DOHaD and Developmental Plasticity 1

1.1.2 DOHaD, birthweight and body composition 3

1.1.3 DOHaD: Evidence from additional human cohorts 5

1.1.4 DOHaD and over nutrition 6

1.1.5 Animal models of maternal malnutrition during pregnancy 7

1.2 The Periconceptional period and DOHaD 8

1.2.1 Neural induction during embryonic development 10

1.2.2 Preimplantation period and undernutrition 10

1.3 Pre-natal adversity and neurodevelopment 11

1.4 Advanced Maternal Age (AMA) 14

1.4.1 AMA and pregnancy associated-risk factors 14

1.4.2 AMA, natural conception and perinatal outcomes 15

1.4.2.1 AMA and chromosomal anomalies 16

1.4.2.2 AMA and positive perinatal outcomes 17

1.4.2.3 AMA and factors associated with reduced fertility 17

1.4.3 AMA: Animal models of reproductive ageing 18

1.5 Assisted reproductive Technologies (ART) 19

1.5.1 ART and DOHaD 20

1.5.2 Factors influencing ART outcomes 21

1.5.2.1 Advanced maternal age (AMA) 21
1.5.2.2 Other procedures used in assisted reproduction (human studies) 22
1.5.3 Animal models of assisted reproduction 23
1.5.3.1 Advanced maternal age (AMA) 23
1.5.3.2 Other procedures used in assisted reproduction (animal models) 24
1.6 Mouse embryonic stem cells as a model system for DOHaD 26
1.6.1 Mouse embryonic stem cells (mESCs): Origin 28
1.6.1.1 Mouse embryonic stem cells (mESCs): Derivation and maintenance .. 29
1.6.1.2 Pathways influencing mESC phenotype 30
1.6.2 Neural induction (NI) in mESCs 31
1.6.2.1 Signalling pathways and *in vitro* NI 33
1.7 Development of working hypothesis 35
1.7.1 Aims and objectives 36
Chapter 2 Effects of Advanced Maternal Age (AMA) on derived mESC lines 39
2.1 Introduction 39
2.2 Materials and Methods 41
2.2.1 Animal Procedures 41
2.2.1.1 Animals and embryo collection 41
2.2.1.2 Embryo staging 41
2.2.2 Cell culture 41
2.2.2.1 Mouse embryonic fibroblasts (MEFs) preparation 41
2.2.2.2 Derivation and culture of mESC clones from E3.5 blastocysts 42
2.2.3 Gender Analysis (Sexing) of mESCs 44
2.2.3.1 Genomic DNA Isolation 44
2.2.3.2 Polymerase Chain Reaction (PCR) 45
2.2.3.3 Gel Electrophoresis 45
2.2.4 Chromosome Counting (Karyotyping) 46
2.2.5 Quantitative PCR (qPCR) analysis 47

2.2.5.1 RNA extraction 47
2.2.5.2 RNA quality 47
2.2.5.3 Reverse transcription (cDNA synthesis) 48
2.2.5.4 Quantitative PCR 49
2.2.5.5 Normalisation of PCR data 50
2.2.5.6 Selection of reference genes 51
2.2.5.7 Data analysis of RT-PCR 52
2.2.5.8 Characteristics of negative controls 52
2.2.5.9 Qualitative analysis of PCR products 54
2.2.6 Cell proliferation and viability assay (Trypan blue dye exclusion) 54
2.2.7 Flow cytometry 55
2.2.7.1 Pluripotency analysis 55
2.2.7.2 Proliferation Assay 56
2.2.7.3 Apoptosis and cell death assay 56
2.2.8 Immunocytochemistry (ICC) staining 58
2.2.9 Statistics 58
2.3 Results 59
2.3.1 Effect of maternal age on embryo development at E3.5 59
2.3.2 Derivation of mouse embryonic stem cells (mESCs) 62
2.3.2.1 Optimization of mESC derivation protocol 64
2.3.3 Effect of Advanced Maternal Age (AMA) on mESC derivation 66
2.3.4 Characterization of derived mESCs 67
2.3.4.1 Sexing of mESC lines 67
2.3.4.2 Karyotype analysis of mESC lines 68
2.3.5 Functional Characterization of derived mESCs 72
2.3.5.1 Pluripotency (Stemness/ markers for mESC) analysis 72
2.3.5.2 Differentiation analysis 76
2.3.5.3 Cell Proliferation and Differentiation analysis 78
2.3.5.4 Cell Apoptosis and Cell Death analysis 85
2.3.5.5 Epigenetic modifiers 88

2.4 General Discussion 90

2.4.1 Effect of Advanced Maternal Age (AMA) on Embryo Development 90

2.4.2 Effect of Maternal Age on derived Young and Old male mESC lines 92

2.4.2.1 AMA increases aneuploidy in Old male mESC lines 93

2.4.2.2 AMA reduces *Sox2* expression in Old male mESC lines 94

2.4.2.3 AMA reduces Cell Viability in Old male mESC lines 95

2.4.3 Effects of Sexual Dimorphism in Old mESC lines 96

2.4.4 Conclusion and Future aspects 97

Chapter 3 Metabolic differences between mESC lines derived from normal and low protein fed dams during the preimplantation period 99

3.1 Introduction 99

3.2 Materials and Methods 101

3.2.1 Animals and early experimental procedures (performed by Dr. Andy Cox) . 101

3.2.2 Sample preparation for metabolic analysis (Conducted by me in Southampton, U.K) 101

3.2.3 Sample processing and data acquisition (Conducted at Metabolon, U.S) 102

3.2.4 Phosphofructokinase (PFK) Activity Assay 104

3.2.4.1 Principle of PFK Activity Assay (Abcam, ab155898) 105

3.2.4.2 Sample preparation for PFK Activity assay 106

3.2.4.3 Calculations for Data Analysis 107

3.2.5 Pierce BCA (Bicinchoninic Acid) Protein Quantification Assay 109

3.3 Results 110

3.3.1 Amino Acids 110

3.3.2 Glucose metabolism 111

3.3.3 Fatty acid metabolism 117

3.4 General Discussion 121

3.4.1 Derivation and Culture of mESCs 121

3.4.2 Glycolysis: In developing embryos and derived pluripotent mESCs 124

3.4.2.1 Impact of Low Protein Diet (LPD) on glucose metabolism 125

3.4.3 Amino Acid metabolism in pluripotent mESCs 127

3.4.4 Polyunsaturated fatty acids (PUFAs) metabolism in pluripotent mESCs.....128
3.4.5 Conclusions and future work 128

Chapter 4 Optimisation of a neural induction protocol and evaluation of differences between the neural induction efficiency of NPD and LPD mESCs.....131

4.1 Introduction.....131
4.2 Materials and Methods 134
4.2.1 Culturing mESCs (at Southampton).....134
4.2.2 Freezing and thawing mESC lines.....134
4.2.3 mESC culture (at Biotalentum Ltd, Gödöllő, Hungary) 134
4.2.4 Neural induction of mESCs.....137
4.2.4.1 Standard neural induction medium (S-NIM).....137
4.2.4.2 Advanced neural induction medium (A-NIM) 139
4.2.5 Quantitative PCR (qPCR) analysis.....141
4.2.5.1 Sample preparation for RNA extraction (conducted at Biotalentum Ltd., Hungary) 141
4.2.5.2 RNA extraction 141
4.2.5.3 Reverse transcription (cDNA synthesis) and quantitative PCR 142
4.2.5.4 Normalization of PCR data and selection of reference genes 142
4.2.6 Immunocytochemistry (ICC) staining.....145
4.2.7 Statistical Analysis 145
4.3 Results 146
4.3.1 PART 1: Optimisation of neural induction (NI) protocol for NPD and LPD mESCs 146
4.3.1.1 Increasing proliferation of mESCs- Serum and serum-free mESC culture conditions 146
4.3.1.2 Optimal cell density for neural induction (NI) of NPD and LPD mESCs 148
4.3.1.3 Characteristics of neural induction protocol.....153
4.3.1.4 Neural induction of KO/SR cultured mESC lines in Standard or Advanced NIM 156

4.3.2 PART 2: Preliminary analysis of differences between NPD and LPD mESCs . 162

4.3.2.1 Pluripotency of KO/SR cultured NPD and LPD mESCs 162

4.3.2.2 Neural induction of ES-FBS and KO/SR cultured NPD and LPD mESCs 165

4.4 General Discussion 174

4.4.1 Effect of serum on pluripotent mESCs 176

4.4.2 Factors influencing NI efficiency 177

4.4.3 Alternative neural induction protocols 179

4.4.4 Effect of LPD on neural induction (NI) 179

4.4.5 Conclusions 180

Chapter 5 General discussion 183

5.1 Key findings emerging from this thesis 183

5.2 Preimplantation development 183

5.3 Programmed cell death 184

5.4 Cell metabolism 185

5.4.1 Fatty acids and neurogenesis 186

5.5 Future directions 187

5.6 Conclusions 191

Appendix A Media and Diet Composition 193

Appendix B Supplementary Figures 197

Appendix C List of Antibodies and Primers 203

Appendix D Supplementary details 205

List of References 207

Table of Tables

Table 2.1 Components of reverse transcription mix.....49

Table 2.2 Primerdesign 2x *PrecisionPlus*^{TM} qPCR Mastermix.....50

Table 2.3 Total number of ES cell lines isolated in Young and Old groups. 67

Table 2.4 Results of PCR sex analysis of mESC lines according to maternal age. 68

Table 3.1 Mean (± S.E.M.) concentrations of essential and branched chain amino acids (AA).111

Table 4.1 Reagents and their concentration for Standard neural induction medium (S-NIM)139

Table 4.2 Reagents and their concentration for Advanced neural induction medium (A-NIM)140

Appendix A. Table 1 Composition of isocaloric experimental (LPD) and control (NPD) diets196

Appendix C. Table 2 Antibodies used for Immunocytochemistry procedures.....203

Appendix C. Table 3 Antibodies used for Flow Cytometry 203

Appendix C. Table 4 Primers used for gene expression (RT PCR).....204

Table of Figures

Figure 1.1 **Periods of adaptive plasticity in the transition between life-history phases (double arrows).** 2

Figure 1.2 **Periconceptional (PC) period and developmental stages of an embryo.** 9

Figure 1.3 **Stages of mouse and human preimplantation development.** 27

Figure 1.4 **Overview of preimplantation development in mice.** 29

Figure 1.5 **Flow diagram representing series of experimental studies undertaken in this thesis.** 37

Figure 2.1 **RNA gel electrophoresis of AMA mESC lines.** 48

Figure 2.2 **geNorm output for reference gene targets analysed for AMA mESC lines.** .53

Figure 2.3 **Reference and target gene real-time PCR product specificity.** 54

Figure 2.4 **Oocytes and pre-implantation stage embryos from day 0 to day 4.5 after fertilization.** 59

Figure 2.5 **Representative images of embryos derived from (A) Young (7-8 weeks) and (B) Old (7-8 months) female mice (C57BL/6 females mated with CBA males) at E3.5.** 59

Figure 2.6 **Effect of maternal age on developmental stage of embryos at E3.5.** 61

Figure 2.7 **Representative images showing transfer and attachment steps of E3.5 blastocysts to mouse embryonic fibroblasts (MEFs).** 62

Figure 2.8 **Representative images of mESC colonies increasing in size (A-E) and associated timeline establishment (F).** 63

Figure 2.9 **Flowchart representing optimization of mESC derivation protocol in a systematic manner.** 65

Figure 2.10 **Increase in mESC derivation efficiency following optimization.** 66

Figure 2.11 **Derivation efficiency of Young and Old mESC lines.** 67

Figure 2.12 **Gender analysis of DNA isolated from mESC lines by multiplex PCR.** 68

Table of Figures

Figure 2.13 **Optimization of karyotype analysis.** 69

Figure 2.14 **Karyotype analysis to detect chromosomal abnormalities.** 70

Figure 2.15 **Effect of maternal age on karyotype of Young and Old mESCs lines.** 71

Figure 2.16 **Relative gene expression for pluripotency markers in undifferentiated male (young (7-8 weeks) vs old (7-8 months)) mESC lines.** 72

Figure 2.17 **Quantitative analysis of protein expression for pluripotency markers in undifferentiated male (Young (7-8 weeks) vs Old (7-8 months)) mESC lines.** 73

Figure 2.18 **Relative gene expression for pluripotency markers in undifferentiated Old (7-8 months, Male vs Female) mESC lines.** 73

Figure 2.19 **Quantitative analysis of protein expression for pluripotency markers in undifferentiated Old (7-8 months, Male vs Female) mESC lines.** 74

Figure 2.20 **Representative images of protein expression for pluripotency markers Oct4 and Sox2 (both green), and Nuclear marker Dapi (blue).** 75

Figure 2.21 **Relative gene expression for differentiation markers in undifferentiated male (young (7-8 weeks) vs old (7-8 months)) mESC lines.** 76

Figure 2.22 **Relative gene expression for differentiation markers in Old (7-8 months, Male vs Female) mESC lines.** 76

Figure 2.23 **Representative images of protein expression for mesodermal marker Brachyury (red) and Nuclear marker Dapi (blue).** 77

Figure 2.24 **Representative phase-contrast images of cell proliferation of Young (7-8 weeks), Old (7-8 months) male and Old female mESCs.** 79

Figure 2.25 **Cell proliferation of undifferentiated male (Young (7-8 weeks) vs Old (7-8 months)) mESC lines by trypan blue dye exclusion assay.** 80

Figure 2.26 **Cell proliferation and differentiation in Young male (7-8 weeks) vs Old male (7-8 months) ES lines.** 81

Figure 2.27 **Cell proliferation of undifferentiated Old ((7-8 months) male vs female) mESC lines by trypan blue dye exclusion assay.** 83

Figure 2.28 **Cell proliferation and differentiation in Old male vs Old female mESC lines.** 84

Figure 2.29 **Quantitative protein expression of early apoptosis marker, Annexin V, in undifferentiated Young (7-8 weeks) vs Old (7-8 months) male mESC lines.** 86

Figure 2.30 **Quantitative protein expression of early apoptosis marker, Annexin V in undifferentiated Old Male vs Old Female mESC lines.** 87

Figure 2.31 **Relative gene expression for DNA methyltransferases in undifferentiated male (Young (7-8 weeks) vs Old (7-8 months)) mESC lines.** 88

Figure 2.32 **Relative gene expression for DNA methyltransferases in undifferentiated Old ((7-8 months) Male vs Female) mESC lines.** 89

Figure 2.33 **Flow diagram representing study layout and findings from Chapter 2 of this thesis.** 91

Figure 3.1 **Glycolytic and gluconeogenic conversion of Fructose-6-Phosphate (F-6-P).**105

Figure 3.2 **Functional mechanism of the PFK Activity Assay Kit, ab155898 (Abcam).** .106

Figure 3.3 **Optical densities at 450nm.** 108

Figure 3.4 **Mean (± S.E.M.) concentrations of key metabolites involved in fructose-mannose and pentose-phosphate pathways from lysates of undifferentiated male NPD and LPD mESCs (P11-13; n=7) cultured in standard mESC medium (KnockOut DMEM + LIF + KO/SR).** 113

Figure 3.5 **Mean (± S.E.M.) glycolytic metabolite concentrations in lysates from undifferentiated male NPD and LPD mESCs (P11-13; n=7) cultured in standard mESC medium (KnockOut DMEM + LIF + KO/SR).** 114

Figure 3.6 **Mean (± S.E.M.) concentrations of glycolytic enzyme phosphofructokinase (PFK) in homogenised NPD and LPD mESC lines.** 115

Figure 3.7 **Mean (± S.E.M.) TCA cycle metabolite concentrations in lysates from undifferentiated male NPD and LPD mESCs (P11-13; n=7) cultured in standard mESC medium (KnockOut DMEM + LIF + KO/SR).** 116

Figure 3.8 **Mean (± S.E.M.) concentrations of selected saturated and monounsaturated fatty acids (FAs) in lysates from undifferentiated male NPD and LPD mESCs (P11-13; n=7) cultured in standard mESC medium (KnockOut DMEM + LIF + KO/SR).** 118

Figure 3.9 **Mean (± S.E.M.) concentrations of selected omega-3 polyunsaturated fatty acids (PUFAs) in lysates from undifferentiated male NPD and LPD mESCs (P11-13; n=7) cultured in standard mESC medium (KnockOut DMEM + LIF + KO/SR** 119

Figure 3.10 **Mean (± S.E.M.) concentrations of selected omega-6 polyunsaturated fatty acids (PUFAs) in lysates from undifferentiated male NPD and LPD mESCs (P11-13; n=7) cultured in standard mESC medium (KnockOut DMEM + LIF + KO/SR).** 120

Figure 3.11 **Flow diagram representing study layout and findings from Chapter 3 of this thesis.** 123

Figure 4.1 **Project timeline representing the series of events from receiving samples to neural induction of NPD and LPD mESCs.** 136

Figure 4.2 **RNA gel electrophoresis of NPD and LPD mESC lines.** 142

Figure 4.3 **geNorm output for reference gene targets analysed for NPD and LPD mESC lines.** 144

Figure 4.4 **Representative images showing proliferation and morphological changes in mESC lines in pluripotent medium (with LIF) under three serum conditions.** 146

Figure 4.5 **Brightfield images showing proliferation and morphological differences in NPD and LPD mESC lines in serum (ES-FBS) and serum-free (KO/SR) culture conditions.** 148

Figure 4.6 **Selecting the most efficient cell density for neural induction protocol.** 149

Figure 4.7 **Effect of mESC density on relative gene expression of pluripotency and differentiation markers during standard neural induction.** 151

Figure 4.8 **Effect of mESC density on relative gene expression of neural stem cell (NSC) and mature neuron markers during standard neural induction.** 152

Figure 4.9 **Immunocytochemistry of neuron marker(s) expression: Beta III Tubulin (Green), Map 2 (Red) and Nuclear marker Dapi (blue).** 153

Figure 4.10 **Representative images of a gradual decrease in pluripotency marker expression- Oct4 (green), Nanog (red) and Sox2 (light blue) from pluripotency to NI.** 154

Figure 4.11 **Changes in neural stem cell (NSC) marker(s) expression, Nestin and Pax6 (red), from D0 to D7 of neural induction (NI).** 155

Figure 4.12 **Presence of other lineage marker expression during Neural Induction (NI).**156

Figure 4.13 **Comparison between neural induction under Standard (S-NIM) and Advanced (A-NIM) culture conditions.** 158

Figure 4.14 **Comparison of relative gene expression for pluripotency, differentiation and apoptosis markers in mESCs undergoing NI under standard and advanced culture conditions.** 160

Figure 4.15 **Comparison of relative gene expression for early neural stem cell (NSC) and mature neuron markers in mESCs undergoing NI under standard and advanced culture conditions.** 161

Figure 4.16 **Comparison of relative gene expression for pluripotency, differentiation and apoptosis markers in pluripotent NPD and LPD mESCs cultured without serum.** 163

Figure 4.17 **Comparison of relative gene expression for early neural stem cell (NSC) and mature neuron markers in pluripotent NPD and LPD mESCs cultured without serum.**.....164

Figure 4.18 **Figure 4.18. Representative images of pluripotency marker expression, Oct4 (green), Nanog (red) and Sox2 (light blue) in pluripotent NPD and LPD mESCs before NI.**.....165

Figure 4.19 **Neural induction (D3-D7) of NPD and LPD mESC lines cultured in ES-FBS and KO/SR.** 167

Figure 4.20 **Neural induction (D10-D14) of NPD and LPD mESC lines cultured in ES-FBS and KO/SR.** 168

Figure 4.21 **Comparison of relative gene expression for pluripotency, differentiation and apoptosis markers in mESCs cultured with or without serum, undergoing standard NI.**.....170

Figure 4.22 **Comparison of relative gene expression for early neural stem cell (NSC) and mature neuron markers in mESCs cultured with or without serum, undergoing standard NI.**.....171

Figure 4.23 **Representative images for mature neuron marker(s) expression: Beta III Tubulin (Green), Map 2 (Red) and Nuclear marker Dapi (Blue) at Day 7, 10 and 14 of NI.** 173

Figure 4.24 **Flow diagram representing study layout and optimisation techniques from Chapter 4 of this thesis.** 175

Figure 4.25 **Flow diagram representing study findings from Chapter 4 of this thesis** ... 176

Appendix B. Figure 1 **Carcass weight of Young (7-8 weeks) v Old (7-8 months) dams at E3.5** 197

Appendix B. Figure 2 **Effect of time on protein expression of pluripotency surface marker, SSEA-1, in undifferentiated male (young (7-8 weeks) vs old (7-8 months)) ES lines.** 197

Appendix B. Figure 3 **Relative gene expression for cell apoptosis marker in undifferentiated male (young (7-8 weeks) vs old (7-8 months)) mESC lines.** 198

Appendix B. Figure 4 **Effect of time on protein expression of pluripotency surface marker, SSEA-1, in undifferentiated old ((7-8 months) male vs female) ES lines.** ... 198

Appendix B. Figure 5 **Relative gene expression for cell apoptosis marker in undifferentiated old ((7-8 months) male vs female) mESC lines.** 199

Appendix B. Figure 6 **BSA Standard Curve at 570 nm absorbance.** 199

Appendix B. Figure 7 **Brightfield images showing proliferation and morphological differences in control mESC line, HM1 in serum-free (KO/SR) and serum (ES-FBS) based pluripotent culture conditions.** 200

Appendix B. Figure 8 **Neural induction (D1-D8) of HM1 control mESC line cultured in S-NIM.** 201

Appendix B. Figure 9 **Neural induction (D9-D14) of HM1 control mESC line cultured in S-NIM.** 202

Academic Thesis: Declaration Of Authorship

I, Pooja Khurana declare that this thesis and the work presented in it are my own and has been generated by me as the result of my own original research.

Mouse embryonic stem cells as a model system for periconceptional developmental programming

I confirm that:

1. This work was done wholly or mainly while in candidature for a research degree at this University;
2. Where any part of this thesis has previously been submitted for a degree or any other qualification at this University or any other institution, this has been clearly stated;
3. Where I have consulted the published work of others, this is always clearly attributed;
4. Where I have quoted from the work of others, the source is always given. With the exception of such quotations, this thesis is entirely my own work;
5. I have acknowledged all main sources of help;
6. Where the thesis is based on work done by myself jointly with others, I have made clear exactly what was done by others and what I have contributed myself;
7. None of this work has been published before submission.

Signed:

Date:

Acknowledgements

I would like to thank my supervisors, Professor Tom Fleming and Dr. Neil Smyth for their guidance, support and valuable advice for my PhD and related research. I have learnt a great deal from them. I would also like to thank Dr. Judith Eckert and Dr. Bhav Sheth for their kind support, guidance and positive criticism throughout my PhD.

I am also thankful to our EpiHealthNet consortium collaborators at Metabolon Inc (U.S), Dr. Edward Karoly and Dr. Brian Ingram, and at Biotalentum Ltd (Hungary), Prof. Andras Dinnyes and Dr Julianna Kobolak for giving me an opportunity to join their research teams and for teaching me new techniques, skills and cultures. A special thanks to Ms. Marianna Tóth from Biotalentum for acquainting me with day-to-day lab work, while we developed new ways of communicating 'Science', given that I could not understand Hungarian and she did not speak English.

I am also very thankful to Mr. Richard Jewell and Dr Carolann McGuire for flow cytometry training, and Dr David Johnson for confocal microscopy training and his helpful inspirational words of wisdom. I am very grateful to Dr. Emilie Simon and Dr. Juliane Obst for their guidance and support, especially with qRT-PCR and flow cytometry techniques. I learnt a lot from them.

A special thanks to Professor Kevin Sinclair for his guidance on matters in and around my PhD. From suggesting courier services for samples abroad, to invigorating scientific discussions, stress buster strategies and after-conference entertainment, he has been a great source of motivation and fun.

I am very appreciative of Ms. Samantha Scott from Student's Union and Mr. Jason Varlow of University Enabling Services for helping me to stay focussed and positive through the challenging times. I am also thankful to Ms. Lorraine Prout for her kind and consistent support, and for answering my frequent administrative and general queries.

Also thanks to fellow lab members of the Developmental Biology group and everyone, I shared the common office space with, for the stimulating discussions, banter and all the fun we had throughout the last four years. I would also like to thank all my friends here, and across the globe for their good wishes and support.

And lastly, I'm immensely grateful to my parents and family for standing by me, through their long-distance support, patience, motivation, love and positivity at each and every step through life, and this unique journey of science, demanding stem cells, research, sleepless nights, fun filled international travels and crazy adventures. It has been a memorable voyage of rich experiences indeed!

Abbreviations

18S	18 S ribosomal RNA
AA	Amino acids
ACT B	Beta-actin
AFC	Antral-follicle count
ALKS	Alkaline-like receptor kinases
AMA	Advanced maternal age
AMH	Anti Mullerian Hormone
AMP	Adenosine monophosphate
AMPA	α-amino-3-hydroxyl-5-methyl-4-isoxazole-propionate
A-NIM	Advanced neural induction medium
APEX1	Apurinic/apyrimidinic endodeoxyribonuclease 1
ART	Assisted reproductive technologies
AS	Angelman syndrome
ATP	Adenosine triphosphate
ATP5B	ATP synthase subunit beta
B2	Riboflavin
B2M	Beta-2-Microglobulin
B6	Thiamine
BCA	Bicinchoninic Acid
BCAA	Branched chain amino acids
bFGF	Basal fibroblast growth factor
BIO	6-Bromoindirubin-3’-oxime
BMI	Body mass index
BMP	Bone morphogenic protein pathway
bp	Base pair
BWS	Beckwith-Wiedmann syndrome
CANX	Calnexin
C(t)	Cycle threshold
$CaCl_2$	Calcium chloride
$CaCl_2.2H_2O$	Calcium chloride dehydrate
CDM	Chemically defined media
CHD	Coronary heart disease
CNS	Central nervous system
CVDs	Cardiovascular diseases
CYC1	Cytochine c1
DAPI	4, 6-diamino-2-phenylindole dilactate
DE	Definitive endoderm
DHA	Docosahexaenoic
DMEM	Dulbecco modified Eagle medium
DMRs	Differentially methylated regions
DMSO	Dimethyl sulphoxide
Dnmt	DNA methyltransferase transcript
DOHaD	Developmental Origins of Health and Disease
EBs	Embryoid bodies
EDTA	Ethylenediaminetetraacetic acid
EGA	Embryonic genome activation

EIF4A2	Eukaryotic initiation factor 4A-II
Epi	Epiblast
EpiSCs	Epi-stem cells
ER	Endometrial receptivity
ERK	Extracellular-signal-regulated kinase
ESC	Embryonic stem cell
ES-FBS	ES-based fetal bovine serum
ESI	Electrospray ionization
ET	Embryo transfer
ETC	Electron transport chain
F1	First generation
F-1,6-bP	Fructose-1,6-bisphosphate
F-2,6-bP	Fructose-2,6-bisphosphate
FA	Fatty acid
FbP-1	Fructose bisPhosphatase 1
FbP-2	Fructose bisPhosphatase 2
FBS	Fetal bovine serum
FDR	False discovery rate
FGF	Fibroblast growth factor
FGF4	Fibroblast growth factor 4
FISH	Fluorescent *in situ* hybridisation
FITC	Fluorescein-5-isothiocyanate
FSH	Follicle stimulating hormone
G0	Resting phase
GAPDH	Glyceraldehyde-3-phosphate dehydrogenase
Gata4	Transcription factor Gata-4
G-6-P	Glucose-6-phosphate
GC	Guanine-cytosine
GIFT	Gamete intrafallopian transfer
GLDC	Glycine decarboxylase
GLUT	Glucose transporters
GSK3	Glycogen synthase kinase 3
HDP	Hypertension during pregnancy
hESCs	Human ESCs
hFF	Human foreskin fibroblasts
HILIC	Hydrophilic interaction chromatography
HK	Hexokinase
HLA	Human leukocyte antigen
IC	Infancy-childhood
ICC	Immunocytochemistry
ICM	Inner cell mass
ICSI	Intracytoplasmic sperm injection
Id	Inhibitor of differentiation
IHD	Ischaemic heart diseases
IL6	Interleukin 6
IUGR	Intrauterine growth restriction
IVF	*In vitro* fertilization
JAK	Janus Kinase
KCL	Potassium Chloride

Klf4	Krüppel-like transcription factor 4
KO/SR	Knockout™ serum replacement
LBW	Low birthweight
LGA	Large for gestational age
LIF	Leukemia inhibitory factor
LIFRß	LIF receptor ß
LPD	Low protein diet
MAPK	Mitogen-activated protein kinase
MBD3	5-methyl-CpG-binding domain protein
MEFs	Mouse embryonic fibroblasts
mESCs	Mouse embryonic stem cells
$MgCl_2$	Magnesium chloride
$MgSO_4.7H_2O$	Magnesium sulphate7-hydrate
MI	meiosis I
MII	meiosis II
mLIMS	Metabolon Laboratory Information Management System
MMC	Mitomycin C
MMC-MEF	Mitomycin C- mouse embryonic fibroblasts
MOSART	Massachusetts Outcomes Study of Assisted Reproductive Technology
MSC	Mesenchymal stem cells
mTOR	Mammalian target of rapamycin
NaCl	Sodium chloride
$NaH_2PO_4.2H_2O$	Sodium dihydrogen orthophosphate
$NaHCO_3$	Sodium bicarbonate
NCDs	Non-communicable diseases
NEAA	Non-essential AAs
NI	Neural induction
NK	Natural killer
NMDA	*N*-methyl-d-aspartate
NPD	Normal protein diet
NSCs	Neural stem cells
O.D	Optical density
Oct3/4	Octamer binding transcription factor 3 or 4
PAR	Predictive adaptive response
PARP	Poly (ADP-ribose) Polymerase
PCD	Programmed cell death
PCOD	Polycystic ovarian disease
PDH	Pyruvate dehydrogenase
PE	Primitive endoderm
PEP	Phosphoenolpyruvate
PEPCK	Phosphoenolpyruvate carboxykinase
pERK	Protein kinase RNA-like endoplasmic reticulum kinase
PFK	Phosphofructokinase
PGD	Preimplantation genetic diagnosis
PGS	Pre-implantation genetic screening
Pi	Inorganic phosphate

PI	Propidium iodide
PI3K	Phosphatidylinositol 3-kinase
PK	Pyruvate kinase
PNS	Peripheral nervous system
POLB	DNA polymerase beta
PPARs	Peroxisome proliferator-activated receptors
PPP	Pentose phosphate pathway
PS	Phosphatidylserine
PTBs	Preterm births
PUFAs	Polyunsaturated fatty acids
QC	Quality control
qPCR	Quantitative polymerase chain reaction
RA	Retinoic acid
ROS	Reactive oxygen species
RPL13A	Ribosomal Protein L13a
RP/UPLC-MS/MS	Reverse phase ultra-performance liquid chromatography-tandem mass spectrometry
SCs	Stem cells
SDHA	Succinate dehydrogenase complex, subunit A
SDS	Sodium dodecyl sulphate
SGA	Small for gestational age
SMIs	Small molecule inhibitors
S-NIM	Standard NI medium
Sox1	SRY-box containing gene 1
Sox2	Sex determining region Y-box 2
STAT3	Signal transducer and activator of transcription-3
TCA	Tricarboxylic acid
TDH	Threonine dehydrogenase
TE	Trophectoderm
TGF-β	Transforming growth factor beta
Tm	Temperature
UBC	Polyubiquitin-C
UV	Ultraviolet
WNT	Wingless/Integrated
XCI	X-chromosome inactivation
Xic	X-inactivation centre
YWHAZ	14-3-3 protein zeta/delta
β-Ctnn	Cytoplasmic β-catenin

Introduction

Several maternal health and lifestyle factors during pregnancy have been linked to the long-term wellbeing of offspring (Barker and Thornburg, 2013; Godfrey et al., 2017; Dhana et al., 2018). Epidemiological evidence has thus far supported the concept of the 'Developmental Origins of Health and Disease' (DOHaD), which proposes that early life events, including poor *in utero* environment, can predispose offspring to non-communicable diseases (NCDs) in later life (Gluckman et al., 2007). Cardiovascular (including hypertension and ischaemic heart diseases (IHD)) and metabolic (including obesity, insulin resistance and type 2 diabetes) disorders are the leading causes of death worldwide. However, emerging evidence has also revealed the deleterious effects of maternal undernutrition on neurodevelopmental comorbidities, including schizophrenia, autism spectrum disorders and behavioral abnormalities (such as anxiety and depression).

Some of the most compelling data have been obtained from human cohorts such as The Dutch Hunger Winter, The Chinese Famine, Sub-Saharan Africa and The Gambia (Prentice et al., 1981; Roseboom et al., 2011; Li et al., 2011). One common denominator among these studies has been the prevalence of extreme undernutrition (associated with additional physical and mental distress) experienced by pregnant mothers, and its effects on offspring health. These historic cohorts continue to provide strong evidence of adverse long-term effects arising from poor nutrition *in utero* and have, therefore, been used to understand the relationship between the timing of nutritional insult and pregnancy outcome. Although environmental stressors throughout pregnancy can affect offspring health, the most adverse outcomes occur when *in utero* insults were experienced during the early stages of gestation (Painter et al., 2006). Several maternal lifestyle factors are known to influence offspring health. These include maternal age, malnutrition, infectious diseases, substance abuse, chemotherapy, and assisted reproductive technologies (ART) (Wu et al., 2004; Severinski et al., 2006; Ornoy and Ergaz, 2010; Calsteren and Amant, 2011; Balasch and Gratacós, 2012; Waldorf and McAdams, 2013).

Industrialization and socio-economic factors have introduced a global trend of increasing maternal childbearing age (Powell et al., 2006). While this may also indicate improvement in women's health, educational and working status, there is growing concern regarding the health of offspring conceived by the reproductively older woman. Several reports indicate that women of advanced reproductive age are more prone to developing complications during pregnancy, such as stillbirths, gestational diabetes and pre-eclampsia (Hansen, 1986; Carolan and Frankowska, 2011; Biro et al., 2012); and their offspring have higher risks of developing chromosomal abnormalities, mental disorders and cardiovascular diseases (CVDs). While the age of both parents has an influence,

women have a shorter reproductive lifespan, with the reserve of ovarian follicles diminishing rapidly from around 35 to 40 years of age (Carolan and Nelson, 2007; Baird, 2013). Additionally, reproductive age varies among women of the same chronological age, which may be influenced by their lifestyle, health, diet and/or genetic constitution. Moreover, given the increasing 'success' of ART such as *in vitro* fertilization (IVF), many AMA women are now choosing this option over early pregnancy (Bühler et al., 2014). While this may seem beneficial, it has compounded the adverse effects of AMA and ART, and increased the susceptibility of offspring to non-communicable diseases in later life.

Although human cohort studies have been invaluable in establishing the long-term effects of adverse *in utero* environments, the data for the most part are observational, compromised by a plethora of unavoidable confounding factors, and lack mechanistic insight. This makes it difficult to identify preventative measures and to develop strategies for intervention. In contrast, animal studies offer controlled experimental settings with fewer ethical issues in addition to facilitating targeted interventions. Given that most reproductive failures occur during the periconceptional period, several mouse models have been developed that focus on programming events that occur during early embryo development (Langley and Jackson, 1994; Watson, 1992; Watson et al., 2004; Eckert et al., 2012; Velazquez et al., 2016, 2018; Fleming et al., 2018). While such studies provide important insights into developmental events and effects of *in utero* environment, they have their limitations. For example, mouse embryos developing *in vivo* after E4.0 are inaccessible, as they initiate the process of implantation. Earlier stage embryos have limited numbers of cells that limit analysis, and restricted number of embryos obtained per mother (8-12 on average) necessitate the use of many animals.

To overcome these issues, recent studies have turned to mouse embryonic stem cells (mESCs) as an *in vitro* model system (Cox et al., 2011; Zhu and Huangfu, 2013; Shyh-chang and Ng, 2017). Mouse ESCs are derived from the inner cell mass (ICM) of early embryos, and will thus have been exposed to the maternal *in utero* environment for the first three days of gestation (i.e. during the preimplantation period). The preimplantation period is now generally recognized as one of the most critical stages of developmental programming, inducing irreversible changes in the embryo that influence adult offspring health (Watkins et al., 2008). Previous studies from Southampton have demonstrated that mESCs derived from embryos of mothers fed a low protein diet (LPD) retain memory of nutritional adversity and propagate the effects *in vitro* (Cox et al., 2011). Phenotypic changes observed in mESCs were further validated by the formation of embryoid bodies (EBs) (Sun et al., 2014, 2015), which are three-dimensional aggregates of pluripotent cells and resemble an *in vivo* embryo. Alterations detected in derived EBs were similar to observations made in the embryos recovered from LPD-fed mothers, further confirming the value of *in vitro* model systems of mESCs.

Therefore, the present series of studies in this thesis utilised the validated *in vitro* model of mESCs to explore the biological mechanisms underlying developmental programming of long-term health as influenced by AMA and maternal LPD. The AMA study broadly focused on derivation and characterising mESC lines derived from Young (7-8 weeks) and Old (7-8 months) females mated with reproductively mature males. Chromosomally normal mESCs were analysed for differences in proliferation, viability and programmed cell death, pluripotency and differentiation capacity. To investigate the impact of maternal LPD on cellular metabolism, derived LPD (9% protein) and normal protein diet (NPD, 18% protein) mESC lines from Cox et al. (2011) were used for global metabolomic profiling. Finally, to assess the impact of maternal undernutrition on neurodevelopmental capacity, derived LPD and NPD mESC lines were differentiated to a neural lineage (for 14 days) and analysed for neural induction efficiency (NI) between the two dietary treatment groups. The overall findings from these series of studies indicated that mESC lines derived from AMA and LPD projects had adverse phenotypes (including poor survival and increased cell death), altered metabolism and increased NI efficiency; thus retaining and propagating programming alterations *in vitro* and serving as emerging model systems for mammalian developmental biology.

Chapter 1 Literature review

1.1 The DOHaD Hypothesis

Scientists have long postulated that the risk of acquiring coronary heart disease (CHD) in adult life is related to an unhealthy lifestyle (particularly in the western world) and inherited genetics (Segall, 1981). The other 'traditional' view of disease origin was a genetic mutation. However, these beliefs failed to offer any preventive measures for the disease and raised questions like why only a limited population becomes affected (Ebrahim and Smith, 1997).

It was David Barker and colleagues at the University of Southampton who, through their epidemiological studies, provided the first clue regarding the origin of non-communicable diseases (NCDs). Their studies proposed a strong geographical correlation between deaths that occurred from ischaemic heart disease (IHD) in 1968-78 and infant mortality rates in 1921-25 across two hundred local authority areas in the United Kingdom (Barker and Osmond, 1986). Other diseases, which showed a similar link to infant mortality, included stomach cancer, bronchitis and rheumatic heart disease. These studies showed that the regions of England and Wales that had the highest rates of infant mortality also had the highest rates of mortality from CHDs decades later (Williams et al., 1979). IHD in these areas was most prevalent in the poorer regions. This suggested that poor nutrition in early development might enhance the susceptibility to CHD just as an unhealthy lifestyle (i.e. high fat and cholesterol diet) could (Barker and Osmond, 1986). Cohorts from different world populations have also demonstrated the impact of poor living conditions on the health of newborns. Maternal nutrition plays a key role in the development and health of the offspring. Hence, any change in maternal diet can directly or indirectly affect the growth trajectory of the embryo (Robinson et al.,1999). Not only is prenatal health affected, but the subsequent postnatal health of the offspring may also be permanently compromised (Barker et al., 1993b; Godfrey and Barker, 2000; Morrison and Regnault, 2016).

1.1.1 DOHaD and Developmental Plasticity

Since the pioneering studies of David Barker, a number of additional related theoretical models have been proposed to explain the underlying phenomena. The ability of a given genotype to produce different phenotypes in response to different environments is termed 'plasticity' and is part of the organism's 'adaptability' to environmental cues (Hochberg, 2011) (Figure 1.1). The DOHaD hypothesis proposes that the intrauterine environment plays a key role in determining offspring development, health and wellbeing. Generally, exposure to adverse environments has a detrimental effect on the developing embryo but, in some cases, this early exposure may modulate

the normal developmental program to improve its immediate or future prospects of survival. For instance, short babies at birth (that have increased head to body size ratios) can arise as a result of poor maternal nutrition during late gestation (Barker et al., 1993b; Barker et al.,1993e; Barker, 1997).

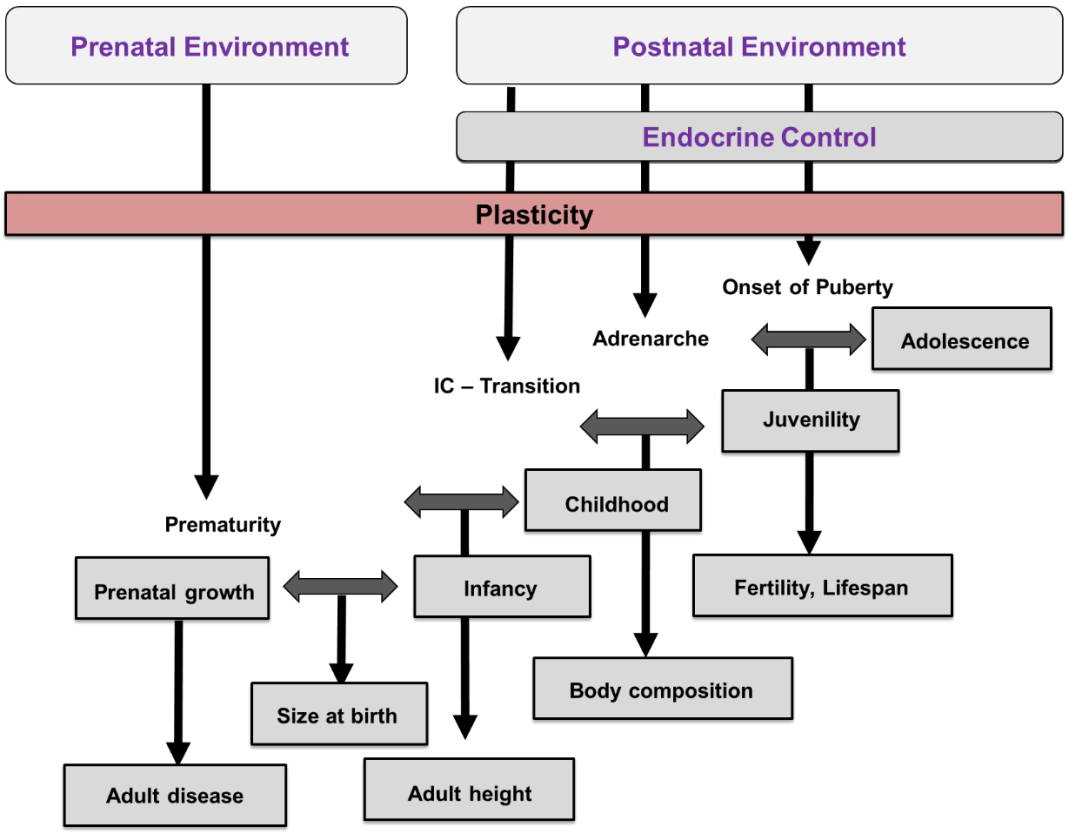

Figure 1.1 Periods of adaptive plasticity in the transition between life-history phases (double arrows).

Prenatal growth affects adult health and disease. The transition from infancy to childhood confers a predictive adaptive response (PAR) that determines adult height (Hanson and Gluckman, 2008). The transition from childhood to juvenility bestows an adaptive response that resolves adult body composition and metabolic consequences. The transition from juvenility to adolescence establishes longevity and the age of reproduction and fecundity. IC, Infancy-childhood (transition) (Adapted from (Hochberg, 2011)).

These infants tend to have a small abdominal circumference resulting in compromised liver size. This could be a compensatory mechanism for redistribution of blood flow to the vital organs of the body, such as the brain and the heart. As the liver is central to the synthesis and excretion of cholesterol, and plays a vital role in blood coagulation, any disturbances in its function could increase the risks of CHD in later life (Martyn et al., 1995). Hence, these immediate 'adaptive responses' may occur to ensure short-term survival and competitive reproductive fitness of the

fetus, but at the cost of compromised postnatal/ adult health (Mcmillen, 2005; Gluckman et al., 2007).

A refinement to the concept of 'developmental plasticity' is the notion of 'predictive adaptive responses' (PARs) (Hanson and Gluckman, 2008), which suggests that the fetus has the potential to forecast, by sensing the current environment *in utero*, and to develop accordingly. Such adaptations might not have immediate advantages, but can improve future postnatal health or optimize body composition/ metabolism to the predicted postnatal environment. The association of outcomes with birthweight is an epi-phenomenon of the relationship between nutrient availability to the fetus and the predictive adaptive response, therefore anticipative of the later life environment (Gluckman and Hanson, 2004; Gluckman et al., 2005a). The adaptive advantage of these responses is determined by the probability that the choices made during early development are suitable for the environment that the offspring will be exposed to in later life (Gluckman et al., 2005a). If the prediction is accurate, then the organism is matched better to its subsequent environment and will cope adequately. An example is poor intrauterine environment inducing the reduced development of skeletal muscle and increased visceral fat deposition. This helps survival of the fetus in a poor postnatal environment, often observed in some South Asian babies (e.g. India) (Yajnik et al., 2003). However, if the developmental choices made are not suited, the fetus may become more susceptible to diseases in later life. This becomes evident when the expected postnatal conditions vary and start challenging the offspring's own physiological system leading to a 'developmental mismatch'. This concept is relevant to the increasing obesity epidemic (Gluckman et al., 2007a) and is observed mostly in populations experiencing rapid dietary alterations such as in India, resulting in increased incidents of metabolic syndrome (Gluckman et al., 2005c). Hence, it is the match-mismatch theory that determines the chances of embryo survival and the health of the offspring in later life.

Although an array of nutritional alterations can inflict similar responses in offspring health, the timing and duration of the alterations affect the severity and nature of the response. The offspring may exhibit different responses to a particular stimulus depending on the stage of development and gestation when the change occurs (McMillen and Robinson, 2005; Gluckman et al., 2007a).

1.1.2 DOHaD, birthweight and body composition

Coronary heart disease (CHD) is associated with low birthweight (LBW). Studies with large British cohorts, showed that men with LBW had higher mortality rates from CHD (Barker et al., 1993b; Osmond et al.,1993). This association between LBW and CHD has also been confirmed in studies of men in Uppsala and Caerphilly (Frankel et al., 1996) and among women in the United States

(Rich-Edwards et al., 1997). LBW has also been associated with increased insulin resistance and incidence of type 2 diabetes mellitus (Beringue et al., 2002). These effects of LBW are accentuated by slow infant growth and rapid weight gain in childhood (Barker et al., 2002) . As shown in the Helsinki cohort, people who developed CHD, hypertension and type 2 diabetes were the ones who were short and thin at birth, had poor growth in the first year, and accelerated weight gain in later childhood (Eriksson et al.,2001; Veening et al., 2003). These diseases were believed to originate through two biological phenomena, that is developmental plasticity and compensatory or 'catch-up' growth (Barker and Thornburg, 2013; Langley-Evans, 2015).

However, neonates with high birthweight are also susceptible to diseases such as polycystic ovarian disease (PCOD) and hormone related cancers in later life, including breast, prostate and testicular cancer (Huang et al., 1997; Mumm et al., 2013; Zhou et al., 2016). These longitudinal studies led to the hypothesis that *in utero* development and infancy were influenced by environment and poor social conditions that increase the probability of acquiring diseases in adult life. Cohorts in Norway (Forsdahl, 1977), Finland (Notkola and Husman, 1988) and the USA (Buck and Simpson, 1982) also supported this hypothesis. The leading cause of neonatal deaths obtained from the cohorts was low birth weight. As this cause was certified as a congenital cause, it was proposed that undernutrition *in utero* and during infancy permanently changed the body's structure, physiology and metabolism, and led to a higher risk of acquiring diseases in later life (Frankel et al., 1996; Rich-Edwards et al., 1997).

In Britain, cohorts demonstrated that children born small at birth (and small stature during infancy) developed high blood pressure, and had high serum cholesterol and plasma fibrinogen concentrations with impaired glucose tolerance in adulthood (Eriksson et. al., 2000). Increased blood pressure, although marginal in childhood, could subsequently be magnified throughout life. This further suggested that not only are diseases initiated during the fetal period, but they may be amplified throughout the adult life span (Barker et. al.1990; Eriksson et. al., 2003).

Such a connection between reduced fetal growth and increased postnatal blood pressure has been associated with the vascular structure of the arteries (reduced elasticity) (Berry et. al.,1976; Martyn et al., 1995). Similar results in men and women showing an association between birthweight with non-insulin dependent diabetes and impaired glucose tolerance in later life have been reported in studies undertaken in Britain, United States and Sweden (Phipps et al., 1993; Mccance et al., 1994; Valdez et. al., 1994)

In addition to birthweight, thinness of the baby at birth has also been associated with disease risk in later life. For instance, insulin resistance is not only associated with low birthweight (LBW), but more precisely with thinness at birth (Barker et al., 1993). Thin babies lack muscle and fat. As

muscle is the peripheral site of insulin action, thin babies tend to become insulin resistant (Phillips et. al., 1994). Small babies, who unlike the thin and short babies, are mostly proportionate and may not develop CHD, may still develop increased blood pressure. Elevated blood pressure is associated with fetal abnormality at almost every stage of gestation and with LBW, thin and short babies.

1.1.3 DOHaD: Evidence from additional human cohorts

Several epidemiological studies have indicated a strong correlation between maternal health and lifestyle, and the prenatal, postnatal and adult development of offspring. These are reviewed extensively elsewhere (Stanner et al., 1997; Barker, 2007; Barker et al., 2009) and so only brief reference is made here. The Dutch hunger winter cohort of children, either conceived or experienced later pregnancy during a 5-month period (1944–1945) towards the end of the war provided a unique opportunity to study the effects of undernutrition during different stages of gestation in humans. Although exposure to famine during any stage of gestation was associated with glucose intolerance, it was found that CHD, disturbed blood coagulation, increased stress responsiveness, obesity and schizophrenia were more prevalent among those exposed to famine in 'early gestation' (Roseboom et al., 2011). Similarly, *in utero* malnutrition during the first trimester, as occurred during the Chinese Great Famine (1959-61) increased the risk of hypertension (Li et al., 2011; Wang et al., 2016), schizophrenia (St Clair et al., 2005) and metabolic disorders such as hyperglycemia (Li et al., 2011) and dyslipidemia (Xin et al., 2018) in adulthood. Some of these effects (e.g. incidence of type-2-diabetes) were also observed in the second generation, hinting at the prospect of transgenerational effect of severe malnutrition (Li et al., 2017).

Similar effects are observed in regions of the world where there are marked seasonal fluctuations in food availability. For example, in rural Matlab region of Bangladesh, Sub-Saharan Africa and in The Gambia. For example, birth cohorts from three Gambian villages (1949-1994) show that people born during the wet season of July-October, also referred to as the 'annual hungry period', are about ten times more susceptible to premature death, than those born in the dry season. These individuals suffered from intrauterine growth retardation, and severe growth faltering in infancy and childhood (Prentice et al., 1981).

In contrast, the Leningrad study (now St. Petersburg) during 1941-1944 showed no differences between individuals who experienced starvation *in utero* (prenatal life) or during infancy. Although subjects in the intrauterine group showed increased correlation between obesity on high blood pressure and endothelial dysfunction than in the infant group, unlike the Dutch cohort, this study

did not show association between maternal intrauterine malnutrition and the development of glucose intolerance, dyslipidemia, hypertension, or cardiovascular disease in adulthood (Stanner et al., 1997). This could be explained by both the timing and duration of exposure (e.g. 5 months for the Dutch Hunger Winter vs >1 year for the famine in China), and whether or not the extended duration of malnutrition in the Leningrad study, led to a 'mismatch' between gestational and post-natal nutritional status. Additionally, criticisms subjected to this study include high ascertainment rates and lack of reliable birth weight data, as most candidates provided a recalled birth weight which could have affected data accuracy (Antonov, 1947; Kramer and Joseph, 1996). Alternate explanations include, as also observed by Godfrey and Barker (1995), that the effect of protein deprivation is more evidently seen in women where protein diets are replaced by high carbohydrate diets (like in developing countries). Other studies have shown more powerful relation between growth retardation and disease development when the insults like malnutrition last for prolonged periods or across generations (Martyn et al., 1996).

1.1.4 DOHaD and over nutrition

Whilst many of the early 'Barker-hypothesis' related studies, including the aforementioned cohort studies, related to the effects of under or malnutrition, in recent years attention has focused more on the effects of obesity, and over nutrition more generally. Indeed, there now exists an overwhelming body of evidence that over nutrition in mothers and children also contributes to later chronic diseases, including CHD, blood pressure and adult-onset type-2 diabetes. Maternal obesity reduces fecundity (Luke et al., 2011; Broughton and Moley, 2017), success rates following assisted reproduction (ART) (Kumbak et al.,2012), and increases the risk of congenital anomalies in offspring (Stothard et al., 2009). Babies born to overweight mothers following natural or assisted conception are more susceptible to obesity, metabolic dysfunction, impaired glucose homeostasis, muscle metabolism and neuroendocrine changes (Wankhade et al., 2016). Maternal obesity may also induce higher risks of neurodevelopmental disorders and affect cognitive performance in offspring. As more studies show the association of maternal obesity with the global obesity epidemic, determination of the factors that lead to such long-term effects has now become an urgent global priority (published in WHO bulletin, Ota et al., 2011).

This association may be due to excess nutrition *in utero* or during infancy. Babies born with high birthweight tend to become obese in adult life (Stettler et al., 2002; Dietz, 2004), although studies also link over-nutrition with low birthweight and small body size during infancy (Frankel et al., 1996). Slow growth patterns during fetal life followed by a rapid increase in body mass index (BMI) after 2 years of age, are related to type-2 diabetes and CHD (Eriksson et al., 2003). Some studies also indicate a relationship between maternal and childhood obesity. This is linked

to shared eating habits and changes in hormonal or metabolic processes. High BMI amplifies the probability of gestational diabetes in the mother and type-2-diabetes in offspring (Farmer et al., 1988; Mccance et al., 1994). These offspring are born with excess adiposity, high birthweight and tend to be overweight during childhood; thereby demonstrating a perfect example of *in utero* events leading to obesity in later life (Nicholas et al., 2016).

1.1.5 Animal models of maternal malnutrition during pregnancy

Whilst studies of malnutrition in human populations under natural settings have been informative, they largely remain observational, offering no mechanistic insights. Animal models on the other hand are both controlled and interventional in nature, and are better to study the effects of specific nutrient deficiencies with minimal confounding factors. Several animal models of maternal malnutrition during pregnancy exist, and these have been reviewed extensively elsewhere (McMillen and Robinson, 2005; Nathanielsz, 2006; Chavatte-Palmer et al., 2016), so only brief reference is made to these later in the current thesis. The subsequent discussion, therefore, focuses primarily on the effects of maternal low-protein diet (LPD) in rodents, which was originally developed in Southampton during the 1990s (Langley and Jackson, 1994) and has been used extensively by several laboratories since (Erhuma et al., 2007).

As mentioned previously, the maternal low-protein diet (LPD) model in rodents, was originally developed in Southampton by Langley and Jackson (1994). In these early studies rat dams were habituated to isocaloric (balanced by addition of carbohydrates), control (18% casein) or LPD (9% casein) diets 14 days before mating, and thereon throughout gestation. The LPD (9%) diet was calculated to meet the minimal nutrient requirements of non-pregnant dams. Lactating dams and pups (normalized to a maximum litter of 8) were switched to standard chow diet (20% casein). In these studies, pregnant LPD-fed dams (9%) typically consumed less energy, and gained less weight compared to dams on control diet (18%). LPD-offspring displayed elevated systolic blood pressure, which was associated with increased pulmonary angiotensin-converting enzyme activity, indicative of physiological and biochemical functional changes in the fetus (Langley and Jackson, 1994). LPD-offspring also developed additional phenotypic alterations in adulthood, including impaired brain, liver and renal function, together with impaired immune responses, cardiovascular disease, and reduced lifespan (Langley-Evans et al., 1996; Langley-Evans et. al., 1999; Aihie et al., 2001; Langley-Evans, 2013). This model was later extended to consider the effects of LPD fed exclusively during the preimplantation period (E0.5 to E3.5) (discussed in detail in Section 1.2). Briefly, the restricted window of maternal LPD revealed significant reduction in the number of ICM and TE cells in the blastocysts, decreased levels of insulin and essential amino acids in maternal serum, which further correlated with elevated incidence of development of abnormal postnatal phenotypes (such as

obesity, hypertension, and behavioral disorders). Moreover, recent studies have also shown that maternal insults experienced exclusively during the limited window of pre-implantation compared to extended periods throughout gestation and/ or through lactation, may already be sufficient in inducing lasting consequences on offspring brain development and cognitive abilities (Gould et al., 2018).

1.2 The Periconceptional period and DOHaD

Several human studies and animal experiments have identified the periconceptional period as the most vulnerable stage of mammalian development. Definitions for this period vary according to species and nutrient-sensitive developmental stages (both pre- and post-conception). They typically range from 3 weeks pre-mating to 4 days post mating in many rodent studies (e.g. Sun et al., 2015), and around 14 weeks pre-mating and 10 weeks post-mating in humans (e.g. Steegers-Theunissen et al., 2013).

The preimplantation embryo initiates and directs a series of metabolic interactions with the uterus to sustain normal fetal development (Watson, 1992; Watson et al., 2004). These interactions are stimulated by autonomous signals from the oviductal and uterine fluid, and activation of the embryo's genome (Yeung et al., 2002; Schultz, 2005). Despite this autonomy, the signals may be influenced by external environmental factors like maternal nutrition (Kwong et al., 2000; Fleming et al., 2012), maternal age (Master et al., 2015), or *in vitro* embryo culture conditions like IVF or cryopreservation techniques (Niemann and Wrenzycki, 2000). Such factors may influence the implantation potential of the embryo directly and/ or reprogramme the embryo and affect its adaptive capacity resulting in abnormal embryonic, fetal and/or postnatal growth, thereby increasing disease susceptibility in adult life. It is therefore critical to understand the basic programme controlling preimplantation development and to track the changes that are induced by environmental factors to minimize the risk of disease development.

Preimplantation development is characterized by a series of cleavage divisions that give rise to three cell lineages and enable implantation of the embryo into the uterus. Following fertilization, the zygote undergoes a series of cell divisions until compaction, which commences around the 8-cell stage in mice (Figure 1.2). It is at this stage that blastomeres undergo an intracellular adhesion mediated by the calcium-dependent E-cadherin/catenin system (Fleming et al., 2000). This coincides with the polarization of blastomeres such that asynchronous cell divisions result in 16-cell morula stage with distinct outer and inner cell populations. The outer cells become the trophectoderm (TE) of the blastocyst (formed from 32-cell stage) and the inner cells become the inner cell mass (ICM) of the blastocyst. The TE comprises epithelial cells and surrounds the

ICM, which constitute the pluripotent progenitor cells of the later fetus and extra-embryonic yolk sac (Johnson and McConnell, 2004).

An important event in the preimplantation stage is the morphogenesis of the blastocyst. Fluid is transported across TE from the embryo exterior forming a blastocoelic cavity (Watson et al., 2004). The TE is the first differentiated cell type (multipotent) of development. It initiates implantation and is the progenitor of chorio-allantoic placenta (Rossant, 2004).

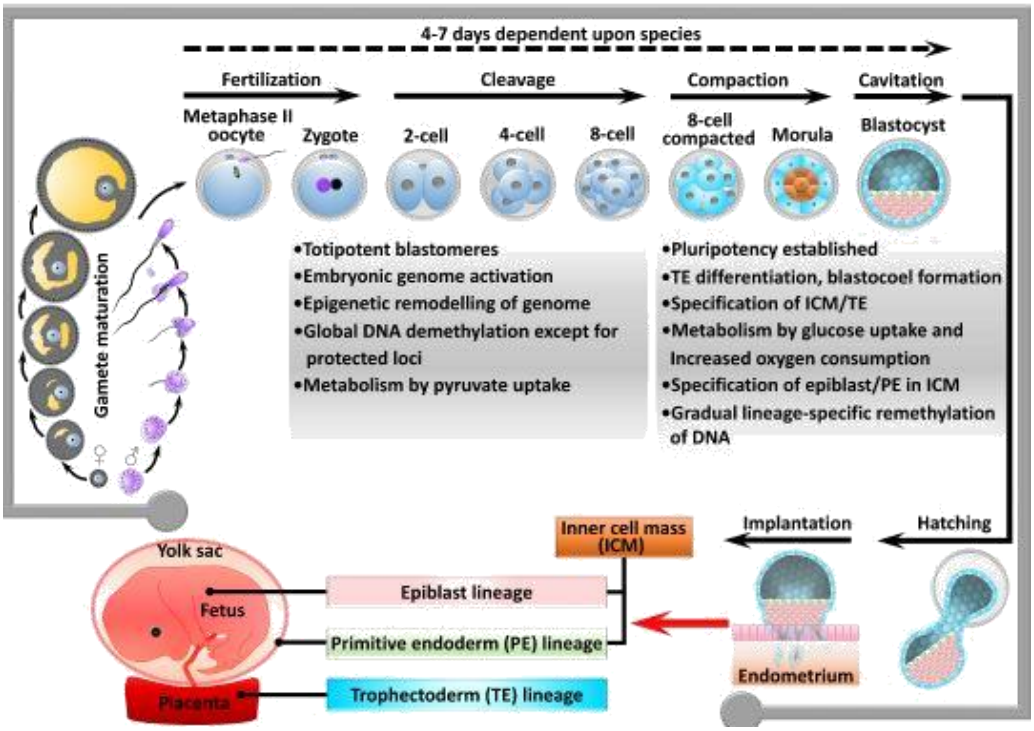

Figure 1.2 Periconceptional (PC) period and developmental stages of an embryo.

(Fleming et al., 2018)

The ICM is responsible for giving rise to all types of fetal tissues and a proportion of extraembryonic membrane (yolk sac and allantois). Prior to hatching of the zona pellucida, the ICM cells specialize to form the epiblast (Epi) and primitive endoderm (PE). The Epi continues to differentiate to form the three fetal germ layers: ectoderm, mesoderm and definitive endoderm (DE); while the PE forms the endoderm layers of the yolk sac placenta during post-implantation pregnancy (Rossant and Cross, 2001). The programming of preimplantation development is therefore, governed by the formation of the TE and the specification of the distinct cell lineages (i.e. Epi and PE) (Duranthon et al., 2008). This stage also involves the activation of the embryonic genome and ultimately the attachment of the embryo to the uterine wall (Watson, 1992). Embryonic genome activation (EGA) is initiated early during pre-implantation development, from around Day 2 in the mouse (Latham, 2001). Transcriptomic analyses suggest the initiation of a

highly regulated gene expression programme as soon as embryonic genome expression begins (Hamatani et. al., 2004; Wang et al., 2004; Zeng et al., 2004).

1.2.1 Neural induction during embryonic development

Neural induction in vertebrate embryos is mediated by coordinated FGF (fibroblast growth factor) and WNT (wingless/ integrated) signalling along with the inhibition of BMP activity (Muñoz-Sanjuán and Brivanlou, 2002). Together, these events contribute to the development of neuroectoderm primordium, which eventually gives rise to the nervous system. In mouse embryos, the initial neuroepithelial progenitors (NPs) express pan neural genes such as *Sox1* and *Sox2* (Wood and Episkopou, 1999). As the primary NPs continue to develop, some mature into neurons and contribute to the neural tube during neurulation, initiated by a signalling switch that controls differentiation whereby FGF is replaced by retinoid signalling (Corral and Storey, 2004). During neurulation, the embryonic tube consists of a layer of neuroepithelial cells with apico-basal polarity that is delineated by apical protein complexes such as the PAR polarity complex and junctional proteins like N-cadherin and β-catenin (Afonso and Henrique, 2006). The timing and production of proliferating NPs and maturing neurons (or glial cells) is further controlled by the cross talk between Delta/Jagged ligands and Notch receptors (Ohtsuka et al., 1999). Such assembly of the neural tube is unique to the embryonic developmental phase.

Even though mouse models serve powerful tools to study mammalian neural tube closure thereby providing deeper insight into neural tube defects, *in utero* development restricts embryo manipulation in a controlled manner. Gray and Ross, (2011) illustrated that embryos cultured *in vitro* in enriched media developed similar neural tube closure patterns as observed *in vivo*, i.e. from neural plate formation (between E7 - E7.5) to the conclusion of cranial fold and caudal neuropore closure (between E9.5 - E10) (Winter, 1993). In vitro neurulation isolates maternal environment and its effect on embryonic and fetal development. However, the complex developmental mechanisms and limited number of cells available at distinct embryonic developmental stages limits the scope of such research. Differentiation potential of mouse embryonic stem cells (mESCs) therefore, represents a valuable cellular system to circumvent such limitations and enhance the sphere of developmental biology studies (discussed in detail in Section 1.6.2).

1.2.2 Preimplantation period and undernutrition

Changes induced within the three progenitor cell lineages (TE, Epi and PE) may have severe effects on the development of the fetus (and/or offspring), establishing the significance of the preimplantation period for fetal and adult health. Previous work at Southampton supports this

hypothesis, where the effect of maternal LPD fed to rodents exclusively during the preimplantation (embryonic) period (denoted as Emb-LPD; 9% casein) compared with isocaloric normal protein diet (NPD; 18% casein), was investigated (Kwong et al., 2000).

The Emb-LPD led to reduced birthweight, postnatal growth rate, hypertension and altered organ/body-weight ratio in rat offspring up to 12 weeks of age (Kwong et al., 2000). Preimplantation embryos collected from LPD-exposed dams displayed significantly reduced cell numbers in both ICM and TE lineages in blastocysts. By the fourth day of development, maternal serum contained significantly reduced insulin and essential amino acids, and increased glucose levels (Kwong et al., 2000). In subsequent LPD model studies, E3.5 LPD-exposed mouse blastocysts also developed abnormal postnatal phenotypes associated with increased weight from birth, sustained hypertension and anxiety-related behaviour (Watkins et al., 2008).

These data provide key insights into changes in the maternal uterine environment and preimplantation embryo that lead to long-term programming of postnatal growth and physiology of offspring. As described above, embryos at this stage are highly sensitive to their environment and may develop irreversible damage depending upon the severity of the change. Data emanating from Emb-LPD studies in mice point to a deficiency in branched chain amino acids (BCAA) and insulin within the local environment which further leads to reduced signalling through the mammalian target of rapamycin (mTOR) pathway (which is responsible for regulating growth within blastocysts) (Eckert et al., 2012a). This altered embryo environment has an impact on the normal development of TE and PE, thereby affecting gastrulation and future growth of the blastocyst. The embryo senses the decrease in protein levels as harmful for its survival, and initiates compensatory cellular responses in order to protect the conceptus. These responses include events to extract more nutrients from the mother, facilitated by enhanced motility and invasiveness of TE cells (forming trophoblast outgrowths) (Eckert et al., 2012a).

1.3 Pre-natal adversity and neurodevelopment

Birth cohorts obtained from the aforementioned famine-struck cities showed increased cases of infant mortality and offspring with low birth weight. Babies conceived at the peak of the famine also had elevated nervous system-related congenital abnormalities such as spina bifida, hydrocephalus, and cerebral palsy (Stein and Susser, 1975). This was one of the first epidemiological studies to link prenatal nutrition and neural tube defects which led to further research, and the supplementation of folate to pregnant mothers to reduce the occurrence of these defects in the offspring (Czeizel and Dudás, 1993). While spina bifida was more prevalent in males, females showed increased cases of epilepsy, cerebral palsy, and spastic diplegia, displaying a sex-dependent

effect of prenatal malnutrition. Gender bias was also observed in neuropsychiatric or behavioural disorders such as affective psychoses and neurotic depression which dominantly affected men (Brown et al., 1995b), while both men and women were diagnosed with schizophrenia (Susser et al., 1996).

The Dutch Hunger Winter records have been very instrumental in providing data to diagnose latent effects of prenatal malnutrition. This is especially beneficial to study age-related neurological disorders in an ecological setting. Decades later the data of babies conceived at the peak of the famine was compared with their adult health records. Many studies evaluated the relationship between offspring born with congenital neural defects and who had also developed other neurodevelopmental disorders in their mid- or late adult life. Amongst all the psychiatric anomalies detected, schizophrenia was the most salient neurodevelopmental disorder in the birth cohort exposed to the height of famine in the winter of 1944-1945 (Brown et al., 1995b).

The psychiatric data obtained from the Dutch Hunger study indicated the prevalence of schizophrenia conceived at the height of the famine (Susser et al., 1997; Van, 1997). Although diagnosed in late adult life, schizophrenia displayed early manifestations, possibly due to environment-genetic interactions leading to disordered fetal brain development, thus classifying it as a neurodevelopmental disorder. Apart from food restriction, *in utero* exposures to viral infections, stress, hypoxia and other complications have also been linked with increased risks of this disorder (Khashan et al., 2008). Schizophrenia is therefore a quintessential condition to study the impact of early life quality on mental disorders.

The Dutch Winter Study also highlighted the critical effect of time of gestation. While- predominant cases of schizophrenia were recorded in babies exposed to famine in the periconceptional period (Susser and Lin, 1992), those exposed in the second and third trimester suffered from affective disorders (Brown et al., 1995a). One drawback of this study, however, was the lack of nutrient information in the total calorie intake of pregnant women, along with other confounding factors (such as stress, anxiety etc.), thus raising many important questions pertaining to the role of nutrient deficiency in such disorders.

Offspring from LPD-fed dams have been associated with neurological disorders and behavioural abnormalities (Watkins et al., 2008) often displayed in open-field activities for locomotion and hyperactivity or anxiety depicting assays (Crossland et al., 2017). Similar data indicating a two-fold increase in the risk of developing mental health conditions, such as schizophrenia, had also been observed in adults who were exposed to the aforementioned Chinese famine (Xu et al., 2009) and Dutch winter famine (Susser et al., 1996); the latter during early gestation.

In rodents, protein deficiency affects the neuroanatomy of the developing brain. It affects thickness of visual cortex, parietal neocortex (Diaz-Cintra et al., 1990), and causes gender-dependent disruption of cerebellar development (Hillman and Chen, 1981; Ranade et al., 2012), thereby affecting overall brain size. Protein malnutrition has also been observed to reduce dendritic arborisation (the process by which dendritic cells branch out to make new synapses) (Angulo-Colmenares et al., 1979), number of neurons in the CA1 region of the hippocampus, and cellular maturation (Lister et al., 2005). Such changes in brain organisation and anatomy, including reduced connectivity and number of neurons, further influence adult behaviour and brain function.

Perinatal LPD has been associated with changes in neurotransmitters and oxidative status in the brain. Apart from being building blocks for proteins, certain amino acids are precursors of many neurotransmitters or are neurotransmitters in their own right, though protein deficiency may not always correlate with effects on neurotransmitters. As observed in the glutamatergic system, protein restriction in rats caused an increased density of hippocampal kainate receptors, but did not affect NMDA (*N*-methyl-D-aspartate) and AMPA (α-amino-3-hydroxyl-5-methyl-4-isoxazole-propionate) receptors (Fiacco et al., 2003). Other studies also suggest a decreased vesicular glutamate uptake during gestational dietary restriction (Rotta et al., 2008), indicating a deregulation of glutamate signalling through kainate receptors on the exposure of gestational and lactation LPD. These effects have further been associated with a reduction in length, number and complexity of dendrites in the cortex and CA3 regions (Noback and Eisenman, 1981; Alamy and Bengelloun, 2012). Similar differential changes are observed in GABAnergic neurons (Díaz-Cintra et al., 2007), and the mRNA expression of GABA receptor subunits (Steiger et al., 2003), by protein malnutrition during gestation and lactation.

Malnutrition also reduces the serotonin (tyrosine) and noradrenaline (tryptophan) precursors (Chen et al., 1997), although serotonin level is increased in the offspring (Resnick and Morgane, 1984). Dopamine levels are also compromised in the hypothalamus and hippocampus of deprived rats (Kehoe et al., 2001). Protein restriction can influence the cellular health and integrity by interfering with the redox status of the neurons (Bonatto et al., 2005). Increased lipid peroxidation and protein oxidative damage (Feoli et al., 2006) is observed in the cortex, hippocampus and cerebellum of deprived rats during gestation and lactation.

Mice born to protein deprived dams show reduced juvenile play and increased non-social rearing (Almeida et al., 1996). Such behaviours are considered essential in preparation for adult life, the disruption of which could impact physical growth, neurological reflexes and evoke neuropsychiatric behaviours of depression and anxiety (Belluscio et al., 2014). In rodents, malnutrition induced changes in the structure and neurochemistry of hippocampus, affect their memory and cognitive

ability (Tonkiss et. al., 1990), while early damage of cerebellum and brain function, causes motor coordination impairment (Ranade et al., 2012). Although malnutrition during gestation and lactation period showed increased risks of anxiety-like behaviour in pups (Belluscio et al., 2014) and juveniles, postnatal deprivation reduced such risks in adult rats (Reyes-Castro et al., 2012). Nutritionally challenged (during gestation and lactation) mice also show increased incidents of depression-behaviour (Belluscio et al., 2014), as compared to the controls indicating the importance of period of protein deprivation and duration of deprived diet, and the susceptibility of developing disorders.

1.4 Advanced Maternal Age (AMA)

The proportion of births in women aged 35 and above has been steadily rising in recent years around the globe (Martin et al., 2017). According to the U.K. and Wales office for National Statistics, from the mid 1970's until 2016, there has been a continuous long-term rise in total fertility rates (defined as number of children born per woman) for women aged 30 and over (Office for National Statistics, 2016). Similarly, fertility rates for women aged 35 to 39; and 40 and over, have trebled since 1980 and 1990 respectively, and are at their highest since 1938. Simultaneously, there has been a steep decline in fertility rates for women under 20 years of age. As of 2016, the largest percentage 'increase' in fertility rates was observed for women aged 40 and over (4.6%); whereas those under age 20 had the largest percentage 'decrease' in fertility rates (5.5%). Overall, since 2004, the age group with highest fertility has shifted from 25-29 to 30-34 (Office for National Statistics, 2016). A similar trend in fertility rates having declined under 20, and increased for 35- 45, including a further increase in 45 – 49, and 50 and over, has been observed in the United States (Martin et al., 2015).

1.4.1 AMA and pregnancy associated-risk factors

It is known that older women (>35 years) have a much greater tendency to develop medical disorders such as hypertension and diabetes mellitus than younger women (Hansen, 1986). They also experience increased abnormal labour patterns such as preterm delivery (Aldous and Edmonson, 1993; Jacobsson et al., 2004), placenta previa and abruptio placenta, often causing late pregnancy bleeding, leading to caesarean section as the preferred method of delivery (Williams and Mittendorf, 1993). Advanced maternal age is associated with increased pregnancy complications including gestational diabetes (Biro et al., 2012), pregnancy-induced hypertension and pre- eclampsia (Delbaere et al., 2007; Carolan, 2013), increasing the incidence of spontaneous abortion and stillbirth in older women (Hansen, 1986).

These risks are further accentuated in older multiparous women (Russell et al., 2003). Parity in older women may also increase their likelihood to have twin or multiple births (Russell et al., 2003; Biro et al., 2012). Older women (aged 30-34, 35-39, and 40-44 years) experienced an increase in multiple births of 62%, 81%, and 110% respectively (Russell et al., 2003). The risk of multiple births in AMA women also increases with ART treatment, where high order pregnancy is regarded as the most important predictor of adverse maternal, obstetrical and perinatal outcomes (Okun et al., 2014). Additionally, women >35 years have increased incidents of breech presentation, postpartum haemorrhage, pre-term birth (birth <32 weeks) (Jolly et al., 2000), post-term pregnancy (birth >42 weeks) (Roos et al., 2010) and severe maternal morbidity (Huang et al., 2008; Knight et al., 2009). These complications increase their probability of having medical interventions (Lialios et al., 1999; Bayrampour and Heaman, 2010). Under extreme circumstances, these risks also contribute to maternal mortality (McCall et al., 2016).

Pregnancy in older women is often associated with confounding factors like underlying pre-existing medical disorders such as diabetes mellitus and hypertension; or parity, which must be taken into account when the risks associated with AMA are quantified (Hansen, 1986; Chan and Lao, 1999; Chan and Lao, 2008). Though older women with pre-existing conditions display increased pregnancy-related risks (Balasch and Gratacós, 2012), other studies have shown a linear increase in risks with advancing age, even in healthy women with no diagnosed medical condition (Carolan and Frankowska, 2011).

1.4.2 AMA, natural conception and perinatal outcomes

Natural conception in AMA women is associated with adverse neonatal and perinatal outcomes compared to that in younger women. Depending on parity, AMA women can have a significantly increased incidence of small (SGA) or large (LGA) for gestational age babies and preterm births (PTBs) (Schimmel et al., 2015; Joseph et al., 2005). AMA can further contribute to adverse outcomes such as antepartum still-birth (Huang et al., 2008); intrapartum-related perinatal death (Pasupathy et al., 2011) and early neonatal death (Gilbert et al., 1999; Joseph et al., 2005; Jacobsson et al., 2004). Several studies highlight the effect of parity in determining maternal as well as neonatal outcomes (Chan and Lao, 2008). When births from older nulliparous women were compared with younger nulliparous counterparts, significantly increased incidence of birth asphyxia, fetal growth restriction and mal-presentation were observed in the older women; similar to the older and younger multiparous group (Gilbert et al., 1999). While older nulliparous women had significantly lower mean birth weight as compared to the younger nulliparous women, no differences were observed in the multiparous groups. Similarly, AMA was independently associated with birth and

spontaneous PTB (<37 weeks); LBW in neonates of older nulliparous women; and PTB in older multiparous women (Chan and Lao, 2008).

AMA is also postulated as an independent risk factor for intrauterine growth restriction (IUGR) (Odibo et al., 2006) and low birth weight (LBW) (Lee et al., 1988; Aldous and Edmonson, 1993; Jolly et al., 2000; Goisis et al., 2017). IUGR is significantly associated with chronic hypertension and pre-gestational diabetes. A positive relationship was observed between increasing age, especially in >35 years, and incidence of IUGR (Odibo et al., 2006). Low-birth weight offspring are more likely to exhibit postnatal 'catch-up' growth, altered body composition and increased adiposity (Varvarigou, 2010). LBW has also been associated with respiratory, cognitive and neurological problems (Hack et al., 1995; Kelly et al., 2001). Thus, fetal growth restriction may predispose offspring to subsequent metabolic dysregulation and development of non-communicable diseases such as cardiovascular disease, type-2-diabetes mellitus, neurological disorders and obesity in adulthood (Sharma et al., 2016).

1.4.2.1 AMA and chromosomal anomalies

In humans, about 20% eggs and 9% sperm display aneuploidy (Martin, 2008). Aneuploidy levels tend to increase with the developmental age being examined. While newborns and stillborns mostly display about 0.3% and 4% of trisomy 21 and sex- chromosome trisomies respectively; clinically recognised abortions and early missed abortions show much higher, i.e. about 35% and 70% of trisomic or monosomic aneuploidy levels respectively (Hassold et al., 1996; Ferro et al., 2003; Philipp et al., 2003).

Spontaneous conception in AMA women imposes additional risks of accumulated damage and mutations in the older oocytes, leading to chromosomal anomalies in the fetus and offspring (Chiang et al., 2012). About 3% of AMA-offspring are born with birth defects out of which about 20% are due to chromosomal or genetic mutations. Abnormalities such as trisomy 13, 18 and 21, and sex-chromosome anomalies increase exponentially with maternal age from 30 years and over, increasing dramatically in women aged > 45 years (Hansen, 1986; Kim et al., 2013). As 10 % of AMA pregnancies result in miscarriage, this may explain the extent of damage induced in older oocytes and embryos.

Although some chromosomal/genetic defects inhibit successful pregnancies and result in miscarriage and stillbirths, others like trisomy 21 (Down's syndrome), are compatible of development into adulthood. With the identification of DNA polymorphisms, it has been possible to classify trisomy 21 to parental origin and stage of the chromosomal error (meiosis I [MI], meiosis II [MII], or postzygotic mitotic) (P. W. Yoon et al., 1996). When blood samples of infants with trisomy

21 and controls were analysed, the distribution was 86% maternal (75% MI and 25% MII), 9% paternal (50% MI and 50% MII) and 5% mitotic. As compared to younger mothers (<25 years), the older mothers (> 40 years) displayed an odds ratio of 5.2 for maternal MI (MMI) errors and 51.4 for maternal MII (MMII) errors., showing a strong association between AMA, and MI and MII errors. It follows that the incidence of Down syndrome pregnancies in AMA mothers has doubled from about 25% in the 1980s to 50% in 2002 (Resta, 2005).

1.4.2.2 AMA and positive perinatal outcomes

In contrast to the studies cited above, some studies report little or no adverse outcomes associated with pregnancy in older women. For example, Barkan and Bracken (1987) reported no evidence of risk of AMA on LBW, preterm delivery, mean birth weight and gestational age in older women. Similarly, Kirz et al. (1985) did not observe any significant differences relating to pregnancy complications, delivery and neonatal outcome in the old (>35 years) vs young (20-25 years) women. Other studies even reported positive effects of AMA. Sutcliffe et al. (2012) found that children born to older mothers had fewer unintentional injuries, increased immunisation schedule by 9 months of age, and improved language development. Similarly, Tearne (2015) reported better behavioural and cognitive outcomes in children born to older mothers. AMA-conceived children were also taller, fitter, displayed less abdominal adiposity and plasma concentration of IGF-2 (Savage et al., 2013). Similarly, fasting glucose levels and cholesterol in adult male offspring were observed to be reduced with increasing maternal age (≥35 years) (Charlotte et al., 2016; Verroken et al., 2017). These findings are more indicative of better socioeconomic status, experience and healthier lifestyle awareness (breastfeeding, nutrition, benefits of exercise etc.) of AMA women, rather than beneficial effects of biological mechanisms induced by reproductive/ chronological ageing (Tearne, 2015).

1.4.2.3 AMA and factors associated with reduced fertility

Reproductive ageing is characterised by the progressive decline in both quantity and quality of oocytes, that further decrease the fertility and fecundity with advancing age (Te Velde and Pearson, 2002). Female fertility is influenced by chronological age, where age-related factors further depreciate or damage the ovarian pool of follicle-enclosed oocytes. Chronological ageing induces changes in several biological processes such as oxidative damage, genomic instability, ribosomal damage, mitochondrial DNA damage, shortening of telomeres, changes in genetic programming, cell apoptosis or senescence leading to cell death and systemic control of ageing (Johnson et al., 1999). While chronological age is determined by the passage of time since birth, 'biological ageing' depends on several additional physiological factors.

1.4.2.3.1 Ovarian reserve, oocyte quality and endometrial receptivity

Physiological factors such as ovarian reserve of follicles and response to stimulation are the most important markers of 'biological age' of an ovary (De Carvalho et al., 2008; Broekmans et al., 2009). Other markers of ovarian ageing and premature ovarian failure, and transition to menopause, include- serum levels of Anti Mullerian Hormone (AMH), inhibin B, oestradiol and follicle stimulating hormone (FSH) (Visser et al., 2006; De Carvalho et al., 2008; Soto et al., 2009; Knauff et al., 2009). In humans, increasing maternal age causes decrease in antral-follicle count (AFC) and serum levels of AMH; whereas FSH levels rise as maternal age progresses (Wiweko et al., 2013). Thus in most ART assessments, AMH and AFC are regarded better markers to determine accurate ovarian follicular status than other hormonal markers (Fanchin et al., 2003). Although chronological ageing is an important factor in infertility, reproductive ageing differs greatly among individuals, depending upon their genetics, environmental factors and lifestyle (Carlo et al., 2009).

Additionally, older women display reduced structural and functional quality of cytoplasmic organelles, especially mitochondria of both oocytes and surrounding granulosa cells (Ford, 2013). Age-related differences have also been reported for ATP content (embryos > zygotes > oocytes) (Zhao and Li, 2012) and structure of human oocytes (de Bruin et al., 2004).

Maternal ageing (≥ 45 years) greatly reduces the incidence of successful pregnancies and deliveries (Ron-El et al., 2000). Apart from decreased ovarian reserve, endometrial receptivity also reduces with advanced reproductive age and causes higher rates of implantation failure (Yaron et al., 1993). Endometrial biopsies of older women show high incidence of delayed or absent secretary maturation (Yaron et al., 1993).

1.4.3 AMA: Animal models of reproductive ageing

Animal models present opportunities to understand the mechanistic basis of maternal reproductive ageing whilst circumventing confounding factors such as ethnicity, general lifestyle and paternal age, which can separately or interactively induce adverse effects on the health outcome of offspring (Kovac et al., 2013).

Delayed motherhood or AMA in mice has been associated with adverse post-natal development of the offspring. Tarín et al. (2005) analysed the long-term effects of AMA on reproductive fitness and longevity of offspring. First generation (F1) young (10 weeks old) or old (51 weeks old) females were mated with 12- to 14-weeks old males. AMA in F1 generation promoted higher pup mortality in the first 3 days of birth; reduced body weight (during pre-weaning period); induced behavioural alterations (at 24-37 weeks of postnatal age); and reduced overall lifespan of F2 offspring.

Similarly, AMA (30 weeks) led to behaviour alterations, increased anxiety, reduced nest-building skills and sociability in female offspring (Lerch et al., 2015). A recent study analysed genome-wide mRNA expression in the hippocampi of 4-month-old male offspring (conceived by 15-18 month females with embryos transferred to 3-month old females) (Sampino et al., 2017). These offspring displayed increased anxiety and ultrasound vocalisation activity when separated from their foster mother, compared to offspring of young control females (2-month old). This was related to altered hippocampal gene expression. Comparable effects have been observed in humans, where embryos from older women were transferred to younger surrogates (Tearne et al., 2016). Collectively, these findings indicate programming of neurological development and subsequent offspring behaviour from the earliest stages of embryonic development.

Due to increased resorption rates, litter size and birth weights are reduced in mouse AMA-pregnancies (Harman and Talbert, 1970). Older dams also display increased infanticide (Mohan, 1974), which is not observed when pups are fostered to younger dams (Sampino et al., 2017), further suggesting age-related changes in maternal behaviour-related hormones (Mann et al., 1983).

AMA in mice also induces long-term effects on metabolic and cardiovascular function of offspring (Velazquez et al., 2016). Similar to the study design described above, blastocysts (E3.5) from old (34–39 weeks) and young (8–9 weeks) C57BL/6 females (naturally mated with young CBA males (13–15 weeks)), were immediately transferred (ET, embryo transfer) to young (MF1, 8–9 weeks) surrogates, hence representing an experimental ART model of AMA. Pregnancy rates were reduced in AMA dams. Sex-dependent postnatal differences were observed in offspring derived from embryos of young and old dams. Whilst 'old-ET' female offspring were heavier and less glucose tolerant compared to their young counterparts, no differences were observed in male offspring between the two treatment groups. However, hypertension appeared to be more persistent in 'Old-ET' male than female offspring, relative to their 'young-ET' counterparts. Once again, these effects appear to originate from events occurring in the pre-implantation embryo. Similar effects of periconceptional programming on altered post-natal behaviour have also been observed in the embryo transfer studies of Watkins et al. (2007), Rexhaj et al. (2013) and Lopez-Cardona et al. (2015).

1.5 Assisted reproductive Technologies (ART)

Since the birth of the first IVF baby in 1978, more than 6.5 million babies (WHO, 2013) have been born through ART worldwide and this number is expected to rise to as high as 10 million by 2020. Despite major technological advances achieved in ART over the last four decades, there is

increasing evidence that ART conceived children may be at greater risk of perinatal complications and NCDs than naturally conceived children (Barnhart, 2013; Hyrapetian et al., 2014). These include a higher incidence of PTB and LBW (Schieve et al., 2002; Declercq et al., 2015; Luke et al., 2017), and congenital abnormalities such as cardiac septal, neural tube defects and esophageal atresia (DeBaun et al., 2003; McDonald et al., 2009; Källén et al., 2010a; Källén et al., 2010b). Furthermore, IVF-children show increased instances of advancement of bone age and potentially subclinical thyroid disorders (Ceelen et al., 2008b; Hart and Norman, 2013). Compared to fertile women, sub-fertile and IVF-treated women tend to be older, often with pre-existing chronic conditions or underlying pathologies that further increase risks of developing complications during pregnancy (Vulliemoz et al., 2012). Thus, ART may induce adverse effects in the developmental programme of the embryo and thereby contribute to the DOHaD hypothesis (Wang and Sauer, 2006).

1.5.1 ART and DOHaD

Human cohort data highlight that IVF children and adolescents suffer from greater risks of increased blood pressure and glucose intolerance (Ceelen et al., 2008a; Valenzuela-Alcaraz et al., 2013; Guo et al., 2017), systemic and pulmonary vascular dysfunction (Scherrer et al., 2012), and cardiovascular remodelling in utero (Valenzuela-Alcaraz et al., 2013), making ART an important cardiovascular risk factor. Several studies have also demonstrated an association of ART with increased incidents of genetic disorders such as Angelman syndrome (AS) (Ludwig et al., 2005; Sutcliffe et al., 2006) and Beckwith-Wiedmann syndrome (BWS) (DeBaun et al., 2003), with cohorts showing 4% of BWS cases from ART conceptions, compared to 1.2% in general population (E. Maher et al., 2003). IVF children have also been associated with perinatal morbidity (Kalra and Molinaro, 2008) and increased risks of chromosomal anomalies, the incidents of which further increase with ICSI (intracytoplasmic sperm injection; Mukhopadhaya and Arulkumaran, 2007).

In addition, ART has been associated with changes in DNA methylation, leading to an increased likelihood of rare genetic disorders (Chiba et al., 2013; Uyar and Seli, 2014; Lazaraviciute et al., 2014). Epigenetic alterations to embryonic DNA during the periconceptional period may induce short or long-term effects in the development of offspring. For instance, though BWS is characterized by genetic heterogeneity, more than 90% of BWS cases are caused by defects in genomic imprinting (Pinborg et al., 2016; Niemitz and Feinberg, 2004). Epigenetic aberrations may also be associated with different aspects of ART (e.g. *in vitro* culture, duration or media used) or manifest in genes due to infertility (Khosla et al., 2001; Calle et al., 2012; Ventura et al., 2015). In some species, these effects may even be inherited over many generations through changes in

the structure of chromatin and lead to transgenerational defects (Seong et al., 2012). However, it should be noted that due to ethical reasons, most human embryo data is derived from poor-quality (discarded) embryos. Without proper comparison with naturally conceived, healthy embryos, the alterations in ART embryos remain to be confirmed. Hence, it is necessary to study the potential of different ART treatments that prompt changes in the early environment of the embryo and the critical processes that affect fetal growth.

1.5.2 Factors influencing ART outcomes

Although the vast majority of children conceived using ART techniques are apparently normal (Beydoun et al., 2010), concerns regarding safe use of ART for the treatment of infertility have been voiced for several years (Caperton et al., 2007). Procedures such as ovarian stimulation, in vitro maturation, or both are used in conjunction with extended periods of embryo culture, and have become increasingly common in human ART (Langley et al., 2001). Their direct and independent effects, however, are difficult to ascertain as inevitably they are confounded by factors such as parental age and underlying fertility disorders. With these considerations in mind, each of these aspects will briefly be considered in greater detail.

1.5.2.1 Advanced maternal age (AMA)

With the advent of ART, sub-fertile, infertile and older women (often past their menopausal age) have increased possibility of becoming pregnant. Moreover with increasing technological advances and simultaneous cultural shift (improvement in social, economic and educational status of women), more and more women are now delaying childbirth. However, the growing evidence of increased risks of maternal age on adverse pregnancy and offspring outcomes have raised ethical concerns regarding the age-limit of women undergoing such artificial procedures (Benshushan and Schenker, 1993; Paulson et al., 2002). Sauer et al. (1993) reported the rescue of age-related decline in female fertility by using eggs from younger women, and that oocyte donation from younger women resulted in comparable pregnancy outcomes following ET to both older (>50 years) and younger (<25 years) surrogates. Similarly, Paulson et al., (2002) performed a retrospective study comparing women >38 years of age undergoing IVF with donor oocytes across different IVF clinics. He reported that the AMA women did not display any maternal or neonatal complications, except for a very few cases of mild preeclampsia (25%), severe preeclampsia (10%) and gestational diabetes (17.5%). His team concluded that women aged 50 years or older could have successful pregnancies with oocytes donated from younger women, and experience similar pregnancy rates without complications. This study confirmed findings from his previous study, where oocyte donation was extended to women over 40 years of age (Sauer et al., 1990). From these and other

studies (Sauer et al., 1992; Pantos et al., 1993; Antinori et al., 1995; Paulson et al., 1997; Cohen et al., 1999; Wang et al., 2012), one can conclude that oocyte 'donor age' is a major determinant of success in ART, and is more important than age of the recipient woman in determining pregnancy success.

In other studies, however, AMA in otherwise medically fit subjects, led to complications during pregnancy which can be harmful to both the mother and baby. In two separate studies (Wennberg et al., 2016; Moaddab et al., 2017) the incidence of adverse maternal outcomes such as hypertension during pregnancy (HDP), gestational diabetes, placental abruption, placenta previa and caesarean delivery increased with maternal age and was greater following ART than with natural conception. Furthermore, in the study of Wennberg et al. (2016), the incidence of adverse neonatal outcomes such as PTB, LBW and perinatal mortality was increased in ART than natural cycles.

1.5.2.2 Other procedures used in assisted reproduction (human studies)

In addition to advanced reproductive ageing, factors such as ovarian stimulation, IVF and ICSI, embryo cryopreservation and transfers also influence ART outcomes. Similar to IVF, ovarian stimulation with gonadotrophins has been associated with increased risks of inducing multiple pregnancies (Ombelet et al., 2006), LBWs (Källén et. al., 2005; Wang et al., 2005) and aneuploidy in pre-implantation human embryos (Baart et al., 2007; Verberg et al., 2009). Separate studies indicate that transfer of frozen embryos influences pregnancy outcomes in terms of PTB, incidence of large (LGA) and small (SGA) for gestational age babies, together with the prevalence of congenital abnormalities (Pandey et al., 2012; Spijkers et al., 2017; Alviggi et al., 2018). LGA babies are further prone to neonatal complications leading to non-insulin-dependent diabetes mellitus, hypertension, and hyperlipidemia (Das and Sysyn, 2004); show slower growth in early infancy (Chiavaroli et al., 2015), and have increased insulin resistance and inflammation in adolescence (Stansfield et al., 2016). In order to increase the success rate of ART, most laboratories prefer multiple to single embryo transfer. Multiple pregnancies, which occur in 1 in 10 from IVF compared to 1 in 80 from natural births (Schachter et al., 2001), are linked to the occurrence of PTB and increased morbidity in offspring. Furthermore, 10-20% of twin gestational sacs undergo spontaneous reduction and lead to singleton pregnancies (Pinborg et. al., 2006) and the singletons born, show significantly increased risks of very low birthweight, PTB, cerebral palsy, ante partum haemorrhage, premature delivery and growth restriction. Given the strong association of LBW and PTB with adult-onset diseases like CHDs, hypertension, type-2 diabetes and neurological disorders (Fleming et al., 2004; Laas et al., 2012), the aforementioned ART-associated factors may, therefore, further develop adverse health outcomes in later life.

1.5.3 Animal models of assisted reproduction

Maternal environment and reproductive technologies can alter the epigenetic status of oocytes and early embryos thereby influencing post-natal health of offspring (Uyar and Seli, 2014; Markunas et al., 2016; Banik et al., 2017). Adverse effects of ART have also been observed in large animals (Young, 1998; Barry et al., 2008). 'Environmental epigenomics' is the interaction between endogenous (hormones/immune status) and exogenous (maternal diet or ART) factors and the epigenome. Genomic imprinting during early embryogenesis, which is characterised by monoallelic gene expression and X-chromosome inactivation, is a critical event (Reamon-Buettner and Borlak, 2007), dysregulation of which induces disorders such as autism, Angelman (AS) and Beckwith-Wiederman Syndromes (BWS), and certain cancers (Sandhu, 2010). In mammals, epigenetic modifications are established during the earliest stages of mammalian development (prior to and following conception) and maintained throughout life although there may be modifications in organs after birth. Animal models lend themselves to the temporal study of mechanisms such as these.

1.5.3.1 Advanced maternal age (AMA)

Following on from the observations reported under Section 1.4.3., maternal ageing increases damage to reproductive and other biological systems with a simultaneous decrease in adaptability and energy utilisation of the body. While genetic factors are necessary for survival (and healthy ageing), they account for only 20-30% of variation throughout lifespan (Herskind et al., 1996; Mitchell et al., 2001). Thus, variations in stochastic events, environmental and non-genetic factors or 'environmental epigenomics', play a vital role in determining ageing phenotype in mammals (Wilson and Jones, 1983; Lipman and Tiedje, 2006; McCauley and Dang, 2014).

Advance maternal ageing (AMA) may induce dysregulation of DNA methylation and alter expression of imprinted genes in oocytes. In mice, maternal age has been associated with the alteration of gene expression patterns in metaphase II oocytes (Toshio Hamatani et al., 2004). These altered genes were found to be involved in mitochondrial function, oxidative stress, chromatin structure, DNA methylation, genome stability and RNA helicases. Similarly, Yue et al., (2012) reported decreased expression of DNMTs (Dnmt1, Dnmt3a, Dnmt3b and Dnmt3L) in MII oocytes, together with changes in genome-wide DNA methylation in oocytes and pre-implantation embryos, which were associated with reduced reproductive potential of AMA mice.

Paczkowski et al., (2015) analysed epigenetic changes in fetal, placental and ovarian tissue collected from 16.5 day of pregnancy from AMA (15 months) and control young (4-5 weeks) mice. Maternal age was associated with fetal growth restriction, placental overgrowth, dysregulation of

methylation in fetal tissue and aberrant DNA methylation patterns in placental tissue with abundant transcripts of imprinted genes. AMA also dysregulated ovarian methylation, and ovarian and uterine gene expression, including nutrient transport genes. Although, gene expression was not altered as much in oocytes (as shown in other studies (Hamatani et al., 2004)), significant changes in *Kcnq1* transcript expression were observed (Paczkowski et al., 2015). *Kcnq1* is a tissue specific imprinted gene located in chromosome 11, and is associated with Beckwith-Wiedemann Syndrome (BWS) (NCBI gene report 3784). Advanced maternal age-induced changes in oocyte competence, gene expression and maternal fertility have also been observed in other studies (Armstrong, 2001; Guglielmino et al., 2011; Liu et al., 2011).

In contrast, some studies have not reported any age-related differences in methylation patterns of the differentially methylated regions of imprinted genes- *Snrpn, Kcnq1ot1, U2af1-rs1, Peg1, Igf2r* and *H19* (Lopes et al., 2009). However, AMA dams displayed increase in resorption sites, morphological abnormalities (including abnormal placental morphology) and developmentally delayed oocytes. This suggested that although AMA affects post-implantation embryo and placental development, embryos that do develop to mid-gestation continue to undergo normal acquisition of DNA methylation.

Thus, maternal ageing has been shown to induce adverse effects on the methylation and gene expression of reproductive tissues, follicular changes in the ovary, oocytes, embryos and reduced implantation capacity of the uterus, thus affecting overall fertility of AMA mothers. Such adverse changes in epigenetic modifications may partly explain the increased incidence of hypertension, obesity and other non-communicable diseases in adulthood offspring born from advance aged mothers (Velazquez et. al., 2016).

1.5.3.2 Other procedures used in assisted reproduction (animal models)

Many studies have reported an association between ART especially ovarian stimulation, imprinted disorders such as AS and BWS, and potential risks of health and development in offspring (Maheret al., 2003; J.R. and C.J., 2005; Chang et al., 2005; Ludwig et al., 2005; Uyar and Seli, 2014). Studies have reported that ovarian stimulation induced aberrations in oocyte pronuclei (Vogel and Spielmann, 1992), increased congression failure at first meiotic metaphase and produced aneuploid oocytes with compromised nuclear and cytoplasmic maturity (Hodges et al., 2002; Roberts et al., 2005) and DNA-lesions in early mouse embryos (Elbling and Colot, 1985). Exogenous gonadotropins have further been shown to both disrupt (Ertzeid and Storeng, 1992) and delay (Auwera and Hooghe, 2001) zygote development, reduce cell number in blastocysts (Champlin et al., 1987), thus impairing preimplantation embryo development, increasing post-implantation embryo loss, thereby reducing litter size and birth weight. During folliculogenesis, the maternal germ-line imprinting process is

vulnerable to environmental influences and epimutations (Waal and Mccarrey, 2010). Some studies also proposed that ovarian stimulated oocytes may have an incompletely programmed maternal genome, which further increase the risks of imprinting errors in oocytes, embryos and placental tissue. The association between increased AS and BWS incidence following ovarian endocrine stimulation, further suggests imprinting errors on the maternal allele, and their origin in the oocytes. This theory is supported by the findings of Shi and Haaf (2002), Sato et al. (2007) and Fauque et al. (2007), who showed a higher rate of abnormal DNA methylation in mouse oocytes and embryos derived from ovarian stimulated dams, compared to those derived from no exogenous endocrine stimulation.

Similar to effects of ovarian stimulation on embryo and offspring growth, in mice, cryopreservation of preimplantation embryos has been found to have long-term developmental consequences, increasing body weight and inducing behavioural abnormalities in offspring (Dulioust et al., 1995). Kader et al., (2009). Cryopreservation induces DNA damage and reduces survival of mouse blastocysts, where the susceptibility increases with advancing stage of blastocyst development (Massip et.al., 1984; Zander-Fox et al., 2013). Slow-controllable freezing also reduces ICM and epiblast cell viability in mouse embryos, and delays blastocyst development, hatching and implantation rate (Uechi et al., 1999; Zander-Fox et al., 2013). Furthermore, Homayoun et al. (2016) observed vitrification-induced changes in morphological (increased zona pellucida thickness) and morphometric (reduced blastomere volume) parameters of the embryos, thereby increasing the incidence of aneuploidy (Wu et al. 1999). High concentrations of cryoprotectants used in vitrification cause intense dehydration and shrinkage in embryos. For example, Dimethyl sulfoxide (DMSO), cryoprotectant used in freezing, has been shown to induce detrimental effects on cellular function (i.e. metabolism and enzymatic activity), growth (i.e. cell cycle and apoptosis) and differentiation (Santos et al., 2003). In mouse preimplantation embryos, DMSO also increased early oxidative stress responses by disrupting pro- and anti-oxidant balance, increased expression of unfolded protein-response genes (*Hspa5, Hsp90b1, Ddit3, Atf4,* and *Xbp1),* subsequently causing dose-dependent developmental arrest along with mitochondrial depolarization/dysfunction, apoptotic cell death (via JNK/ATF2 pathway), and excessively increased autophagy and mitophagy expression (Kang et al., 2017). This further led to decrease in ICM and trophectoderm cell number, and decreased implantation and developmental rates (Zhou et al., 2014; Kang et al., 2017). Gene ontology studies in mouse embryos have also revealed slow-freezing-induced altered expression of genes involved in protein metabolism, transcription, cell organization, signal transduction, intracellular transport and development (Mamo et al., 2006; Dhali et al., 2007; Larman et al., 2011). Vitrification and culture can also lead to epigenetic dysregulation. Jahangiri et al. (2014; 2018)

reported increased histone (H3) modifications in *H19* imprinted genes, significantly increased levels of *Igf2* and, contrastingly, decreased expression of *Oct4* in mouse blastocysts.

1.6 Mouse embryonic stem cells as a model system for DOHaD

Like humans, mice can develop most NCDs such as certain cancers, hypertension and diabetes, making them a desirable animal model for studies in developmental biology and DOHaD more generally (Edwards et. al., 1980; Bongso and Tan, 2005; Cockburn and Rossant, 2010). In addition, mouse embryos share many common features to human embryos (Harlow and Quinn, 1982; Edwards et al., 1981; Trounson et al., 1982). Physiological similarities in the temporal sequence of events of cleavage, compaction and blastocoel formation make the mouse a good model to study human preimplantation development. Specifically, the first three to four cleavage divisions occur within 10 h of syngamy in the mouse embryo and within 13-16 h in the human embryo. Cell cycle length thereafter is ~12 h for each species, reaching the fully expanded blastocyst stage after 84-96 h (mouse) and 108-120 h (human) (Figure 1.4). It is around this time that the three major cell lineages of the embryo and extraembryonic membranes are specified. As described in Section 1.2 (Figure 1.2), the epiblast (Epi) will give rise to the fetus, the trophectoderm (TE) will give rise to the fetal contribution to placenta, and the primitive endoderm (PE) will develop into the parietal and visceral endoderm, later forming the yolk sac (Cockburn and Rossant, 2010).

Human embryos, however, do differ in several subtle ways. For example, they differ with respect to zygote centromere inherence (Mercader et al., 2006; Biggers and Summers, 2008), gene expression patterns (Dobson et al., 2004; Hamatani et al., 2004; Bell et al., 2008), susceptibility to genetic instability (Vanneste et al., 2009) and interval to embryonic genome activation (Braude et al., 1988; Duranthon et al., 2008) relative to the mouse. Additionally, the average diameter of mouse embryos at 70 µm is about half that of human embryos, thus making the volume of the human embryo ~8-fold larger than the mouse embryo.

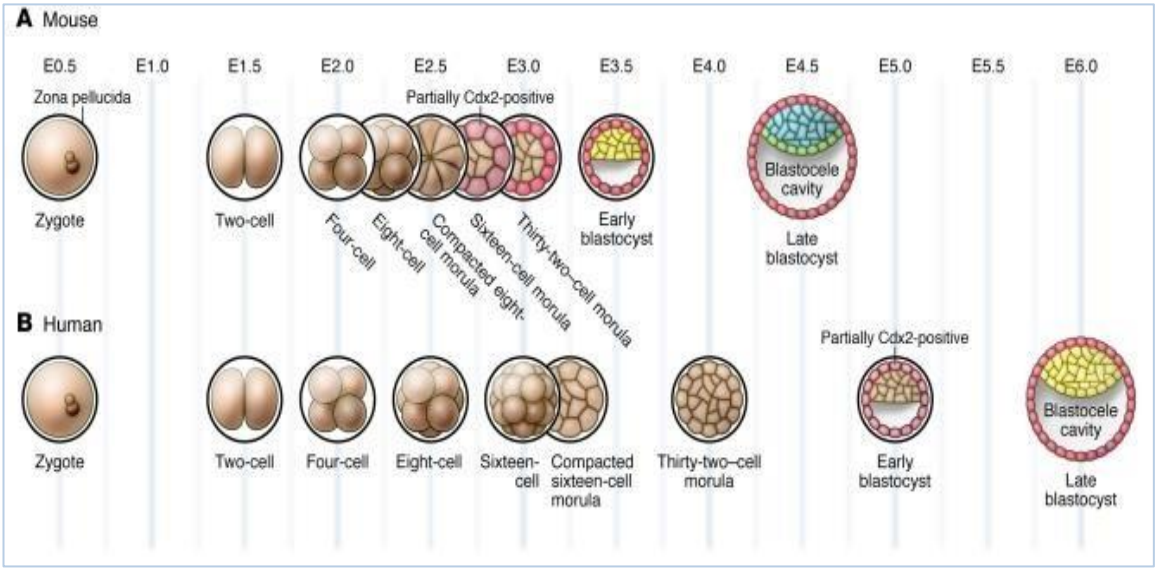

Figure 1.3 Stages of mouse and human preimplantation development.

(A) In the mouse, the fertilized egg undergoes three rounds of cell division to produce an eight-cell embryo which later undergoes compaction. The blastocoel cavity forms on the inside of the embryo at around the 32-cell stage and continues to expand as the embryo grows and matures into a late blastocyst at E4.5. (B) Development is similar in the early human embryo, although compaction occurs at the 16-cell stage and as development progresses. The timing of blastocyst formation occurs around 36 h later in the human embryo which undergoes an additional round of cell division prior to implantation, at ~256-cell stage compared to ~164 cells in the mouse blastocyst (Niakan et al., 2012).

Additionally, mouse and human embryo metabolism is also similar. In both species, the early preimplantation embryo relies, to a greater or lesser extent, on endogenous energy sources such as ATP and glycogen and, for several mitotic cell cycles, they both use pyruvate, lactate and amino acids to maintain intermediary substrate and cofactor levels (Quinn and Wales, 1973; Wales, 1975; Blerkom et al., 1995). During compaction (from the 8-cell stage), and at the onset of blastocoel cavity formation, the energy demand of the embryo increases and relies to a greater extent on aerobic glycolysis (Barnett and Bavister, 1996; Lane and Gardner, 1996).

These changes have been studied during *in vitro* culture and endogenously by analysing the metabolic components of the reproductive tract fluid (Quinn, 1997). The early mouse and human embryo also has a requirement for glutamine and other non-essential amino acids (Quinn et al., 1995; Lane and Gardner, 1996), together with inorganic phosphate (Pi). Above certain threshold levels (typically > 1.5 mM) glucose and Pi together are inhibitory (Leese, 1995; Barnett and Bavister, 1996). The utilization of exogenous glucose increases during the latter half of preimplantation development, and its presence in culture medium together with glutamine and other amino acids is beneficial for development in both species (Conaghan et al., 1993; Lane and Gardner, 1996).

These similarities in metabolism, therefore, render the mouse a valuable model to study the effects of maternal age, diet and ART.

Previous work in Southampton (using the mouse as a model species) found that poor maternal nutrition during the periconception period affects the formation and characteristics of early embryo cell lineages leading to adult offspring cardiometabolic disease (Watkins et al., 2008; Watkins et al., 2015; Sun et al., 2015). These developmental modifications could be retained and propagated (possibly by epigenetic means) in embryonic stem cell (ESC) lines derived from nutritionally deprived embryos. As changes in lineage specification causes permanent alterations in the physiology and functionality of tissues (Morris and Zernicka-Goetz, 2012; Condic, 2014), analysing the processes that regulate pluripotency and cellular differentiation during and following preimplantation development would provide key insights into the adverse effects of advanced maternal age (AMA), diet and ART.

1.6.1 Mouse embryonic stem cells (mESCs): Origin

Stem cells (SCs) are characterized by their developmental potential for self-renewal and differentiation (Gardner and Beddington, 1988). In mammals, only the zygote and early blastomeres are considered to be totipotent. Totipotent cells are capable of generating an entire organism by self-replication and differentiation into all cell types including extra-embryonic tissues that form the fetal placenta and membranes (Rossant and Tam, 2009; Mitalipov and Wolf, 2009). As the zygote and early blastomeres undergo cleavage divisions to form a blastocyst, they lose this potential. In mice, this formation occurs typically by 3.5 days after fertilization. After fertilization, the zygote and the morula up to the early blastomere stage consist of totipotent stem cells. Mouse embryonic stem cells (mESCs) are derived from the ICM of the pre-implantation blastocyst (E3.5), and are said to be pluripotent. That is, these cells can self-renew and generate into almost all cell types in the body, but not the entire organism as they lack the placenta forming cells (extraembryonic trophoblast lineage) (Nagy et al., 1993; Brons et al., 2007). This is depicted in Figure 1.5. The ICM of the blastocyst develops into the pluripotent epiblast (red) and primitive endoderm (blue). Epi-stem cells (EpiSCs) are obtained from the pluripotent epiblast, present in post-implantation embryos (E5.5-6.75) (Czechanski et al., 2014).

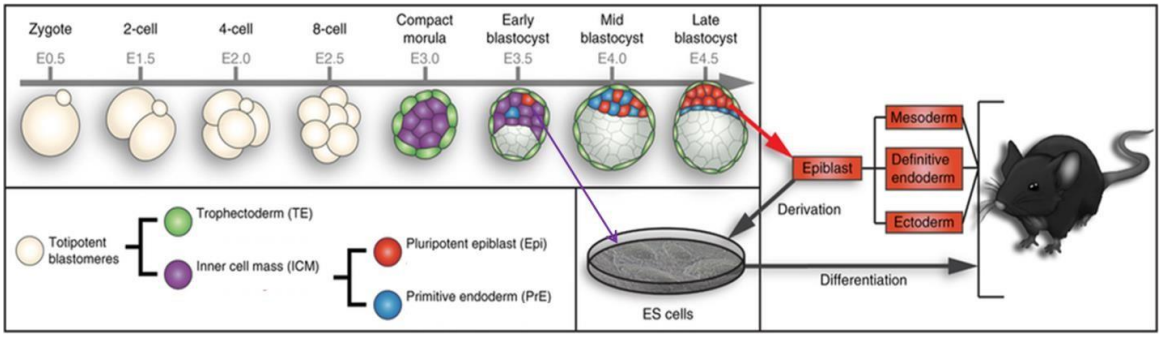

Figure 1.4 Overview of preimplantation development in mice.

(Czechanski et al., 2014)

1.6.1.1 Mouse embryonic stem cells (mESCs): Derivation and maintenance

In the 1980s, two laboratories independently and simultaneously reported that they had derived and cultured pluripotent mESCs *in vitro* (Martin, 1981; Evans and Kaufman, 1981). Embryonic stem cells possess several fundamental properties including *'self-renewal, multi-lineage differentiation, clonogenicity, a normal karyotype, extensive proliferation, and the ability to be frozen and thawed'* (Smith, 2001). Ever since, a plethora of culture conditions and techniques have been developed to derive mESC lines by the dissociation of ICM cells from plated blastocyst outgrowths (Nagy et al., 1993; Czechanski et al., 2014). Murine embryonic fibroblasts (MEFs) (also called feeder or helper cells) were first used in the 1970s to establish pluripotent teratocarcinoma (stem) cell lines (Martin and Evans, 1974). Since then, feeder cells have also been used for studying embryonal carcinoma cells and in the derivation of mESCs (Evans and Kaufman, 1981). Typically, MEFs are mitotically inactivated using Mitomycin C (MMC) or by γ-irradiation; although they continue to metabolise by maintaining gene transcription and protein synthesis. Whilst MMC efficiently and specifically crosslinks with the CpG regions of DNA; γ-irradiation induces breaks in DNA strands (Ponchio et al., 2000; Conner, 2001; Michalska, 2007).

Mitotic inactivation is an essential step in mESC derivation and prevents feeders from growing over the stem cells. Though feeders are a different cell population, and their use in conjunction with stem cells has been debatable, the cellular matrix assists embryos to attach and encourages stem cells to proliferate (Li et al., 2004). *In vitro*, feeders release embryo trophic factors and reduce the inhibitory effects of fetal bovine serum (FBS) in culture media. They overcome the developmental block, activate the embryonic genome and promote embryonic survival and development by secreting various growth factors. They also protect the embryo against oxygen toxicity (Vanroose et al., 2001). Although human foreskin fibroblasts (hFF) also support the propagation of human and mouse ESCs (Hovatta et al., 2003), MEFs are more commonly used for maintenance of mESCs (Eiselleova et al., 2008).

Additionally, FBS conditioned media has been used as a universal growth supplement media for cell and tissue culture, including mESCs (Li and Kirschner, 2014). Fetal bovine serum contains a combination of cell replication stimulators and cell differentiation inducers. As it is a biological product, it has never been completely characterised, raising major concerns about its immunogenicity and potential pathogenicity (i.e. presence of endotoxins, mycoplasma, viral contaminants or prion proteins) (Jochems et al., 2002), along with batch to batch variations (Gstraunthaler et al., 2013). Therefore, many researchers have replaced the use of FBS with chemically defined media (CDM) (Lee et al., 2012) containing chemically-defined Knockout™ serum replacement (KO/SR) (Goldsborough et al., 1998) and N2B27 (Nichols and Ying, 2006) supplementation.

Mouse embryonic stem cells have a high rate of cell division and differentiation. Maintenance of their phenotype (including pluripotency) *in vitro* requires their endogenous differentiation capacity to be inhibited while maintaining their proliferation rate. This is achieved by using a haemopoietic regulator, myeloid leukaemia inhibitory factor (LIF). LIF induces differentiation in M1 myeloid leukemic cells and assists in the derivation and maintenance of mESCs pluripotency (Williams et al., 1988; Smith et al., 1988) in feeder- and serum- free culture conditions (Nichols and Ying, 2006).

1.6.1.2 Pathways influencing mESC phenotype

LIF is an active constituent of the many pathways that play a role in the self-renewal, pluripotency and proliferation of mESCs (Williams et al., 1988; Smith et al., 1988; Murray and Edgar, 2001). It is a member of the interleukin 6 (IL6) family of cytokines and interacts with cell surface complex of a heterodimeric receptor LIFRß (LIF receptor ß) and the transmembrane signalling molecule glycoprotein 130 (gp 130). The ligand binding results in the activation of three signalling cascades: Janus Kinase (JAK)/ STAT3 (Signal transducer and activator of transcription-3), the phosphatidylinositol 3-kinase (PI3K)-mediated pathway, and the mitogen-activated protein kinase (MAPK) cascade.

LIF is sufficient in triggering JAK-STAT3, which is essential in maintenance of pluripotency (Smith et al., 1988; Niwa et al., 1998; Matsuda et al., 1999). Signal transduction occurs when LIFRß-gp130 binds to JAK in the intracellular gp-130 domain (Yoshida et al., 1994); where it is phosphorylated by STAT3 and translocated to the nucleus to express genes involved in self-renewal (Niwa et al., 1998). LIF also plays a key role in activating the MAPK/ERK (extracellular-signal-regulated kinase) pathway, which induces mESC differentiation (Niwa et al., 2009; Li and Ding, 2010), thus maintaining synergistic association to ensure a regulated mESC response.

Although LIF is essential for the derivation and maintenance of many mESC lines, some strains lose their derivation efficiency in its presence (Kawase et al., 1994; Li et al., 2005). As LIF's efficiency is limited to supporting mESCs, (Brevini et al., 2007; Keefer et al., 2007), the scope of other regulatory and signal transduction mechanisms and pathways for self-renewal, proliferation, differentiation and apoptosis have since been explored (Burdon et al., 2002; Liu et al., 2007). The canonical Wnt/ß catenin signalling is endogenously involved in the short-term self-renewal and pluripotency maintenance of both hESCs and mESCs (Aubert et al., 2002), though its main role is in the regulation of ES differentiation (Lee et al., 2010). Wnt/ß catenin pathway upregulates the mRNA expression for *STAT3*. It therefore allows LIF to act along with Wnt proteins to inhibit ES differentiation (Hao et al., 2006) and to enhance self-renewal by activation of pluripotency genes, including transcription factors Nanog, Oct3/4 (Octamer binding transcription factor 3 or 4), and Klf4 (Krüppel-like transcription factor 4).

Glycogen synthase kinase 3 (GSK3), a serine threonine kinase, is a key enzyme involved in conversion of glucose to glycogen (Rayasam et al., 2009). In addition to its association with insulin signalling and embryonic development, it plays a crucial role in the regulation of Wnt/β-catenin, Hedgehog, and Notch signalling pathways. It is inactivated in its phosphorylated form. Upon de-phosphorylation it enhances glucose synthesis, destabilizes the cytoplasmic β-catenin (β-Ctnn) and inhibits cell proliferation. Wnt inhibits and degrades the GSK3β complex and allows the β-Ctnn to translocate in the nucleus where the target genes such as c-Myc and Cyclin D1, promote cell proliferation and self- renewal.

More recently, novel mitogen-activated protein kinase (MAPK)/extracellular signal- regulated kinase (ERK) or MEK inhibitors such as PD0325901 or SU5402 have been used to eliminate differentiation-inducing signalling from MAPK. Additionally, the GSK3 inhibitor CHIR99021 has also been used to enhance ESC growth capacity and viability in mouse (Q.-L. Ying et al., 2008b) and rat ESC lines (Buehr et al., 2008). Therefore, in recent years several ESC lines have been derived and established using biochemical inhibitors in the absence of feeders. Most recently, a GSK3 inhibitor, BIO (6- Bromoindirubin-3'-oxime), was also used to successfully derive ES cells from Kunming mice IVF blastocysts in feeder- and serum- free conditions (Liu et al., 2015).

1.6.2 Neural induction (NI) in mESCs

As discussed in Section 1.6.1, mESCs are pluripotent cells derived from the ICM of preimplantation blastocyst (E3.5) and have been observed to be capable of resuming back their proliferative and differentiating abilities when re-introduced into the blastocyst. As stated previously, mESCs maintain their self-renewing capacity mostly via the transmembrane gp130, LIF, the removal of

which, induces spontaneous differentiation into the mesoderm, endoderm and ectoderm. *In vitro,* the pluripotent characteristics of mESCs have been further utilised by introducing specific genetic alterations and thus inducing targeted differentiation across specific cell lineages. This was initially achieved through the formation of suspended multicellular aggregates called embryoid bodies (EBs). For targeted neural differentiation, EBs are cultured in the presence of retinoic acid (RA) (Bain et al., 1995), or co-cultured with stromal cells/ conditioned medium (Kawasaki et al., 2000) and plated on to laminin or gelatin. Cells within the EBs displayed a range of cells with neural morphology, and neuron- and glial- (including for astrocytes and oligodendrocytes) specific genes. Most neurons generated from EB cultures were GABAergic (where GABA stands for γ -aminobutyric acid), although other studies also produced dopaminergic and serotonergic neurons (Lee et al., 2000). However, as EBs depict a complex interaction of heterologous population of differentiating stem cells at distinct stages of cell cycle, unless other lineages are strictly inhibited, they may result in the formation of derivatives from all three germ layers (Brickman and Serup, 2017). Furthermore, cell-to-cell communication and transportation of growth molecules varies across the compact structure of the EBs, often with varying density, cell number and shape. Thus to reduce undefined variables and increase culture homogeneity, neural commitment has been observed to be better attained by monolayer differentiation of adhered mESCs, methods initially developed by Ying et al, (2003). However, in order to develop rational strategies to utilise the ES-based culture system, it is important to perform systematic and detailed characterisation of neural differentiation in these cells.

Most extensively studied mESC differentiation has been directed towards the production of neural lineages such as neurons, radial glial cells, oligodendrocytes and astrocytes (Visan et al., 2012). Such *in vitro* culture systems aim at recapitulating complex *in vivo* events occurring in the inaccessible embryo to multi-step processes of neural differentiation i.e. from the initial stages of neural induction to terminal differentiation of neurons and/ or glial cells. As a result, they have achieved to produce distinct stages of neural stem cells, progenitors and intermediate neural cell populations with neurosphere-like morphology. Additionally, mature neurons (tested positive for MAP2 protein) derived from these protocols expressed synaptic proteins, neurotransmitters such as serotonin and γ-aminobutyric acid, and the presence of functionally active glutamate and dopamine receptors. Therefore, derived neural cells represent an efficient and malleable culture system to compare *in vivo* and *in vitro* neural lineage differentiation and to detect the effects of *in vivo* maternal environment on the neural population of the developing embryo.

1.6.2.1 Signalling pathways and *in vitro* NI

While several protocols have used a combination of RA and sonic hedgehog (Shh) to differentiate mESCs into mature neurons (Wichterle et al., 2002), their differentiation efficiency has only been moderately successful. Within most of the 2D *in vitro* culture systems, mESCs are grown in serum- and feeder- free cultures in the absence of BMP signals, as BMPs have been implicated in maintaining pluripotency and thus inhibiting neural differentiation (Di-Gregorio et al., 2007). In mESCs, BMPs and STAT3 are involved in self-renewal (Ying et al., 2003) and thus act as inhibitor of differentiation (Id) genes and differentiation-promoting pathways such as the mitogen-activated protein kinases (MAPK) (X. Qi et al., 2004). As BMP-mediated inhibition is also observed *in vivo*, it is suggestive of similar mechanisms that control differentiation and in particular, the neural fate during embryo development until E7.25, as the anterior neural markers are not expressed until then (Yang and Klingensmith, 2006).

Noggin and Dorsomorphin are two specific BMP antagonists that block BMP activity and thus are commonly used as default models during *in vitro* neurogenesis for the growth and patterning of the neural tube and somites (McMahon et al., 1998; Graham et al., 2014). Similar to *in vivo* development, neurogenesis is further enhanced by FGF signaling that serves pivotal in the autocrine induction mechanism, hence promoting an efficient neural commitment of mESCs (Kunath et al., 2007). This is achieved by inhibition of BMP signaling by MAPK-mediated phosphorylation of SMAD1 linker (Sapkota et al., 2007), although some studies have also shown that FGF/Erk can induce NI in mESCs independent of BMP activity (Stavridis et al., 2007). Together with Noggin, FGF promotes a posterior neural identity and induces neural tissue formation (Sinha and Chen, 2006). FGF signaling also plays an important role in initiating and later maintaining the neural precursor (NP) characteristics, and so some protocols use FGF as an instigator of neural commitment, which once established, is cultured in its' absence to promote further differentiation of NP cells (Ying et al., 2003).

Fate of NPs within the embryonic neuroepithelium is also controlled by the activity of the Notch Pathway, inhibition of which leads to precocious neural differentiation (Yoon and Gaiano, 2005). Monolayer *in vitro* cultures of neural differentiation consisting of NPs and neural rosettes expressed *Notch 1*, *2* and *3,* genes along with *Delta-like*, *Jagged* and *hes* genes, that are also expressed during early embryonic neural development, further displaying similarities between the *in vivo* and *in vitro* differentiation during the early NI period (Ohtsuka et al., 1999). Similar to FGF signaling, the inhibition of Notch signaling induces differentiation of NPs demonstrated by the expression of neuron markers such as Beta III Tubulin and morphological changes, i.e. from rosettes to large rounded ganglion-like clusters of differentiating neurons, with extensive neurite outgrowths

(Abranches et al., 2009a). Interestingly, as the cultures continue to differentiate, the extent of Notch inhibition increases (especially at Day 8 of differentiation) however, Notch receptors are still observed to be active (at lower levels) even at Day 16 of differentiation. It has been observed that at later stages of differentiation, the specificity of Notch receptors shifts from neuronal to gliogenic, as also observed during embryo neural development (Qian et al., 2000; Shen et al., 2006).

1.7 Development of working hypothesis

Adverse maternal environment during the periconceptional period influences embryo and fetal development, and predisposes offspring to adult-onset non-communicable diseases. Previous work using mouse models has demonstrated that advanced maternal age (AMA) and maternal low protein diet (LPD) program the preimplantation embryo (E3.5) in a manner that alters its formation (ICM:TE), metabolism and subsequent lineage allocation thus enhancing the risk of cardiometabolic and neurodevelopmental disorders in offspring. AMA and LPD-induced modifications in the numbers and ratio of ICM and TE cells of the blastocysts suggests effects on cell proliferation and lineage specification.

The current thesis is based on the premise that mESCs derived from E3.5 blastocysts provide a powerful model to investigate environmental effects on the preimplantation embryo; i.e. they provide an unlimited supply of pluripotent cells that can be induced to differentiate into lineages that go beyond the normal period of implantation during *in vivo* development. Using such a model, preliminary studies undertaken at Southampton with LPD mESCs and embryoid bodies (EB) indicated changes in phenotype and epigenetic programming of ICM derived ESCs (Cox et al., 2011; Sun et al., 2014, 2015).

The present series of studies, therefore, sought to assess the effects of two major aspects of maternal environment; specifically, advanced maternal age (AMA) and maternal LPD, that each contribute to DOHaD. The studies utilised C57BL/6 female mice mated with sexually mature CBA males as an animal model. To determine the consequence of AMA and LPD on founder ICM cells within the blastocyst, a process that is difficult to study *in vivo*, maternal effects were analysed on mESC lines derived from E3.5 blastocysts. For the AMA study, mESC lines were derived and established from Old (7-8 months) and Young (7-8 weeks) dams; whereas the LPD studies were based on normal and low protein diet (NPD and LPD) mESC lines derived by a former PhD student, Dr. Andy Cox. Pluripotent mESC lines were derived and evaluated to assess changes in their phenotype and responsible molecular mechanisms, thus overcoming limitations posed by small numbers of cells and rapidly changing development of *in vivo* blastocysts. Thus, in the current thesis, mESC lines acted as a model of the inaccessible blastocyst within the mother.

1.7.1 Aims and objectives

Therefore, this thesis sought to assess the effects of advanced maternal age and dietary restriction during the periconceptional period on aspects of subsequent development using mESCs as an experimental model. This overall aim was addressed as three objectives listed below and depicted in Figure 1.6.

Objective 1: To determine the effects of advanced maternal age (AMA) on embryo development and characteristics of mESC lines derived from E3.5 blastocysts.

Objective 2: To establish the effects of maternal low protein diet (LPD) on metabolomic profiles of derived mESC lines

Objective 3: To investigate the effects of maternal low protein diet (LPD) on neural differentiation of derived mESC lines

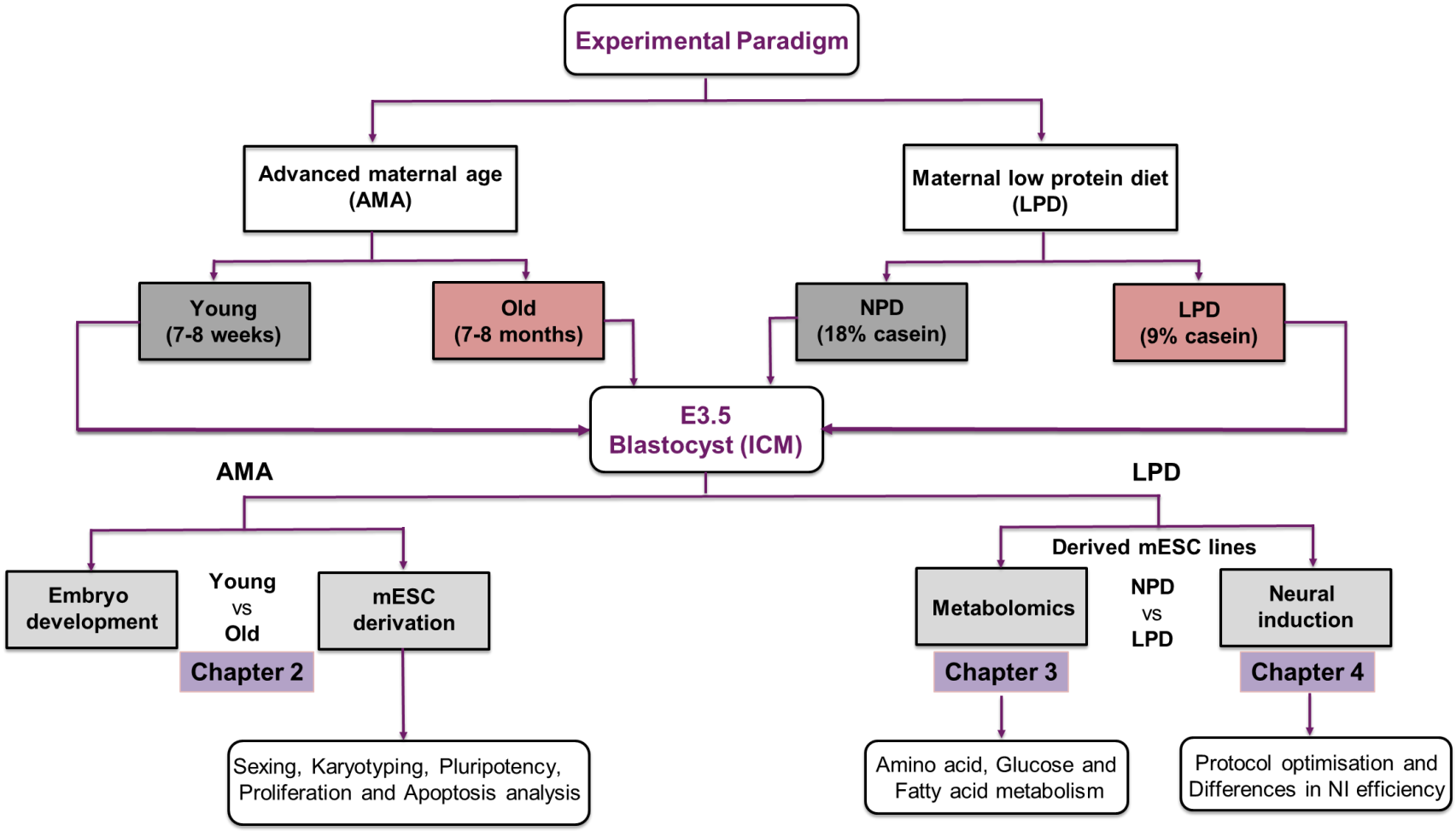

Figure 1.5 Flow diagram representing series of experimental studies undertaken in this thesis.

Chapter 2 Effects of Advanced Maternal Age (AMA) on derived mESC lines

2.1 Introduction

Advanced maternal age (AMA) is associated with increased gestational diabetes (Biro et al., 2012), preterm births, hypertension, pre-eclampsia and other complications (Delbaere et al., 2007; Carolan, 2013; Ferré et al., 2016) that induce adverse neonatal and perinatal outcomes (Laopaiboon et al., 2014). As discussed in Section 1.4.2.3, AMA has detrimental effects on the ovarian reserve and oocyte quality, maternal uterine environment including endometrial receptivity; thereby affecting embryo formation, fetal development and postnatal health of offspring (Pellicer et al., 1995; Janny and Menezo, 1996; Meden-Vrtovec, 2004; Carolan and Frankowska, 2011a; Rasool and Shah, 2017; Shirasuna and Iwata, 2017).

Human-based studies have also observed AMA-induced decrease in placental weight, along with decreased surface antigen and transcript expression of CD105 and CD29 (markers of angiogenesis) in placenta-derived mesenchymal stem cells (MSC) (Alrefaei et al., 2015). Maternal ageing is known to induce structural and functional changes in cytoplasmic organelles, especially in the mitochondria of oocytes and granulosa cells of older females (Kushnir et al., 2012). This further reduces ATP content, telomerase activity and telomerase length in stem cells inducing cell senescence (Bruin et al., 2004). As reproductive ageing in humans is a multifaceted phenomenon and depends on maternal genetics and epigenetics that are influenced by environmental aspects including paternal health and lifestyle (Carlo et al., 2009), it emphasises the need for controlled experimental studies in animals.

AMA in mice decreases blastocyst cell number, and increases blood pressure and reduces glucose tolerance in offspring, in a sex dependent manner (Velazquez et al., 2016). As these offspring were derived from the blastocysts (E3.5) of older dams that were transferred to younger dams until birth, observed AMA effects were restricted to E3.5. Reduced cell number in blastocysts have further been associated with AMA- induced growth-restriction in offspring (Master et al., 2015), and decreased placental and fetal weight (Wakefield et al., 2011). Additionally, AMA reduced embryo size and somite number, without altering litter size (Lopes et al., 2009). Alterations in cell proliferation (induced by periconceptional diet) during blastocyst development has also been associated with metabolic and mitochondrial dysfunction in embryos (Mitchell et al., 2009). Although the importance of maternal environment and the periconceptional period have been

demonstrated previously (Watkins et al., 2007; Rexhaj et al., 2013; Lopez-Cardona et al. 2015; Velazquez et al., 2016), little is known about how 'AMA' impacts the underlying mechanisms at the sensitive stage (i.e. periconceptional period) of development.

MESC lines derived from E3.5 blastocysts of low protein diet (LPD) fed dams showed phenotypic differences (including reduced proliferation, pluripotency and survival) compared to control, normal protein-derived mESC lines (Cox et al., 2011). Furthermore, embryoid bodies derived from LPD mESC lines also showed persistent periconceptional programming in histone modifications to regulate *Gata6* expression and PE growth (Sun et al., 2015). Collectively, these studies demonstrated the propagation of nutritional programming adaptations *in vitro,* mimicking the inaccessible blastocyst within the mother while propagating blastocyst-stem cell population (i.e. inner cell mass, ICM). This further led to reducing animal use, in accord with the principles of the 3Rs (replacement, reduction, and refinement).

Similarly, the present study utilised the self-renewal potential of mESCs in exploring the impact of AMA. Young (7-8 weeks) and Old (7-8 months) C57BL/6 female mice were mated with sexually mature (4-5 weeks) CBA males. Mouse ESC lines were derived from E3.5 blastocysts and were maintained in low passage numbers (P9-P11) on mouse embryonic fibroblasts (MEFs). Due to limited number of derived Female mESC lines, impact of AMA was analysed only between Male mESC lines, although sex differences were observed within the 'Old mESC group'. Mouse ESC lines were observed for phenotypic differences based on mESC line derivation efficiency, pluripotency, proliferation rate and cell senescence between the groups (i.e. Young male v Old male and Old Male v Old Female). The current study focussed on the effects of 'reproductive ageing' and not on chronological ageing in mice, and thus the chosen period of 7-8 months reflects the onset of reproductive ageing (depicted by oocyte damage), rather than a substantial or complete loss of reproductive function. Although animal studies offer no direct comparisons with humans, the age model used in the present study represents the practice of delayed childbearing in the current society.

2.2 Materials and Methods

2.2.1 Animal Procedures

All mice and experimental procedures were conducted using protocols approved by, and in accordance with, the UK Home Office Animal (Scientific Procedures) Act 1986 and local ethics committee at the University of Southampton under UK Home Office Project License PPL30/3001.

2.2.1.1 Animals and embryo collection

C57BL/6 mice (University of Southampton Biomedical Research Facility) were housed on a controlled 07.00-19.00 h light cycle at 21°C and fed standard laboratory chow (Special Diet Services) and water *ad libitum*. For advanced maternal age (AMA) experiments, Young (7-8 weeks) and Old (7-8 months) C57BL/6 females were naturally mated with sexually mature CBA males (3-4 months old). Mating was confirmed the following morning (E0.5) by the presence of a copulation plug (vaginal plug). Mice were subsequently culled by cervical dislocation, an approved Schedule 1 method. In order to flush E3.5 embryos, oviducts and uterine horns were dissected and immediately placed in pre-warmed H6-BSA (buffer with 4mg ml^{-1} bovine serum albumin, Sigma, embryo culture tested, A3311, Appendix A). Once the embryos were collected, they were transferred to a fresh dish containing embryo culture media, KSOM (Potassium supplemented simplex optimized medium, Appendix A) drops covered with a layer of mineral oil (Sigma Aldrich). Embryos were moved across the drops and washed thrice. Females were culled at E3.5 for AMA experiments and blastocysts were directly used for mESC derivation.

2.2.1.2 Embryo staging

To evaluate the effect of maternal age on development, the embryos derived at E3.5 from ten female C57BL/6 dams (Young and Old) were staged according to their morphology, number of cells (if countable), compaction of morula, and the proportion of inner cell mass (ICM) and trophectoderm (TE) (see Figure 2.4).

2.2.2 Cell culture

2.2.2.1 Mouse embryonic fibroblasts (MEFs) preparation

Primary mouse embryonic fibroblasts (MEFs) were isolated from fetuses of MF1 female mice with timed pregnancies (E14-E15). Fetuses were surgically dissected from both uterine horns and all steps were performed under a sterile hood with autoclaved dissection equipment. The brain and visceral organs were removed and the trunks were washed with pre-warmed PBS to get rid of blood

before finely mincing and incubating in trypsin: Ethylenediaminetetraacetic acid (EDTA) (0.05%; Gibco, 25300) at 37°C in 5% CO_2 for 15 min with intermediate pipetting to ensure proper tissue dissociation. Trypsin activity was reduced with the addition of MEF medium ((Dulbecco modified Eagle medium (DMEM) [Gibco, 42430] supplemented with 10% FBS [Sigma], 2 mM glutamine and penicillin [50 U/ml]/ streptomycin [50 µg/ml] (Gibco, 10378)), and DNAse (100 µg/ml) to cleave and break DNA strands. Cells were washed and centrifuged at 1,500 rpm for 5 minutes and the resultant pellet was re-suspended in MEF medium. Cells were plated onto 15 cm tissue culture dishes and cultured in a humidified environment at 37°C, 5% CO_2. Once MEF cells were 80 % confluent, they were frozen (at -80°C for short-term and liquid N_2 tanks for long-term) in MEF medium supplemented with 20% FBS and 10% dimethyl sulfoxide (DMSO, Sigma, D5879).

2.2.2.1.1 Preparation of Mitomycin C treated MEF cells

MEFs were thawed and expanded for up to 2-3 passages in MEF medium (Section 2.2.2.1.) before they were mitotically inactivated. To ensure proper mitotic inactivation, MEFs were treated with mitomycin-C (MMC, Fisher Scientific, 10182953). MMC arrests the MEF cells at metaphase. Once the untreated MEFs were 80-90% confluent (observed as area covered by adherent cells under a Brightfield microscope), they were treated with 1 mg/mL MMC to get a final concentration of 10 µg/ ml. MMC was added directly to the MEF medium and the dishes were incubated for 3 h at 37°C, 5% CO_2 in air in humidified incubator. Gelatin (Sigma, G1393; 0.01% in PBS) coated dishes were prepared. After 3 h of incubation with MMC, MEF dishes were washed 2-3 times with PBS and trypsinized with 0.05% trypsin-EDTA (20 ml) at 37°C and 5% CO_2 for 5 min. Single cells were washed and centrifuged at 1,200 rpm for 5 min. The pellet was re-suspended in fresh MEF medium and seeded on pre-prepared gelatin coated dishes. Once the MEFs were MMC-treated, they were used within 3-4 days. Media were changed the following day and then every alternate day.

2.2.2.2 Derivation and culture of mESC clones from E3.5 blastocysts

MMC-treated MEF dishes were prepared as describes in Section 2.2.2.1.1 about two days before collecting E3.5 blastocysts. Thirty minutes before the blastocysts were transferred to MEF dishes, the MEF culture medium was replaced by mESC medium (knockout-DMEM supplemented with 15% knockout serum replacement (KO/SR) (Gibco, 10828), non-essential amino acids (Gibco, 11140), 1 mM sodium pyruvate (Gibco, 11360), 100 µM 2 mercaptoethanol (Sigma, M7522), 2 mM glutamine, penicillin (50 U/ml)/ streptomycin (50 µg/ml) (Gibco, 10378) and 1000 U/ml of leukemia inhibitory factor (LIF)), and incubated under standard humidified conditions of 37°C in 5% CO_2 in air. Blastocysts were washed in H6-BSA to get rid of any oil residue and then transferred to the pre-prepared MEF dishes for mESC isolation. The number of embryos recovered from C57BL/6 mice

varied between 7- 9. Blastocysts from different mothers were plated onto different dishes. Plated blastocysts were transferred to MEF dishes in mESC medium and incubated for 48 h. On the fourth day, almost all blastocysts had hatched and attached to MEFs. The mESC medium was replaced with PBS. ICM clumps were carefully isolated and picked using a 10 µl micropipette (Gilson) under a sterile hood and an inverted phase microscope without taking the surrounding MEFs.

Each isolated ICM outgrowth was collected in a different well of a 96-well U-shaped plate containing 30-50 µl/ well of pre-warmed trypsin-EDTA (0.25% diluted 1:1 with PBS). Once all the outgrowths were collected, they were incubated (5% CO_2, 37˚C). Plates were taken out of the incubator after 5-6 min and the outgrowths were pipetted a few times to isolate the cells. The medium was neutralized by adding 10% FBS-containing MEF medium (100 µl). The trypsinized outgrowths were pipetted a few more times and the entire cell suspension was then transferred to a fresh 96-well MMC-MEF plate (Section 2.2.2.1.1). mESC medium was changed daily. Once the protocol was established, it took 4-5 days for the first mESC clones to appear (round, tomb-like small clusters of cells). After 8 to 9 days, mESC colonies were transferred to fresh 24-well MMC-MEF dishes and cultured in mESC medium.

mESC colonies were cultured to 70% confluency on MMC-treated MEF cells in ESC medium (with 15% KO/SR and 1000 U/ml of LIF) under standard incubation conditions. mESCs were passaged by dissociating cells by gentle pipetting before spinning at a low speed (~1200 rpm). The resultant pellet was re-suspended, first in a small volume (1-2 ml) of mESC medium, and then diluted in a larger volume, before they were seeded on fresh MMC-MEF dishes. mESC medium was changed daily.

2.2.2.2.1 Freezing and thawing mESC lines

Once mESCs were expanded for 8-9 passages, mESCs were either used directly or frozen for later use. For freezing, cells were counted (Section 2.2.6) and frozen at a concentration of approximately 1 million cells per cryovial. The cells were trypsinized and after centrifugation, the pellet re-suspended in ice-cold freezing medium. The mESC freezing medium was always prepared fresh and consisted of mESC medium supplemented with 20% KO/SR and 10% DMSO. No LIF was added to the freezing medium. About 1 ml of mESC suspension was aliquoted into 1.8 ml cryovials, transferred to ice immediately and then frozen slowly at -80˚C overnight before storing in liquid nitrogen. Cell stocks were quick-thawed in a water bath at 37˚C, spun (~300 g) to get rid of DMSO and re-suspended in mESC culture medium. They were seeded onto a fresh MMC-MEF dish. mESCs were cultured on feeders for at least one passage before they were used.

2.2.3 Gender Analysis (Sexing) of mESCs

2.2.3.1 Genomic DNA Isolation

a) **Pre-plating of mESCs- Process to eliminate MEFs**

For gender analysis, mESCs were grown on gelatin-coated dishes in the absence of MEF cells. This was achieved by pre-plating the cells in mESC medium, i.e. post trypsinization, mESCs were transferred to gelatin-coated dishes for 30-40 min after which the supernatant (containing floating mESCs) was gently aspirated and transferred to fresh gelatin-coated dishes. This process eliminated MEFs as they stuck to gelatin while the mESCs remained in suspension.

b) **Genomic DNA isolation from mESCs**

On the first day, confluent cells from each cell line were washed with PBS and trypsinized. The cells were centrifuged with ice-cold PBS at 500 *g* for 5 min. To the resultant pellet, fresh lysis buffer containing 10 mM Tris, pH 8, 100 mM NaCl, 10 mM EDTA, pH 8, 0.5% sodium dodecyl sulphate (SDS), and 1 mg/ml proteinase K was added fresh. For cells ≤ $3.7x10^7$, 300 µl of lysis buffer was added, which was increased with increasing cell density. The samples were gently pipetted and transferred to individual Eppendorf tubes and incubated overnight at 55°C in humid environment to avoid evaporation (Ramírez-Solis et al., 1992). On the following day, lysates were centrifuged at 13,000 rpm for 15 min. The supernatant was carefully transferred to fresh thin-walled nuclease-free tubes, to which 30 µl 5M NaCl was added (the volume of NaCl added depended on the volume of lysis buffer used initially). The samples were incubated for 5 min at room temperature and centrifuged at 13,000 rpm for 15 min.

The supernatant was removed and added to pre-prepared tubes containing 100 µl of isopropanol. The tubes were gently shaken by hand until DNA strands were visible and the surrounding solution appeared clear. The tubes were left on bench at room temperature for 10 min and spun later at 13,000 rpm for 30 min (the samples could be stored overnight at 4°C at this stage). The supernatant was discarded carefully without disturbing the pellet. To this pellet, 1 ml of 70% ethanol was added, incubated (15 min, room temperature), and spun at 13,000 rpm for 30 min. The supernatant was discarded and the tubes were put on a heating block set at 37°C for a few minutes. The pellets were re-suspended in nuclease-free water (50 µl) (Thermo Fisher, 10977049). The volume of water added depended on the size of the DNA pellet. Initially, low volume (20-30 µl) was added which, when required, was re-diluted later. Stocks of 25 ng/µl DNA were also prepared for performing PCR reactions later. To ensure proper dilution in water, the tubes with DNA samples were left at room temperature for 10-

15 min. Genomic DNA concentration and quality was quantified using the Nanodrop ND-100-spectrophotometer (as described below, Section 2.2.3.1, d). Samples were stored either at 4°C (short term) or at -20°C (long term).

c) **Genomic DNA Isolation from mouse tails (as control samples)**

A few micrometres of tail tips were cut and stored in sterile Eppendorf tubes from male and female C57BL/6 mice as control samples. The tail tips were either directly used for gDNA extraction or stored at -20°C for later use. Genomic DNA from mouse tails were derived as described previously (Section 2.2.3.1. b, without trypsinisation). Caution was taken while transferring supernatants after the lysis step to avoid transfer of mouse hair. An extra washing step with isopropanol was added (when required) to ensure this. Genomic DNA concentration and quality was quantified using the Nanodrop ND-100- spectrophotometer (as described below, Section 2.2.3.1, d). Samples were stored either at -20°C (short term) or at -80°C (long term).

d) **Measuring DNA concentration using Nanodrop ND-100- spectrophotometer**

The correct sample type was chosen on the Nanodrop software - i.e., genomic DNA. The machine program was initialized by placing 1 µl of RNase-free H_2O (Thermo Fisher, 10977049) on the measuring tip. The samples (1 µl) were run and, the concentration (ng/ml) and quality (260/280 and 260/230- to assess sample purity) of measured gDNA samples was noted.

2.2.3.2 Polymerase Chain Reaction (PCR)

PCR samples containing final concentrations of primer mix, 1x PCR buffer (20 mM Tris–HCl, pH 8.4, 50 mM KCl), 2.5 mM $MgCl_2$ (Invitrogen), 250 µM of each dNTP (Invitrogen), 250 nM of each oligonucleotide primer, 0.625 U HotStar Taq (Qiagen), RNase-free H_2O) and 50 ng gDNA sample were prepared in a total volume of 25 µl. Each sample was measured in triplicate. The PCR was performed on a DNA Engine® Peltier Thermal Cycler (BioRad, UK). PCR program included initiation by HotStar Taq activation at 95°C for 15 min, followed by 40 cycles each consisting of a denaturation step at 94°C for 60 sec, annealing at 55°C for 30 sec and extension at 72°C for 60 sec. After the last cycle, samples were incubated at 72 °C for 10 min.

2.2.3.3 Gel Electrophoresis

Amplified DNA products were separated by gel electrophoresis with 1% agarose gel in 1X TBE (50 mM Tris, 100mM Borate, 10 mM EDTA, pH 8.) buffer. TBE was also used as running buffer. Bands were analysed by nucleic acid gel stain, GelRed (Cambridge Bioscience, BT41003). A 100 base pair (bp) ladder (6 µl) was added to the first lane, and the samples were mixed with 6X DNA loading

dye (Thermo Scientific, SM1331) and loaded on to subsequent wells. The gel was run at 70 V for about 20-30 minutes and immediately visualized under ultraviolet (UV) illumination using a UV camera.

2.2.4 Chromosome Counting (Karyotyping)

Embryonic Stem Cells (ESCs) are expected to show a stable euploid karyotype, but in the last decade, chromosomal aberrations have been systematically described in ESC lines when maintained *in vitro*. Culture media and duration, along with other conditions have long been regarded as factors involved in the acquisition of such abnormalities (Draper et al., 2004). Thus, it is imperative to analyse the chromosome constitution in mESCs derived from different *in vitro* ART processes such as AMA, cryopreservation and IVF, as many ART-conceived offspring have shown increased risks of chromosomal abnormalities (Feng et al., 2008).

To assess the chromosome status, the mESC lines were cultured as described in Section 2.2.2.2. MESCs (between P9-P11) were harvested and seeded onto MMC-MEF 6-well plates. The cells were cultured in mESC medium (Section 2.2.2.2.) that was changed every day. In order to obtain a large number of metaphase spreads, cultures were arrested at metaphase using Colcemid (Gibco, 15212-012) at a final concentration of 0.1 µg/mL once they reached 70% confluency. Colcemid was directly added to the existing mESC medium in the culture dishes and incubated for 3 h at 37°C and 5% CO_2 (Campos et al., 2009). MESCs were then washed with PBS, trypsinized using 0.05% trypsin-EDTA and centrifuged at 122 *g* for 5 min. Hypotonic KCl solution (KCl 75 mM, pre-warmed to 37°C) was added to the cell suspension and incubated at 37°C for 15 min in a water bath. To this, fixative solution containing methanol and glacial acetic acid (3:1) were added. Immediately afterwards, the cell suspension was centrifuged at 122 *g* for 5 min. 200 µl of supernatant was left and fixed overnight at 4°C. Slides used for karyotyping were cleaned using 6 M HCl for at least 3 h at room temperature and stored in 96% ethanol and dried with a lint-free tissue.

On the following day, the fixed cells were centrifuged at 122 *g* for 5 min and washed three times. At the last centrifugation step, sufficient amount of solution was left behind to homogenize the cell pellet. 20-30 µl of the fixed cell suspension was dropped onto a cleaned slide from a vertical distance of about 15-20 cm and left for air-drying at room temperature. The slides were stained with Giemsa staining solution (Sigma, G500; 1:25 dilution) for 25 minutes, gently washed and air-dried. Slides were analysed under a phase contrast microscope at a magnification of 100x.

While dropping the fixed cells on the slides, a slightly different protocol was also practised. Instead of dropping the cells from a distance, they were placed parallel to the slide's surface using a micropipette. The slides were immediately exposed (face up) to steam (90°C) for 30 sec. This caused the cells to blow up. The reason behind steam exposure was to evaporate the methanol from the fixative solution and increase the acetic acid concentration, which with water, stimulates chromosome spreading. Although this step helped in getting spread-out chromosomes, often the steam caused the chromosomes from different spreads to mix and induced difficulty in distinguishing and counting the chromosomes accurately. Hence, the previous method was adopted. A total of 60-70 distinguished spreads were counted from each mESC line using Image J software.

2.2.5 Quantitative PCR (qPCR) analysis

2.2.5.1 RNA extraction

Mouse ESCs (400,000 cells/well) were seeded on 6-well cell-culture dishes coated with mitotically inactivated MMC-MEFs (135,000 cells/well) (Section, 2.2.2.2). mESCs were cultured for 3-4 days after which they were trypsinised, disaggregated to single cells, neutralized with medium and transferred to 15 ml Falcon tubes (Section, 2.2.2.2). The cells were washed with PBS and pre-plated on 10 cm gelatin-coated dishes for 45 min and incubated (5% CO_2, 37°C). Pre-plating eliminates the majority of MEFs which can act as contaminants in mESC RNA samples. The derived pellet was gently mixed (without pipetting) with ~200 µl undiluted RNA Later (Sigma, R0901) (to maintain the integrity of the cell samples), and stored at -80°C until required. Total RNA from mESCs was isolated using the RNeasy mini kit (Qiagen, UK) as described in the RNeasy handbook. RNA was quantified using the Nanodrop ND-1000 spectrophotometer (Section 2.2.3.1, d).

2.2.5.2 RNA quality

RNA is highly susceptible to degradation due to ubiquitous presence of RNase. Isolation of intact and high integrity RNA is essential for precise downstream applications. All RNA extraction samples (derived AMA mESC lines) were analysed and qualified for concentration, purity and integrity. Quantitatively, RNA samples were analysed by ultraviolet absorbance using Nanodrop spectrophotometer and were classified as pure (and protein free) if the 260 to 280 nm absorbance ratios were between 1.9 to 2.0. Although Nanodrop is widely used for analysing concentration and purity of samples, it lacks specificity i.e., all nucleic acids (dsDNA, RNA and ssDNA) absorb at 260 nm. Thus, while the A_{260}/A_{230} ratio estimates RNA purity, it cannot determine the amount of genomic DNA present in the RNA sample. In addition, Nanodrop also lacks sensitivity for low-level samples, which was observed with our samples and has also been reported by others (Simbolo et

al., 2013). Moreover, the method may not be reflective of RNA integrity or display degradation, as single nucleotides also contribute to the 260 nm reading. Therefore, qualitatively, total RNA integrity was analysed by running diluted RNA samples (1 µl RNA sample + 4 µl of 6X DNA loading dye) on a 0.8 % agarose gel (diluted with GelRed), at 120 V for 15 mins.

Intact RNA shows clear 28S and 18S rRNA bands, where 28S is twice as intense as the 18S rRNA band (as observed in Figure.2.1) and the 2:1 ratio acts as a good indicator of integrity and purity of RNA. Partially degraded RNA samples exhibit smears, lack sharp bands and do not show 2:1 band ratio, whereas completely degraded RNA samples appear as very low molecular weight smears (Sigma).

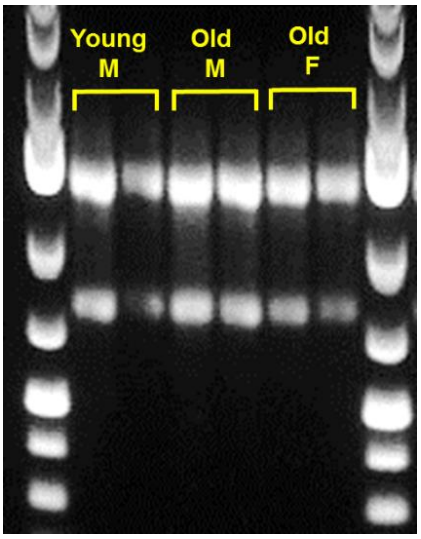

Figure 2.1 RNA gel electrophoresis of AMA mESC lines.

A representative 0.8% agarose gel showing RNA (~ 400 ng/µl) extracted from AMA (Young and Old) mESC lines (2 lines/group; where M and F stand for Male and Female respectively). The 18S and 28S ribosomal RNA bands are visible, showing no lower molecular smears (degraded RNA) indicating that the RNA samples are intact. Band sizes were determined using GeneRuler 1 kb Plus DNA Ladder (left and right column; ladder).

2.2.5.3 Reverse transcription (cDNA synthesis)

First-strand cDNA was synthesized using 400 ng RNA using GoScript™ Reverse Transcription System (Promega, UK). Experimental RNA was combined with 0.5 µg/ reaction of each Oligo$(dT)_{15}$ and random primers, diluted with nuclease-free water to bring the total volume to 5 µl. The mix was heated in a controlled heat block at 70°C for 5 min, immediately chilled on ice until used for reverse transcription. Table 2.1 summarises the components used for reverse transcription mix (15 µl in total for each cDNA reaction). The reverse transcription mix (15 µl) was combined with RNA and primer mix (5 µl), making a total of 20 µl reaction volume in thin walled, nuclease-free tubes and transferred to DNA Engine® Peltier Thermal Cycler (BioRad, UK). The primer-templates were

annealed at 25°C for 5 min, extended at 42°C for 1 h, and reverse transcriptase was inactivated at 70°C for 15 min. cDNA products were divided into multiple (thin walled, nuclease-free) tubes and stored at -20°C for later use in qPCR.

Table 2.1 Components of reverse transcription mix

Components	Volume
GoSriptTM 5X Reaction Buffer	4 µl
$MgCl_2$ 3mM	2.4 µl
PCR nucleotide mix (0.5 mM each dNTP[2])	1 µl
Recombinant RNasin ® Ribonuclease Inhibitor	0.5 µl (20 units)
GoSriptTM Reverse Transcriptase	1.0 µl
Nuclease-free water	6.1 µl

2.2.5.4 Quantitative PCR

Quantitative polymerase chain reaction (qPCR) has been established as a powerful technique to assess transcriptional differences between samples of varying origin in a short period. It is sensitive, specific and has a broad quantification range making it a high-throughput gene expression analysis technique. Here, specific gene targets were detected using SYBR-green from the SYBR-green 2x *PrecisionPlus™* Mastermix (Primerdesign, UK) protocol. SYBR-green is a dye-based fluorescent labeling method that enables the quantification and collection of data as it intercalates with every new copy of dsDNA molecule. The fluorescence is measured in each cycle and increases as the PCR progresses or in 'real-time'. Therefore, the fluorescence intensity is proportionate to the number of dsDNA copies formed i.e., the PCR product, which constitutes to the target gene expression. Although it is a convenient and widely adopted method of detecting dsDNA amplification, it does have a few drawbacks. This method allows the detection of only one target gene at a time and binds to any dsDNA present in the sample. Therefore, careful RNA extraction and cDNA conversion from a clean sample is imperative. However, accurate normalization of quantitative real-time PCR by reference or house-keeping genes minimizes such errors.

Each lyophilised primer mix vial (forward and reverse primer mix; Primerdesign, UK) was diluted with 220 µl nuclease-free water, from which 1 µl was used for each PCR reaction tube. Reverse transcribed samples were thawed (on ice) and spun in a table centrifuge before added directly to the PCR plates. Primerdesign 2x *PrecisionPlus™* qPCR Mastermix consisted of the following components:

Table 2.2 Primerdesign 2x *PrecisionPlus*^{TM} qPCR Mastermix

Components	Volume (per 20µl reaction)
Re-suspended primer mix (300nM/ 20 µl reaction)	1 µl
Primerdesign 2x *PrecisionPLUS*^{TM}	10 µl
RNAse/DNAse free water	8 µl
cDNA sample	1 µl

Each sample (20 µl) was analysed in duplicate using low profile, non-skirted, clear 96-well plates (Starlab). As controls, a few RT-negative samples were tested to confirm absence of genomic DNA, and water samples were introduced in each run as no template controls. Product amplification took place in a Chromo4 Real-time Detector (BioRad, UK) and analysed with Opticon Monitor v3.1 software. Amplification program included enzyme activation at 95°C for 2 min, followed by 40 cycles of denaturation at 95°C for 10 s, annealing (and data collection) at 60°C for 1 min, and a final extension step at 72°C for 10 min.

Melting curves were generated for each sample to confirm target-specific amplification by fluorescence detection between 60°C and 95°C at 1°C steps, holding for 15 s before the program was terminated and maintained at 4°C until the plates were retrieved from the machine. The data was saved from the Opticon Monitor and the plates were stored in the fridge until required for gel electrophoresis.

2.2.5.5 Normalisation of PCR data

Quantitative RT-PCR is an efficient and sensitive technique, which has been used for decades to detect and compare patterns of gene expression. As it works on the principle of exponential amplification of the target DNA sequences, any variants or errors in the starting material such as-sample-to-sample variation, RNA integrity/ degradation (Lossos et al., 2003), RT efficiency (Bustin, 2000) or cDNA sample loading errors, could be compounded and contribute to flawed data (Ståhlberg et al., 2003). Such variations can cause misinterpretation of the derived gene expression data especially when the samples are taken from several cell lines, at different time points and varying culture conditions. Therefore, it is essential to have a standard comparison or normalisation of the target gene levels in the samples, that suppress or compensate sample-to-sample and run-

to-run (intra and inter-kinetic) variation as much as possible (Pfaffl and Hageleit, 2001). Although there are methods to normalise for these variations (such as total RNA, cDNA, mRNA input etc.), these may be influenced by experimental conditions. Thus, normalising to a stable reference gene is the most accredited method available for such variations (Radonić et al., 2004). However, careful assessment and selection of the reference gene is required for reliable transcriptional differences between control and experimental groups.

2.2.5.6 Selection of reference genes

Reference or house-keeping genes are an invariant endogenous control that remains most consistent in expression across given experimental conditions. They are required for basic cell function and are expressed in all cells of the organism under either normal (control) or patho-physiological (experimental) conditions. Therefore, these unaltered genes are used to normalise mRNA levels from different samples within a given experiment. Caution should be taken while selecting these genes as any variation in the normaliser would conceal actual changes in the data and reduce accuracy and sensitivity of the assay (Bustin, 2000).

The Primerdesign geNorm kit with 12-candidate reference genes (for *Mus musculus*) was used to measure gene expression by quantitative PCR using SYBR-green fluorescent dye. Specific product amplification was determined by the generation of a single peaked melting curve, while the melting temperature (Tm) was determined by the composition of the base and length of the oligonucleotide. When assessing expression stability in different groups, the same number of samples were used from each group to avoid bias towards a group with larger number of samples. Reference gene stability was determined using qbase+, a relative quantification framework and software, provided with Primerdesign geNorm kit. Data was uploaded following the instructions in the Primerdesign qBase+ software manual. geNorm analysis is based on geNorm M and geNorm V, detailed explanation of which is provided in Appendix D.

For AMA experiments, four mESC lines from each age group, i.e. Young male, Old Male, and Old Female were used for the evaluation of stable reference genes. Out of the twelve candidate genes within the Primerdesign geNorm kit, five genes showed a high average expression stability of low M value (M<0.5). Figure 2.2 A displays the M value for individual genes and ranking of the least to the most stable genes (from left to right side). As observed in Figure 2.2 B, the optimum number of reference genes required for the current experimental group was two, calculated by V 2/3, where the normalising factor was <0.10. Therefore, genes *Ywhaz* and *Rpl13a* (with least M values) were identified as the most stable reference genes.

2.2.5.7 Data analysis of RT-PCR

To normalise absolute quantification of qPCR, multiple steps in the sample processing need to be optimised and normalised. In general, normalising to a set of reference genes is the most acceptable approach to reduce processing errors and variations caused in experimentation. However, under certain circumstances, expression of several reference genes has been reported to vary, thus misinterpreting the target gene expression. Therefore selecting the most stable reference genes during all experimental treatments is essential. Here, C(t) values of twelve most commonly used reference genes were analysed by the geometric averaging normalisation approach by Vandesompele et al (2002).

Quantitative real time PCR analysis was stored in Opticon Monitior v3.1 software and further details of the process are provided in Appendix D. Samples were prepared from the same batch of RNA and cDNA for the entire set of qPCRs- geNorm for reference gene selection, and for assessing target genes. Relative cycle threshold, C(t) values were normalised with two genes (as calculated by the normalisation factor) with the lowest M values, as determined by the geNorm qbase+ software analysis.

2.2.5.8 Characteristics of negative controls

Negative RT or water controls should not show amplification in the quantitation graphs. If there is amplification, but the melting curves do not coincide with positive targets' curves, then they may be ignored. If the melting curves and Tm coincide, then the C(t)s of the negative controls should be 10 C(t) values less than the samples' (i.e., if a sample is amplified 10 cycles after, then it would theoretically have 1000 times less cDNA amplified and may be discounted). Negative controls in the present study did not show amplification in the quantitation graphs.

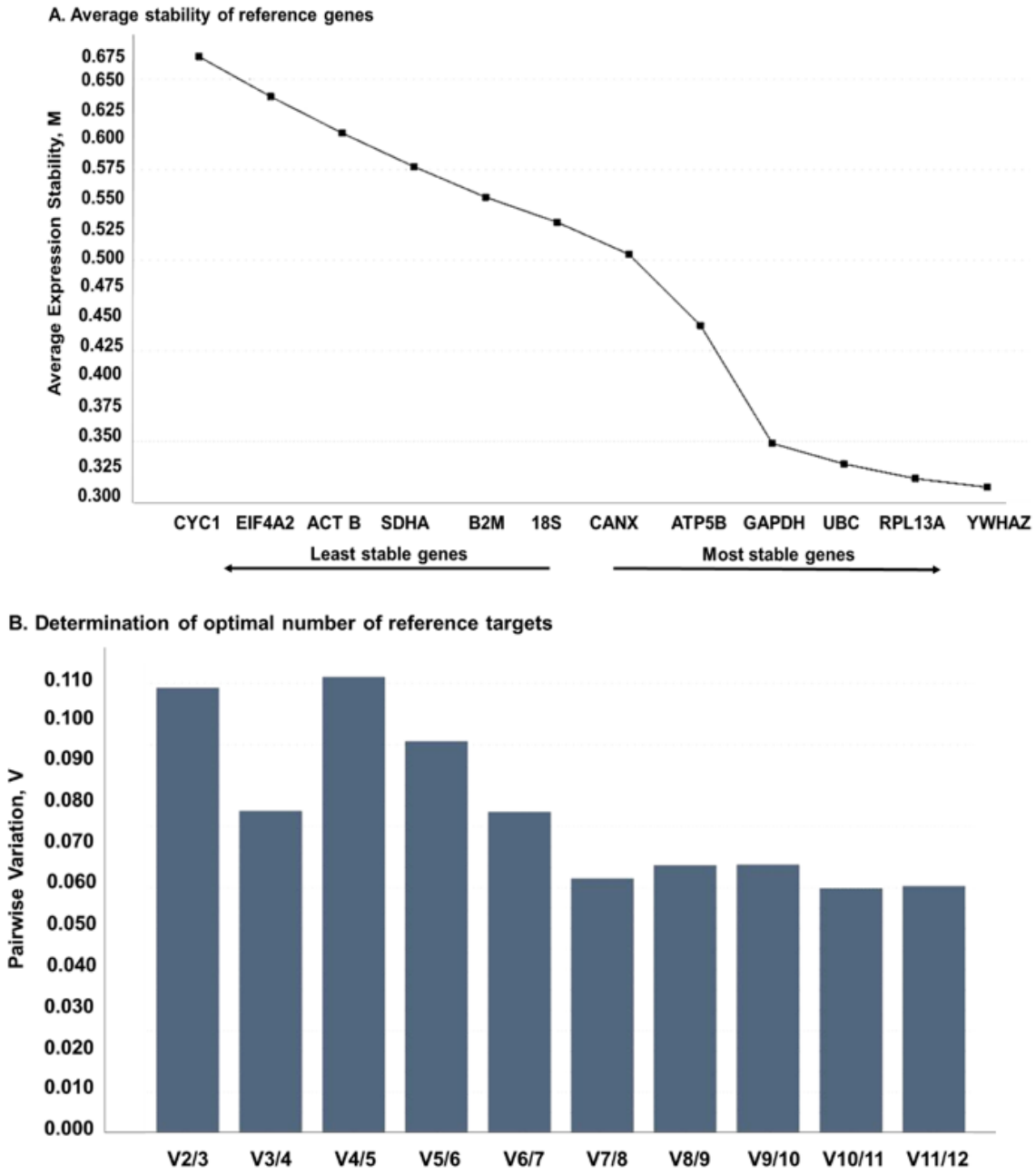

Figure 2.2 geNorm output for reference gene targets analysed for AMA mESC lines.

(A) geNorm analysis showing average gene expression stability M. M was calculated by comparing average pairwise variation of expression between 12 target reference genes (x-axis). M was calculated for each gene individually, and the least stable gene was excluded from the next round of calculations. Two genes with highest reference target stability (average geNorm, M ≤ 0.5) are shown on the right most side on the x-axis (i.e. *Rpl13a* and *Ywhaz*) and were selected for normalisation. (B) Shows optimal number of reference genes selected for normalisation. geNorm V is less than 0.10 when comparing a normalisation factor based on the 2 or 3 most stable targets and suggests that no more than 2 or 3 genes are required for accurate normalisation. In the present AMA mESC experiments, V< 0.15, therefore an optimal number of reference targets= 2.

2.2.5.9 Qualitative analysis of PCR products

PCR products and primers were qualitatively analysed by gel electrophoresis (Section 2.2.3.3.). Briefly, 5 µl of samples were premixed with 1 µl of loading dye and transferred to 1.2% agarose gel (with GelRed™), and run at 100 V for 20 minutes in TBE buffer (Section 2.2.3.3.). Figure 2.3 shows the representative agarose gel electrophoresis image of PCR products of selected reference and target genes for AMA RT PCR experiments.

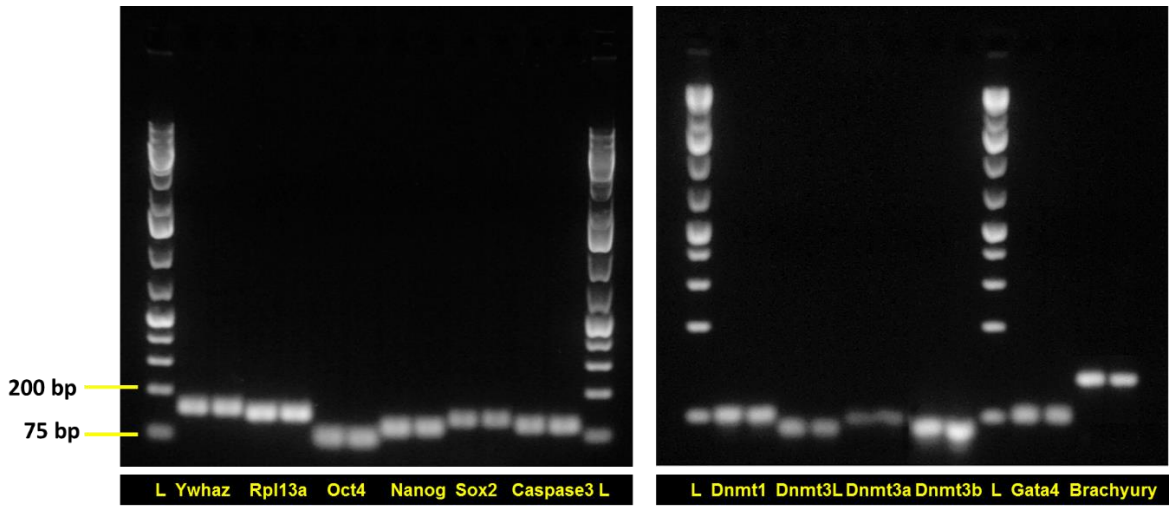

Figure 2.3 Reference and target gene real-time PCR product specificity.

Representative images of PCR products in 1.2% agarose gel electrophoresis. PCR products for selected reference (*Ywhaz* and *Rpl13a*), pluripotency (*Oct4*-61 bp, *Nanog*-76 bp and *Sox2*-105 bp), early apoptotic (*Caspase 3*- 97 bp) markers, epigenetic (*Dnmt1*, *Dnmt3L*- 60 bp, *Dnmt3a*- 65 bp and *Dnmt3b*- 63 bp), and differentiation (*Gata4*-72 bp and *Brachyury*- 117 bp) markers. Genes show single bands at correct amplicon size. Band sizes were determined using GeneRuler 1 kb Plus DNA Ladder.

2.2.6 Cell proliferation and viability assay (Trypan blue dye exclusion)

Proliferation assays were performed on established mESC lines after expansion up to passage 9-11 (P9-P11). mESCs were cultivated (see Section 2.2.2.2) and at the selected passage number, cells were harvested and seeded onto freshly prepared mitomycin C treated MEFs on 24-well plates. Cells were cultured in mESC medium. Cells were harvested up to 96 h and cell counts were performed at every 24 h interval. For counting floating or dead cells, spent media were collected and centrifuged at 14,000 rpm for 5 min. The cell pellet from each sample was re-suspended and cells were counted using a haemocytometer. Viable cells were detected by trypan blue dye exclusion assay. Adhered cells were dissociated with 0.05% trypsin-EDTA and neutralized with the addition of an equal volume of FBS containing MEF medium. Cell clumps were separated from which cell suspension (10 µl) was taken and mixed with an equal volume of 0.4% trypan-blue dye (Sigma, T8154). 10 µl of cell suspension was mounted on the conventional Neubauer

haemocytometer, where the cells were visualized and counted using a phase-contrast microscope. The mean number of cells per well was calculated at each assay time-point i.e., 24 h, 48 h, 72 h and 96 h.

2.2.7 Flow cytometry

Data acquisition was performed using a FACS Calibur flow cytometer and was assessed using FlowJo (version 10) software. To analyze cell samples, live mESC populations were first identified with pluripotency markers (i.e. surface marker, SSEA-1 for apoptosis and intracellular marker, Oct 4 for Ki-67 staining). ES cell size and granularity of overall cell population predicted where the cell population was displayed on the screen. Accordingly, forward scatter (FSC, indicating cell size) vs side scatter (SSC, indicating cell granularity) plots were adjusted and the mESC population was gated to exclude cell debris and MEF cell populations. To make sure there was no contamination by MEFs in the results, they were also analyzed for pluripotent (i.e. Oct4, Nanog, Sox2 and SSEA1) and cell proliferation (Ki67) markers. MEFs did not show any staining, confirming that the pluripotent and cell proliferation markers were selective for mESCs only. The percentage of cells in each population and gate of interest were quantified and presented as graphs using Prism software. (For details of antibodies used, see Appendix C, Table 2; and Additional details of the flow cytometry process are provided in Appendix D.

2.2.7.1 Pluripotency analysis

In addition to relative gene expression, pluripotency of derived mESCs was also determined by analyzing protein expression of the triad of pluripotency markers i.e. Oct4, Nanog and Sox2, by flow cytometry. mESCs (200,000 cells/well) from AMA groups were seeded on 6-well gelatin (0.01%) coated dishes, pre-plated with mitomycin C treated MEF cells (135,000 cells/well). Cells were cultured in mESC medium with KO/SR and LIF for 3 days. On the fourth day, cells were washed, trypsinized and stained with Oct4 only, Sox2 only, Nanog only, Oct4 and Sox2. Cells were prepared following the intracellular (nuclear) proteins staining protocol (Thermo Fisher Scientific, UK) using Foxp3 Fixation/ Permeabilization working solution. Pluripotency markers (Oct4-APC, Nanog-APC and Sox2-PE, Milteni Biotec, UK) were added in 1:10 dilution. After staining, cell samples were re-suspended in flow cytometry staining buffer (PBS with 3% FBS, fetal bovine serum) and stored on ice, until analyzed on FACS caliber. Cells were segregated by size, granularity and fluorescence (Section 2.2.7).

2.2.7.2 Proliferation Assay

Effect of maternal age on cell proliferation of mESCs was determined by analysing protein expression of a cell proliferation marker, Ki67. Ki67 is a 360 kDa nuclear protein, commonly used to detect proliferating cells (Preusser et al., 2008). Antigens are detected only within the nucleus during interphase, although during mitosis, proteins are relocated on chromosomal surface (Scholzen and Gerdes, 2000). Ki67 is induced when quiescent arrested cells enter G1-S phase, and is present (and expressed) in all phases of cell cycle, i.e. G1, S, G2 and mitosis, but not during the resting phase (G0) (Endl et al., 1997; Pozarowski and Darzynkiewicz, 2004). This strict association of Ki67 exclusively with proliferating cells makes it a suitable indicator of 'growth fraction' in a given population of cells.

Protein expression of Ki67 was analysed using flow cytometry. Mouse ESCs (150,000 cells/well) were seeded on 6-well, gelatin (0.01%) coated pre-plated mitomycin C treated MEF cells (135,000 cells/well). Cells were collected and processed for analysis every 24 h, up to a total of 96 h. Briefly, cells were washed with PBS, trypsinized and stained for Ki67 only, Oct4 only, Ki67 and Oct4, where Oct4 was used as a positive mESC marker. While Ki67 was conjugated with FITC, Oct4 was APC conjugated. Cells were prepared following the intracellular (nuclear) protein staining protocol (Thermo Fisher Scientific, UK), as described in detail in Section 2.2.7.1. Ki67 expression was also analyzed by fixing the mESCs with 70% ethanol, as practiced in several established protocols. However, as both protocols (i.e. fixation by ethanol and Foxp3 Fixation/ Permeabilization working solution, Section 2.2.7.1) gave identical results, intracellular (nuclear) protein staining protocol was chosen as the final working protocol for all experiments. Experiments were performed twice, with an n= 4 per AMA group.

2.2.7.3 Apoptosis and cell death assay

Apoptosis is a natural process involved in development and maintenance of health of an organism. Unlike necrosis, apoptosis is a regulated and controlled process that is essential for a cell's life cycle. A damaged cell's DNA may undergo apoptosis to maintain normal functioning of an organism. The events generally include blebbing, cell shrinkage, nuclear fragmentation, chromatin condensation and chromosomal nuclear fragmentation. In this chapter, cell apoptosis and cell death were measured using Annexin V-PI binding assay. Briefly, annexins are a family of calcium-dependent phospholipid-binding proteins which play an important role in the communication between cellular membranes and their cytoplasmic environment. Annexins bind to phosphatidylserine (PS) to identify apoptotic cells, therefore influencing cell life cycle and exocytosis. In healthy cells, PS is predominantly located along the cytosolic side of the plasma membrane. Upon initiation of apoptosis, PS loses its asymmetric distribution in the phospholipid bilayer and translocate to the

extracellular membrane. Based on the annexin V affinity to PS, apoptotic cells are distinguished from live cells. Annexin V staining conjugated with a fluorescent tag, such as Fluorescein-5-isothiocyanate (FITC) paired with viability dyes such as propidium iodide (PI) is widely used to identify apoptotic stages by flow cytometry techniques. In early stages of apoptosis, the plasma membrane excludes PI. Therefore, cells display only annexin V+/PI- staining. During late-stage apoptosis, loss of cell membrane integrity allows annexin V binding to cytosolic PS, as well as cell uptake of PI. Hence, the annexin V-PI binding assay is a robust tool for distinguishing between live (annexin V-/PI-), early apoptotic (annexin V+/PI-), necrotic or late apoptotic (annexin V+/PI+) and dead (annexin V-/PI+) cells.

Mouse ESC lines were cultured (see Section 2.2.2.2) and expanded between P9 to P11. The cells were trypsinized and seeded at a starting cell density of 100,000 cells/well on freshly prepared MMC-treated MEFs (135,000 cells/well), on 6-well plates under standard humidified conditions (at 37 °C in 5% CO_2 in air). Cells were analyzed at every 24 h interval for a time course of 96 h from the day of seeding the cells. To assess cell viability, floating cells were collected, centrifuged and added to adherent cells, which were harvested by trypsinization. After centrifugation, cells were stained with AnnexinV-FITC only, PI only, SSEA-1-APC only, Annexin V-FITC with PI and SSEA-1-APC, and left unstained as negative control. SSEA-1 staining was used as a positive marker for pluripotent mESCs, in order to separate mESCs from MEFs. Positive control for apoptosis was derived by treating the cells with Etoposide. Etoposide is an antitumor agent that blocks the cell cycle in S-phase and G2 phase, and induces apoptosis. Initially, three concentrations of Etoposide were tested- 10µg/ml, 20 µg/ml and 30µg/ml for either 4 h or overnight (12 h) incubation. Based on cell survival rates and positivity for Annexin V, final concentration of 20 µg/ml Etoposide, incubated for 4h was selected for future experiments. Floating or dead cells were considered as positive samples for PI stain. These cells accounted for the positively apoptotic and necrotic population of cells before getting impacted by the attrition caused during processing the samples for flow cytometry analysis.

Cells stained for SSEA-1 only and triple staining were incubated with the conjugated antibody SSEA-1-APC at 4°C in the dark for 10 min, while remaining samples were incubated in the same conditions but without the antibody. For apoptosis analysis, cells were prepared and stained following the eBiosciences AnnexinV-FITC Apoptosis kit protocol (BMS500FI). Immediately after, the samples were stored on ice, and analyzed by flow cytometry.

For data analysis, population of cells positive for SSEA-1-APC fluorophore i.e. mESC or pluripotent cells, were selected first and only the positive cells were gated and analyzed for Annexin V-FITC and PI staining. Annexin V-FITC exhibited anti-phospholipase activity and bound to PS. FITC labelling allowed direct detection by flow cytometric analysis and counterstaining by PI enabled the

discrimination of apoptotic cells by staining necrotic cells. 20,000 cell events were recorded using a FACS Calibur flow cytometer. Data were acquired as detailed in Section 2.2.7. SSEA-1 staining and FSC-SSC gates were used to exclude MEF cell populations and cell debris. The percentage of apoptotic cells was determined by generating a dual-colour dot plot (Annexin V-FITC (FL-1) vs. PI (FL-2)) and then setting a quadrant marker based on unstained and single-labelled control samples. No electronic compensation was required.

2.2.8 Immunocytochemistry (ICC) staining

Mouse embryonic stem cells (30,000 cells/ well) were cultured on inactivated gamma irradiated MEFs (27,000 cells/ well) at the given density (on sterile coverslips) on 24-well plates. mESCs were fixed at 70% of confluency. The density and days of culture were fixed to make sure any changes in cell proliferation between the groups were also recorded. Once the cells reached the desired confluency, they were washed with PBS, fixed with 4% paraformaldehyde (PFA) solution for 15 min and stained directly after or stored in PBS at 4°C until required.

For staining, cell samples were washed (with PBS) and permeabilized in 0.2% Triton X-100 in PBS for 20 min at RT. Non-specific antibody binding was blocked with 3% BSA containing 0.2% Triton X-100 in PBS for 30 min at RT after which the samples were incubated with the optimised dilution of primary antibody, in a moist chamber at 4°C overnight. Cells were incubated with the appropriate Alexa-Fluor conjugated secondary antibody in the blocking solution, in the dark, for one hour at RT (for details of antibodies used, see Appendix C, Table 1). Cell nuclei were counterstained with DAPI (4', 6-diamino-2-phenylindole dilactate), which was pre-diluted in Mowiol mounting media. Coverslips were left to set on the microscope slide at RT for 30 minutes before images were captured by fluorescence microscopy.

2.2.9 Statistics

Statistical analysis was performed using Statistical Package for the Social Sciences (i.e. IBM SPSS Statistics 24) or independent Student's t-test. Data was tested for assumptions of normality using the Shapiro-Wilk normality test (GraphPad Prism 7 software) and considered normal where values were over significance cut off ($P > 0.05$). Variance homogeneity was analysed using the F-test. All data are expressed as means ± SEM. $P<0.05$ was considered statistically significant and $P<0.1$ was considered as trending towards significance.

2.3 Results

2.3.1 Effect of maternal age on embryo development at E3.5

Preimplantation embryos (from C57BL/6 females mated with CBA males) were flushed and collected in warm embryo culture medium, KSOM. Figure 2.4 illustrates oocytes and different stages of preimplantation embryo development (E1.5-E4.5) from C57BL/6 females.

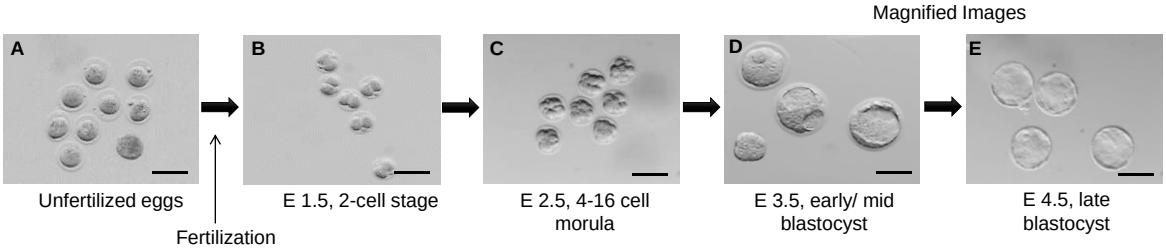

Figure 2.4 Oocytes and pre-implantation stage embryos from day 0 to day 4.5 after fertilization.

Representative images of oocytes and embryos of C57/BL6 females mated with CBA males. Mouse embryonic stem cells were derived from mid blastocysts, E3.5 (D). Magnification bar = 200µm.

To assess the effects of maternal age on pre-implantation embryo development *in utero*, embryos were flushed and collected at E3.5. Embryos were separated by maternal age (Young, 7-8 weeks or Old (advanced maternal age, AMA, 7-8 months) and based on their morphology (as described in Section 2.2.1.2), they were classified as unfertilized oocytes, morulae, early-, mid- and late-stage blastocysts, or degenerated embryos. Figure 2.5 shows representative images of embryos derived at E3.5 from young and old mothers.

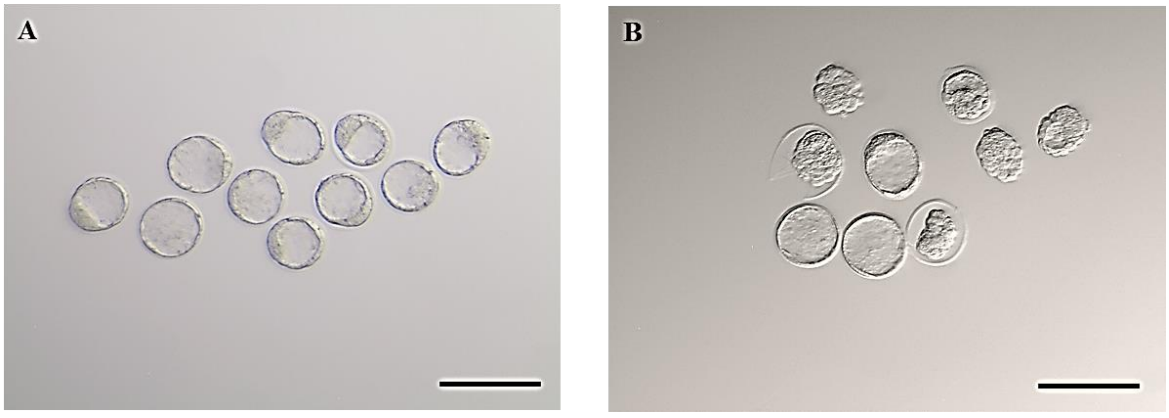

Figure 2.5 Representative images of embryos derived from (A) Young (7-8 weeks) and (B) Old (7-8 months) female mice (C57BL/6 females mated with CBA males) at E3.5.

Embryos were flushed and morphologically categorized into differed stages of development. Magnification bar= 200 µm.

Embryos were collected from ten Young and ten Old mothers, and differences in embryo stage assessed. As recovered embryos also included a small population of unfertilized oocytes and degenerated embryos, differences in proportions are explained as 'of fertilized' (i.e. of fertilized embryos only), 'of total blastocysts' (i.e. of early-, mid-, and late- blastocysts only), and as 'of total' (i.e. all stage- embryos, including the unfertilized oocytes and degenerated embryos). After embryos were retrieved, weight of dams was also recorded (Appendix B, Figure 1).

Although no differences in the total number of embryos derived between the Young and Old group were observed, older mothers (7-8 months) had increased proportions of early stage embryos and therefore yielded fewer mid-stage and total blastocysts compared to younger mothers (7-8 months) (Figure 2.6). Retrieved embryos were frozen and stored at - 80°C for later use.

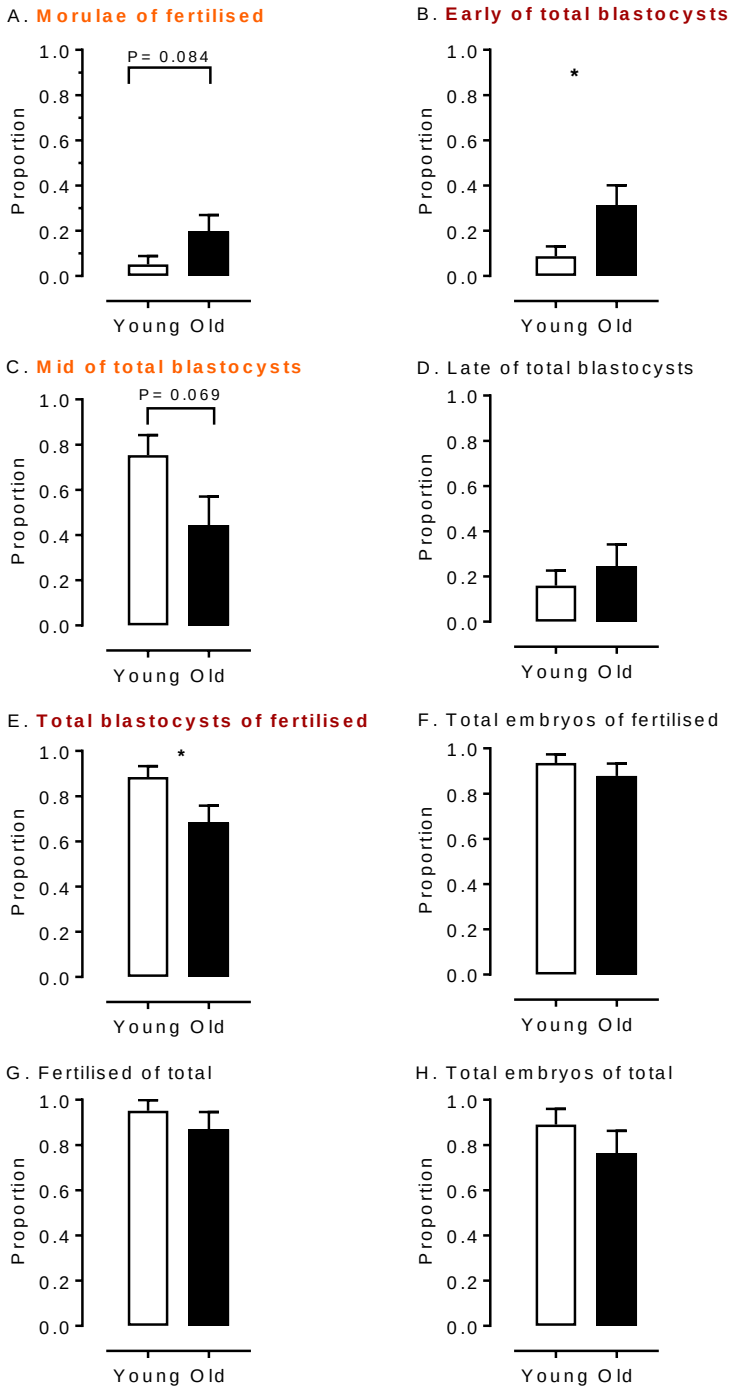

Figure 2.6 Effect of maternal age on developmental stage of embryos at E3.5.

Embryos were flushed from Young (7-8 weeks) and Old (7-8 months) C57BL/6 females at E3.5 and classified into different stages of development. Data highlighted in red are significant at P<0.05, and those in orange at P <0.1. Older dams yielded fewer (P = 0.069) mid (C) and total (P = 0.039) (E) blastocysts, and more (P = 0.084) morulae (A) and early blastocysts (P = 0.034) (B) than younger dams. In graphs G) and H), 'total' also includes degenerated embryos and unfertilised eggs (n=10 dams with 8-9 embryos/ dam). Vertical bars represent SEM. * indicates P<0.05.

2.3.2 Derivation of mouse embryonic stem cells (mESCs)

As described in Section 2.2.2.2, mouse embryonic stem cells (mESCs) were derived from mid-blastocysts collected at E3.5. Briefly, blastocysts were flushed from Young and Old dams, washed in H6BSA, and immediately transferred to 6-cm dishes with pre-plated MMC-treated MEFs containing mESC medium. Dishes were incubated at 37°C in 5% CO_2. The first 2-3 days are critical for embryo adaptation to *in vitro* culture, therefore culture dishes were left undisturbed. Figure 2.7 shows the early stages of blastocyst hatching that occur after 3 days in culture. As shown in Figure 2.7, E and F, the inner cell mass (ICM) grows out of the zona and attaches to the fibroblast cell matrix.

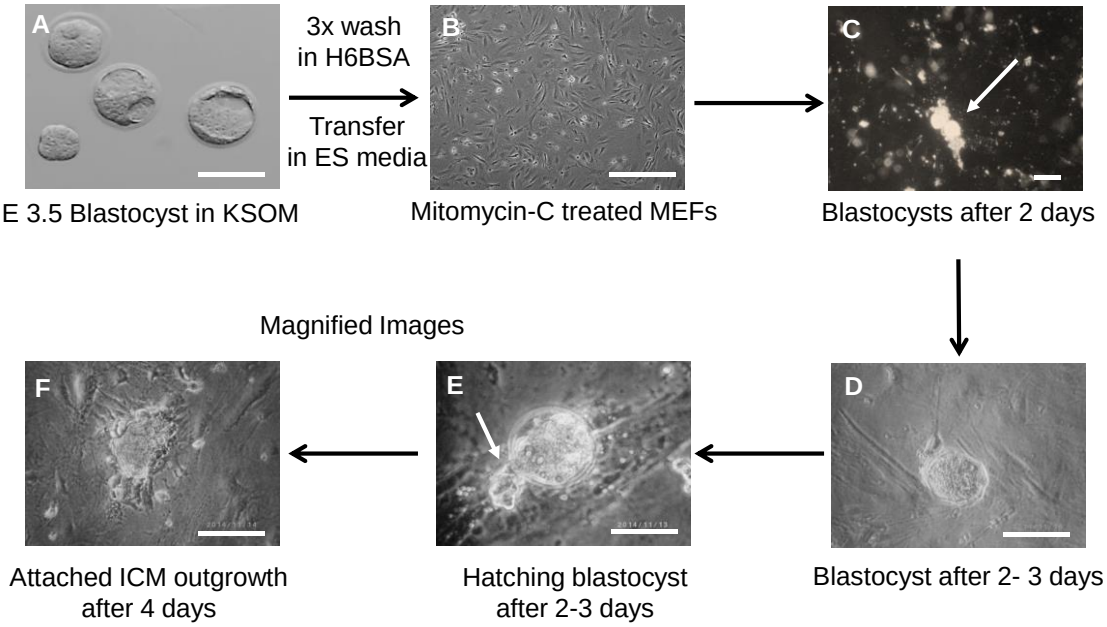

Figure 2.7 Representative images showing transfer and attachment steps of E3.5 blastocysts to mouse embryonic fibroblasts (MEFs).

(A) Mid blastocysts at E3.5 were flushed in saline solution, washed in H6BSA and transferred to (B) MMC treated MEFs in ES medium and (C, D) left undisturbed for two days. The arrow in (C) shows two blastocysts on a MEF dish. (E) On the third day from transfer, the embryo hatches from the zona pellucida and the inner cell mass (ICM) of the blastocyst grows out (indicated with an arrow) and (F) attaches to the fibroblast matrix. Magnification bar= 200 µm, except for C) = 50 µm.

Once ICM cells attached to MEFs (i.e. 3 to 4 days after transferring blastocysts), the outgrowths were picked, dissociated with trypsin-EDTA, and transferred to individual wells of fresh MMC-MEF 96-well dishes. The first ES clones were observed after 4-5 days from the day of seeding, and were further cultured for 3-4 days. Initially, cells grew at a slower rate (up to P4) compared to later passages. This may be influenced by the low cell density at lower passages. Therefore, a sequential increase in

surface area of culture dishes also plays an important role in the growth of ES colonies. Figure 2.8 (A-E) illustrates the increasing size of ES colonies with time and subsequent passaging.

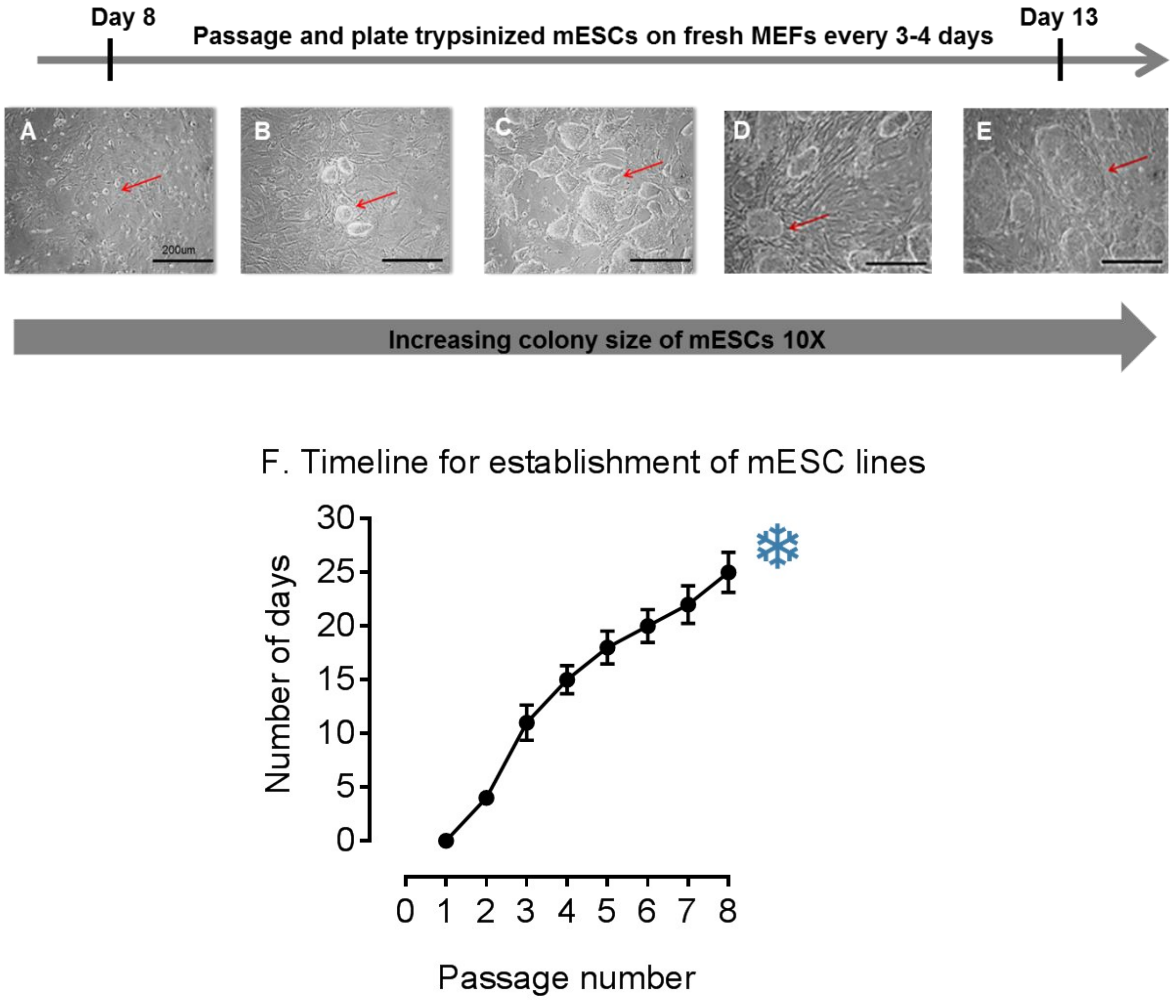

Figure 2.8 Representative images of mESC colonies increasing in size (A-E) and associated timeline establishment (F).

E3.5 blastocysts were transferred and developed into embryonic stem cells (mESCs) on mitomycin C-treated mouse embryonic fibroblasts (MMC-MEFs). Images (A-E) show increase in mESC colony size with passaging and culture in mES medium. From the day of blastocyst transfer to MEFs (day 0), it took 8-9 days for the first mESC clones to appear (A). The number of cells and colony size increased subsequently with time (B-E). ES cell timeline (F) represents the average time of establishing a mESC line (i.e. 26 days) before freezing and the standard deviations for n= 43 mESC lines, and the time interval between subsequent passages (i.e. 3-4 days). Magnification bar= 200 µm.

Cells were maintained at 70-80% confluency, and passaged every 3 to 4 days to avoid overcrowding. This is essential for maintaining a pluripotent state in ES cells, as high cell density can induce metabolic shifts, contributing to cell differentiation (Singh et al., 2017). From the time of collecting

and transferring blastocysts to MEF cells at E3.5, it took around eight passages (lasting 27-30 days) to establish each mES cell line (Figure 2.8 F). Although the growth rate of ESCs improved in the later passages, the overall derivation efficiency of mESC lines remained low (see next paragraph).

2.3.2.1 Optimization of mESC derivation protocol

It is known that different mouse strains require different culture conditions for establishment of ESC lines (Kawase et al., 1994; Baharvand and Matthaei, 2004). Furthermore, ESCs derived from the same strain, same mother, or even the same blastocyst (ICM), display heterogeneity (Hayashi et al., 2008; Martinez et al., 2012). Such differences further enhance with multiple in vitro culture, which may induce exaggerated phenotypic characteristics in the cells. It is therefore essential to practice optimized derivation procedures to minimize confounding factors while interpreting data.

In the present study, preliminary mESC lines were derived using our standard protocol. Females used for these derivations were limited to the Young group (7-8 weeks) due to the unavailability of Old mothers (7-8 months) when the experiments were carried out. Given the low efficiency of the initial protocol, the method of derivation was subsequently modified and an optimized protocol established. The flow diagram (Figure 2.9) illustrates the initial protocol with the modifications highlighted in red.

Derivation efficiency was influenced by the time taken to transfer blastocysts from embryo culture medium (KSOM) to the MMC-MEF dish with mESC medium. Prolonged washing in H6BSA also affected embryo quality, developmental ability, and ESC derivation efficiency. Other factors that lowered the efficiency included poor enzymatic dissociation and mechanical disaggregation of ICM cells, which often gave rise to clumps of differentiated cells. Additionally, avoiding centrifugation steps during early passages (P1-P3), and a systematic increase in the surface area of culture dishes, also improved mESC survival, growth, ultimately increasing the number of ES lines derived.

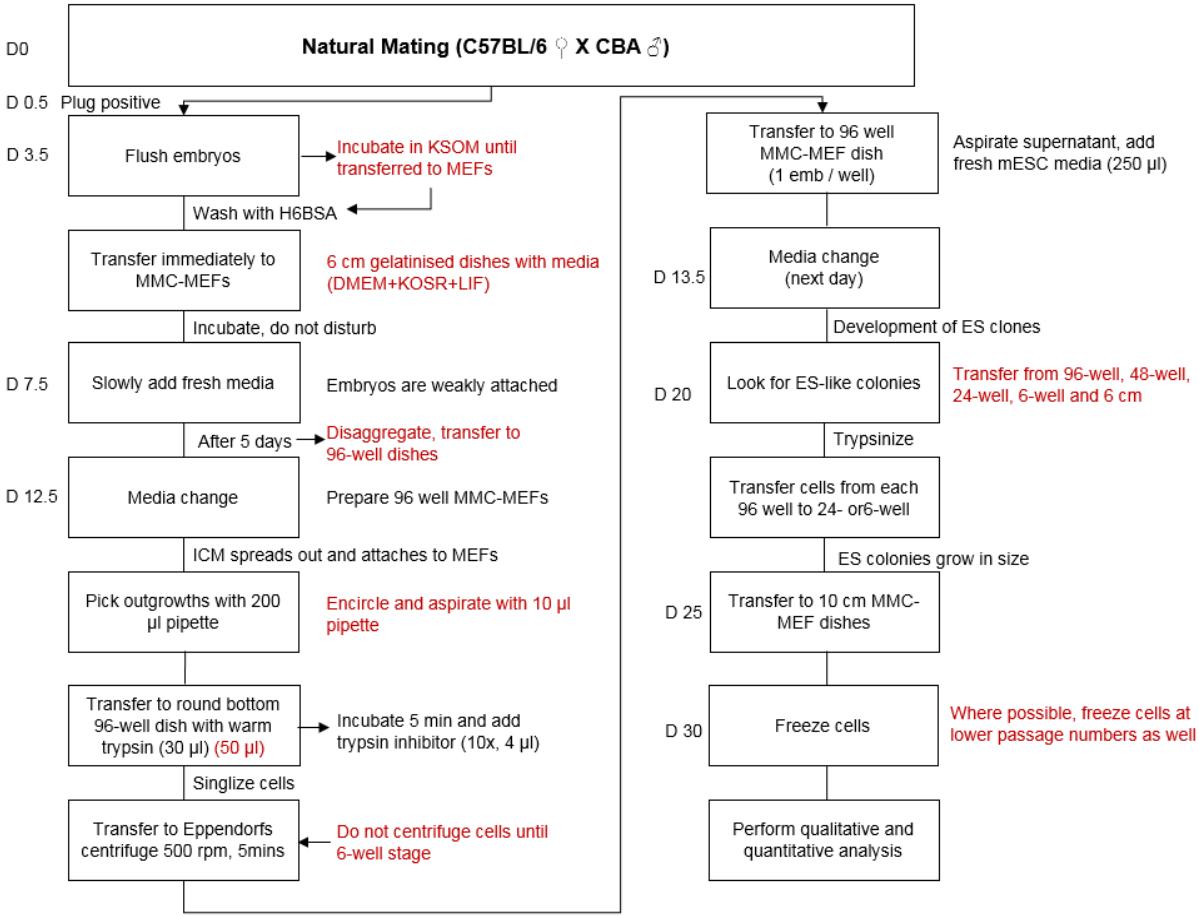

Figure 2.9 Flowchart representing optimization of mESC derivation protocol in a systematic manner.

The modifications made in intermediate steps are illustrated in red.

Although the initial protocol was modified only slightly, altogether, it increased the developmental potential of mESC lines (Figure 2.10). The x-axis represents the time of blastocyst transfer to MMC-MEFs, or the beginning of mESC-derivation process, and the y-axis indicates the derivation efficiency calculated by the ratio of the number of embryos that produced mESC lines to the total number of embryos collected from the dam.

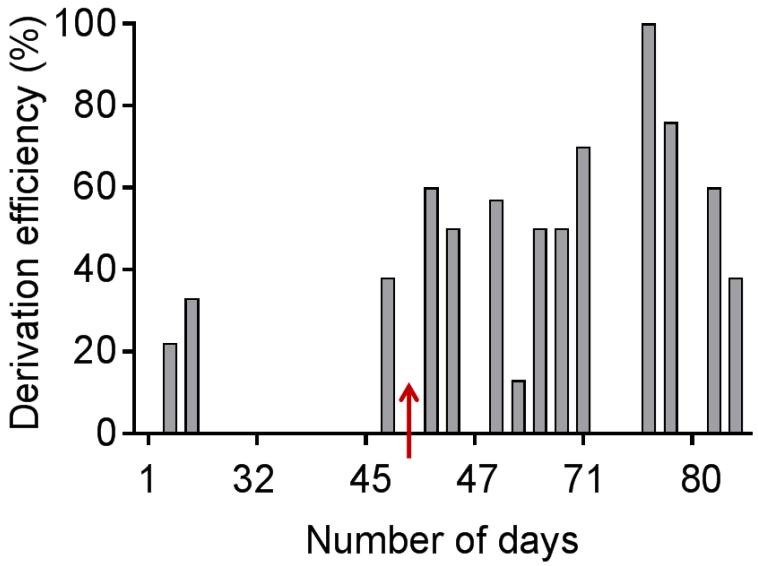

Figure 2.10 Increase in mESC derivation efficiency following optimization.

The number of mESC lines derived and established increased 5-fold after optimization. The grey bars represent cell lines derived from C57BL/6 females. The red arrow on x-axis indicates the time of when the optimized protocol for mESC lines was introduced. Days from date of first derivation (14th January 2014).

Following optimization (indicated by red arrow), there was a five-fold increase in derivation of ES lines. The modified protocol was therefore adopted for deriving the remaining ES lines reported in this thesis.

2.3.3 Effect of Advanced Maternal Age (AMA) on mESC derivation

As described in Section 2.2.2.2, mESC lines were derived from E3.5 blastocysts of both Young (7-8 weeks) and Old (7-8 months), and cultured on MMC-MEFs in ES medium. ICM outgrowths were cultured individually and each mESC line was generated from an individual blastocyst. Table 2.3 presents the total number of C57BL/6 females used for the derivation of mESC lines, the number of females that ultimately gave rise to mESCs, and the total number of embryos collected at E3.5 for derivation of mESC lines. The derivation efficiency of mESC lines isolated from

individual Old dams (45%) was slightly higher compared to Young dams (36%), although statistically insignificant (Figure 2.11).

Table 2.3 Total number of ES cell lines isolated in Young and Old groups.

Maternal age	Total dams	Dams producing embryos	Dams deriving mESCs	Total embryos	mES lines derived
Young (7-8 weeks)	14	11	4	28	10
Old (7-8 months)	14	13	9	62	28

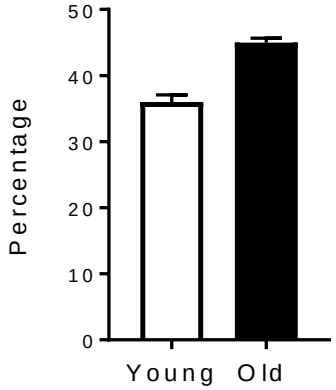

Figure 2.11 Derivation efficiency of Young and Old mESC lines.

The percentage of blastocysts yielding ES cell lines isolated from young (7-8 weeks) and old (7-8 months) C57BL/6 females. The number of blastocysts collected per mother was recorded and the percentage of those blastocysts yielding mESC cell lines calculated. Young, n=28 total blastocysts from 11 mothers vs. old, n= 62 total blastocysts from 13 mothers. Young mothers gave rise to n=10 mESC lines, and old mothers gave rise to n=28 mESC lines. Vertical bars represent SEM.

2.3.4 Characterization of derived mESCs

2.3.4.1 Sexing of mESC lines

To analyse gender of the derived mESCs, genes- *Sry* and *Zfy*, and *DxNds3 (*or *Nds3),* located in the sex-determining regions of the Y- and X-chromosome respectively, were amplified by multiplex PCR. The amplified PCR products were run on agarose gel following gel electrophoresis and bands were observed at 617 bp for *Zfy*, 404 bp for *Sry*, and 244 bp for *DXNds3*. Figure 2.12 shows a representative gender specific reaction where a mESC line shows positive amplification for both X and Y chromosome genes indicating male gender cell line. A female cell line shows an amplified band for only X-chromosome gene, *DxNds3*.

Figure 2.12 Gender analysis of DNA isolated from mESC lines by multiplex PCR.

Band sizes were determined using a Bioline Hyperladder II DNA size marker (left column; ladder). The lanes contained 50 ng of DNA isolated from mESC lines, and 50 ng of pure DNA from positive male and female control tail biopsies. In this image the mESC line was identified as male as it displayed strong bands for Y- *Sry* (619 bp) and *Zfy* (404 bp), and X- *Nds3* (244 bp) chromosomal genes.

Table 2.4 shows the proportion of male and female ESC lines for both Young and Old groups. The total number of male lines isolated was much higher than the number of female lines for both treatments (86.84% total male mESC lines).

Table 2.4 Results of PCR sex analysis of mESC lines according to maternal age.

Maternal Age	Total number of mESC lines	Male (%)	Female (%)
Young (7-8 weeks)	10	9 (90)	1 (10)
Old (7-8 months)	28	24 (86)	4 (14)
Total	38	33 (86.84)	5 (13.15)

As the Young group generated only one female mESC line, effects of maternal age were evaluated only between male mESC lines (i.e. Young male vs Old male mESC lines). However, as animal studies have displayed maternal age effects on sexual dimorphism (Velazquez et al., 2016), gender comparisons were made (although limited to) within the Old group (Old Male vs Old Female mESC lines).

2.3.4.2 Karyotype analysis of mESC lines

2.3.4.2.1 Optimization of karyotyping techniques

For analysis, 70% confluent mESCs were treated with Colcemid. The addition of Colcemid improved chromosome counting as it arrested the mES cells in metaphase, producing

distinguishable chromosome spreads (Figure 2.13, C-F). The cells were washed, trypsinized, treated with KCl (hypotonic solution) and fixed (see Section 2.2.4). After drying the fixative, slides were incubated with Giemsa stain.

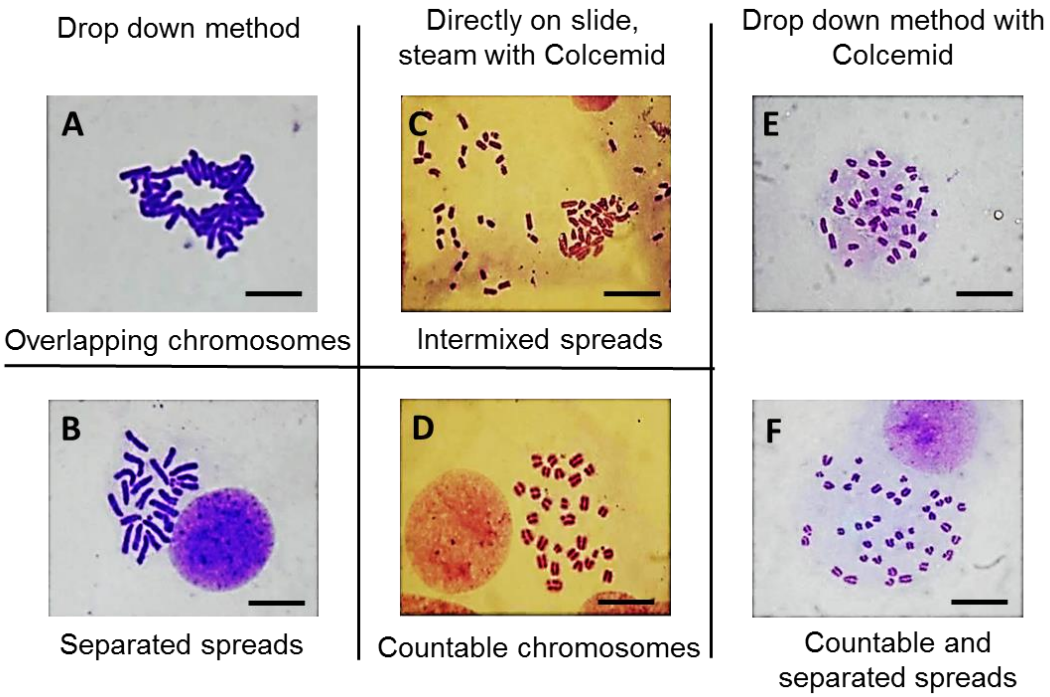

Figure 2.13 Optimization of karyotype analysis.

Confluent mES cells were isolated and prepared for chromosome spreads. Results for three methods (A, B) drop-down method without Colcemid, (C, D) placing the cells directly on the slide with Colcemid, and (E, F) drop-down method with Colcemid. The drop-down method with Colcemid (E, F) proved to be the most efficient method as it produced high numbers of separated and countable spreads, and was adopted for karyotype analysis of all mESC lines. Chromosomes were stained with Giemsa stain. Images were captured at 460 µm under oil.

Slides were prepared either by dropping the cells on the slides from an approximate height of 20 cm (drop-down method, Figure 2.13, A and B), or directly on the slide surface using a micropipette, after which they were briefly exposed to steam (Figure 2.13, C and D). While the drop-down method produced separated spreads, the chromosomes (often in asynchronous mitotic phases) overlapped (Figure 2.13, A), generating erroneous data. Steam helped in swelling chromosomes thereby generating distinguishable spreads (Figure 2.13, D). However, it caused spreads to float and intermix with each other, making it difficult to count individual spreads accurately (Figure 2.13, C). As the drop-down method produced separated chromosome spreads and Colcemid helped in arresting cells in metaphase thereby increasing accuracy of counts, the combined treatment i.e. drop-down method with Colcemid (Figure 2.13, E and F) was the most efficient, and therefore practiced for all future Karyotype experiments.

2.3.4.2.2 Effect of Maternal Age on mESC karyotype

To assess the effect of maternal age on karyotype (number of chromosomes) in the derived mESCs from Young and Old dams, chromosome spreads were prepared from lines between passage numbers 10-11. At least 70 chromosome spreads (individual cells) were counted per mESC line. They were categorised as aneuploid, euploid or polyploid spreads (Figure 2.14, A-C).

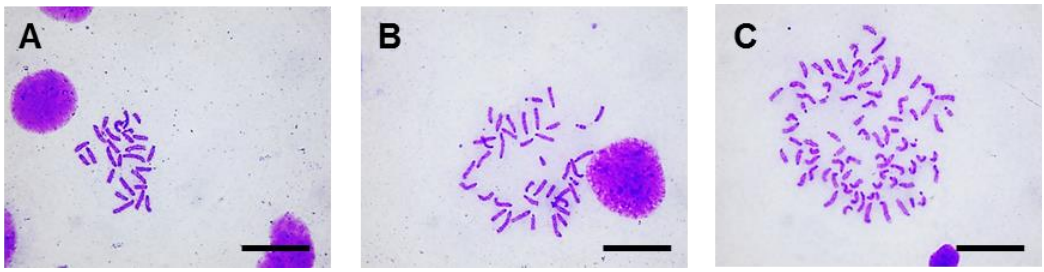

Figure 2.14 Karyotype analysis to detect chromosomal abnormalities.

(A-C) Representative images of metaphase chromosome spreads (derived by drop-down method, with Colcemid) of mESC lines showing (A) aneuploidy (27, 2n<40), (B) euploidy (40, 2n=40) and (C) polyploidy (81, 2n>40). Chromosomes were stained with Giemsa stain. All images were captured at 460 µm under oil.

Overall, the majority of derived mESC lines were euploid. Separated by maternal age, Young male mESCs showed greater euploidy (P=0.039) (Figure 2.15 A), and consequently reduced aneuploidy with 38 chromosomes (P=0.090) (Figure 2.15 B) and with chromosomes with less than 37 chromosomes (P=0.005) compared to the Old male mESC lines (Figure 2.15 C). Separated by gender, Old females showed greater number of cells with 38 chromosomes (P=0.033) (Figure 2.15 E) compared to Old male mESC lines, although no differences were observed between euploidy (Figure 2.15 D). Proportion of cells assessed for polyploidy were not statistically significant in either groups, however the Old male mESC lines (0.140 ± 0.071) had greater number of polyploid spreads compared to the Young male mESC lines (0.079 ± 0.052). Old male mESC lines (0.181 ± 0.100) also displayed increased polyploid spreads than Old female mESC lines (0.121 ± 0.083), although they were not statistically significant.

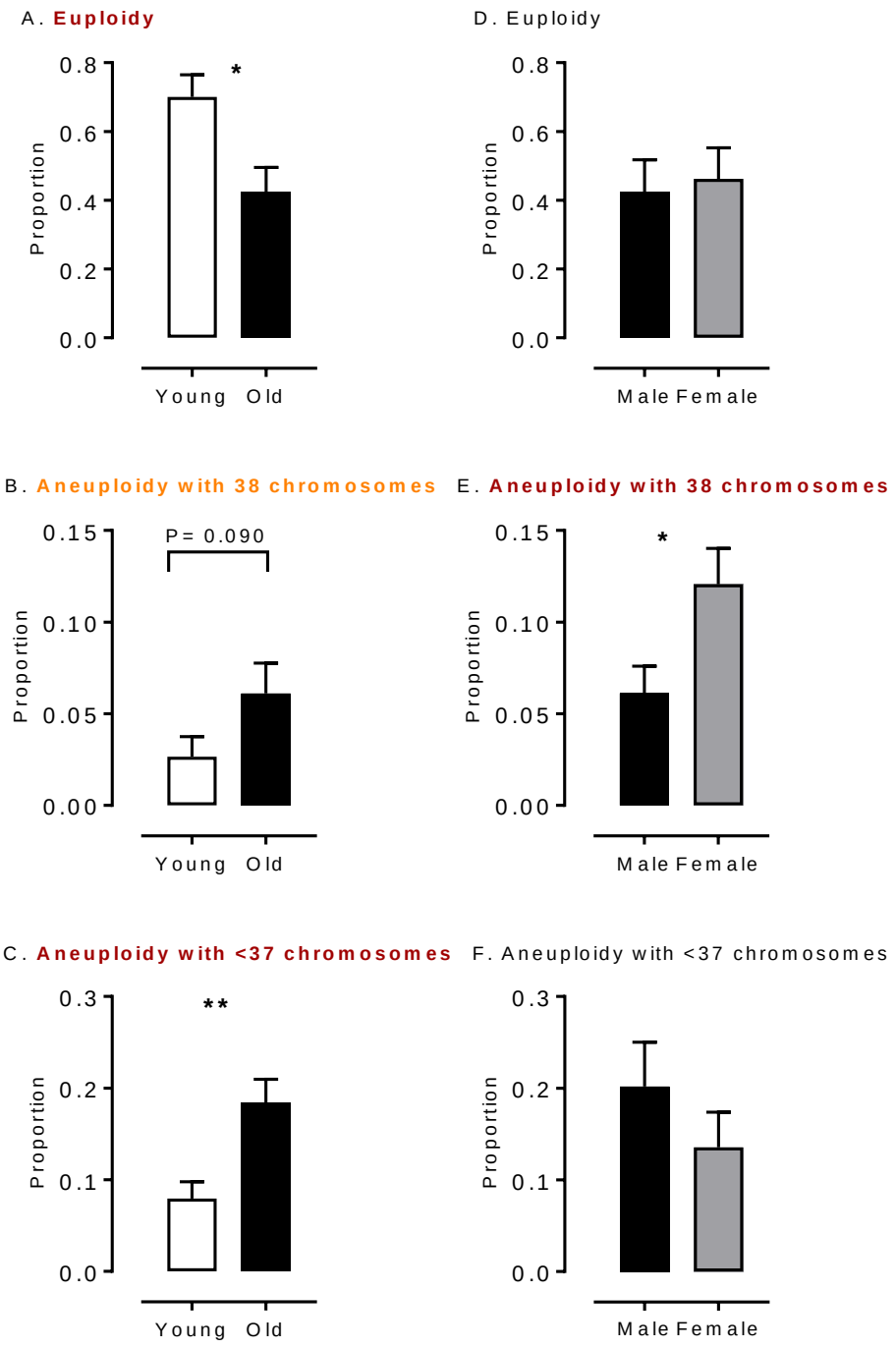

Figure 2.15 Effect of maternal age on karyotype of Young and Old mESCs lines.

Distribution of euploid and aneuploid cells. Data presented as proportion of total number of spreads counted, where data highlighted in red are significant at P<0.05, and those in orange at P <0.1. Old male mESC lines exhibit reduced (P=0.039) incidences of euploidy (A) and increased incidences of aneuploidy with 38 chromosomes (P=0.090) (B) and <37 chromosomes (P=0.005) (C) compared to Young male ES lines. Old Female mESC lines showed no difference in proportion euploid cells (D) and aneuploid cells with <37 chromosomes (F). However, Old Female mESC lines had a greater (P=0.033) proportion aneuploid cells with 38 chromosomes compared to Old Male mESC lines (E). Data presented as means ± SEMs based on n = 6 for Young and Old male mESC lines; n=4 for Old Female mESC lines. * indicates P<0.05 and ** indicates P<0.005.

As stated previously, cell lines with more than 50% euploid (2n = 40) spread counts were selected for further experiments. It is known that mESC karyotype may also vary with extended *in vitro* culture (Rebuzzini et al., 2008). Likewise, lines with even seemingly normal karyotype (>50%) may have an increased percentage of a specific type of aneuploidy, for instance a high number of spreads with 39 or 41 chromosomes (as observed by Gaztelumendi and Nogués (2014)), which may be noteworthy.

2.3.5 Functional Characterization of derived mESCs

2.3.5.1 Pluripotency (Stemness/ markers for mESC) analysis

2.3.5.1.1 Differences between Young male vs Old male mESC lines

a) Relative gene expression (RT PCR)

While no differences were observed in the relative expression of pluripotency genes *Oct4* and *Nanog, Sox2* expression was reduced (P=0.049) in Old male compared to Young male mESC lines (Figure 2.16). Additionally, significant interaction was observed between the expressions of *Oct4* (P=0.018) and *Sox2* (P=0.003) on *Nanog*.

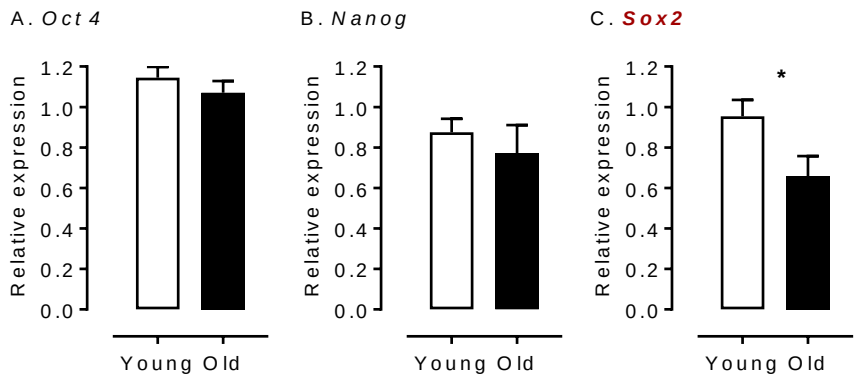

Figure 2.16 Relative gene expression for pluripotency markers in undifferentiated male (young (7-8 weeks) vs old (7-8 months)) mESC lines.

Genes of interest were normalized to *Ywhaz* and *Rpl13a* within geNorm. Old male mESC lines showed reduced expression for *Sox2* (P=0.049), highlighted in red. Data presented as means ± SEMs based on n = 4 mESC lines. * indicates P< 0.05.

b) Protein expression (Flow cytometry)

Expression of pluripotency markers Oct4, Nanog and Sox2 was analysed by flow cytometry following intracellular (nuclear) staining protocol (Section 2.2.7.1) and revealed no differences between Old and Young male mESC lines (Figure 2.17). However, interaction was observed between the expressions of Oct4 (P=0.01) and Sox2 (P=0.029) on Nanog.

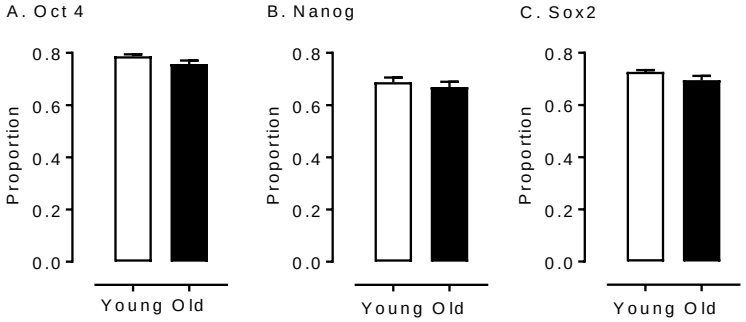

Figure 2.17 Quantitative analysis of protein expression for pluripotency markers in undifferentiated male (Young (7-8 weeks) vs Old (7-8 months)) mESC lines.

Pluripotent cells are presented as the proportion positive of total cells (stained and unstained). No differences were observed between the groups. Data are presented as means ± SEMs based on n = 4 cell lines.

2.3.5.1.2 Differences between Old Male vs Old Female mESC lines

a) **Relative gene expression (RT PCR)**

No differences were observed in the relative expression of pluripotency genes *Oct4, Nanog* and *Sox2* between Old Male and Old Female mESC lines (Figure 2.18). Additionally, an interaction was observed between the expressions of *Oct4* (P=0.075) and *Sox2* (P<0.001) on *Nanog*.

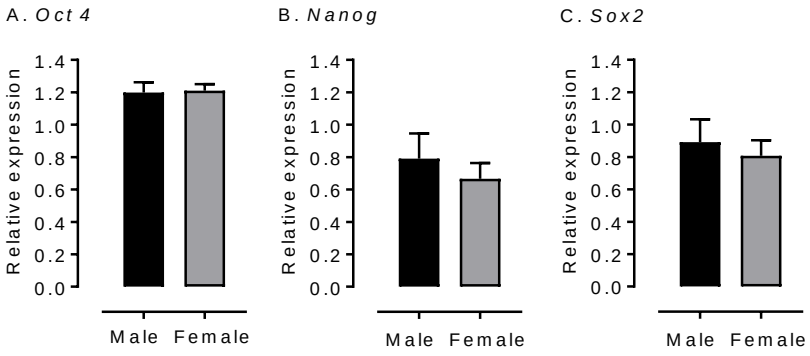

Figure 2.18 Relative gene expression for pluripotency markers in undifferentiated Old (7-8 months, Male vs Female) mESC lines.

Genes of interest were normalized to *Ywhaz* and *Rpl13a* within geNorm. No differences were observed between the groups. Data presented as means ± SEMs based on n=4 mESC lines.

b) Protein expression (Flow cytometry)

No differences were observed in the proportion of cells expressing pluripotency markers Oct4 and Sox2 between Old Male and Old Female mESC lines (Figure 2.19 A and C), although the proportion of mESCs expressing Nanog was reduced (P=0.033) in Old Female compared to Old Male cell lines (Figure 2.19 B). Additionally, interaction was observed between the expression of Sox2 and Nanog (P=0.0018), but not between Oct4 and Nanog.

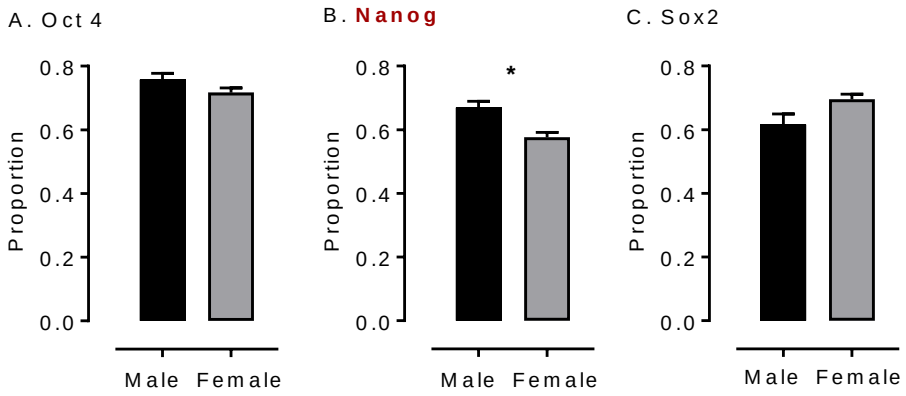

Figure 2.19 Quantitative analysis of protein expression for pluripotency markers in undifferentiated Old (7-8 months, Male vs Female) mESC lines.

Pluripotent cells are presented as the proportion positive of total cells (stained and unstained). Old Female mESCs lines showed reduced proportion of cells positive for Nanog (P= 0.033), highlighted in red, compared to Old Male cell lines. Data are presented as means ± SEMs based on n=4 mESC lines. * indicates P<0.05.

2.3.5.1.3 Qualitative pluripotency expression analysis (Immunocytochemistry)

Mouse ESC lines were cultured for three days and fixed on the fourth day and stained with pluripotency markers Oct4 and Sox2, and nuclear marker Dapi. The culture duration and density was similar to that for protein expression analysis by flow cytometry. Strong expression of both Oct4 and Sox2 was evident in both Young male and Old male mESC lines (Figure 2.20). Old Female mESC lines however, showed relatively low intensity of immunostaining and smaller ESC colonies, compared to the Old Male mESC lines (Figure 2.20 C and F).

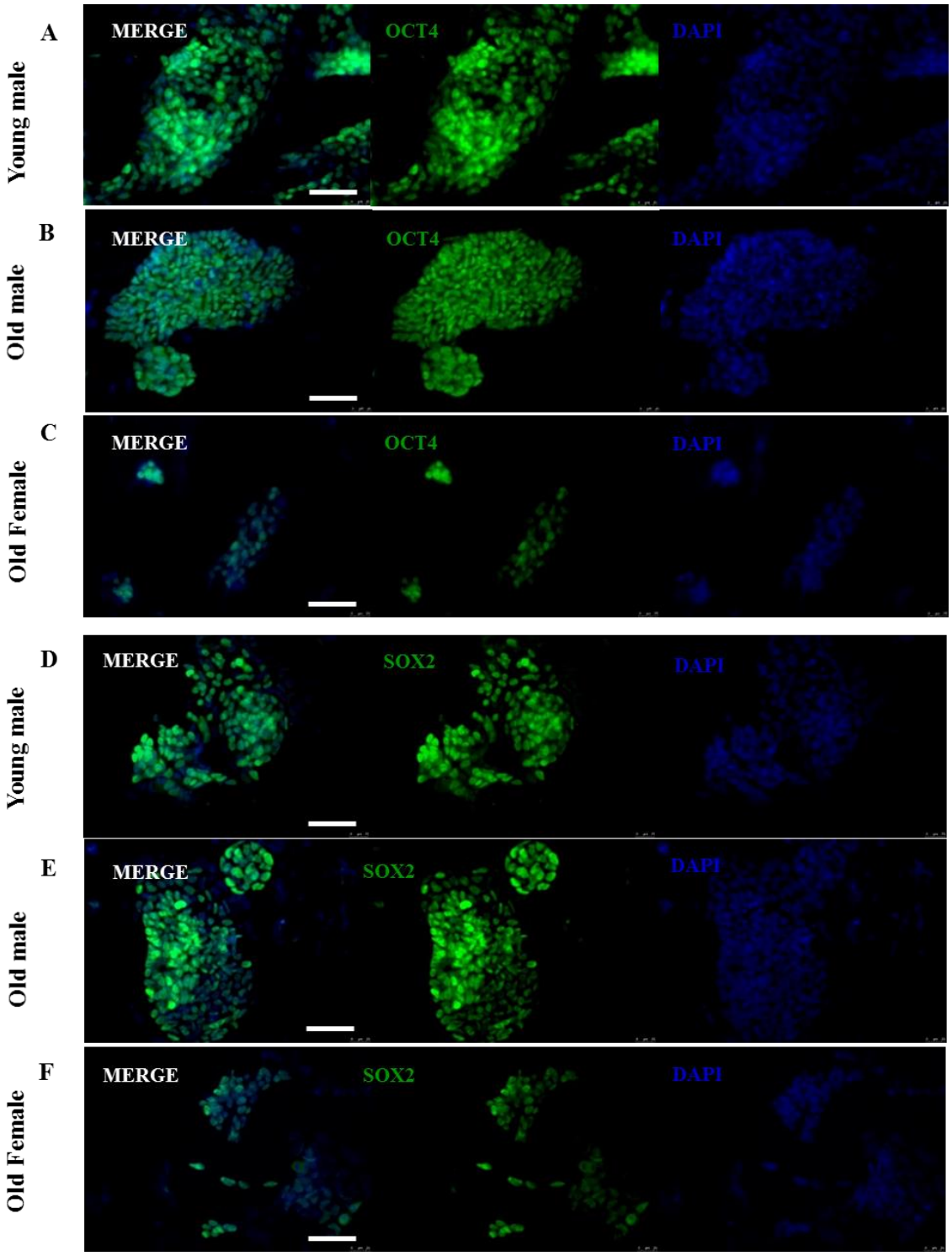

Figure 2.20 Representative images of protein expression for pluripotency markers Oct4 and Sox2 (both green), and Nuclear marker Dapi (blue).

mESC lines were cultured in triplicate. While Young male (A, D) and Old male (B, E) mESC lines stained strongly for both Oct4 and Sox2, Old Female mESC lines (C, F) appeared relatively dim. They also had smaller colonies and with fewer cells/ colony. Magnification = 200µm.

2.3.5.2 Differentiation analysis

2.3.5.2.1 Differences between Young male vs Old male mESC lines (RT PCR)

To analyse the influence of maternal age on potency of mESCs, undifferentiated ES cells were analysed for relative gene expression of endodermal *Gata4* and mesodermal *Brachyury* genes. Although Old male mES lines had higher relative expression for *Gata4* and reduced expression for *Brachyury*, no significant differences were observed compared to Young male mESC lines (Figure 2.21).

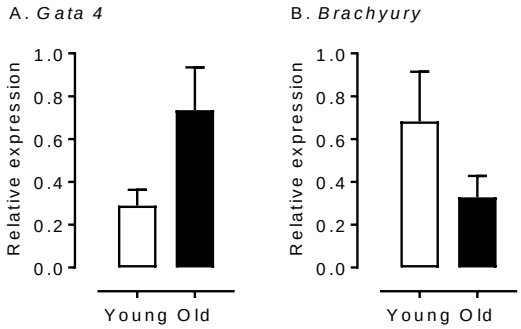

Figure 2.21 Relative gene expression for differentiation markers in undifferentiated male (young (7-8 weeks) vs old (7-8 months)) mESC lines.

Genes of interest were normalized to *Ywhaz* and *Rpl13a* within geNorm. No differences were observed between the groups. Data presented as means ± SEMs based on n = 4 mESC lines.

2.3.5.2.2 Differences between Old Male vs Old Female mESC lines (RT PCR)

No differences were observed for the relative gene expression of endodermal *Gata4* and mesodermal *Brachyury* markers between Old Male and Old Female mESC lines (Figure 2.22).

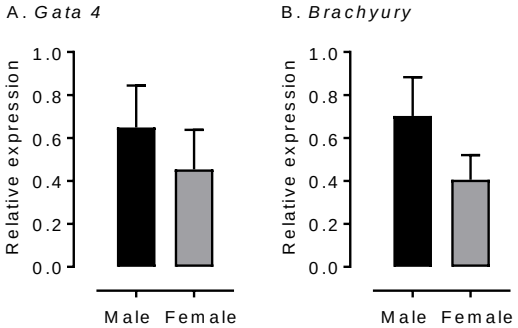

Figure 2.22 Relative gene expression for differentiation markers in Old (7-8 months, Male vs Female) mESC lines.

Genes of interest were normalized to *Ywhaz* and *Rpl13a* within geNorm. No differences were observed between the groups. Data presented as means ± SEMs based on n = 4 mESC lines.

2.3.5.2.3 Qualitative differentiation expression analysis (Immunocytochemistry)

Mouse ESC lines were cultured for three days and fixed on the fourth day and stained with differentiation (mesodermal) marker Brachyury, and nuclear marker Dapi. Strong expression of Brachyury and reduced colony size were evident in both Old Male and Old Female mESC lines (Figure 2.23 B and C). Young male mESC lines however, show no expression for Brachyury (Figure 2.23 A). MEFs were used as positive control and showed a strong expression for the mesodermal marker (Figure 2.23 D).

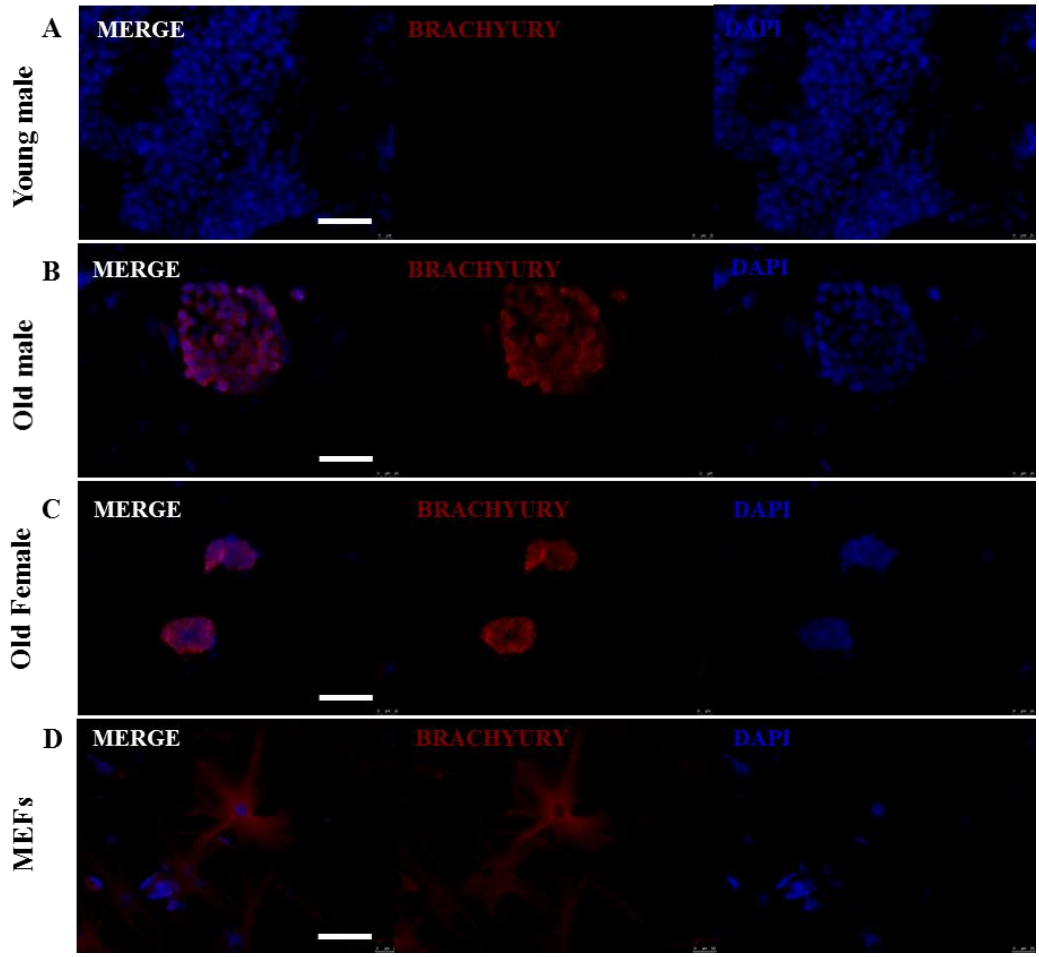

Figure 2.23 Representative images of protein expression for mesodermal marker Brachyury (red) and Nuclear marker Dapi (blue).

mESCs were cultured in triplicate. While Young male (A) mESC lines did not show any staining for Brachyury, several cells within Old (B) Male and (C) Female mESC colonies stained strongly. (D) MEFs were used as control for positive Brachyury staining. Magnification = 200µm.

2.3.5.3 Cell Proliferation and Differentiation analysis

The effect of maternal age was analysed on the growth and proliferation of mESC lines from the three groups. Briefly, mESC lines were seeded in defined density for 96 h as the cells are generally passaged every 72-96 h. Cells were harvested and analysed every 24 h. Figure 2.24 shows phase contrast images of proliferating mES colonies. Young male mESC lines (Figure 2.24 A to D) appeared to have a high cell density and number of colonies at all time points compared to Old male mESC lines (Figure 2.24 E to H). Old Female mESC lines (Figure 2.24 I to L) appeared to be smaller with fewer colonies compared to Old Male mESC lines at all time points.

2.3.5.3.1 Differences between Young male vs Old male mESC lines

a) Cell proliferation and Viability (Trypan Blue Dye Exclusion Assay)

Mouse ESC lines were seeded in defined density for 96 h and harvested every 24 h. For analysis, mESCs were separated into floating and adhered cells. While floating (dead) cells were centrifuged and counted (without trypan blue staining) using haemocytometer, adhered cells were trypsinized, stained with trypan blue dye and counted as proportions of live (trypan blue negative) and dead (trypan blue positive) cells. Old male mESC lines showed fewer proportions ($P=0.001$) (Figure 2.25 A) and reduced number ($P<0.001$) of live adherent cells (Figure 2.25 C) compared to Young male mESC lines. Old male mESC lines also showed increased proportion of floating cells ($P<0.001$) compared to young mESC lines (Figure 2.25 B). Additionally, effect of time ($P<0.001$) was observed in all three analysis (Figure 2.25).

b) Cell proliferation and Differentiation (Flow Cytometry)

Mouse ESC lines were seeded in defined density for 96 h. Cells were harvested and counted every 24 h. For analysis, cells were separated into Oct4 only, Ki67 only, and Ki67 and Oct4 both positive cells. Oct4 was used as a pluripotency marker for mESC cells. While Oct4 expression presented differences over time ($P<0.001$) in both Young and Old male mESC lines (Figure 2.26 A), Ki67 expression was reduced ($P=0.01$) in Old male mESC lines, compared to Young mESC lines (Figure 2.26 B). Changes in Ki67 expression were observed at 24 h ($P=0.011$) and 48 h ($P=0.001$), although no treatment (age) and time induced differences were observed in cells expressing both Oct4 and Ki67 (Figure 2.26 C). Here, cells expressing both Oct4 and Ki67 represent pluripotent mESCs undergoing proliferation, whereas cells expressing only Ki67 are proliferating and perhaps undergoing differentiation (as they are Oct4 negative), and the cells expressing only Oct4 are the stem cells which are not actively proliferating.

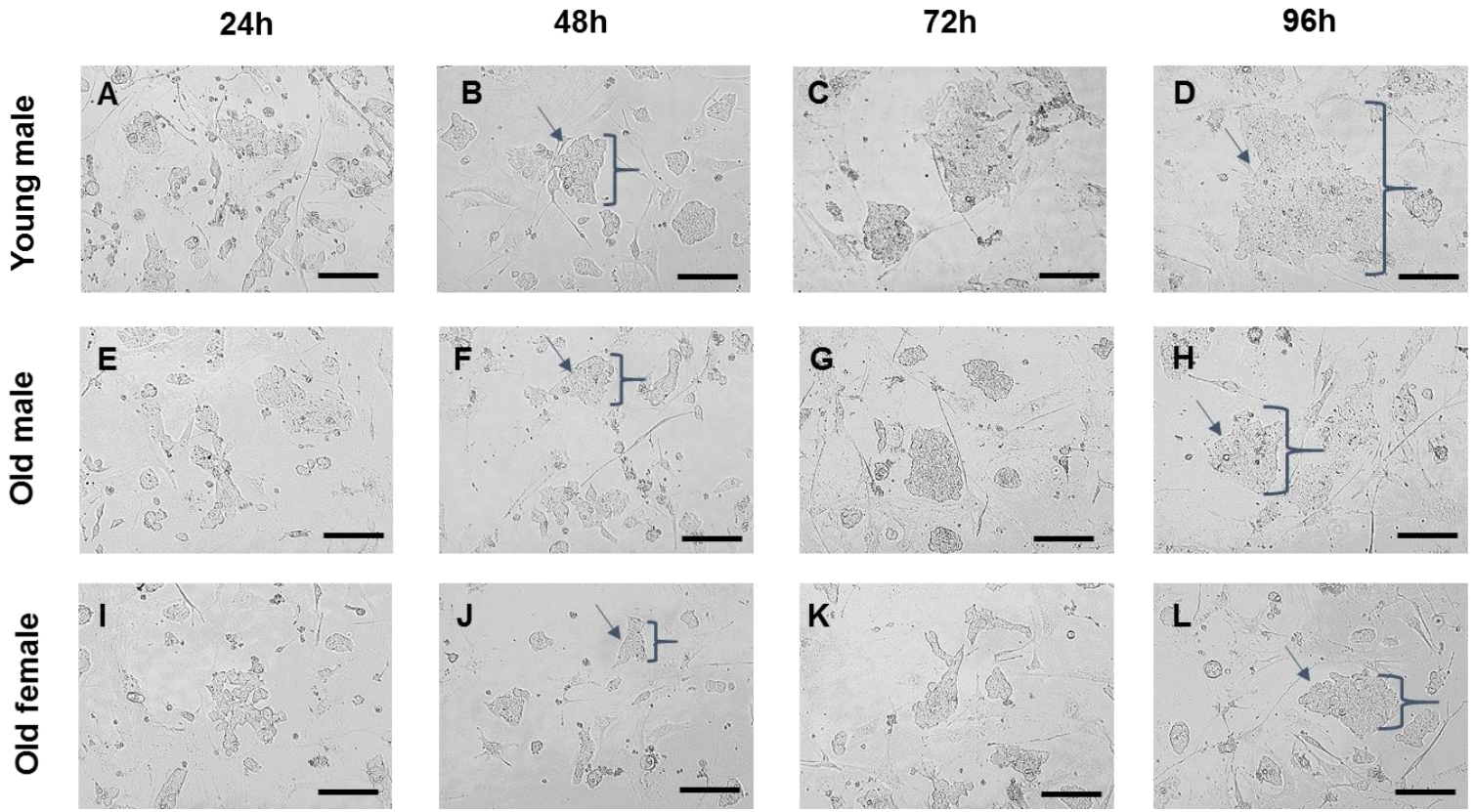

Figure 2.24 Representative phase-contrast images of cell proliferation of Young (7-8 weeks), Old (7-8 months) male and Old female mESCs.

Cells were cultured in triplicate. After seeding, images were captured every 24 h over a period of 96 h. Images show that Young male (A-D) mESC lines have larger colonies with increased density of cells/ colony compared to Old male (E-H) mESC lines. Old Female mESC lines (I-L) present much smaller colony size and fewer mESC clones compared to Old Male mESC lines. Arrows and parenthesis point toward the colony size differences across the groups. Magnification = 100 µm.

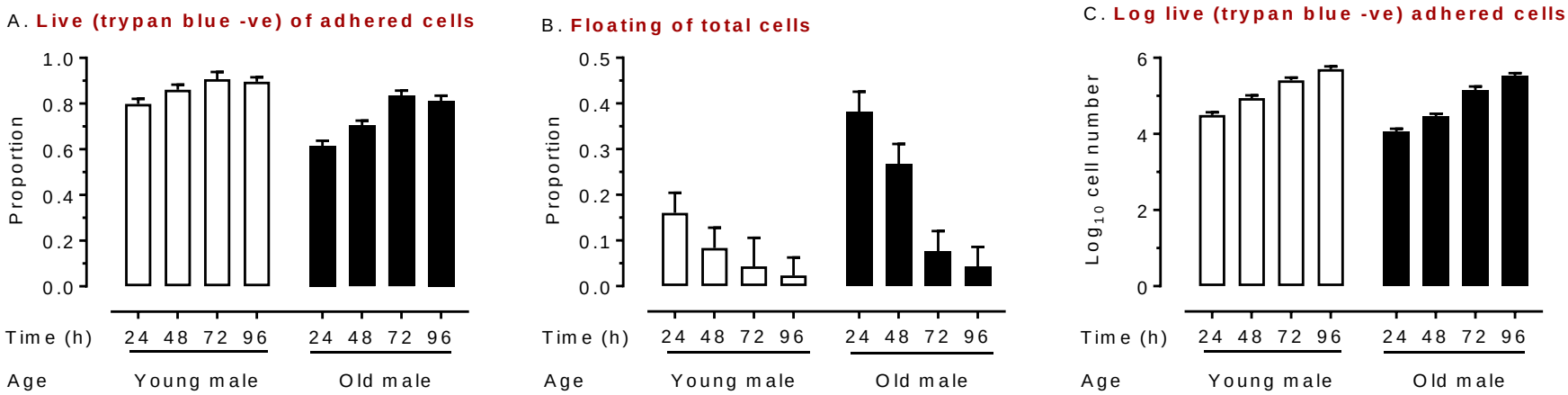

Figure 2.25 Cell proliferation of undifferentiated male (Young (7-8 weeks) vs Old (7-8 months)) mESC lines by trypan blue dye exclusion assay.

mESCs were cultured in triplicate. Trypan negative (live) cells presented as proportion of adherent (live and dead) cells, and floating cells as proportion of total (live, dead and floating) cells. Old male mESC lines had fewer (A) proportions (P=0.001) and (C) number (P<0.001) of live adherent cells, and (B) increased number of floating cells (P<0.001), highlighted in red, as compared to Young mESC lines. Data presented as means ± SEMs based on n = 4 mESC lines.

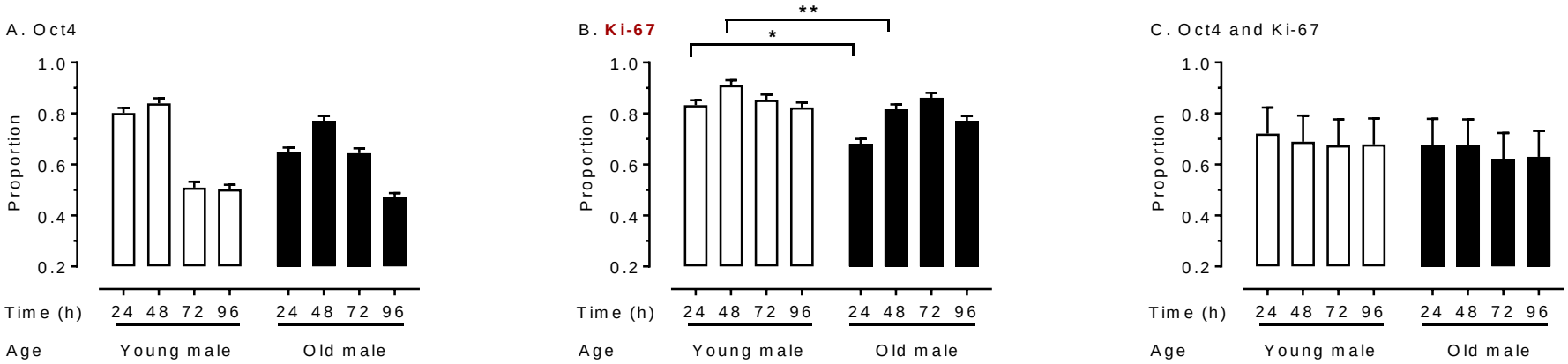

Figure 2.26 Cell proliferation and differentiation in Young male (7-8 weeks) vs Old male (7-8 months) ES lines.

Protein expression of Ki-67 and Oct4 in mESC lines. Marker expression presented as the proportion positive of total cells (stained and unstained). Both Young and Old male mESC lines showed differences in (A) Oct4 expression over time ($P<0.001$). Ki-67 expression was lower ($P=0.01$) in Old vs Young mESC lines (B), highlighted in red. Ki67 expression also differed between Old and Young mESC lines at 24 h ($P=0.011$) and 48 h ($P=0.001$). Oct4 and Ki-67 positive cells were unaffected by treatment and time (C). Data presented as means ± SEMs based on n = 4 mESC lines. * indicates $P<0.01$ and ** indicates $P<0.001$.

2.3.5.3.2 Differences between Old Male vs Old Female mESC lines

a) Cell proliferation and Viability (Trypan Blue Dye Exclusion Assay)

Mouse ESC lines were seeded in defined cell density for 96 h. Cells were harvested and counted every 24 h. For analysis, cells were separated into floating and adherent cells. While floating cells were centrifuged and counted (without trypan blue staining) using haemocytometer, adherent cells were trypsinized, stained with trypan blue dye and counted as live (trypan blue negative) and dead (trypan blue positive) cells.

No gender-based differences were observed between Old Male and Old Female mESC lines. Differences were observed in proportion (Figure 2.27 A) and number (Figure 2.27 C) of live adherent cells, and proportion of floating cells (Figure 2.27 B) over time ($P<0.001$).

b) Cell proliferation and Differentiation (Flow Cytometry)

Mouse ESC lines were seeded in defined density for 96 h. Cells were harvested and counted every 24 h. For analysis, cells were separated into Oct4 only, Ki67 only, and Ki67 and Oct4, both positive cells. Oct4 was used as a pluripotency marker for mESC cells.

While both Old Male and Old Female mESC lines showed differences in Oct4 (Figure 2.28 A) and Ki67 (Figure 2.28 B) expression over time ($P<0.001$), no treatment- (gender) and time-based differences were observed in cells expressing both Oct4 and Ki-67 (Figure 2.28 C).

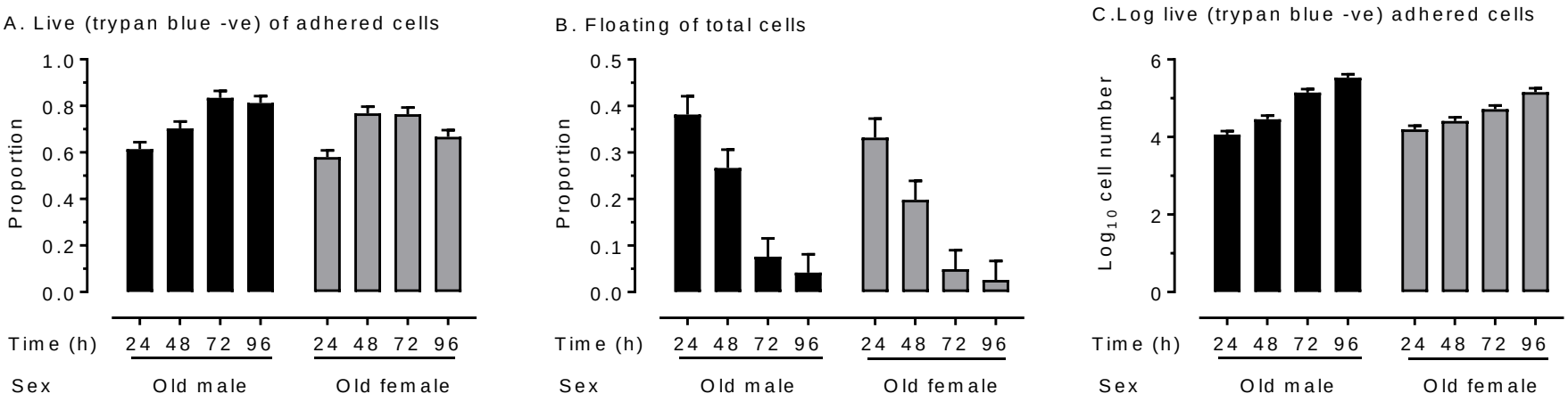

Figure 2.27 Cell proliferation of undifferentiated Old ((7-8 months) male vs female) mESC lines by trypan blue dye exclusion assay.

mESCs were cultured in triplicate. Trypan negative (live) cells presented as proportion of adherent (live and dead) cells, and floating cells as proportion of total (live, dead and floating) cells. Both Old male and Old female mESC lines showed differences in (A) proportion and (C) number of live adherent cells, and (B) proportion of floating cells over time ($P<0.001$), although no gender based differences were observed between the two groups. Data presented as means ± SEMs based on n = 4 mESC lines.

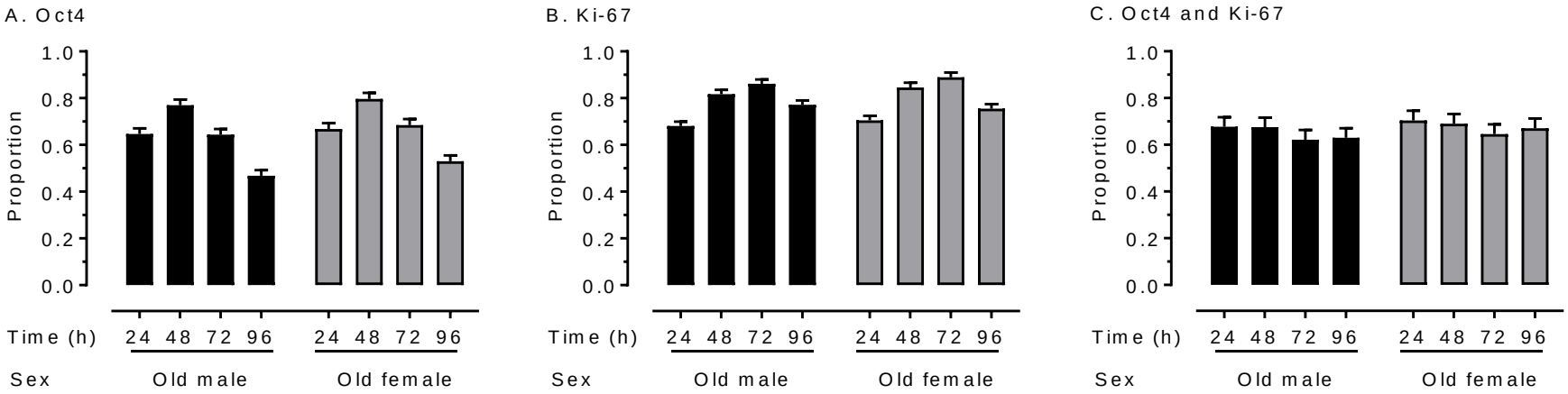

Figure 2.28 Cell proliferation and differentiation in Old male vs Old female mESC lines.

Protein expression of Ki-67 and Oct4 in mESC cells. Marker expression presented as the proportion positive of total cells (stained and unstained). Both Old male and Old female mESC lines showed differences in (A) Oct4 and (B) Ki67 expression over time ($P<0.001$). Oct4 and Ki-67 positive cells were unaffected by treatment and time (C). Data presented as means ± SEMs based on n = 4 mESC lines.

2.3.5.4 Cell Apoptosis and Cell Death analysis

The effect of advanced maternal age on cell apoptosis and death was assessed by analysing the protein expression of Annexin V- FITC and PI in the mESC lines from Young and Old groups using flow cytometry (see Section 2.2.7.3). Briefly, mESCs were simultaneously seeded in defined cell density and analysed every 24 h for a period of 96 h. ES cells were selected from a combined population of mESC and MEF cells using a pluripotency surface marker, SSEA-1. Only SSEA-1 positive cells were further analysed for Annexin V and PI negative (live cells), Annexin V positive and PI negative (early apoptotic cells), Annexin V and PI positive (late apoptotic or necrotic cells), and Annexin V negative and PI positive (dead cells). Data is presented as proportion positive of total cells (stained and unstained cells).

2.3.5.4.1 Differences between Young male vs Old male mESC lines

Both Young and Old male mESC lines showed differences in SSEA-1 expression over time ($P<0.001$) (see Appendix B, Figure 2).

While proportion of live ($P= 0.068$), necrotic ($P= 0.062$) and dead ($P= 0.056$) cells changed over time in both Young and Old male mESCs (Figure 2.29 A, C and D), no differences were observed in the proportion of apoptotic cells by treatment (age) and time (Figure 2.29B). Old male ESC lines showed slightly increased proportion of necrotic cells at 24h ($P=0.075$) compared to Young mESC lines (Figure 2.29 C).

In addition, no difference was observed in the relative gene expression of early apoptosis marker, *Caspase 3* (see Appendix B, Figure 3).

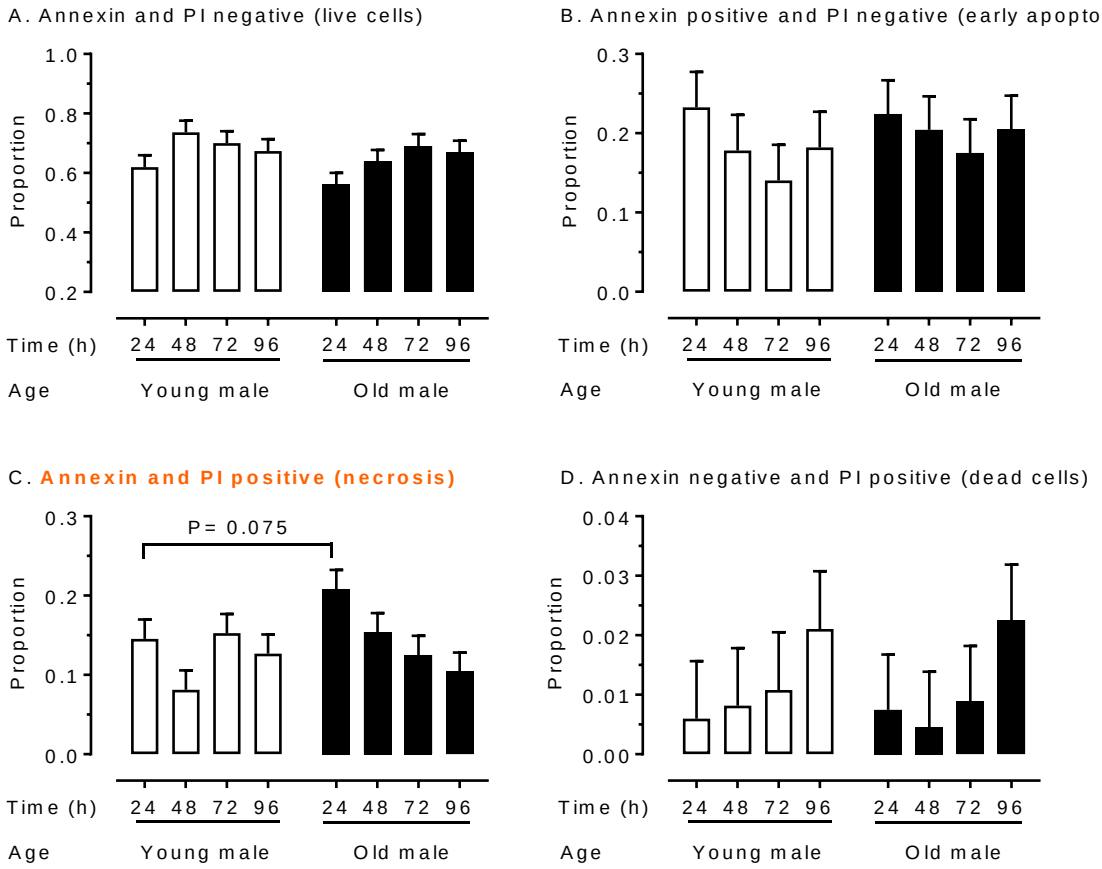

Figure 2.29 Quantitative protein expression of early apoptosis marker, Annexin V, in undifferentiated Young (7-8 weeks) vs Old (7-8 months) male mESC lines.

mESCs were cultured in duplicate. Cells are presented as the proportion positive of total cells (stained and unstained cells). Proportion of (A) live (P=0.065), (C) necrotic (P=0.062) and (D) dead (P=0.056) cells changed over time in both Young male and Old male ESCs. Proportion of necrotic cells also differed between Old and Young ESC lines at 24 h (P=0.075), highlighted in red. Proportion of apoptotic cells (B) were unaffected by treatment (age) and time. Data presented as means ± SEMs based on n = 4 mESC lines.

2.3.5.4.2 Differences between Old Male vs Old Female mESC lines

Old Male mESC lines showed differences in SSEA-1 expression (P=0.02) compared to Old Female mESC lines. Both Old Male and Old Female mESC lines showed changes in SSEA-1 expression over time (P<0.001). Old Male mESC lines showed reduced SSEA-1 expression at 48 h of culture (P<0.001) compared to Old Female mESC lines (see Appendix B, Figure 4).

Old Female mESC lines showed differences in proportion of live (P=0.095) and necrotic (P=0.003) cells compared to Old Male mESC lines (Figure 2.30 A and C). Both Old Male and Old Female mESC lines showed differences over time in live (P=0.084), apoptotic (P=0.009) and dead (P=0.003) cells. Proportion of early apoptotic cells were increased (P=0.059) at 24 h, and reduced (P=0.055) at 48 h

in Old Female mESC lines compared to Old Male mESC lines (Figure 2.30 B). Old Female mESC lines also showed increased proportion of late apoptotic cells at 72 h (P=0.035) and 96 h (P=0.035) compared to Old Male mESC lines (Figure 2.30 C). Additionally, no difference was observed in the relative gene expression of early apoptosis marker, *Caspase 3* (see Appendix B, Figure 5).

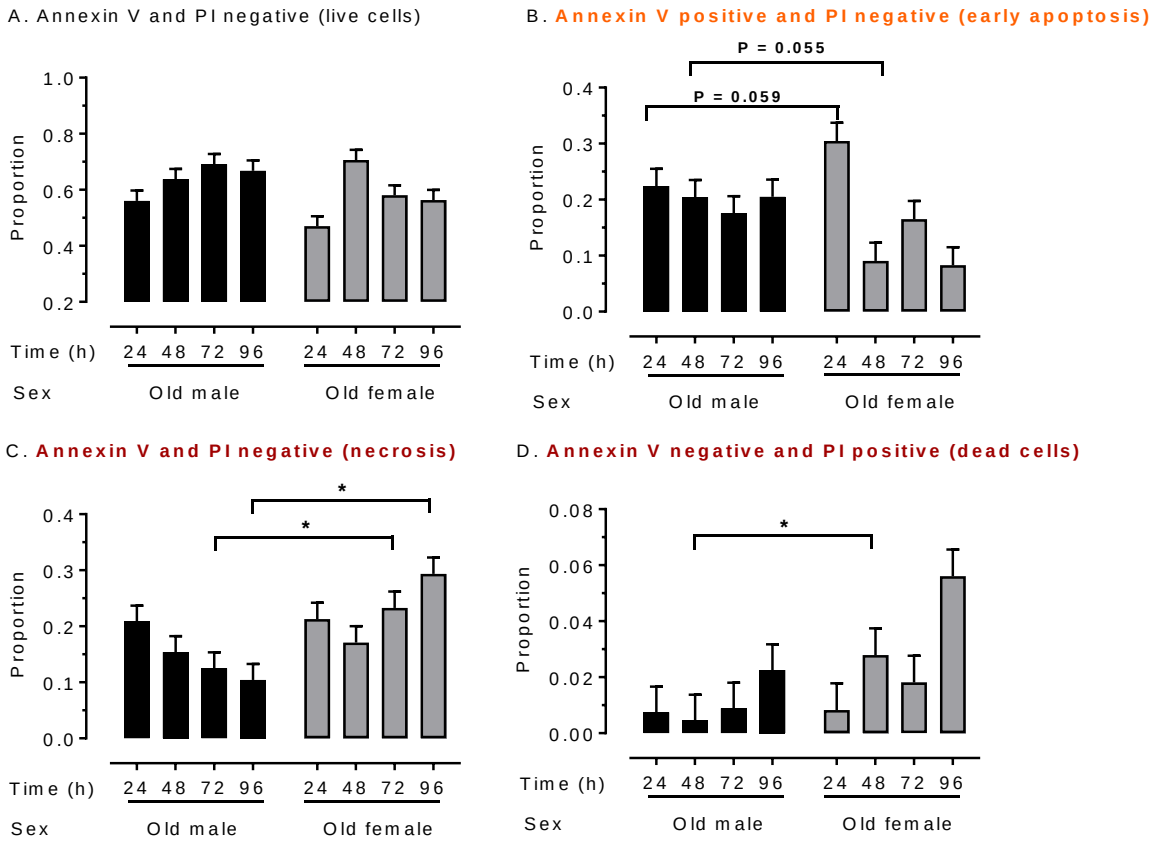

Figure 2.30 Quantitative protein expression of early apoptosis marker, Annexin V in undifferentiated Old Male vs Old Female mESC lines.

mESCs were cultured in duplicate. Cells are presented as the proportion positive of total cells (stained and unstained cells). Old Female mESC lines showed differences in proportion of (A) live (P=0.095) and (C) late apoptotic or necrotic (P=0.003) cells compared to Old male mESC lines, highlighted in red. Both Old Male and Old Female mESC lines showed differences in (A) live (P=0.084), (B) apoptotic (P=0.009) and (D) dead (P=0.003) cells, over time. Old Female mESC lines presented (B) proportion of early apoptotic cells to be increased (P=0.059) at 24 h, and decreased (P=0.055) at 48 h, compared to Old Male mESC lines. Old female mESC lines also showed increased (C) proportion of necrotic cells at 72 h (P=0.035) and 96 h (P=0.035) and (D) proportion of dead cells at 48 h (P=0.013) compared to Old male mESC lines. Data presented as means ± SEMs based on n = 4 mESC lines. * indicates P<0.05.

2.3.5.5 Epigenetic modifiers

2.3.5.5.1 Differences between Young male vs Old male mESC lines

While Old and Young male mESC lines displayed no differences between the relative expression of DNA methyltransferases *Dnmt1, Dnmt3L* and *Dnmt3b*, Old male mESC lines showed reduced expression of *Dnmt3a* (P=0.049) compared to Young male mESC lines (Figure 2.31).

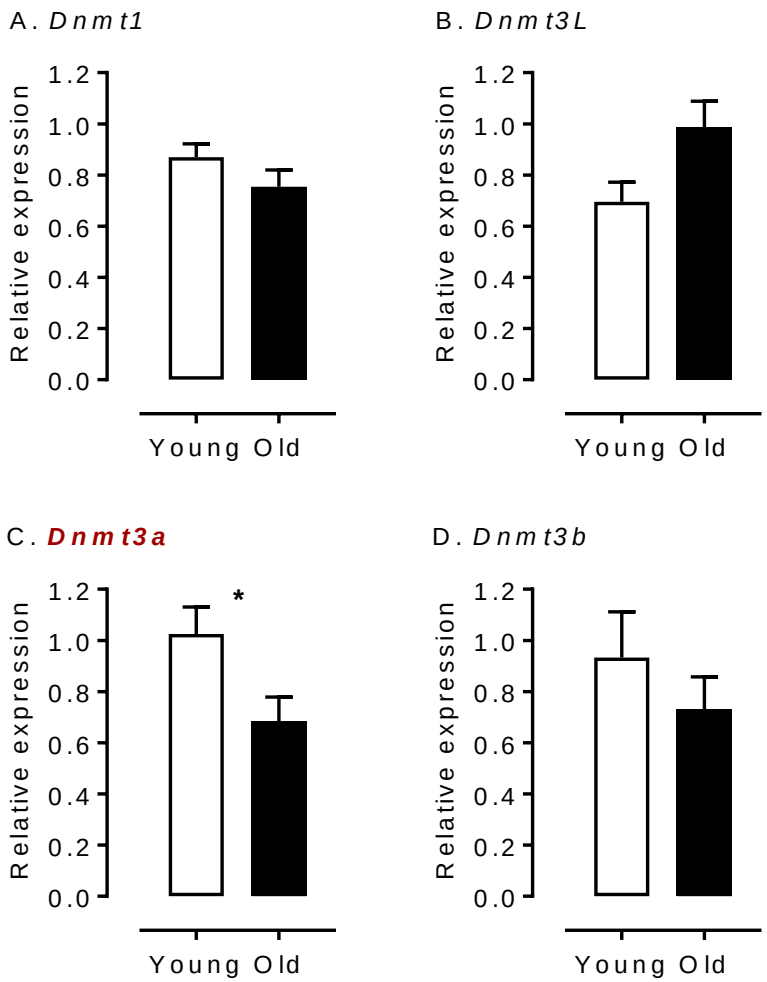

Figure 2.31 Relative gene expression for DNA methyltransferases in undifferentiated male (Young (7-8 weeks) vs Old (7-8 months)) mESC lines.

Real-time PCR analysis of DNA methyltransferases *Dnmt1, Dnmt3L, Dnmt3a* and *Dnmt3b.* Genes of interest were normalized to *Ywhaz* and *Rpl13a* within geNorm. Old mESC lines showed reduced expression of *Dnmt3a* (P=0.049) highlighted in red, compared to young mESC lines (C). Data presented as means ± SEMs based on n = 4 mESC lines. * indicates P<0.05.

2.3.5.5.2 Differences between Old Male vs Old Female mESC lines

While Old Male and Old Female mESC lines displayed no differences between the relative expression of DNA methyltransferases *Dnmt1, Dnmt3L* and *Dnmt3a*, Old Female mESC lines showed reduced expression of *Dnmt3b* (P=0.078) compared to Old Male mESC lines (Figure 2.32).

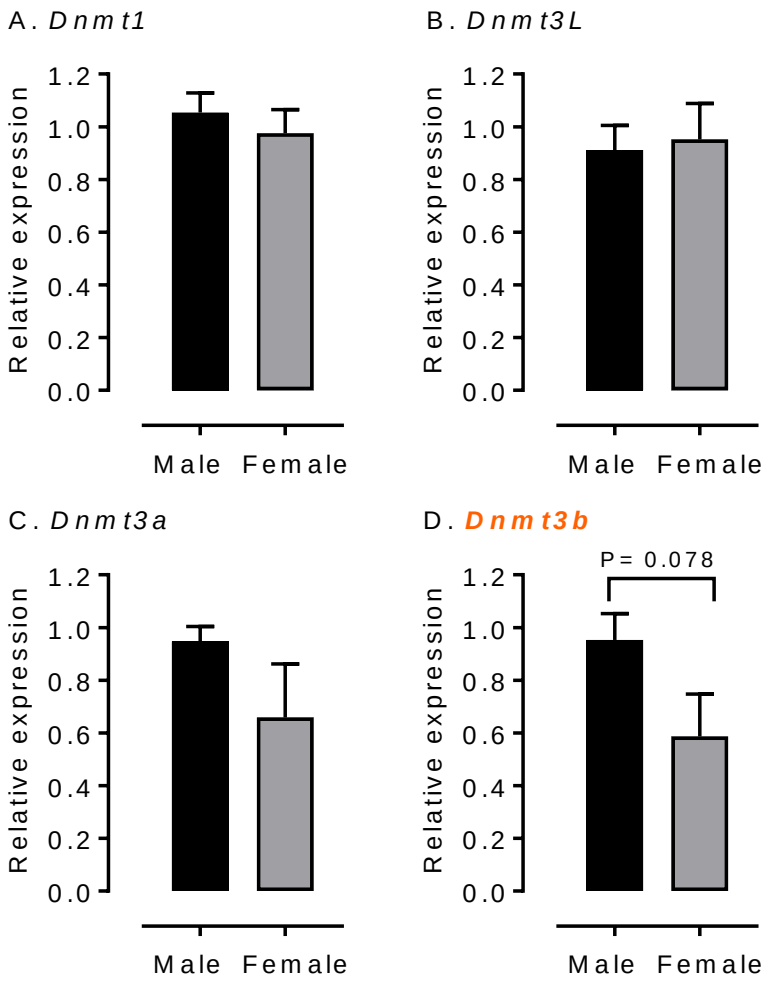

Figure 2.32 Relative gene expression for DNA methyltransferases in undifferentiated Old ((7-8 months) Male vs Female) mESC lines.

Real-time PCR analysis of DNA methyltransferases *Dnmt1, Dnmt3L, Dnmt3a* and *Dnmt3b.* Genes of interest were normalized to *Ywhaz* and *Rpl13a* within geNorm. Old Female mESC lines showed reduced expression of *Dnmt3b* (P=0.078) highlighted in orange, compared to Old Male mESC lines. Data presented as means ± SEMs based on n = 4 mESC lines.

2.4 General Discussion

The current study investigated the effects of maternal age (Young, 7-8 weeks v Old, 7-8 months) using mESCs as model. These cells were derived from the stem cell population (ICM) within blastocysts (E3.5). Key findings from this study were that embryos from Old dams were less well developed than those from Young dams. mESC lines derived from these embryos also exhibited higher incidences of aneuploidy and a lower proportion of viable and proliferating cells. In contrast, differences between Old Male and Female mECS lines were minor. Collectively, these results indicate that advanced maternal age (AMA) delays embryo development and gives rise to a higher proportion of karyotypically abnormal mESCs. Furthermore, these mESC lines were generally less viable and showed of precocious loss of pluripotency. Figure 2.33 summarizes the AMA model, analysed characteristics and results presented in Chapter 2, in a schematic format.

2.4.1 Effect of Advanced Maternal Age (AMA) on Embryo Development

In the present study, AMA had no effect on the total number of embryos retrieved at E3.5, which was similar to the observations of Velazquez et al. (2016) and comparable to the lack of differences shown between litter-size of young and old dams (Yue et al., 2012). Although the present study showed no differences in fertilization rates, maternal age did have an impact on the developmental stage of embryos recovered at E3.5. Old dams (7-8 months) had an increased number of morulae and early blastocysts and, consequently, a reduced number of mid and total blastocysts compared to those retrieved from Young dams (7-8 weeks), indicating AMA-induced retardation of blastocyst development. Other studies have also reported that aged dams produce an increased number of delayed and morphologically abnormal embryos, with reduced embryo size (measured as crown-rump length of embryo) and somite number (Lopes et al., 2009). In the same study, aged dams also showed an increased number of early and late resorption sites, indicating implantation failures at different stages of embryonic development, comparable to reduced fertilization rates (Velazquez et al., 2016) and litter-size (Care et al., 2015). Decrease in fertilization rates and embryo quality with AMA has also been observed in humans. This was represented by reduced number of oocytes and an increased number of arrested morulae, which in turn reduced blastocyst formation and expansion rates (Janny and Menezo, 1996). Ageing oocytes display increased chromosomal aberrations in addition to alterations in chromatin structure and genome stability compared to younger oocytes (Toshio Hamatani et al., 2004). Although eggs contain equal amounts of maternal and paternal DNA, it mostly constitutes of maternal (oocyte) cytoplasm and mitochondria, therefore being more vulnerable to adverse maternal environment (Veleva et al., 2008). The present study focussed only on the number, quality and developmental stages of the embryos retrieved at E3.5, and did not culture the early-stage embryos (i.e. morulae or early blastocysts)

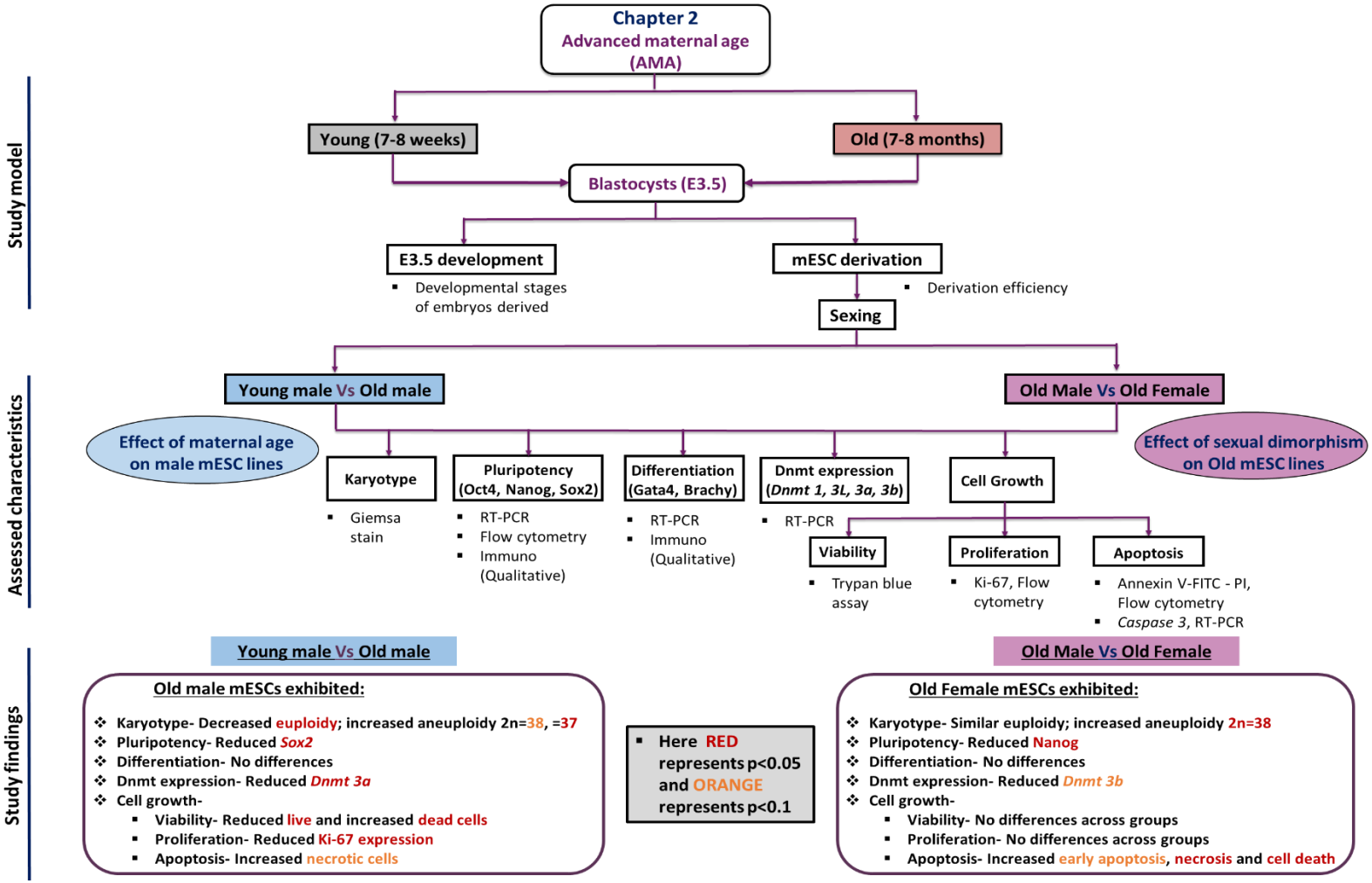

Figure 2.33 Flow diagram representing study layout and findings from Chapter 2 of this thesis.

further to test their viability or developmental potential. Nevertheless, as AMA delayed blastocyst development in the current study, and has been shown to reduce pregnancy outcomes in other studies, collectively, these observations highlight the possibility of reduced developmental potential of the delayed embryos.

2.4.2 Effect of Maternal Age on derived Young and Old male mESC lines

Given the aforementioned detrimental effects of AMA on the development of blastocysts, the current study utilised the self-renewal and pluripotent potential of ICM-derived mESCs, *in vitro*. No statistical differences in the derivation efficiency of mESC lines from Young and Old dams were observed, which is comparable to the similar number of ICM cells obtained from E3.5 blastocysts of young and old dams in another study with similar maternal age groups (Velazquez et al., 2016). It is noteworthy that due to unavailability of Old dams (7-8 months) at the time, most of Young mESC lines were established before mESC-derivation protocol optimisation and the majority of Old mESC lines were derived after optimisation. While it may be argued that the optimised culture conditions could have been favourable in improving the derivation efficiency of Old mESC lines, significant differences observed in several phenotypic aspects (discussed below) between the Young and Old dam derived mESC lines, suggest otherwise.

In the current study, both Young and Old age groups showed a strong bias towards male embryos (~80-90%). Therefore, age-related differences were limited to male mESC lines. This is quite common in ESC derivation, as compared to Male (XY) ESC lines, Female (XX) ESC lines are more prone to developing abnormal karyotypes (with frequent loss of one chromosome), related to reduced cellular function and proliferation (Hadjantonakis and Papaioannou, 2001; Zvetkova et al., 2005). Mammalian females undergo dosage compensation of X-chromosome by an essential epigenetic event during early embryonic developmental transition, called X-chromosome inactivation (XCI). In mice, it is developmentally regulated and occurs during preimplantation development (by a single *cis*-acting X-inactivation centre (Xic)), on the onset of cellular differentiation by upregulating *Xist* expression (Monk and Harper, 1979). This results in functional hetero-chromatinization and silencing of the X chromosome, which continues through subsequent cell divisions, thus having only one functionally active X chromosome in both sexes. In mice, XCI occurs in two forms. In the extra-embryonic trophectoderm and primitive endoderm lineages (during preimplantation), XCI is imprinted and paternal X-chromosome is inactivated (Takagi and Sasaki, 1975). This starts as early as two- to eight- cell stage and continues from extra-embryonic trophectoderm through to development of fetal placenta (Huynh and Lee, 2003). In contrast, paternal X-chromosome is reactivated in the ICM, followed by random X inactivation that initiates post implantation, in the epiblast (around E5.5). As ESC lines are derived from ICM, they lack X-

inactivation, and therefore have both XX chromosomes activated, which induces instability and interferes with propagation of the ES lines, a phenomenon also observed in human ESCs (Rastan and Robertson, 1985; Barakat and Gribnau, 2010; Dvash et al., 2010; Xie et al., 2016). Similar to this notion, other studies have reported that male blastocysts have an increased number of blastomeres which are metabolically more active, which may favour the isolation of pluripotent ESCs compared to female blastocysts (Sato et. al., 1995). Global methylation patterns of ESCs suggest increased hypomethylation of XX ESCs relative to XY and XO cells, which could be responsible for two active XX-chromosomes and inducing instability in female ESC lines (Zvetkova et al., 2005).

2.4.2.1 AMA increases aneuploidy in Old male mESC lines

Karyotype analysis of male mESC lines revealed increased aneuploidy (< 40 chromosomes) including a greater proportion of cells with less than 38 and 37 chromosomes in Old male mESC lines compared to Young male mESC lines. *In vitro* culture conditions, such as passaging with Trypsin, handling and prolonged cultures, have been shown to influence ESC karyotype over time (Baker et al., 2007). Cytogenetic studies suggest that karyotypic aberrations could be representative of progressive adaptation of ESC lines to their culture conditions, thus increasing *in vitro* proliferation. However, as all mESC lines used in the present study were cultured in a similar fashion, the effects of *in vitro* cultures are less likely to be responsible for the differences observed. Moreover, all mESC lines used for further analysis in the present study had a normal karyotype (>50% euploidy) in accordance with the guidelines of American Type Cell Culture, ATCC.

Aneuploidy increases with maternal age contributing to reduced implantation and fertility rates (Munné, 2006), making it one of the leading causes of IVF-failures in older mothers (Annette et al., 1997; Harton et al., 2013). In mice however, aneuploidy in embryos may also depend on the strain background, making it a quantitative genetic trait (Yun et al., 2014; Schulkey et al., 2015). In AMA human and mouse studies, aneuploidy is also associated with poor embryo development (Gabrielsen et al., 2000; Steuerwald et al., 2007; Mohammadzadeh et al., 2018). Increased aneuploidy in ageing oocytes and preimplantation embryos is caused by (i) recombination errors in early meiosis, (ii) defective and weakened spindle assembly checkpoint in meiosis I, (iii) deterioration of sister chromatid cohesion or chromosome non-disjunction, (v) premature segregation of sister chromatids (MI and MII) and (v) higher errors of microtubule-kinetochore interactions (Chiang et al., 2012; Stuppia, 2013). Additionally, altered patterns of degradation of maternal mRNAs (during oocyte maturation), reduced BRCA1 expression in ageing oocytes, further perturbing spindle formation and chromosome congression, and decreasing DNA methylation (Pan et al., 2008; Yue et al., 2012). Together, these alterations reduce cleavage, blastocyst and pregnancy

rates, and increase still birth and fetal malformations. As observed in the present study, and in mice models generally, AMA significantly increased maternal body weight, making it an additional factor contributing to increased aneuploidy in oocytes (with increasing maternal weight) (Luzzo et al., 2012) and reduced fertility in older mothers (Comstock et al., 2015).

2.4.2.2 AMA reduces *Sox2* expression in Old male mESC lines

Embryo and ESC pluripotency is maintained by the core intrinsic factors including octamer-binding transcription factor 4 (Oct4), Nanog and sex determining region Y-box 2 (Sox2) (X. Chen et al., 2008). Following zygote genome activation, pluripotent cells (eventually forming ICM) specialise to give rise to the three germ layers (ectoderm, mesoderm and endoderm). While Oct4 and Nanog inhibit differentiation, Sox2 acts as Oct4 coactivator and synergistically regulates pluripotency factors (Ambrosetti et al., 1997). Sox2 is first detected at the morula stage, becoming more specifically located in the ICM and epiblast (Avilion et al., 2003). It is one of the most essential factors for regulating embryonic development, the absence of which is embryonically lethal. Like other pluripotency factors, Sox2 maintains self-renewal and assists in proliferation of ES cells (Thomson et al., 2011).

All mESC lines used in the current study displayed high levels of pluripotency, congruent to all putative ESC lines expressing characteristics of *in vivo* ICM of blastocysts (Mitsui et al., 2003). However, Old male mESC lines showed reduced *Sox2* expression compared to Young male mESC lines. It must be noted that although derived from ICM, ESCs are not 'identical' to the cells in the ICM, and could undergo alterations depending on the duration and conditions of *in vitro* culture. Nevertheless, loss of *Sox2* expression may induce similar effects in both cell types, and reduce pluripotency, change in cell morphology and increase differentiation of ESCs (Masui et al., 2007). As Sox2 synergistically maintains Oct4 expression, reduction in Sox2 would therefore influence Sox2-Oct4 target genes, disturbing the dynamic equilibrium between Oct4 and Nanog, eventually perturbing the core regulatory circuitry in pluripotent stem cells and inducing differentiation (Boer et al., 2007; Kopp et al., 2008)

Although no study has yet made a direct comparison to assess pluripotency of Old and Young blastocyst-derived ESCs, Huang et al. (2010) succeeded in generating ESCs from artificially activated aged oocytes. They observed no age-induced differences in derivation efficiency and pluripotency expression (*Oct4, Nanog* and *SSEA1*) of the ES lines, and only little difference in the global gene expression. However, ES derivation efficiency was reduced in the old group lines derived from parthenogenetic blastocysts. Additionally, greater global gene expression differences were observed in the eggs of Old and Young dams, compared to the ES lines derived from the artificially activated oocytes. Similar differences in gene expression, DNA methylation patterns and

aneuploidy rates have been observed between aged oocytes and aged eggs (Pan et al., 2008). Therefore, assessing effects of maternal age at different stages of development (i.e. eggs vs embryos) may reveal different results. The current study focussed on ICM-derived mESCs at the preimplantation stage (E3.5) of development as ICM is responsible for fetal development and has been identified as the most critical developmental period of gestation (Sun et al., 2015; Velazquez et al., 2018). Moreover, it is the preimplantation stage that is mostly used for embryo transfers in IVF treatments (which corresponds to E5- E6 in humans).

2.4.2.3 AMA reduces Cell Viability in Old male mESC lines

Studies have indicated that AMA in mice increases the rate of embryo fragmentation during *in vivo* fertilisation, which occurs during the first cell cycle (Jurisicova et al., 1998). This was observed to increase even further when oocytes were fertilised *in vitro*. Embryo fragmentation restricts and arrests embryo development thereby contributing to programmed cell death (PCD) in the preimplantation embryos. Excessive chromatin condensation, DNA degradation, presence of cell death and apoptotic bodies in blastomeres of fragmented human embryos suggest the initiation of PCD at early developmental stages; that is prior to blastocyst formation, eventually causing death of the preimplantation embryo (Jurisicova et al., 1996). Likewise, in the present study, Old male mESC lines showed an increased proportion of dead cells and consequently reduced number of live cells (by Trypan blue dye exclusion assay). Additionally, Old male mESC lines displayed reduced cell proliferation (by Ki67, flow cytometry) and increased proportion of necrotic cells compared to Young male mESC lines (Annexin V- PI assay, flow cytometry).

While pre-established PCD in 'Old blastocysts' could have induced cell death and necrosis in 'Old mESC lines', an additional factor could have been reduced *Sox2* expression. As described before, positive-feedback loops between core-regulatory transcription factors are essential in maintaining pluripotency as well as continuous ESC self-renewal (Ivanova et al., 2006). Moreover, reduced expression of these factors, especially Oct4-Sox2, lead to decreased cell proliferation and increased cell death as indicated by the death of Sox2-null mice embryos, post implantation (Avilion et al., 2003). Although the apoptosis marker, *Caspase3*, showed no transcriptional differences between the two groups, further evaluation of cell death mechanisms such as the Ras/Raf/extracellular signal-regulated kinase (Erk) signalling pathway is required (Cagnol and Chambard, 2010).

Additionally, 'Old male mESC lines' showed reduced levels of DNA methyltransferase transcript (*Dnmt3a*) expression, which is essential for de novo methylation, cell division and proliferation, ageing, germline determination and early mouse development and survival (Okano et al., 1999; Robertson and Wolffe, 2000; Trasler, 2006). Together with *Dnmt1* and *Dnmt3b*, *Dnmt3a* regulates cytosine methylation in CpG dinucleotides and promotes gene silencing thereby maintaining

genome integrity (Tsumura et al., 2006). A common belief is that the *de novo* methytransferases Dnmt 3a/3b, establish methylation in the CG landscape in the hypomethylated genome of early embryos prior to implantation, which is later copied from parent to daughter strands during replication by Dnmt1 (Probst et al., 2009). These patterns are faithfully maintained by Dnmt1 during DNA replication to ensure epigenetic inheritance across generations DNA methylation patterns change with age and stages of embryonic development (Reik et al., 2001; Morgan et al., 2005). Aged oocytes and preimplantation embryos show reduced DNA methylation both *in vivo* and *in vitro* (Yue et al., 2012). These oocytes lead to reduced cleavage, blastocyst and pregnancy rates, and increased stillbirth and fetal malformations compared to the young group. This further highlights the importance of DNA methylation in embryonic and mammalian development. Moreover, in stem cells, de novo DNA methyltransferases maintain self-renewal, pluripotency and, therefore, affect proliferation and differentiation capacity of these cells (Tadokoro et al., 2007); although some studies show contrasting results (Tsumura et al., 2006). However, it remains unclear how DNA methyltransferases affect mESCs derived from aged blastocysts and how their expression varies with *in vitro* culture conditions. This requires further research.

2.4.3 Effects of Sexual Dimorphism in Old mESC lines

Human and animal studies have demonstrated the influence of parental age on offspring health and longevity (Lansing, 1947; Palomares et al., 2009; Gillespie et al., 2013). Although maternal age plays a critical role in determining offspring health and development, the parental age effect may also depend on the offspring's sex (Gavrilov and Gavrilova, 1997; Grottenthaler, 2004). For instance, in humans, paternal age has been shown to influence life span of daughters, although no correlations were observed between maternal or paternal age and son's longevity. Such differences have also been displayed in mouse models where effects of maternal undernutrition and ageing varied with sex of offspring (Watkins et al., 2008a; Velazquez et al., 2016).

In AMA mice, 'aged blastocysts' depicting delayed development gave rise to male offspring with shorter life spans compared to those with normal rates of development, thus displaying a strong correlation between maternal age, sex of blastocyst, it's development rate and postnatal life-span (Lind et al., 2015). In the current study, as only one Young female mESC line was derived, it restricted age-related comparisons between Young and Old Female mESC lines. However, given the aforementioned differences and importance of sex in determining blastocyst development and offspring health, the present study also focussed on analysing possible sex-induced differences within the Old group; i.e. between Old Male and Old Female mESC lines. Old Female mESC lines displayed smaller colony sizes, reduced pluripotency (Nanog, flow cytometry and Oct4 and Sox2 by immunocytochemistry) and increased Brachyury (by immunocytochemistry) expression. While no

differences were observed in proliferation rates, Old Female mESC lines showed a decreased proportion of live cells and consequently increased proportion of apoptotic and necrotic cells compared to Old Male mESC lines; in addition to decreased trends of DNA methyltransferases, especially *Dnmt3b.*

2.4.4 Conclusion and Future aspects

The current study revealed an AMA-induced delay in embryo development (E3.5) which is congruent with previous data (Lopes et al., 2009). The current data indicates that maternal age increases aneuploidy and reduces pluripotency, proliferation and cell viability of the ICM. While the present mESC model depicted possible AMA-induced changes in the E3.5 blastocysts, the Old mESC group also showed signs of sexual dimorphism, suggesting increased vulnerability of Female mESC lines compared to Male mESC lines. Collectively, the data showed interesting similarities between *in vivo* E3.5 blastocyst and *in vitro* derived mESC lines, and highlighted possibility of AMA-induced differences in the core pluripotency circuitry altering cell survival mechanisms in derived Old mESC lines.

During the course of the present study, E3.5 embryos retrieved from Young and Old dams were individually frozen for comparative gene analysis studies between E3.5 blastocysts and derived mESC lines. Although protocols for single-embryo sex, transcript analysis and karyotype (from fresh embryos) were optimised, time limitations prohibited a formal comparison between the two groups (i.e. embryos and mESC lines), which can be explored in future studies.

Collectively, the present study shows promising parallels between changes induced within the preimplantation embryo and the derived mESC lines. This provides an opportunity to further investigate the underlying mechanisms that are responsible for altering the phenotypic expression of these cells, providing deeper insights on AMA-induced changes in the inaccessible embryo, thereby reducing animal numbers required for research.

Chapter 3 Metabolic differences between mESC lines derived from normal and low protein fed dams during the preimplantation period

3.1 Introduction

In mice, maternal low protein diet (LPD, 9% casein) fed during either the preimplantation period (i.e. E0.5 - E3.5) or throughout gestation alters embryonic and fetal development, and predisposes adult-offspring to various non-communicable, late-onset cardiometabolic diseases and neuro-behavioural dysfunction (Watkins et al., 2008, 2011; Gould et al., 2018).

It has also been reported that maternal LPD alters various metabolic hormones and metabolites, including insulin and glucose levels in maternal serum at E3.5 (Eckert et al., 2012b). Furthermore, LPDs also reduce both maternal serum and uterine fluid amino acids (AA) concentrations, particularly branched chain AAs (BCAAs) such as leucine, isoleucine and valine, at this stage of gestation. These maternal changes corresponded with alterations in the AA composition of blastocysts which were accompanied by reduced mTORC1 signalling and an increased number and expansion of TE cells; which in turn corresponded with previous observations of compensatory mechanisms of enhanced maternal-fetal nutrient transport via the visceral yolk sac (Watkins et al., 2008). Importantly, similar observations were made when mouse embryos were cultured in media containing low levels of insulin and BCAAs (Miguel A. Velazquez et al., 2018), confirming the importance of these metabolic factors in a more chemically defined system.

Mouse ESC lines derived from blastocysts of dams fed LPD (9% casein) for E0.5 - E3.5, showed reduced derivation efficiency and survival, and increased apoptosis compared to lines derived from NPD blastocysts (normal protein diet, 18% casein) (Cox et al., 2011). Furthermore, embryoid bodies (EBs) derived from these mESC lines exhibited persistent changes in pERK (Protein kinase RNA-like endoplasmic reticulum kinase) signalling and histone modifications involved in *Gata6* expression and PE differentiation (Sun et al., 2015; 2016); congruent to the previously reported *in vivo* data (Watkins et al., 2008; Eckert et al., 2012). Thus, the mESCs and EBs appear to retain and propagate nutritionally-induced adaptations *in vitro,* making them a suitable model for analysis of underlying mechanisms. Collectively, these observations indicate a maternal LPD-induced compensatory (or adaptive) response on the part of the maternal uterine environment and/or blastocyst; aspects of which can be modelled in an *in vitro* system using mESCs.

It is not known, however, to what extent metabolic alterations in the early embryo persist beyond the period of implantation *in vivo* to influence subsequent fetal development. Carryover effects from the preimplantation period may be epigenetic in nature, and it is possible that these could relate to genes encoding enzymes involved in key metabolic processes (Denisenko et al., 2016). As an initial step to address this hypothesis, the current study undertook a comprehensive metabolomic profile of mESC lines derived from E3.5 blastocysts of dams fed either a NPD or LPD.

Metabolomic profiling provides an instantaneous snapshot of cellular physiology. In the current study, metabolomic analyses were conducted in collaboration with Metabolon Inc (North Carolina, U.S). The study utilised the undifferentiated NPD and LPD mESC lines described by Cox et al. (2011), Sun et al. (2015, 2016). The defining characteristics of ESCs (i.e. their ability to self-renew and differentiate into virtually any cell type (Weissman et al., 2001)) is mostly regulated by their high glycolytic index. Thus, it is the metabolic profile of ESCs that enables biological stability and distinguishes their undifferentiated state from differentiated state, where increased glycolysis is replaced by mitochondrial oxidative phosphorylation. Additionally, changes in the metabolomic profile of mESC lines may be related to additional cellular phenotypic changes induced by maternal LPD on ICM of E3.5 blastocyst *in vivo.*

NPD and LPD mESC lines (7 per group) with stable karyotype (i.e. >70 % euploid) were cultured and expanded in Southampton as described previously (Cox et al., 2011). Lysates were also prepared in Southampton according to Metabolon Inc guidelines before shipment for metabolomic analyses. This was undertaken at Metabolon by their staff in collaboration with myself on a secondment. Multivariate data analyses conducted by Metabolon followed blanket transformation. In order to confirm statistical significance, those metabolites that displayed the greatest dietary effects, were subsequently tested for normality, homogeneity of variance and additivity, and re-analysed individually by myself.

3.2 Materials and Methods

3.2.1 Animals and early experimental procedures (performed by Dr. Andy Cox)

Animal procedures were conducted in accordance with UK Home Office Animal Act (as described in Chapter 2, Section 2.2.1). For protein restriction studies, inbred C57BL/6 females (7-10 weeks) were mated with sexually mature C57BL/6 males. Once mating was confirmed, females were separated from males, and divided into two groups. From the day of conception (E0.5) to early blastocyst developmental stage (E3.5), dams were fed either normal protein diet (NPD) or low protein diet (LPD) (Appendix A, Table 1). On E3.5, dams were culled, embryos were retrieved (as described in Chapter 2, Section 2.2.1.1), and blastocysts were cultured for the derivation of NPD and LPD mouse ESCs (Chapter 2, Section 2.2.2.2). A former PhD student at University of Southampton, Dr. Andy Cox, performed the animal and experimental procedures mentioned in this section. Mouse ESC lines were derived and cultured on mitotically inactivated MEFs (DMEM and 15% FBS), in mESC medium (KnockOut™ DMEM, LIF, 15% KO/SR) and characterised (i.e. gender analysed and karyotyped), using similar protocols to those described in Section 2.2.2, and Section 2.2.3 and Section 2.2.4, respectively.

3.2.2 Sample preparation for metabolic analysis (Conducted by me in Southampton, U.K)

To investigate the metabolite profiles of established NPD and LPD mESC lines (Sun et al., 2014; Sun et al., 2015), seven mESC lines were cultured (in duplicate) from each dietary group. All mESC lines used in this study were male and karyotypically normal (i.e. >70% euploid). Cells were harvested and prepared for shipment to Metabolon Inc (USA) for metabolomic analysis, in accord with protocol provided by Metabolon Inc. mESC lines (7 NPD and 7 LPD) were thawed on mitomycin-C treated-MEF dishes (Chapter 2, Section 2.2.2.2.1). mESC lines were cultured and expanded in serum-free mESC medium (KnockOut™ DMEM, LIF, 15% KO/SR, Section 3.2.1) after which they were split 1:2 and grown in duplicate for the final passage. mESC lines were maintained at low passage numbers (P9- P11) and precautions were taken to keep the culture conditions (i.e., thawing, handling of cells, warming and changing medium, passaging time, centrifugation time, freezing conditions) as similar as possible for each set of cell lines. Once the cells reached 70-80 % confluency, they were trypsinized (Section 2.2.2.2) and counted using a haemocytometer. For metabolomic profiling, a packed cell pellet (50-100 µl) was prepared and flash-frozen in liquid nitrogen and immediately stored at -80°C until shipped to Metabolon (on dry ice). A sample manifest detailing sample description including sample type (i.e. NPD and LPD mESC lines), unique cell line codes, passage number, cell number per cryovial, date of freezing and any other necessary details about samples, was also shipped along with the samples. Collectively, the entire process including cell culture, expanding and lysate preparation took around 3 to 4 months.

3.2.3 Sample processing and data acquisition (Conducted at Metabolon, U.S)

Each step conducted at Metabolon Inc. underwent quality control (QC) assessment. Once received, samples were assigned a unique identifier which contained the details provided in the sample manifest and was used for subsequent tasks like sample handling, methods and results. Samples were homogenized and frozen at -80°C immediately after, until ready for processing. Samples were prepared using the automated MicroLab STAR® system (Hamilton). They were thawed on ice and diluted with methanol. This step ensured the removal of proteins and the dissociation of protein bound metabolites. Once methanol was added, the samples were distributed (as 4 experimental and 1 spare), sealed and vigorously shaken (GenoGrinder 2000, Glen Mills) and centrifuged (3000 rpm). The shaking aided in the precipitation of proteins with methanol. Cell pellet was discarded at this step and the resulting extract was divided into 5 fractions (for analysis with 4 solvents and 1 reserved for backup).

Samples were reconstituted with 4 solvents i.e. Pos (positive) Early, Pos Late, Polar and Neg (negative). Two solvents were used for analysis by two separate reverse phase ultra-performance liquid chromatography-tandem mass spectrometry (RP)/UPLC-MS/MS methods with positive ion (Pos Early and Pos Late- depending on their size and hence time of elusion) mode electrospray ionization (ESI). The other two solvents were used with negative ion (Neg and Polar) mode ESI for analysis by (RP)/UPLC-MS/MS and hydrophilic interaction chromatography for UPLC-MS/MS (HILIC/UPLC-MS/MS) methods, respectively. Each 384-well plate was reconstituted with different solvent, placed on TurboVap® (Zymark), sealed and sonicated. This further reconstituted the metabolites. Each 384-well plate contained a duplicate of an internal control matrix (MTRX, with human plasma) and 4 samples of combined matrix (combination of all samples). These were essential QC steps to ensure that all aspects were operating within defined specifications (by using MTRX) and to assess the effect of a non-plasma matrix on the Metabolon process, and to distinguish biological variability from process variability (by using CMTRX). The plates were dried overnight under a N_2 hood before proceeding to analysis.

Samples were run on the UPLC-MS/MS Platform. Each platform consisted of 3 identical units of UPLC (Waters ACQUITY) and a high resolution MS/MS (Thermo Scientific Q-Exactive) platform. The platforms were interfaced with a heated ESI source and a mass analyser (for 35,000 mass resolution). The samples were dried and reconstituted with 4 solvents as described above. Each solvent contained several standards at fixed concentrations to ensure consistency with each injection and chromatographic phase. Based on the metabolite's biochemical properties (i.e., mass and ionic charge), ions were eluted in different systems. Some metabolites, however, were eluted in more than one system.

Before initiating the run, samples were randomized and each platform was connected to a common computer where raw data was simultaneously archived. Samples mostly ran overnight, after which raw data was extracted, peak identified and processed for QC using Metabolon's hardware and software services. Once the data was extracted, the compounds were identified by comparison to purified standards of other (known or unknown) biochemicals stored in the libraries depending on the sample source (i.e. mouse ESCs in the present study) and project design (i.e. NPD and LPD). The comparison was based on the biochemical's mass to ionic charge ratio, retention index (or elution time) and other chromatographic data (including MS/MS spectral data) on all molecules present in the library. Once identified, biochemicals were scored based on the number of times they were detected in previous studies and sample type.

Collected data was curated to ensure accurate and consistent identification of the metabolites. It was important to make sure that only true chemical entities were processed further for statistical analysis, thereby removing artefacts and background noise. This was done using Metabolon's proprietary visualization and interpretation software, which eliminated any inconsistent peaks, compared each compound for every sample, to the ones archived in the library, and corrected where errors were discovered. Curated relative ion intensity data were normalized by either protein (Bradford assay by Metabolon) or cell number (haemocytometer at Southampton) analysis. Viable cells were detected by trypan blue dye exclusion assay (as described in Chapter 2, Section 2.2.6) and provided to Metabolon as a part of the sample manifest (Section 3.2.2).

Prior to statistical evaluation, data was normalised and missing values were imputed to ensure improved data quality and to preserve biological variability of the samples. As sample ion intensities may range from a few thousands to many millions (relative abundance/protein), which could be difficult to display and visualise, the values for a given metabolite were normalised (i.e. rescaled) according to the median value recorded for the metabolite, such that, its' median value across all samples was equal to 1. Additionally, in a given study, there can be instances where certain metabolites are not detected. This could occur if a given metabolite's ion intensity is lower than the limit of detection (threshold) in a given sample. This results in 'blank' or 'missing' values. To counter this issue (where required), the current study used a 'minimum imputation approach' whereby, the 'missing values' were imputed by the lowest observed value in the given dataset or sample set.

Finally, once the dataset was normalised (median scaled and protein or cell normalised) and missing values were imputed, data were log-transformed (by Metabolon). This method was selected to ensure a normal or near-normal distribution. Data were then back-transformed (as simple geometric means) and the Welch's 2-sample t-test was performed to evaluate significance. It is important to note that in a metabolomic study of this magnitude, which includes analysis of hundreds of

metabolites and thus data points, it is difficult to test which dataset requires log-transformation, and which does not. Therefore, in metabolomic studies, it is a common practice to log-transform the entire dataset as it is likely to make the data less erroneous and the process more time efficient. Additionally, the large dataset was also adjusted for false discovery rate (FDR, *q*-value). Generally, 5% of the analysed data could meet the significance cut-off (i.e. $P \leq 0.05$) by random chance. Hence, data with a low *q*-value (i.e. $q < 0.10$) are indicative of high confidence, whereas a higher *q*-value indicates diminished confidence.

In the current Chapter, only the most important metabolites out of the 530 analysed are reported, i.e. these metabolites were selected based on Metabolon's multivariate analyses, after they were corrected for FDRs. Therefore, the limited number of metabolites (57 in total) allowed a re-evaluation of normal distribution of the dataset (at Southampton). As evaluated by Shapiro-Wilk normality test (GraphPad Prism 7 software) for each metabolite and sample group, the dataset was normally distributed. Thus, data presented in this Chapter were not log-transformed, although the statistical test for significance was the same as used by Metabolon, i.e. Welch's 2-sample t-test.

3.2.4 Phosphofructokinase (PFK) Activity Assay

Glycolytic activity is tightly controlled by the irreversible reactions catalysed by three important enzymes namely hexokinase (HK), phosphofructokinase (PFK) and pyruvate kinase (PK) (Berg et al., 2002). Activities of these enzymes are regulated by reversible binding of allosteric effectors or by covalent modifications, and the enzyme amounts vary with changing metabolic needs that are regulated by transcription.

Given the findings from Metabolon data (provided later in Section 3.3.2), the current study focused on evaluating the activity of one of the glycolytic enzymes (i.e. PFK) in the same mESC lines that were used in the Metabolon study (Section 3.2.2). As displayed in Figure 3.1, PFK comes as two isoforms- PFK 1 and PFK 2 which, in the presence of adenosine triphosphate (ATP), catalyse the conversion of fructose-6-phosphate to fructose-1,6-bisphosphate (F-1,6-bP) and fructose-2,6-bisphosphate (F-2,6-bP), respectively, thereby releasing ADP as a by-product (Uyeda et al., 1981; Hers et al., 1982). During glycolysis, F-2,6-bP along with adenosine monophosphate (AMP) act as stimulators of PFK and inhibitors of F-1,6-bP, which is converted back to F-6-P by fructose 2,6-bisphosphatase during gluconeogenesis (Figure 3.1).

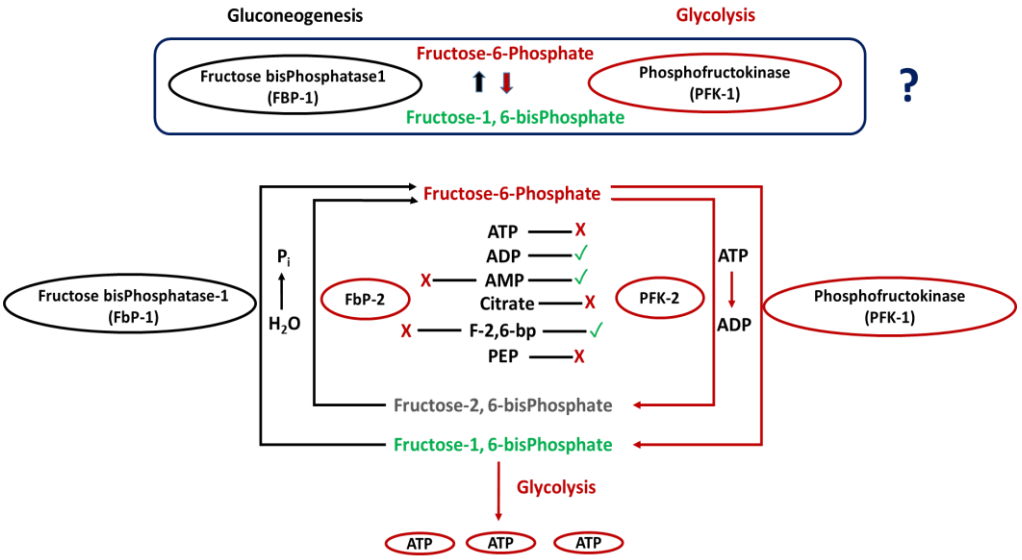

Figure 3.1 Glycolytic and gluconeogenic conversion of Fructose-6-Phosphate (F-6-P).

F-6-P is converted to Fructose-1,6-bisPhosphate (F-1,6-bP) and Fructose-2,6-bisPhosphate (F-2,6-bP) by the glycolytic enzymes PFK1 and PFK2, respectively, by utilizing ATP and releasing ADP. The process is activated by AMP, ADP and F-2,6-bP, and inhibited by ATP, Citrate and phosphoenolpyruvate (PEP). F-1,6-bP and F-2,6-bP undergo gluconeogenesis, utilize H_2O and release Pi to convert back to F-6-P assisted by enzymes Fructose bisPhosphatase 1 (FbP-1) and Fructose bisPhosphatase 2 (FbP-2) respectively. ATP and downstream glycolytic metabolites like citrate and phosphoenolpyruvate (PEP) inhibit the activity of the allosteric enzyme (i.e. PFK).

3.2.4.1 Principle of PFK Activity Assay (Abcam, ab155898)

To assess PFK activity, the current study used the 6-Phosphofructokinase Activity Assay kit (Abcam, ab155898). The assay works on the principal that PFK present in the samples (i.e. NPD and LPD mESC lines) converts fructose-6-phosphate to fructose-diphosphate by utilising ATP, and releasing ADP (Figure 3.1). The released ADP then combines with the substrate (a combination of sugars, proprietary information of Abcam) in the presence of commercial enzyme mix that assists to dephosphorylate ADP to AMP, and release NADH. NADH acts as a reducing agent, which in the presence of a probe/ developer (salt that is reduced by NADH to produce chromophore, proprietary information of Abcam) reduces the colourless probe to a coloured product, detected with strong absorbance at 450 nm (Figure 3.2). To verify accurate functioning of the kit and the reagents, the assay also includes a positive control (i.e. purified PFK enzyme from Bacillus species), that was run with every assay during optimisation and also during the final experiments.

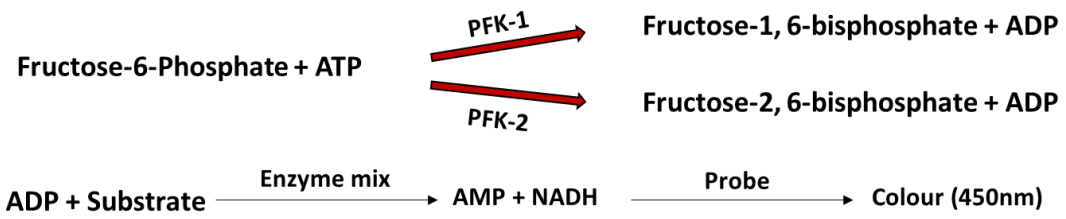

Figure 3.2 Functional mechanism of the PFK Activity Assay Kit, ab155898 (Abcam).

It is a calorimetric assay that works in a kinetic mode; i.e. the conversion rate, which is determined by optical density, changes (i.e. increases, saturates, and then decreases) with time. It is also important to note that the assay utilizes total ADP released; i.e. during the phosphorylation of both F-1,6-bP and F-2,6-bP, which is then used to produce NADH and measure the change in colour intensity. Thus, it is not possible to distinguish between the activities of PFK 1 and PFK 2, and the measured activity is therefore total PFK activity.

3.2.4.2 Sample preparation for PFK Activity assay

PFK activity was analysed in fourteen male mESC lines, i.e. 7 NPD and 7 LPD (derived by Dr. Andy Cox, Section 3.2.1). mESC lines were processed directly from frozen vials (from liquid N_2) and thus, were not cultured. Samples were thawed and washed with PBS (Gibco™, 10010023) to remove any traces of phenol red from the KnockOut™ DMEM. Live cells were counted by Trypan Blue exclusion (Chapter 2, Section 2.2.6). After discarding PBS, cells were diluted to obtain 2 million cells in 200 µl of assay buffer and transferred to UV-radiated 2 ml microcentrifuge Eppendorf tubes. Cells were gently homogenized while the samples were maintained on ice and centrifuged at high speed (12,000 rpm, 5 min, 4˚C). The retrieved supernatant was spun again in a 0.2 µm VectaSpin Micro centrifuge tube filter (Z338591, Sigma Aldrich) to filter out any residual debris. Around 170-180 µl was recovered from the initial 200 µl assay buffer, which was divided into smaller aliquots of 20-30 µl and stored at -20°C. Therefore, the final PFK assay experiment was performed from aliquots/ samples that were frozen and thawed at the same time, and analysed in the same run, using the same batch of reagents.

Samples for assessing PFK activity were processed in accordance with the PFK activity assay kit (ab155898). All steps were performed in a 96-well clear plate with flat bottom. To inhibit initiation of the biochemical reaction (Figure 3.2), samples were loaded as quickly as possible while the 96-well plate was placed on ice at all times until it was analysed in the plate reader. Each sample and standard were plated in duplicate. The assay was run in a multi-well spectrophotometer, pre-warmed and maintained at 37˚C throughout experiment, set at kinetic mode for 80 min, where the optical density (O.D) was measured and recorded at the interval of every 60 seconds.

Additionally, prior to running the final experiment, the kit was optimised for the NPD and LPD mESCs line samples by testing the sample volumes including 50 µl, 25 µl, 15 µl, 10 µl, 5 µl and 1 µl (data not presented). From these, the final sample volume of '0.5 µl' was selected for further analysis, as it fell within the NADH standard curve range. It must be noted that sample volume optimisation was based on 'cell number counts'. As mentioned earlier, a total cell volume of 2 million cells was homogenised in 200 µl of assay buffer. Therefore, assuming that the cell proportion was consistent through different steps of the assay, final sample volume of 0.5 µl would equal to 5000 cells in the analysed sample. However, as there was no confirmative way to verify this assumption of using exactly the same number of cells for each sample well, in addition to cell normalisation, PFK Activity Assay data was also normalised by protein (Bicinchoninic Acid (BCA) Assay, Section 3.2.5).

3.2.4.3 Calculations for Data Analysis

Readings at 0 standard were subtracted from all standard before the NADH standard curve was plotted. As stated before, NADH standards were run for 80 min and O.Ds were recorded after every minute. Standard curves were plotted for every 5 minutes and produced identical standard linear curves throughout the run. Figure 3.3 A shows a representative standard curve at 10 min of incubation time. Value of the intercept in the given figure, X = (Y- 0.0072) / 0.0418, where, Y = O.D. at final time point (T2) subtracted by O.D. at initial time point (T1) for each sample, where T1 and T2 refer to the two chosen time points of linear scale in NPD and LPD mESC samples. Sample background (i.e. interference from ADP and NADH in the sample) was corrected by subtracting value derived from the background control from all sample readings. Based on linearity, the limit of reaction time selected for NADH standard curve and PFK activity calculations were initial time, T1 = 5 min and final time, T2 = 10 min. Calculations for PFK activity were performed using the following equation:

$$\boldsymbol{Sample\ PFK\ Activity\ = \frac{B}{\Delta T\ x\ V} * Dilution\ factor = \ nmol/min/ml\ = \ mU/\ ml}$$

Where**,** x = B (value of intercept), Y = A2-A1 (linear equation), Δ O.D = A2-A1; A1= O.D. at T1 (5 min) and A2= O.D. at T2 (10 min), Δ T (T2-T1) = 10 – 5 = 5 min, Volume of sample, V = 0.5 ul = 0.0005 ml, and the dilution factor = 1 (this was calculated by the number of cells used for homogenisation). Figure 3.3 A shows a representative NADH standard curve where y = (0.418) x + 0.0072. Hence using the above equation in the data provided in Figure 3.3 C, y = 0.0380 for NPD 1 and y= 0.0482 for LPD 1, and the dilution factor =1. Hence, in the presented example, PFK activity for NPD 1 = 392.82 mU/ ml and PFK activity for LPD 1= 294.73 mU/ ml (Figure 3.3 C).

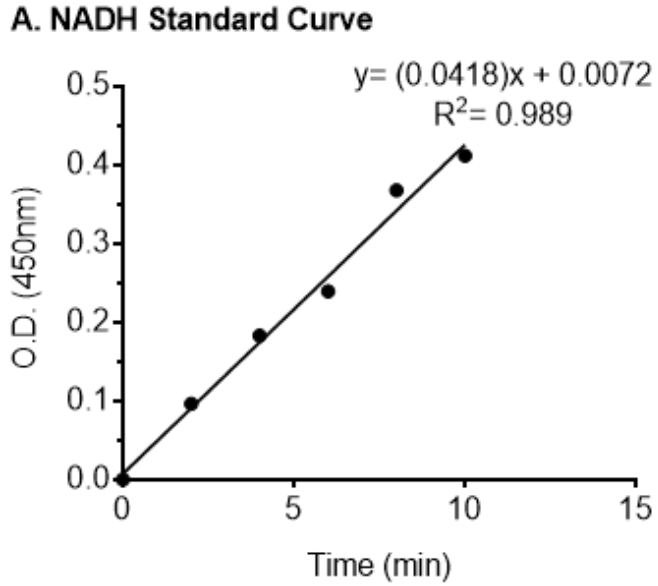

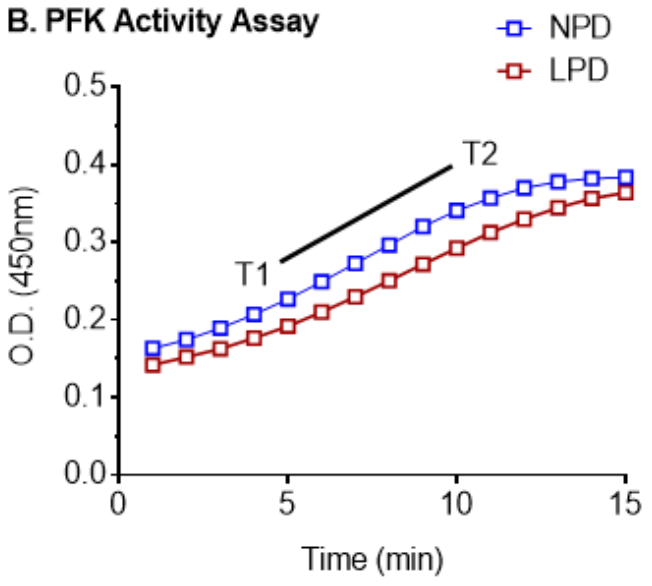

C. Raw Data

Diet Group	O.D. at 5 min A1	O.D. at 10 min A2	Δ O.D. (A2-A1)	ΔT T2-T1	Volume (ml)	y - 0.0072 (y = Δ O.D.)	X (B)	Δ T x V	PFK Activity (B/ Δ T x V)
NPD 1	0.0663	0.1043	0.0380	5	0.0005	0.0308	0.7368	0.0025	392.82
LPD 1	0.0850	0.1287	0.0482	5	0.0005	0.0410	0.9820	0.0025	294.73

Figure 3.3 Optical densities at 450nm.

(A) NADH Standard Curve and (B) PFK Activity Assay for NPD and LPD male mESC lines (n = 7 per group) for the first 15 minutes of reaction time where T1 = 5 min and T2 = 10 min. Table (C) illustrates representative raw data from NPD and LPD mESC lines (n=1) and calculations for estimation of PFK activity (mU/ ml).

3.2.5 Pierce BCA (Bicinchoninic Acid) Protein Quantification Assay

As mentioned earlier, in addition to cell number, PFK activity was also normalised to protein. Protein levels were estimated from the same fourteen NPD and LPD mESC homogenised aliquot samples (n = 7) that were used for the PFK assay (Section 3.2.4). Samples were stored at -20˚C, in assay buffer (PFK assay kit), which is known to be compatible with Pierce BCA Protein Assay Kit (23225, Thermo Scientific).

The Pierce BCA assay is based on the principle of using protein in an alkaline medium (biuret reaction) to reduce Cu^{+2} to Cu^{+1} by selective colorimetric detection of Cu^{+1} in the presence of Bicinchoninic Acid (BCA) (Smith et al., 1985). Chelation of Cu^{+1} produces a purple-coloured reaction which is linear with increasing concentration of protein. The chromophore formation depends on several aspects of protein, i.e. structure, number of peptide bonds and the presence of specific amino acids such as cysteine, cystine, tryptophan and tyrosine (Wiechelman et al., 1988). As the colour formation depends on the combination of several proteins, protein quantity is estimated with reference to an internal standard, generally constituting a common protein like bovine serum albumin (BSA). Therefore, a dilution series of known BSA concentrations was prepared and analysed along with the unknown NPD and LPD samples for protein estimation.

Multiple sample volumes were also tested for 1 µl, 2 µl, 3 µl (data not presented) and 4 µl from which the final sample volume of '4 µl' was selected for further experiments. Working reagents and samples were prepared following company guidelines (23225, Thermo Scientific). Samples and standards were plated in UV radiated, clear 96-well flat bottom microplates. Plates were analysed for 15 minutes in kinetic mode, at an absorbance of 570 nm and maintained at 23˚C (room temperature). For calculating estimated protein concentrations, samples and standards were corrected for background by subtracting the standard sample containing no BSA; i.e. containing only working reagent and water. Standard curve is presented in Appendix B, Figure 6.

3.3 Results

Metabolic reprogramming consequences associated with maternal low protein diet intake (E3.5) were investigated by analysing global metabolomic profiles of 7 NPD (18% casein) and 7 LPD (9% casein) male mESC lines. These mESC lines were maintained at low passage numbers (P10-P12) and cultured on mouse embryonic fibroblasts (MEFs) under serum free (KO/SR) conditions until they were snap frozen as lysates for metabolomic profiling using ultra-performance liquid chromatography-tandem mass spectrometry (UPLC-MS/MS) at Metabolon Inc. (North Carolina, U.S).

Based on Metabolon's findings, a total of 530 metabolites were identified. Data were normalised by both protein concentration and cell counts, log transformed, imputed for missing values and analysed for significance by Welch's two-sample t-test (Section 3.2.3, pointers 8 and 9). Given the multiple comparisons undertaken in a huge dataset such as this, predictions were adjusted for false discovery rate (FDR, q-value). Differences in metabolite levels reported in this chapter are restricted to protein-normalised data. Out of the 530 metabolites, 28 qualified as significant (22 upregulated and 6 downregulated) ($P < 0.05$), whereas 26 (20 upregulated and 6 downregulated) tended towards significance ($0.05< P <0.10$). Most differences centred on changes relating to amines (3), carbohydrate metabolism (5), lipid metabolism (15), miscellaneous nucleotides and vitamins (6). Suggestive differences were also reported in pyrimidine homeostasis (4) and phytosterol levels (1).

Therefore, in the current chapter, the three most significant groups of metabolites (i.e. amino acids, carbohydrates and fatty acids) were reanalysed. As mentioned previously, large datasets of metabolites usually undergo blanket transformation (e.g. log or square root- depending on data type) to reduce or correct skewed data. However, it may induce errors in data that are normally distributed and therefore do not require transformation. As the focus of the chapter was limited to the most significant findings by Metabolon, the data were tested individually for normality and homogeneity of variance, and re-analysed using Welch's 2-sample t-test. As the reported data were observed to be normally distributed, it was not transformed.

3.3.1 Amino Acids

Undifferentiated male NPD and LPD mESC line lysates were analysed for differences between twenty proteinogenic amino acids including essential and branched chain amino acids (BCAA). Out of these, only two (i.e. asparagine ($P = 0.049$) and threonine ($P = 0.073$)) amino acids were observed to be statistically different. Table 3.1 displays the mean concentration of protein-normalised amino acids.

Table 3.1 Mean (± S.E.M.) concentrations of essential and branched chain amino acids (AA).

Amino Acids	NPD mESCs, n=7	LPD mESCs, n=7
Alanine - ala	0.902 ± 0.080	1.047 ± 0.120
Arginine - arg	1.010 ± 0.087	0.997 ± 0.043
Asparagine - asp	**0.845 ± 0.074**	**1.090 ± 0.083**
Aspartate - asp	1.008 ± 0.074	0.989 ± 0.075
Cysteine - cys	1.023 ± 0.085	1.106 ± 0.123
Glutamine - gln	0.939 ± 0.107	0.960 ± 0.038
Glutamate - glu	1.106 ± 0.102	1.009 ± 0.072
Glycine - gly	1.044 ± 0.117	1.087 ± 0.131
Histidine - his	0.928 ± 0.079	1.011 ± 0.038
Isoleucine - ile	1.088 ± 0.103	0.989 ± 0.044
Leucine - leu	1.012 ± 0.080	1.004 ± 0.056
Lysine - lys	0.956 ± 0.087	1.021 ± 0.064
Methionine - met	0.982 ± 0.060	1.103 ± 0.075
Phenylalanine - phe	1.042 ± 0.076	1.022 ± 0.058
Proline - pro	1.047 ± 0.069	0.951 ± 0.061
Serine - ser	0.995 ± 0.063	0.983 ± 0.042
Threonine - thr	**1.136 ± 0.075**	**0.973 ± 0.023**
Tryptophan - trp	0.983 ± 0.074	1.053 ± 0.044
Tyrosine - tyr	0.999 ± 0.085	1.005 ± 0.052
Valine - val	1.024 ± 0.088	1.010 ± 0.042

Concentrations of essential and branched chain AA in lysates of NPD and LPD mESC lines (P11-13; n=7) cultured in serum free mESC medium. Metabolites highlighted in red are significant at $P<0.05$, and those in orange at $P < 0.1$.

3.3.2 Glucose metabolism

Global metabolomic profiling of LPD mESC lines identified significant changes in glucose utilization. LPD mESC lines exhibited increase in some glucose-derived intermediates at either trend or significant levels such as mannose-6-phophate ($P = 0.090$), glucose 6-phosphate ($P = 0.086$) and fructose 6-phosphate ($P = 0.046$), although downstream metabolites appeared to be trending towards reduced levels (Figure 3.4 and 3.5). Additionally, LPD mESC lines also displayed increased concentration of

glycerate (P = 0.049). However, no differences were observed in mannose and glucosamine-6-phosphate, and the pentose phosphate pathway (Figure 3.4).

Given the increased uptake of glucose-6-phosphate (G-6-P) and fructose-6-phosphate (F-6-P), and the suggestion of decreased levels of downstream metabolites (i.e. fructose-1,6-bisphosphate (F-1,6-bP), dihydroxyacetone phosphate, 3-phosphoglycerate, phosphoenolpyruvate and pyruvate), the data indicated inhibited conversion of F-6-P to F-1,6-bP (Figure 3.5). Given the role of the glycolytic enzyme PFK in catalysing ATP and F-6-P to yield ADP and F-1,6-bP (Section 3.2.4), differences in PFK activity of NPD and LPD mESCs were analysed (Section 3.2.4.1).

Frozen aliquots of mESC lines (6 NPD, 6 LPD), same as those that underwent metabolic analysis (Section 3.2.2) were processed for PFK activity (Section 3.2.4.2). Data were normalised by cell number (10,000 cells/ sample well) (Section 3.4.2.2) and protein (Pierce BCA assay, Section 3.2.5), and tested for significance using an unpaired t-test. Protein normalised data displayed decreased PFK activity (P = 0.029) in LPD mESC lines compared to NPD mESC lines (Figure 3.6 a), although this difference was only observed at trend level (P = 0.089) when data were normalised by cell number (Figure 3.6 b). However, two mESC lines (one from each treatment group) were removed prior to analysis as 'statistical outliers' that could not be corrected following transformation (square root or log). When the outliers were included (i.e. n=7), no statistical differences were observed between NPD and LPD mESC lines (Figure 3.6 c and d).

In addition to fructose-mannose, glycolysis and pentose phosphate metabolism, NPD and LPD mESC lines were also analysed for differences in metabolites within the tricarboxylic acid (TCA) pathway. TCA metabolites including citrate, cis-aconitate, α-ketoglutarate, succinate, fumerate and malate showed similar concentrations between NPD and LPD mESC lysate samples (Figure 3.7).

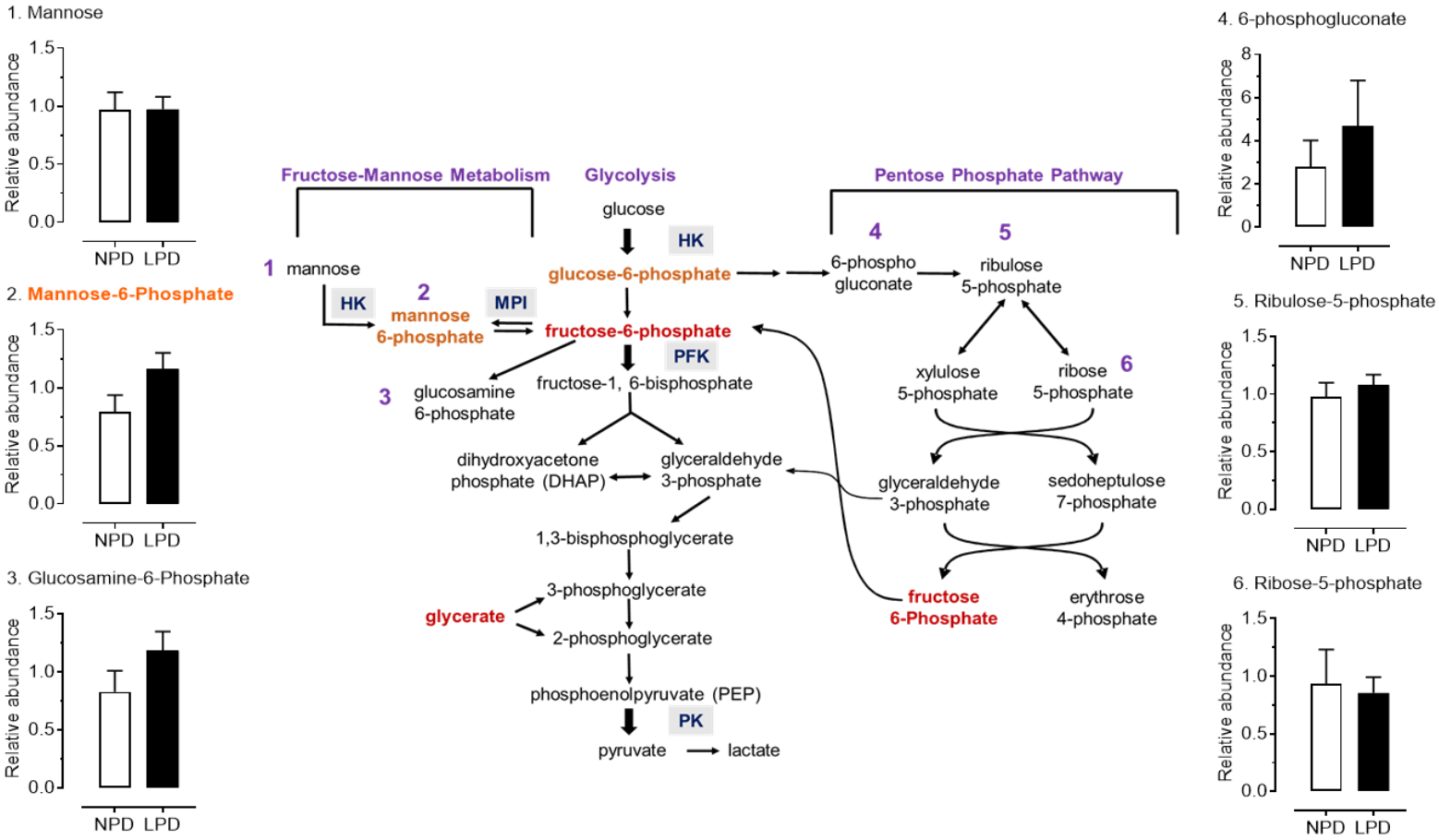

Figure 3.4 Mean (± S.E.M.) concentrations of key metabolites involved in fructose-mannose and pentose-phosphate pathways from lysates of undifferentiated male NPD and LPD mESCs (P11-13; n=7) cultured in standard mESC medium (KnockOut DMEM + LIF + KO/SR).

Metabolite concentrations are protein normalised. Metabolites highlighted in red are significant at P<0.05, and those in orange at P<0.1. HK = Hexokinase, MPI = mannose-phosphate isomerase, PFK = Phosphofructokinase, PK = pyruvate kinase.

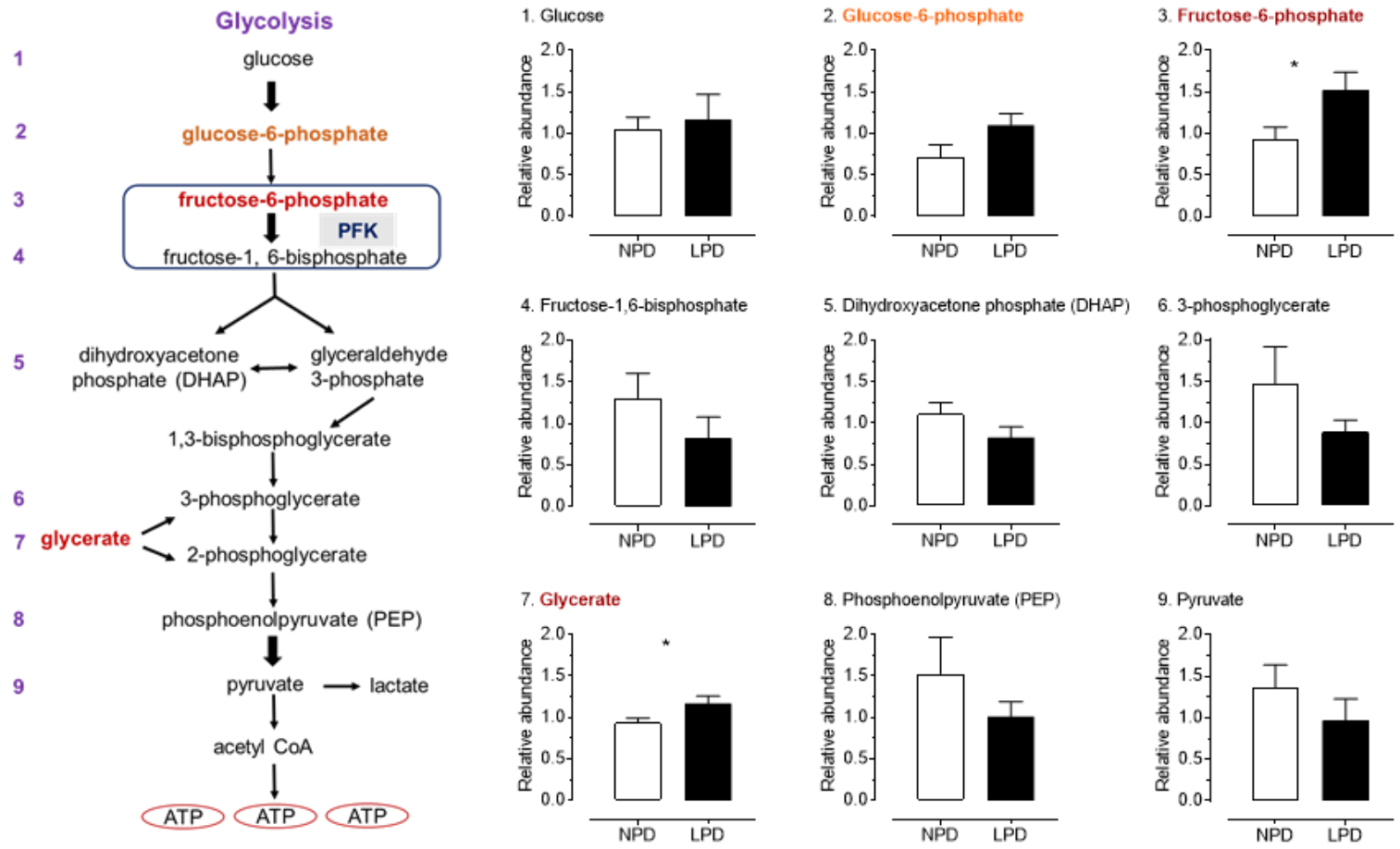

Figure 3.5 Mean (± S.E.M.) glycolytic metabolite concentrations in lysates from undifferentiated male NPD and LPD mESCs (P11-13; n=7) cultured in standard mESC medium (KnockOut DMEM + LIF + KO/SR).

Metabolite concentrations are protein normalised. Metabolites highlighted in red are significant at P<0.05, and those in orange at P<0.1.
PFK = Phosphofructokinase.* indicates P < 0.05.

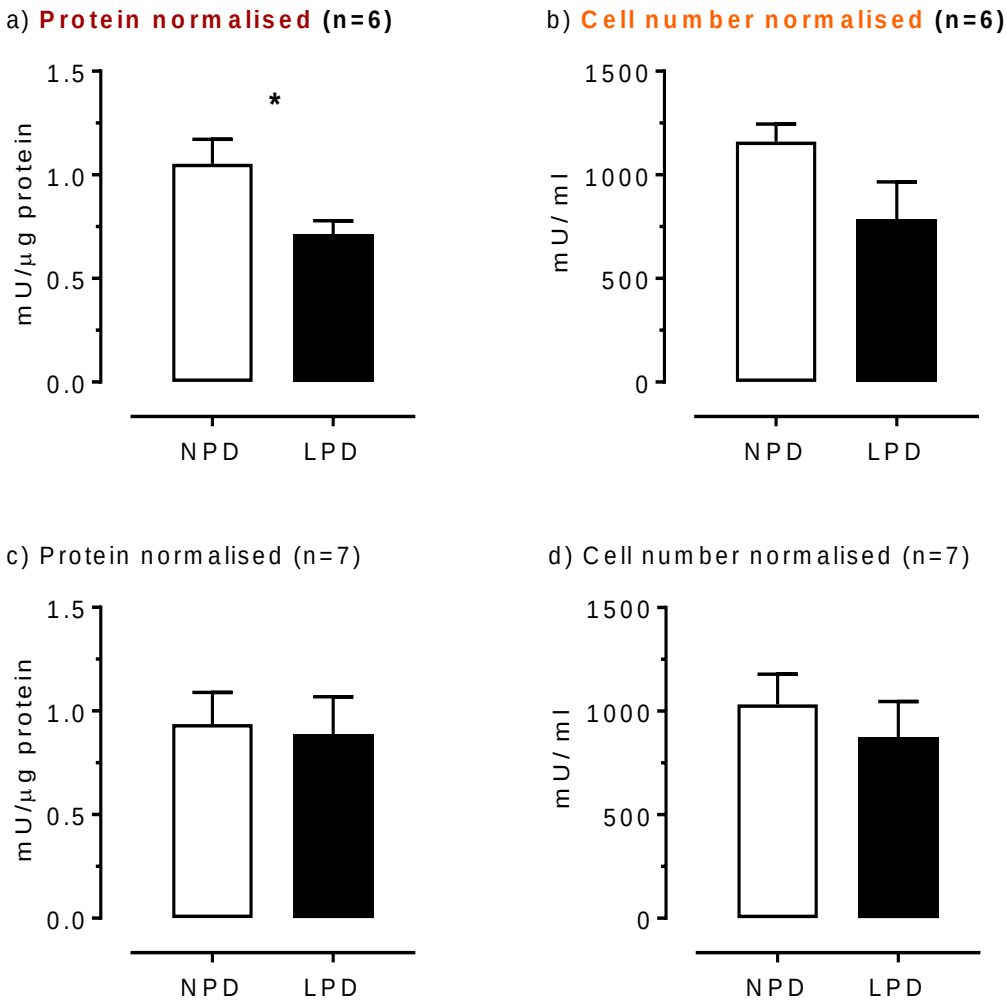

Figure 3.6 Mean (± S.E.M.) concentrations of glycolytic enzyme phosphofructokinase (PFK) in homogenised NPD and LPD mESC lines.

Frozen NPD and LPD mESC line (P11-13) aliquots were homogenised and processed for PFK Activity Assay. LPD samples showed decreased PFK activity compared to NPD samples when data was normalised by a) protein (BCA Protein Assay), (P = 0.029), highlighted in red and by b) cell number (trypan blue dye exclusion assay), (P = 0.089), highlighted in orange, when outliers were removed and n=6. * indicates P < 0.05. However, no statistical differences were observed between the two dietary groups when n=7 and data was normalised by c) protein and by d) cell number. Data presented as means ± SEMs based on n=6 for a) and b); and n=7 for c) and d) NPD and LPD male mESC lines.

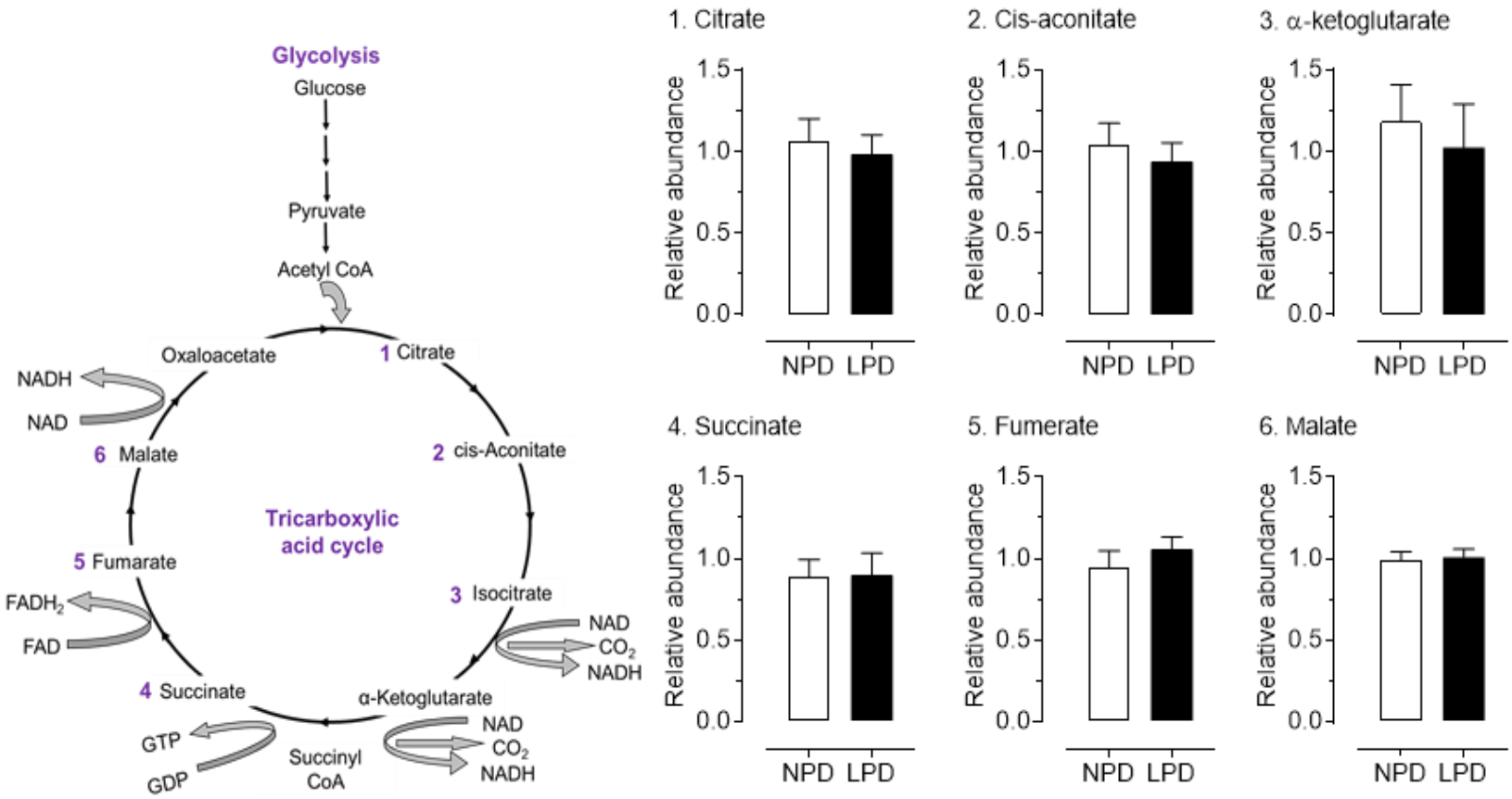

Figure 3.7 Mean (± S.E.M.) TCA cycle metabolite concentrations in lysates from undifferentiated male NPD and LPD mESCs (P11-13; n=7) cultured in standard mESC medium (KnockOut DMEM + LIF + KO/SR).

Metabolite concentrations are protein normalised.

3.3.3 Fatty acid metabolism

Some of the most significant differences between NPD and LPD mESC lysates were observed within fatty acid metabolism. The following results are presented under three broad categories (i.e. (i) saturated and monounsaturated, (ii) omega-3 polyunsaturated and (iii) omega-6 polyunsaturated fatty acids). While LPD mESC lines showed a consistent general trend of increased fatty acids, significant differences between LPD and NPD mESC lines were observed for (i) myristoleate ($P = 0.025$) and palmitoleate ($P = 0.027$) (Figure 3.8), (ii) Linolenate ($P = 0.010$), dihomo-linolenate ($P = 0.051$), eicosapentaenoate ($P = 0.066$) and docosapentaenoate ($P = 0.075$) (Figure 3.9), and (iii) linoleate ($P = 0.030$), dihomo-linoleate ($P = 0.029$), adrenate ($P = 0.068$) (Figure 3.10).

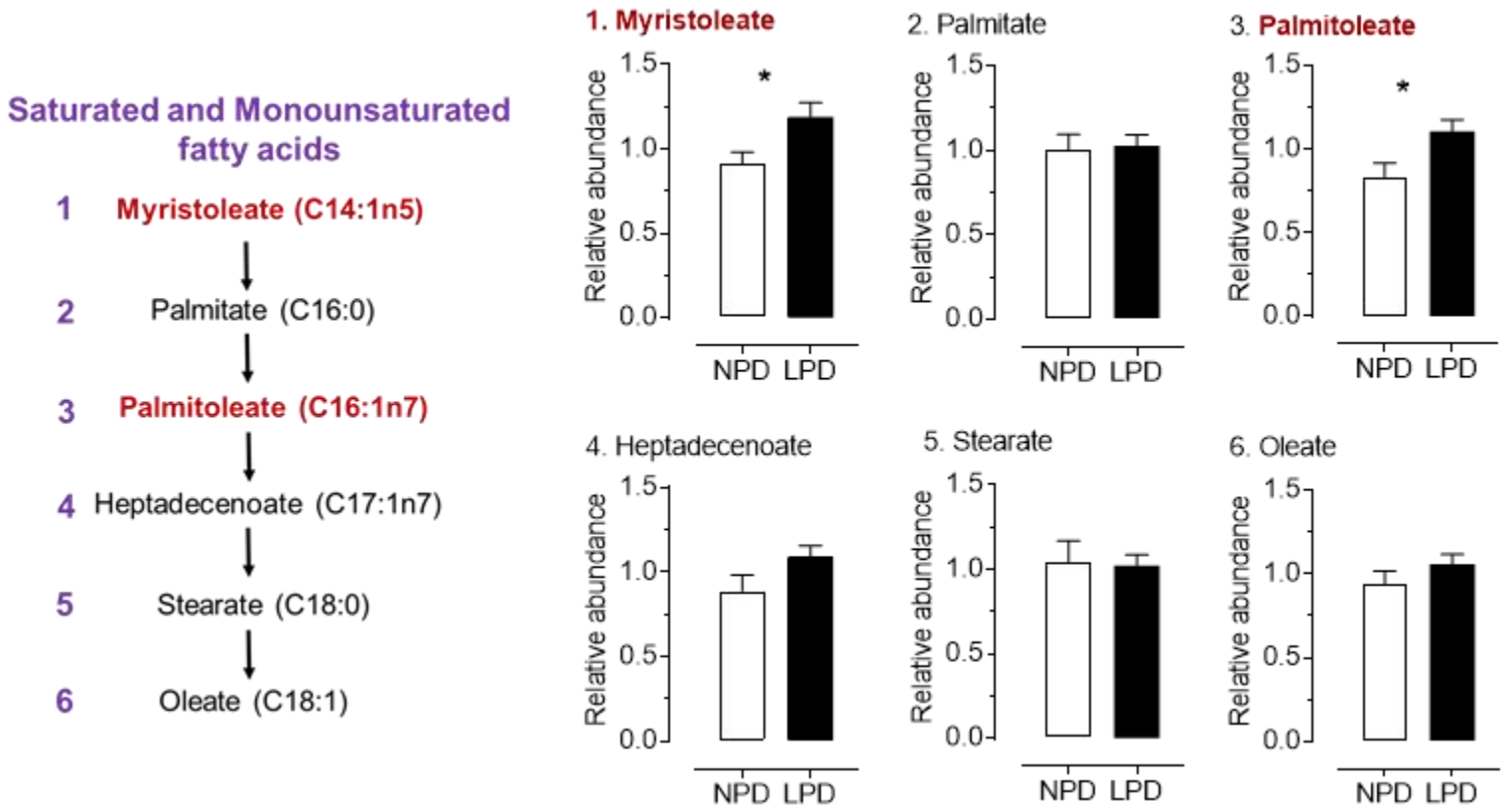

Figure 3.8 Mean (± S.E.M.) concentrations of selected saturated and monounsaturated fatty acids (FAs) in lysates from undifferentiated male NPD and LPD mESCs (P11-13; n=7) cultured in standard mESC medium (KnockOut DMEM + LIF + KO/SR).

FA concentrations are protein normalised. FAs highlighted in red and with an * are significant at $P<0.05$.

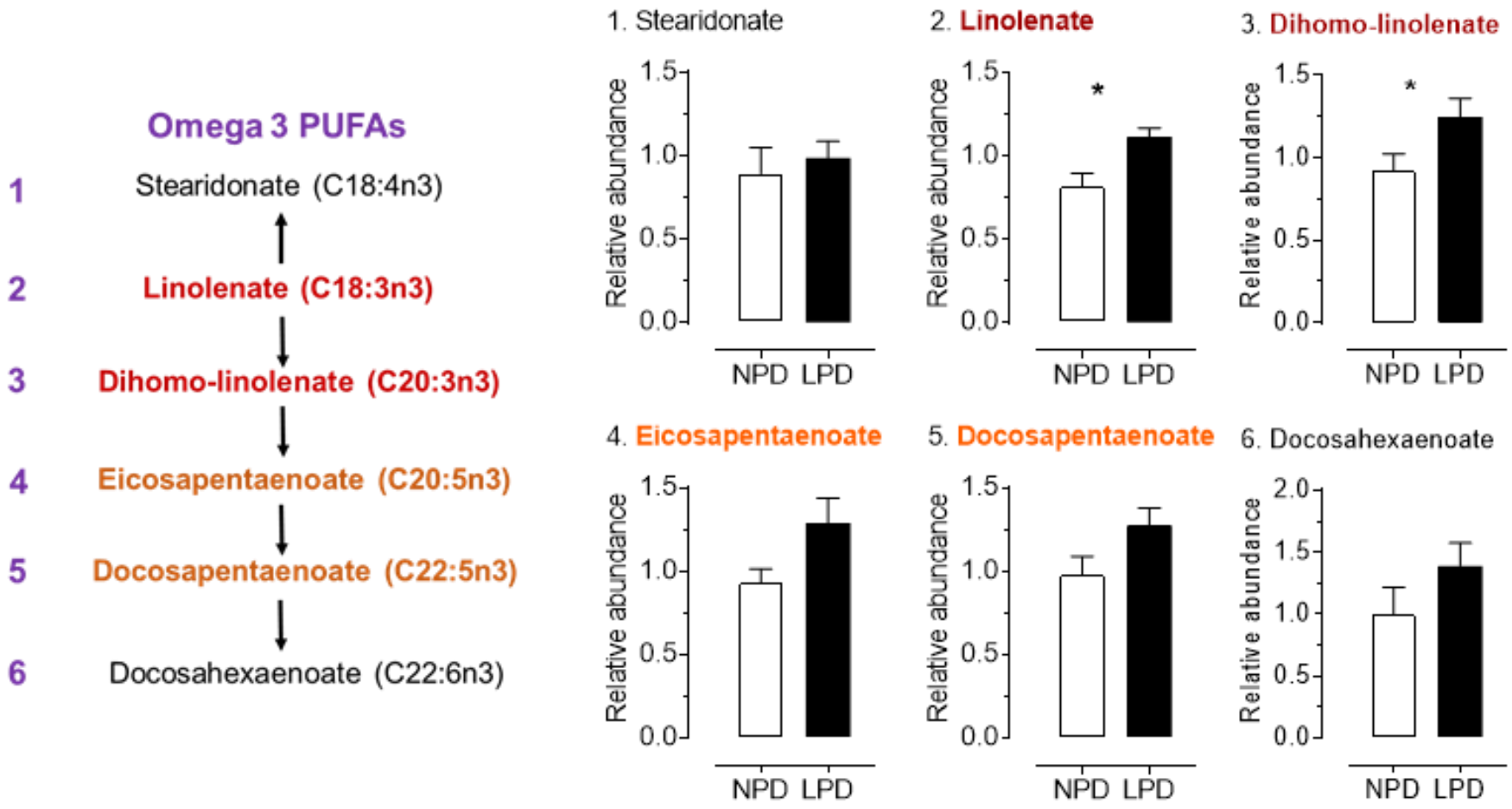

Figure 3.9 Mean (± S.E.M.) concentrations of selected omega-3 polyunsaturated fatty acids (PUFAs) in lysates from undifferentiated male NPD and LPD mESCs (P11-13; n=7) cultured in standard mESC medium (KnockOut DMEM + LIF + KO/SR

PUFA concentrations are protein normalised. PUFAs highlighted in red and with an * are significant at P<0.05, those in orange at P<0.1.

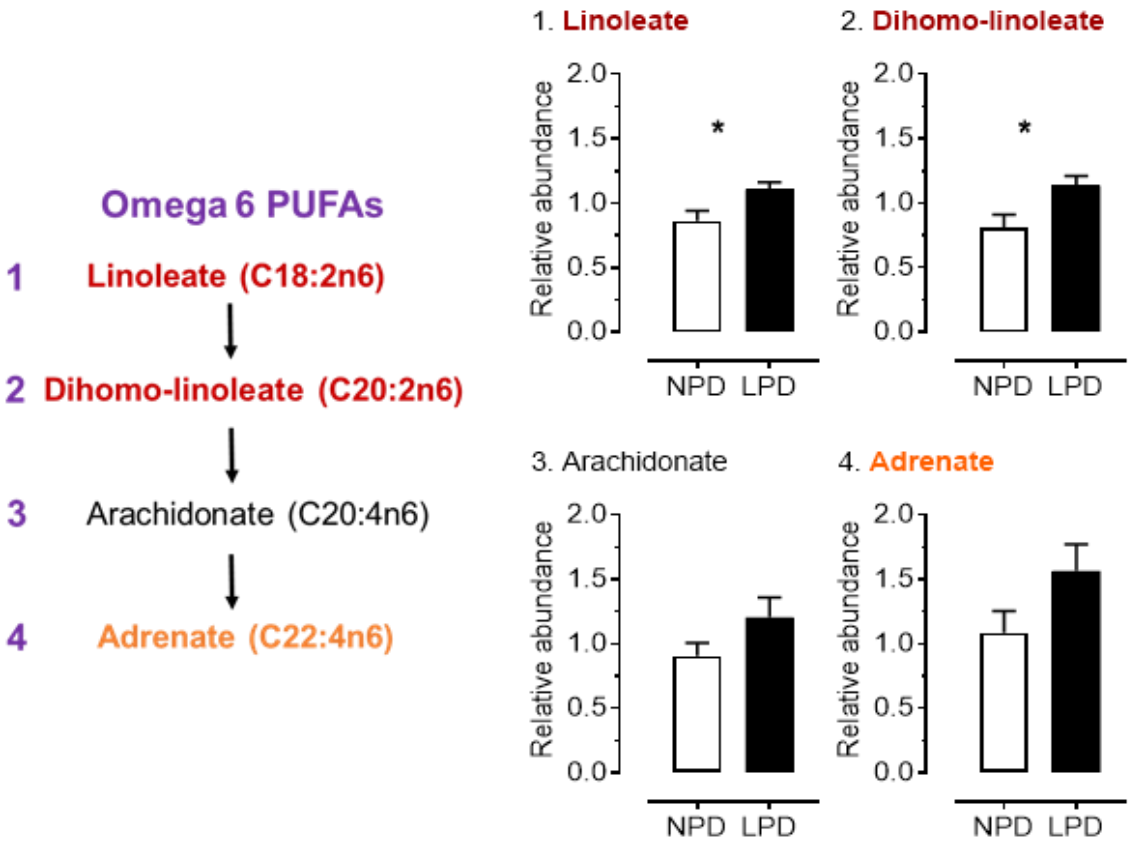

Figure 3.10 Mean (± S.E.M.) concentrations of selected omega-6 polyunsaturated fatty acids (PUFAs) in lysates from undifferentiated male NPD and LPD mESCs (P11-13; n=7) cultured in standard mESC medium (KnockOut DMEM + LIF + KO/SR).

PUFA concentrations are protein normalised. PUFAs highlighted in red are significant at $P<0.05$, those in orange at $P<0.1$.

3.4 General Discussion

Metabolomics data of mESC lines derived from embryos of dams fed NPD and LPD diets represent a snapshot of their metabolic status in response to maternal diet. In this respect, it is noteworthy that these lines were derived from the ICM of blastocysts exposed to dietary changes for only three days (i.e. up to E3.5) after which they were cultured for a protracted period (P9-P12) in commercial mESC media. The composition of this media (Appendix A) differs markedly from that of mouse uterine luminal fluid reported in previous LPD studies (Eckert et al., 2012b), although that study only investigated the amino acid content. Unsurprisingly, therefore, there was a general lack of significant FDR-adjusted differences in the metabolite composition of mESCs derived from each of the two dietary treatment groups. Nevertheless, modest alterations in carbohydrate and fatty acid metabolism between male NPD and LPD mESC lines were detected. Specifically, analysis of the glycolytic pathway revealed increased levels of upstream metabolites (including G-6-P and F-6-P) and reduced levels of downstream metabolites (i.e. F-1,6-bP onwards), suggesting an obstruction in the conversion of F-6-P to F-1,6,-bP. Indeed, subsequent investigations appeared to suggest phosphofructokinase (PFK) enzyme activity to be reduced in LPD mESC lines. Differences between NPD and LPD mESC lines were also observed in omega 3 and 6 families of PUFAs. The former is significant because of the key role of n-3 PUFAs in neurological development and function (McNamara and Carlson, 2006; Innis, 2008). Surprisingly, however, in the current study there were modest increases in both n-3 and n-6 PUFAs in mESCs from the LPD compared to the NPD treatment group. On first inspection this would appear to be at odds with previous studies investigating effects of LPDs on PUFAs (Burdge et al., 2002); albeit these PUFAs were measured in the fetal brain at a much later stage of development, in a study that assessed the effects of diet throughout gestation. Interestingly, the two dietary groups did not show differences (except for asparagine) in levels of essential and branched chain amino acids, unlike previously reported findings of maternal LPD in *in vivo* blastocysts (Eckert et al., 2012b). Figure 3.11 summarizes the NPD-LPD mESC model, analysed characteristics and results presented in Chapter 3, in a schematic format.

3.4.1 Derivation and Culture of mESCs

In the present study, mESCs were derived from the ICM of blastocysts of mothers fed either NPD (18% casein) or LPD (9% casein) for only the preimplantation period (i.e. E0.5-E3.5). After a quick wash in embryo culture media (KSOM, Appendix A) and serum (H6BSA, Appendix A), mid blastocysts from both treatment groups were transferred to mESC media (Chapter 2, Section 2.2.2.2) containing 15% KO/SR (Chapter 2, Section 2.2.2.2) and 1000U/ml LIF. Mouse ESC

derivation, cell line establishment (i.e. P4-5) and expansion (up to P8-10) procedures generally takes around 27-30 days (Chapter 2, Section 2.3.2, Figure. 2.8 F). ESCs exhibit cell plasticity that

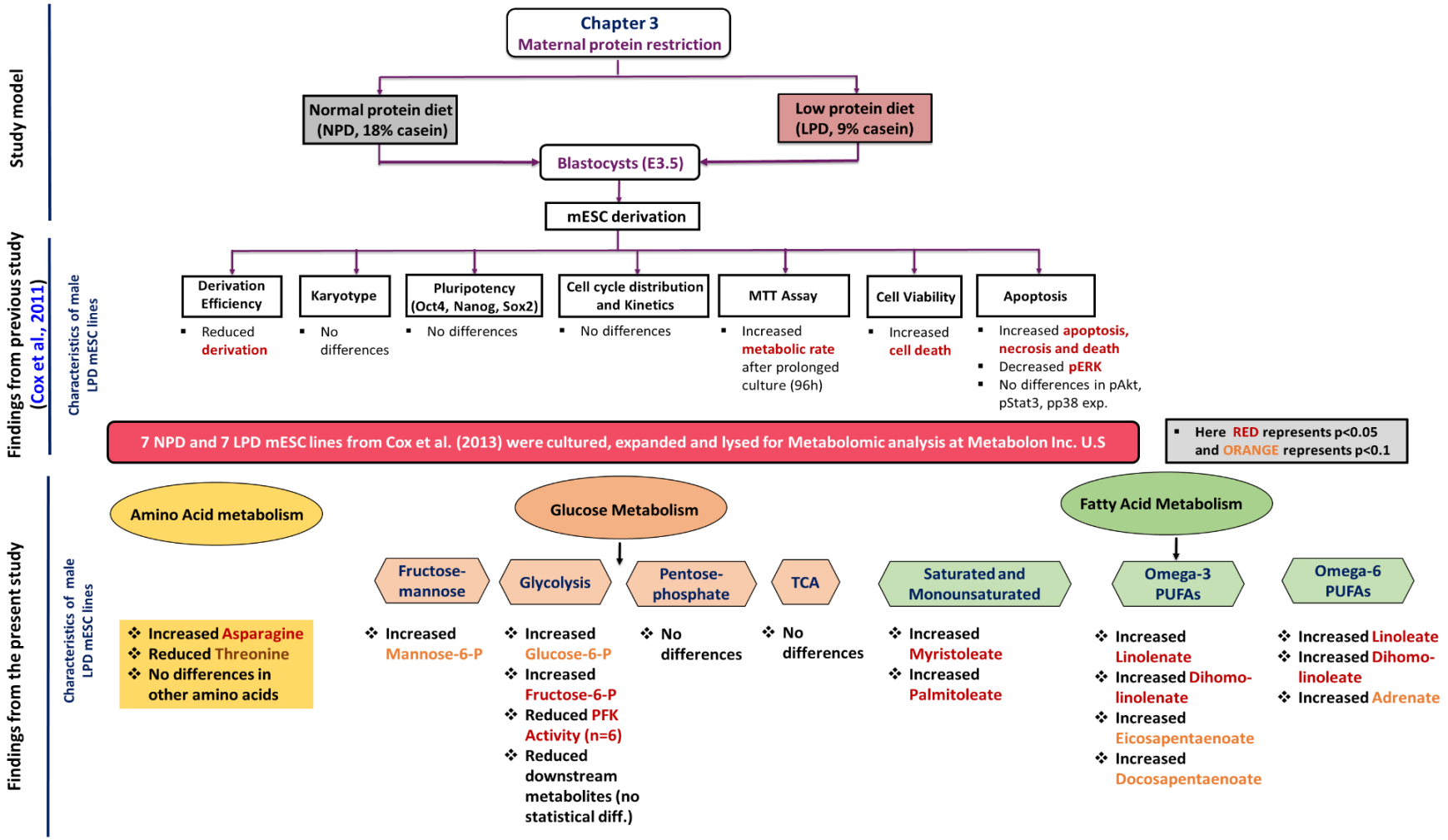

Figure 3.11 Flow diagram representing study layout and findings from Chapter 3 of this thesis.

assists them to adapt to the suboptimal (compared to maternal *in vivo* environment) *in vitro* culture system. Thus, the 'adaptation phase' induces changes in ESC transcript expression, in turn affecting their stemness (i.e. stem cell traits such as pluripotency and self-renewal capacity) (Burdick and Vunjak-Novakovic, 2009). ESC gene expression and phenotype are also affected by *in vitro* culture factors such as media composition, cellular matrix (feeder v feeder-free) frequency of media change, passaging (including frequency and methods of colony dissociation; i.e. enzymatic v non-enzymatic) freezing procedures (including concentration of cryoprotectant and serum) and general handling (Verganiet al., 2004; Park et al., 2015). The current study used KnockOut DMEM (Appendix A), which contained a high concentration of glucose (24.8 mmol/l), inorganic salts, amino acids and vitamins, and was supplemented with pyruvate, L-glutamine and non-essential AAs (NEAA). Additionally, mESC media contained KO/SR and LIF in a feeder-based culture system. Moreover, it has been reported that maternal LPD reduces insulin and increases glucose levels in maternal serum, and decreases AA levels in maternal serum, uterine fluid, which induce programing alterations in the developing blastocyst (Eckert et al., 2012b). Thus, metabolic modifications observed in NPD and LPD mESC lines represent a combination of the above mentioned alterations. Moreover, it is noteworthy that blastocysts and stem cells have different metabolic states and requirements at different stages of development (Shyh-Chang et al., 2013), and thus may respond differently, even under a similar set of environmental conditions.

3.4.2 Glycolysis: In developing embryos and derived pluripotent mESCs

The developing embryo undergoes distinct series of metabolic states with varying energy requirements to cater for fluctuating proliferation rate(s) and cell-specificity; which varies between totipotent (i.e. blastomeres), pluripotent (i.e. ICM) and multipotent states. During totipotency (up to 8-cell stage), although blastomeres undergo continuous self-renewing and DNA replication, the embryo as a whole does not show any net growth (Henry J. Leese, 1995) and uses its own protein reserve (up to 26 %), thus maintaining a low glycolytic rate (Brinster and April, 1966). Metabolism in totipotent blastomeres is tightly regulated and mostly controlled by the glycolytic enzymes hexokinase (HK) and phosphofructokinase 1 (PFK1) (Barbehenn et al., 1978). It is important to note that the only energy (and carbon) sources available at this stage of early embryo development are pyruvate analogues, and that development (at this stage) is inhibited under high glucose concentrations (Brinster and Troike, 1979). Oxidation of pyruvate in the mitochondria activates the Krebs cycle, thus generating carbon intermediates that activate oxidative phosphorylation, while maintaining low O_2 consumption and consequently have truncated mitochondrial cristae. As the embryo develops and the oxygen demand increases, mitochondrial cristae become elongated, although the numbers reduce to half with each cell division (Jonathan Van Blerkom, 2009). The

initial high amount of total ATP, and the ATP:ADP ratio, start to decrease, although the NADH:NAD^+ ratio remains high (Quinn and Wales, 1971; Wales, 1974). Reduced ATP levels further assist activation of PFK1 at the blastocyst stage, as ATP is an allosteric inhibitor of PFK (Johnson et al., 2003).

As morulae undergo compaction, totipotent blastomeres differentiate to ICM and TE, with a consequent increase in net growth and metabolic activity. Upregulation of glucose transporters such as GLUT1 and GLUT3, increase glucose uptake (Pantaleon and Kaye, 1998), thus increasing glycolytic flux, lactate synthesis (Leese and Barton, 1984), oxidative phosphorylation and overall oxygen consumption (Brinster, 1974). Given the role of the TE in forming the blastocyst cavity, the aforementioned changes in glycolysis are driven by high membrane potential of TE mitochondria, and not of the ICM (Jonathan Van Blerkom, 2009). Therefore, ESCs derived from ICM *in vitro,* inherit a high glycolytic rate (Kondoh et al., 2006), a characteristic feature often observed in highly proliferative cells (Hanna et al., 2009; Hansson et al., 2012).

In order to prolong the high rate of cell proliferation, mESCs show increased pentose phosphate pathway (PPP) activity and divert their intermediates towards nucleotide synthesis (Filosa et al., 2003). For ATP synthesis, mESCs depend on glycolysis, and O_2 consumption to oxidize NADH to NAD^+ and to maintain the Krebs cycle flux, which depends on the electron transport chain (ETC) (J. Zhang et al., 2011). Embryonic SCs maintain adequate redox potential to synthesise lipids from citrate, and amino acids from oxaloacetic acid or α-ketoglutarate (Shyh-Chang et al., 2011). Thus, ESCs with increased mitochondrial membrane potential proliferate and form teratomas more efficiently compared to those with less membrane potential (Schieke et al., 2008); and blastocysts with deficient mitochondrial oxidation enzymes (such as the pyruvate dehydrogenase (PDH) complex), are developmentally defected (Johnson et al., 1997; Johnson et al., 2001).

3.4.2.1 Impact of Low Protein Diet (LPD) on glucose metabolism

Maternal LPD decreases insulin secretion thus impairing glucose homeostasis, thereby contributing towards gestational diabetes and increased risk of type 2 diabetes mellitus in adult offspring (Souza et al., 2012; Su et al., 2016). In rodents, maternal LPD (9%, casein) for only first 3 days of gestation, decreased insulin and increased glucose levels in maternal serum, and induced glucose intolerance in the young offspring (Eckert et al., 2012b). In other studies, maternal LPD (10%) during pregnancy and/or lactation also showed altered glucose metabolism with increased insulin sensitivity, along with increased levels of cholesterol and reduced serum leptin in the offspring (Zambrano[1] and Ledesma[1], 2006). A recent study showed maternal LPD (9.6%)-induced impaired glucose tolerance and lowered insulin secretion to be associated with perturbation in programmed epigenetic expression of key miRNAs in offspring liver (J. Zheng et al., 2017).

Consistent with increased glucose levels reported in *in vivo* findings, the present study also showed increased uptake of upstream metabolites such as G-6-P and F-6-P, altered enzymatic activity of PFK and, thus, reduced levels of the downstream glycolytic metabolites in derived LPD mESC lines compared to NPD group. In a separate study, LPD altered glucose metabolism by lowering plasma glucose levels and increasing concentrations of glycogen, F-2-6-bP and F-1-6-bP, and increasing enzymatic activity of pyruvate kinase (PK) and phosphoenolpyruvate carboxykinase (PEPCK) in liver of 3 week old pups (Claeyssens et al., 1992). These alterations were observed when dams were fed normal chow diet during gestation and lactation, and the pups received LPD (6%) for 3 weeks post-weaning; making it a very distinct model compared to the previously discussed studies. Nevertheless, the study showed that irrespective of time, exposure to LPD at an early developing age could alter glucose metabolism; which in this case arose by delaying the down-regulation of the glycolytic pathway and altering glycolytic enzyme(s) activity, as also observed in the current study.

It has been documented that LPD alters maternal uterine environment, changes insulin and glucose homeostasis, and predisposes the developing embryo and fetus to increased risks of metabolic and cardiovascular disorders in adult life (Eckert et al., 2012; Fleming et al., 2012; Zheng et al., 2015; Velazquez et al., 2018). Although several of those studies have focussed on the preimplantation stage of development fewer have focussed on how early in development maternal dietary protein restriction begins to induce detrimental effects. One such study, however, focussed on 2-cell embryos and showed that LPD-embryos had reduced mitochondrial membrane potential, increased mitochondrial calcium and ATP levels, although no differences were observed in pyruvate uptake, compared to the control diet group (Mitchell et al., 2009). Additionally, these embryos showed decreased mitochondrial clustering around the nucleus, further suggesting slow metabolic rate (perhaps as an adaptive mechanism) to mitigate the effects of low protein. LPD 2-cell embryos that developed into blastocysts had reduced number of cells within the ICM, which might also explain the decreased derivation efficiency of mESC lines from LPD blastocysts (Cox et al., 2011). Interestingly, embryos exposed to high protein diets also showed damaging effects (such as increased levels of reactive oxygen species (ROS) and ADP concentrations), indicating metabolic stress (Mitchell et al., 2009). Collectively, these results indicate that perturbed maternal protein environments have a debilitating effect on mitochondrial metabolism, which then induces (possibly an irreversible) metabolic and mitochondrial dysfunction in the developing embryo, as early as the 2-cell stage.

To ensure that diets remain isocaloric, the LPD is supplemented with dietary sugars (such as sucrose). Accumulation of sugars due to LPD-induced insulin sensitivity further disturbs glucose metabolism. In the current study, mESC lines were derived from ICMs of E3.5 blastocysts developing

in a similar (i.e. 'reduced insulin-high sugar-low protein') maternal environment. They were further cultured in a high-glucose medium for a protracted period. Hence, elevated levels of G-6-P and F-6-P observed in the current study could be a result of continued exposure to high glucose concentrations (both *in vivo* and *in vitro*), possibly inhibiting allosteric regulators and thus reducing PFK enzymatic activity. In turn this could lead to reduced downstream metabolites and increased upstream metabolite levels. Increased levels of sugars alone have been shown to impair spatial learning and memory, and hippocampal insulin resistance, reducing hippocampal dependent cognitive functions (Jurdak and Kanarek, 2009; Wu et al., 2015).

3.4.3 Amino Acid metabolism in pluripotent mESCs

Mouse ESCs depend on AA metabolism to maintain a pluripotent epigenetic state. Restriction of threonine alone (and methionine and cysteine to a lesser extent) inhibited mESC growth (Jian Wang et al., 2009). Hence, healthy early blastocysts and mESCs maintain increased expression of the catabolizing enzyme threonine dehydrogenase (TDH) (Wang et al., 2009; Shyh-Chang et al., 2013), and consequently increased amounts of glycine and activity of the mitochondrial enzyme glycine decarboxylase (GLDC). Given that THD also controls regulation of histone H3K4 tri-methylation that maintains epigenetic plasticity of pluripotent mESCs, collectively, these studies illustrate the importance of metabolites produced by degradation of threonine in mESC self-renewal and cell proliferation (Azuara et al., 2006; Wang et al., 2009; Gaspar-Maia et al., 2011).

Blastocysts recovered form LPD-fed mothers had significantly reduced levels of methionine and a trending reduction in threonine at E3.5 and E4.5 respectively, along with reduced insulin and increased glucose levels in maternal serum (Eckert et al., 2012b). Regulated by the mTORC1-signalling pathway, these changes invoked compensatory mechanisms by increasing cell number and expansion of TE, and induced endocytosis. Similar effects on fetal and adult phenotypes were observed when blastocysts were cultured in a reduced insulin and BCAA environment, suggesting pre-programming of preimplantation blastocysts (Miguel A. Velazquez et al., 2018). Consequently, mESC lines derived from *in vivo* LPD blastocysts showed reduced self-renewal and proliferation compared to NPD mESC lines (Cox et al., 2011). Furthermore, EBs derived from LPD mESC lines propagated the effects observed in TE endocytosis (Sun et al., 2014), as observed previously in *in vivo* studies (Eckert et al., 2012). Consistent with these findings, metabolomic analysis of the same NPD-LPD mESC lines (Cox et al., 2011) as used in the present study, showed a trending ($P<0.073$) reduction in threonine levels for LPD compared to NPD mESC lines. Although diet did not seem to affect the levels of AAs in the derived mESC lines, LPD mESC lines showed increased levels of asparagine ($P<0.049$), in contrast to the reduced levels reported in E3.5 LPD blastocysts (Eckert et al., 2012b).

3.4.4 Polyunsaturated fatty acids (PUFAs) metabolism in pluripotent mESCs

Essential fatty acids and their metabolites play a critical role in maintaining stem cell pluripotency and self-renewal by controlling cellular programming. By being incorporated into membrane phospholipids, polyunsaturated fatty acids (PUFAs, especially n-3s), are able to alter cell membrane (chemical and physical) properties, lipid rafts and membrane-associated proteins, thereby affecting signal transduction, gene expression, stem cell self-renewal, cell cycle regulation, and programmed cell death (PCD) (Yamazaki et al., 2006; Lee et al., 2010). Additionally, PUFA-derived eicosanoids and lipid mediators act as coactivators of key transcriptional factors (such as peroxisome proliferator-activated receptors (PPARs) (Rajasingh and Bright, 2006), nuclear factor kappa B (Chapkin et al., 2009), and activator protein-1 (Iwahashi et al., 2000) that further affect stem cell proliferation, differentiation and energy metabolism (Lands, 2012).

As long-chain n-3 and n-6 PUFAs are not synthesised in the body, they can only be supplemented from diet. Although n-6 PUFAs are readily available in the human diet (including grains, plant-based oils, poultry and eggs), the sources for n-3 are limited. The current study used an LPD diet consisting of 9% casein as the main protein source, starch maize as a carbohydrate together with sucrose, and corn oil as FA source. In the LPD casein was replaced by additional maize starch and sucrose. As diets in the present study included FAs in the form of maize oil, they were deficient in n-3 PUFAs which, as mentioned earlier, is essential in neural development (Beltz et al., 2007; Vaca et al., 2008). Consequently, several rodent maternal LPD studies show impaired fetal and adult brain function and development (Bennis-Taleb et al., 1999; Marwarha et al., 2017; Gould et al., 2018), along with an altered state of lipid metabolism (Kang et al., 2011).

Contrary to these findings, in the present study, LPD mESC lines displayed increased levels of n-3 and n-6 PUFAs, which could represent an adaptive/ catch-up response to the sudden shift from a protein-deficient *in vivo* environment to an artificial, nutrient-rich *in vitro* culture environment which may enhance their PUFA levels. Although constituents of commercial mESC culture media (including Knockout DMEM and KO/SR) are not completely known, it does not appear that they are supplemented with FAs. However, mESC medium contains high D-glucose, pyruvate, L-glutamine, vitamins (including folic acid, thiamine (B6) and riboflavin (B2)) and AAs, which may collectively, provide a nutrient rich environment for the proliferation of mESCs and ease the effects of n-3 deficiency (Tsuge et al., 2000).

3.4.5 Conclusions and future work

Collectively, these studies show LPD-induced programing of E3.5 blastocysts and its propagation during *in vitro* culture of mESC lines as depicted by differences in phenotype (Cox et al., 2011) and

metabolomic analysis (current study). The LPD mESC lines showed increased G-6-P and F-6-P uptake, reduced PFK activity and subsequently reduced levels of downstream glycolytic metabolites. It is noteworthy that when PFK activity was evaluated with n=7, no statistical differences were observed. However, as data could not be normalised by transforming the outliers (one from each diet group), it was additionally analysed by removing the two outliers, i.e. n=6, which fell in line with the metabolomic analysis thus displaying significantly reduced PFK activity, and indicating an effect on the reduced levels of downstream metabolites. Moreover, as small n values and outliers can indeed produce false negatives, the experimental findings require to be confirmed with larger dataset. It is known that LPD impairs insulin levels in the maternal serum and uterine fluid, thus inducing glucose intolerance in the offspring (Eckert et al., 2012b), further indicating that LPD mESC lines were maintained in a high-glucose environment (during *in vivo* development and *in vitro* culture). Interestingly though, mESC lines did not display great differences in the levels of AAs, although a modest increase in levels of specific n-3 and n-6 PUFAs was observed. Similarities between previous *in vivo* and *in vitro* findings, and the nature of metabolomic differences observed between NPD and LPD mESC lines could probably be reflective of differences in composition of diets (Appendix A).

However, it is unclear how the protracted period of *in vitro* cell culture, the complex mix of constituents in the commercial media, and the ability of (adaptive) plasticity of mESCs interact with 'preprogramed developmental events' experienced by the blastocyst to modify the metabolomic profile of mESC lines. Moreover, the high false discovery rate (FDR) in this dataset necessitates further research to confirm these findings. One of the ways to test the reliability of *in vitro* metabolomic analysis is to validate the findings by assessing transcript and protein expression for key enzymes as well as enzyme activity. Additionally, mESCs could be profiled under conditions that enhance their phenotype further (i.e. either increased protein restriction *in vivo* or creating a nutritionally challenged *in vitro* culture environment). To assess if protracted culture duration could be depleting mESC memory (i.e. epigenetic marks), mESC metabolomic profiles could be assessed at additional time points and passage numbers, to determine if these may have been altered or lost.

Chapter 4 Optimisation of a neural induction protocol and evaluation of differences between the neural induction efficiency of NPD and LPD mESCs

4.1 Introduction

Maternal LPD in mice restricted to one ovulatory cycle for 3.5 days up to mating induced abnormal anxiety-related behaviour and signs of decreased responsiveness to environmental stimuli in the offspring (Watkins et. al., 2008a). This was indicated by reduced exploratory behaviour and increased resting periods in open field activities. Similarly, when dams were fed LPD exclusively during the preimplantation period (up to E3.5), adult offspring displayed increased anxiety (Watkins et. al., 2008b) and short-term memory deficit (in a novel object recognition assay) (Gould et. al., 2018). Furthermore, extended periods of maternal LPD throughout gestation and weaning affected offspring growth and neurodevelopment (Belluscio et. al., 2014). It also induced signs of anxiety and depression (i.e. reduced juvenile social play and exploratory activity), impaired motivation, learning and memory (Castro et al., 2011). The effect of maternal LPD, therefore, includes disturbance of neurodevelopment and behaviour but the specific character of these consequences depends upon LPD timing in relation to developmental events, the nature and severity of deprivation and genotype (Alamy and Bengelloun, 2012; Besson et. al., 2015).

Maternal LPD in rodents also reduces the size of the cerebrum and alters brain function (Sasaki et. al., 1982; Belluscio et al., 2014; Chertoff, 2015; Jahan-Mihan et. al, 2015). It is important to note that the cerebellum alone constitutes 60% of the brain's neurons in mice (Houzel et. al., 2007), and has a protracted time scale of development compared to that of the cortex or hippocampus (Ranade et al., 2012). These factors could enhance its structural and functional vulnerability to effects of maternal malnutrition at different (and extended) stages of development. Additionally, maternal LPD increases cortical neuron proportion and thickness (Gould et. al., 2018), delays motor development, reduces granular cells, and impairs hippocampal and hypothalamic neuronal proliferation (Ranade et al., 2012).

Neuroplasticity of the prenatal brain makes it vulnerable to such developmental (dietary) insults which may affect metabolism, growth, cell migration and differentiation (Morgane et al., 1993; Gallagher et. al., 2005). In turn, these changes may lead to social isolation, learning disabilities and brain pathologies, such as impaired neuronal circuits and neurotransmitter systems, cell death and axonal-dendritic pruning. As neurogenesis in the rodent brain is mostly completed during the fetal

period (Finlay and Darlington, 1995), developmental insults at this time cause long-lasting brain functional defects in offspring (Takahashi et al., 1999).

Multipotent neural stem cells (NSCs) proliferate *in vivo* via symmetric cell division but also undergo asymmetric divisions to produce neural progenitor cells, which have a restricted differentiation potential to either neuronal or glial lineages (Juliandi et. al., 2010). Normal hippocampal functioning depends on the timing of proliferation and differentiation of NSCs (Shors et al., 2001), which is controlled by extrinsic neural signals and intrinsic cellular memory interacting through epigenetic mechanisms (Juliandi et al., 2010).

Whilst the processes affecting neural proliferation and differentiation are well characterised *in vivo*, few studies have investigated the *in vitro* effects of maternal diet on these cells. A recent study, however, revealed that maternal LPD (9% casein) in mice (either limited to E0.5 to E3.5 as Emb-LPD or throughout gestation) both reduced neurosphere formation (NSCs and progenitor cells) and NSCs analysed through flow cytometry from ganglionic eminence and cortex primary cells at E12.5, E14.5 and E17.5 (Gould et. al., 2018). Maternal Emb-LPD in turn upregulated neural differentiation in remaining NSCs. As these enduring effects throughout gestation were observed following LPD only during the preimplantation period, and also shown during *in vitro* culture of derived NSCs and neurospheres, it indicates that maternal dietary effects on NSCs are persistent.

Embryonic stem cells (ESCs) derived from E3.5 blastocysts evolve into neural progenitors by a default differentiation mechanism (i.e. formation of primitive NSCs before definitive NSC stage) (Tropepe et al., 2001), and act as a road map to neurogenesis in the embryo (Abranches et al., 2009b). Consequently, several distinct mouse ESC (mESC) neural differentiation protocols have been developed (Bain et al., 1995; Kawasaki et al., 2000; Ying et. al., 2003; Abranches et al., 2009; Cha et al., 2017).

The present study used eight established mESC lines derived from embryos of dams fed either a normal protein diet (NPD, 18% casein, n=4) or a low protein diet (LPD, 9% casein, n=4) for the first 3.5 days of embryo development (Congshan Sun et al., 2014). The two primary objectives of the current study were (i) to establish an efficient neural induction (NI) protocol for derived NPD and LPD mESC lines and (ii) to use this protocol to perform preliminary analysis of differences between NI efficiency of the NPD and LPD mESC lines.

As a protocol for NI of mESCs had not been established at Southampton, and given that this was undertaken routinely by our collaborators at Biotalentum Ltd (Gödöllő, Hungary), it was decided to adopt their standard NI protocol (Klincumhom et al., 2012). A key feature of this protocol is that it involves culturing mESCs in the presence of ES-based fetal bovine serum (ES-FBS), which promotes

cell proliferation and maintains a pluripotent cell-cycle state (Li and Kirschner, 2014). However, as the NPD and LPD mESC lines established in Southampton were derived and cultured under serum-free (knock out serum replacement, KO/SR) conditions so, initially, mESC lines were maintained under these culture conditions prior to NI. The following study therefore began by optimising the NI protocol for KO/SR cultured pluripotent NPD and LPD mESC lines (Section 4.2.4). It began by culturing two mESC lines from each dietary group. During the course of these initial experiments, however, it transpired that the revived cell lines from Southampton did not thrive under these conditions. Consequently, it was decided to culture these cells according to the standard, serum-based mESC protocol established at Biotalentum. Morphological changes in these pluripotent cells, however, suggested non-specific differentiation. As serum is known to restrict lineage-specific differentiation and increase heterogeneity in mESCs (Tamm et al., 2013; Guo et al., 2016), the remaining four cell lines (2 NPD, 2 LPD) were cultured only under serum-free (KO/SR) conditions. This, however, led to just two replicates per treatment (NPD vs LPD) for each of the two culture conditions (ES-FBS vs KO/SR), which prohibited a formal statistical analyses of the data. Time constraints associated with shipment from Southampton to Hungary, quarantine, expansion and NI of additional cell lines (which would take approximately 2 months) meant that it was not possible to replace the four lines cultured in the presence of serum during the secondment period. Consequently, this chapter describes the optimisation of a NI protocol for mESCs (Part 1) and a subsequent preliminary analysis of differences in NI efficiency between NPD and LPD mESC lines (Part 2).

4.2 Materials and Methods

4.2.1 Culturing mESCs (at Southampton)

As detailed in Chapter 3 (Section 3.2.1), mESC lines were derived from E3.5 blastocysts of NPD and LPD fed C57BL/6 dams by a previous PhD student, Andy Cox. Briefly, female (C57BL/6) and male (CBA) mice were fed normal chow diet up until successful mating was identified (E0.5), after which the dams were divided into two groups, NPD (18% casein) vs LPD (9% casein). At E3.5, blastocysts were cultured for derivation of mESCs (Chapter 2, Section 2.2.2.2). Once the NPD and LPD lines were established (in mESC medium, i.e. KnockOut DMEM, KO/SR and LIF) and characterised (i.e. pluripotency analysis, sexing and karyotyping), they were frozen and stored in liquid nitrogen until required. Seven mESC lines from each group were expanded (see Section 3.2.1) by me and utilized for metabolic analyses between the NPD and LPD mESC lines (Section 3.2.3). Four representative NPD and LPD mESC lines were selected for the present study, which was undertaken by me at Biotalentum Ltd. (Gödöllő, Hungary) as part of a PhD secondment.

4.2.2 Freezing and thawing mESC lines

As described in Chapter 2 (Section 2.2.2.2.1), mESCs were frozen in freshly prepared, ice-cold freezing medium (20% KO/SR and 10% DMSO). Cells were frozen slowly at -80°C overnight before storing in liquid nitrogen. Cell stocks were quick-thawed in a water bath at 37ºC, spun (~300 g) to remove DMSO and re-suspended in mESC culture medium (with 15% KOSR and 1000 U/ml of LIF). Mouse ESCs were seeded onto fresh Mitomycin C (MMC) treated mouse embryonic fibroblasts (MEFs) and cultured on MEFs for at least one passage before use in further experiments.

4.2.3 mESC culture (at Biotalentum Ltd, Gödöllő, Hungary)

Cells were cultured, expanded and directed towards neuronal induction (i.e. neuronal progenitors and neurons) following pre-established cultured conditions established at Biotalentum Ltd. (Klincumhom et al., 2012). Figure 4.1 summarizes the timeline of events from receiving the samples by courier at Biotalentum, optimisation of NI protocol (Part 1), neural differentiation of NPD and LPD mESCs (Part 2). Following pre-established pluripotency culture conditions (see Section 2.2.1), two mESC lines from NPD and two mESC lines from LPD group (500,000 cells/ 6-cm dish) were thawed and plated onto 6-cm mitomycin-C (MMC) treated MEF dishes (700,000 cells/ 6-cm dish) in mESC medium (Knockout™ DMEM (1X), 10829-018, Gibco® by Life Technologies), 15% KO/SR or ES-FBS (ES-009-B, EmbryoMax ®, Merck) and 1000 U/ml LIF) (discussed in Section 4.3.1.1). As per Biotalentum policy, mESC lines were quarantined for 1-2 weeks. Samples were periodically tested

for mycoplasma using LookOut® Mycoplasma PCR Detection Kit (MP0035, Sigma-Aldrich). All eight mESC lines used in the present study tested negative for mycoplasma throughout the project. mESCs were then expanded and maintained in a pluripotent state (with or without serum) until neural induction (NI) was initiated. mESC medium was changed daily and cell lines were trypsinized (0.05% Trypsin-EDTA, Sigma- Aldrich, Section 2.2.2.2.) once they reached 70% confluency or every 3-5 days, depending upon their growth rate.

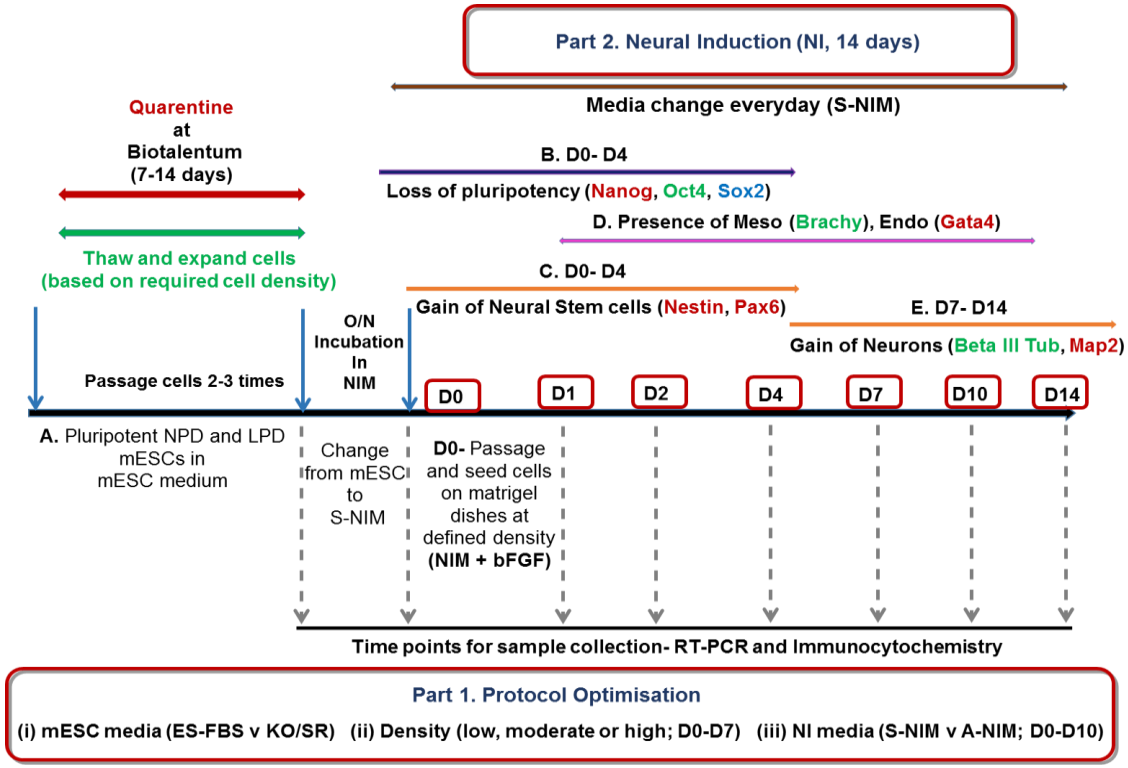

Figure 4.1 Project timeline representing the series of events from receiving samples to neural induction of NPD and LPD mESCs.

Cells were quarantined and expanded for 2 weeks, after which they were directed towards optimisation, followed by neural induction. Part 1 (at bottom) represents the optimisation of neural induction (NI) protocol on the basis of (i) mESC medium (ES-FBS v KO/SR) before NI, (ii) density of plated cells (low, moderate or high; D0-D7) and (iii) use of NI medium (Standard- v Advanced- NIM; D0-D10). In Part 2 of the study (top), NPD and LPD mESCs were differentiated for 14 days, and samples for RT-PCR and immunocytochemistry were collected on the day before start of the NI, followed by Days 0, 2, 4, 7, 10 and 14. Samples were collected to assess (A) initial pluripotent state of mESC lines, (B) loss of pluripotency, (C) gain of NSC expression, (D) presence of other lineages, and (E) the gain of mature neuron expression in the differentiating cells.

4.2.4 Neural induction of mESCs

NPD and LPD mESCs were expanded in pluripotent mESC medium (Section 4.2.3), gently washed with PBS (without passaging), starved of LIF, and conditioned in neural induction (NI) medium overnight. The following day, cells were, trypsinized (0.05% Trypsin-EDTA), centrifuged (300 *g*, 5 mins), and pre-plated for 45 mins, on 0.01% gelatin (G1393, Sigma-Aldrich) coated tissue culture dishes. Cells were , centrifuged, counted and seeded on 24-well (with sterilized cover slips) and 6-well Matrigel (BD Matrigel; Stem Cell Technologies) coated dishes. Cell density was optimised by plating one NPD line 36P12 at three different cell densities of 12,500 cells/cm^2, 25,000 cells/cm^2 and 35,000 cells/cm^2, and culturing them in NI medium for 7 days (see Section 4.3.1.2). After choosing the optimal cell density of 28,500 cells/cm^2, the rest of NPD and LPD mESCs were cultured and differentiated in NI medium. NI medium was changed daily and cells were cultured (without passaging) for 14 days.

For the selected time points (i.e. a day before the start of NI, then on Days 0, 2, 4, 7, 10 and 14 of induction), cell lines were either fixed with 4% PFA (Section 4.2.6) or trypsinized (for gene expression analysis (Section 4.2.5.1; Figure 4.1). Samples were collected at the chosen time points to observe differences between NPD and LPD mESC lines for the following parameters: a) before overnight starvation of LIF to measure original pluripotency expression of NPD and LPD mESCs; b) early NI days 0, 2 and 4 to gauge reduction of pluripotency markers (Nanog, Oct4 and Sox2), increase in early neural stem cell (NSC) markers (Nestin and Pax6), and changes in mesodermal (Brachyury) and primitive endoderm marker expression (Gata 4); c) day 7 to assess reduction of NSCs and appearance of mature neuron markers (beta-III tubulin and Map2); d) late NI, day 10 to estimate gain of mature neuron marker expression, and lastly e) the end of NI, day 14 to measure mature neuron marker expression at the termination of protocol.

In order to establish an efficient neural induction protocol, this study evaluated two different NI media compositions. For ease of representation, neural induction medium (NIM) without the addition of small molecule inhibitors is termed Standard NIM (S-NIM), and medium with inhibitors is referred to as Advanced NIM (A-NIM).

4.2.4.1 Standard neural induction medium (S-NIM)

In the given study, the optimised version of neural induction protocol for mESCs (Section 4.3.1) established at Biotalentum Ltd. (Klincumhom et al., 2012) was adopted. As detailed in Table 4.1, Standard-NI medium (S-NIM) consisted of DMEM/F12, non-essential amino acids (NEAA), N2 and B27

supplements and basal fibroblast growth factor (bFGF, 10 ng/ml). N-2 supplement is a chemically defined, concentrate of Bottenstein's N-2 formulation (Bottenstein, 1985). It is used for the growth and expression of post-mitotic neurons in primary cultures from both the peripheral nervous system (PNS) and the central nervous system (CNS). Its selectivity and specificity towards promoting only neuronal cell line growth makes it a valuable component of the NI medium in the present study.

B-27 is an optimized serum-free supplement used to support the low- or high-density growth, and short- or long-term viability of hippocampal and CNS neurons. B-27 supplement is used with a medium for neuronal cell culture without the need for an astrocyte feeder layer. Fibroblast growth factor (FGF) signalling plays a significant role in both embryonic development, and tissue homeostasis and repair (Coutu and Galipeau, 2011). FGF promotes self-renewing cellular proliferation by inhibiting senescence. FGF has also been used as an essential factor in inducing neural induction (NI) in several protocols. Cells treated with FGF-inhibitors show reduced efficiency of NI (Delaune et. al., 2005) and instead promote the growth of pluripotent stem cells (Ying et al., 2008). However, the effect of FGF on mESCs or human ESCs (hESCs) is rather controversial. While some studies show the inhibition of FGF to increase (Greber et al., 2010) or to block (Vallier et al., 2009) neuronal differentiation in both mESCs as well as hESCs, others indicate its importance, but not necessarily in promoting neural commitment in hESCs (Cohen et. al., 2010).

Table 4.1 Reagents and their concentration for Standard neural induction medium (S-NIM)

Reagents (Standard NIM)	Volume (per 100 ml medium)
DMEM F-12+ GlutaMAX, Gibco (31331-028)	100 ml
N2 Supplement, Gibco (17502-048)	1%
B27 Supplement, Gibco (17504-044)	2%
Non-essential amino acids	1%
Pen-Strep (if required)	1%
bFGF (always add fresh)	10 ng/ml

Although pluripotent ESCs can differentiate into multiple cell types, they proliferate as heterogeneous cell populations, with distinct gene expression, cell cycle and epigenetic states (Hayashi et. al., 2008; Cannon et. al., 2015). Thus during neural differentiation, unless other lineages (i.e. endoderm and mesoderm) are restricted and mESCs are directed specifically towards neuronal lineage, the cell population is non-homogeneous, consisting of multi-lineage cell types and resulting in limited efficiency (Li et. al., 1998). To overcome these issues, along with the Standard NI medium (SNIM), the current study also explored an alternative approach of NI, using defined 'small molecule inhibitors' (SMIs).

4.2.4.2 Advanced neural induction medium (A-NIM)

SMIs are low-molecular weight (<900 daltons) organic compounds with a size of the order of around 1 nm. Their small size enables them to better penetrate cell populations, which further assists them in controlling specific cell cycle and metabolic states of mESCs that is rather heterogeneous otherwise. They do so by targeting specific signalling pathways and cellular processes, thereby inducing lineage-specific differentiation across the embryonic lineages (Kalantar Motamedi et al., 2016). Therefore, as detailed in Table 4.2, the current study evaluated the combinatory effect of two small molecules (SB431542 and LDN193189) on the efficiency of neural induction and on the suppression of other lineage markers, to generate more homologous neural stem cells (Zhang et al., 2012). The medium with SMIs has been referred as Advanced NI medium (A-NIM).

Table 4.2 Reagents and their concentration for Advanced neural induction medium (A-NIM)

Reagents (Advanced NIM)	Stock	Working concentration
Neurobasal medium	500ml	50 %
DMEM/F-12+ GlutaMAX, Gibco (31331-028)	500ml	50 %
N2 Supplement, Gibco (17502-048)	100ml	1 %
B27 Supplement, Gibco (17504-044)	50 ml	1 %
L-Glutamine	200mM	1 %
Non-essential amino acids (NEAA)	100 ml	1 %
Pen-Strep (if required)	100 ml	1 %
B-mercaptoethanol	50 mM	100 µM
LDN193189,	0.2 mM	0.2 µM
SB431542, Sigma (S4317-5MG)	13 mM	10 µM
bFGF (always add fresh)	100µg/ml	5 ng/ml
Insulin	10 µg/ml	5 µg/ml

SB431542 is an established small molecule inhibitor used selectively to inhibit the TGF-β (Transforming growth factor beta)/Activin/Nodal signalling pathway (Inman, 2002). Given the association between the alkaline-like receptor kinases (ALKS) with TGF-β and BMP, they have been an attractive target of such inhibitors. Unlike SB431542, LDN193189 (LDN) is a potent cell-permeable SMI of the bone morphogenic protein pathway (BMP). LDN is used to study BMP inhibition in ES cells (Vogt et al., 2011). Active BMP signalling is known to maintain self-renewal in ESCs, thereby preventing neural differentiation (Ying et. al., 2003). Therefore, an efficient neural differentiation of ES cells requires an effective inhibition of the BMP.

Dual SMAD inhibitors LDN193189 and SB431542 (also referred as the LSB protocol), show a combined effect in directing hESCs into Pax6 positive neural progenitors (G. Lee et al., 2009) and functional cortical neurons (Y. Qi et al., 2017). In the current study, A-NIM culture conditions (as detailed in Table 4.2) combined the effects of small molecular dual SMAD inhibitors (LSB), along with neural supplements (N2 and B27) and bFGF to assist the differentiation of NPD and LPD mESC lines to neuronal lineage.

4.2.5 Quantitative PCR (qPCR) analysis

4.2.5.1 Sample preparation for RNA extraction (conducted at Biotalentum Ltd., Hungary)

RNA samples were collected from NPD and LPD mESC lines at pluripotent stage (i.e. one day before initiation of NI) and then at Days 0, 2, 4, 7, 10 and 14 during NI. For pluripotent samples, cells were cultured as described in Section 4.2.3. mESCs were cultured until 70% confluency after which they were trypsinized (as described in Section 4.2.3) and centrifuged (300 *g*, 5 mins). Cells were pre-plated on 10 cm gelatin-coated dishes for 45 min and incubated (5% CO_2, 37°C, Section 2.2.3.1) to remove MEFs. During pre-plating, pluripotent mESC samples were incubated in mESC medium (Section 4.2.3) with LIF. After 45 minutes, floating cells were carefully collected in and centrifuged (300 *g*, 5 mins). mESCs were washed with PBS and the pellets were snap frozen on dry ice and stored at -80°C until they were shipped back to Southampton for extraction. For NI RNA samples, cells were cultured at 28,500 cells/ cm^2 density, in duplicates for each time point, on 6-well Matrigel-coated dishes. Cells were harvested, frozen and stored as described above, on Day 0, 2, 4, 7, 10 and 14 of induction.

4.2.5.2 RNA extraction

Derived cell pellets were thawed and centrifuged shortly at maximum speed to remove excess PBS. Total RNA was isolated using the RNeasy mini kit (Qiagen, UK) as described in the RNeasy handbook. RNA was quantified using the Nanodrop ND-1000 spectrophotometer as described in Chapter 2 (Section 2.2.5.1).

4.2.5.2.1 RNA quality

RNA quality was determined by gel electrophoresis as described in Section 2.2.5.2. Diluted total RNA samples (1 µl RNA sample + 4 µl loading dye) were run on a 0.8 % agarose gel, diluted with GelRed (Bioscience, BT41003-T), at 120 V for 15 min. Figure 4.2 shows intact RNA with clear 28S and 18S rRNA bands, where 28S is twice as intense as the 18S rRNA band.

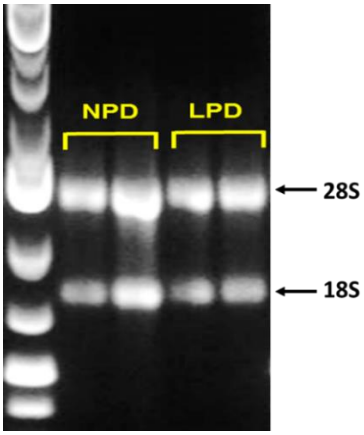

Figure 4.2 RNA gel electrophoresis of NPD and LPD mESC lines.

A representative 0.8% agarose gel showing RNA (~ 300 ng/µl) extracted from NPD and LPD mESC lines (2 lines/group). The 18S and 28S ribosomal RNA bands are visible, showing no lower molecular weight smears (degraded RNA) indicating that the RNA samples are intact. Band sizes were determined using GeneRuler 1 kb Plus DNA Ladder (left column; ladder).

4.2.5.3 Reverse transcription (cDNA synthesis) and quantitative PCR

First-strand cDNA was synthesized using 300 ng RNA using GoScript™ Reverse Transcription System (Promega, UK), as previously described in Section 2.2.5.3. Quantitative polymerase chain reaction (qPCR) was performed following the steps described in Section 2.2.5.4. Briefly, the specific gene targets were detected using SYBR-green from the SYBR-green 2x *PrecisionPlus™* Mastermix (Primerdesign, UK) protocol. Lyophilised primers (Primerdesign, UK) were diluted with nuclease-free water. qPCR was performed using 2x *PrecisionPlus™* qPCR Mastermix kit. Product amplification took place in a Chromo4 Real-time Detector (BioRad, UK) and analysed with Opticon Monitor v3.1 software (Section 2.2.5.4).

4.2.5.4 Normalization of PCR data and selection of reference genes

Quantitative RT-PCR data was normalised using the Primerdesign geNorm kit with 12-candidate reference genes (for *Mus musculus*) as described in Section 2.2.5.5. Specific product amplification was determined by single peaked melting curve, and specific melting temperature (Tm) of the oligonucleotide. Expression stability was assessed by running two cell line samples from three different time points (i.e. pluripotent mESCs, and NI Day 7 and Day 14) from NPD and LPD groups, cultured with and without serum. Reference gene stability was determined using an RT-PCR data analysis software, qBase+. Data was uploaded following the instructions in the Primerdesign qBase+ software manual.

Out of the twelve candidate genes within the Primerdesign geNorm kit, nine showed a high average expression stability of low M value (M<0.5). Figure 4.3A displays the M value for individual genes and

ranking of the least to the most stable genes (from left to right side). As observed in Figure 4.3 B, the optimum number of reference genes required for the current experimental group was two; calculated by V 2/3, where the normalising factor was <0.85. Therefore, genes *Canx* and *Rpl13a* (with least M values) were identified as the most stable reference genes, as they had C(t) values more comparable to those of the target genes. C(t) values of reference and target genes were analysed by the geometric averaging normalisation approach by Vandesompele et al. (2002), as described in Section 2.2.5.7.

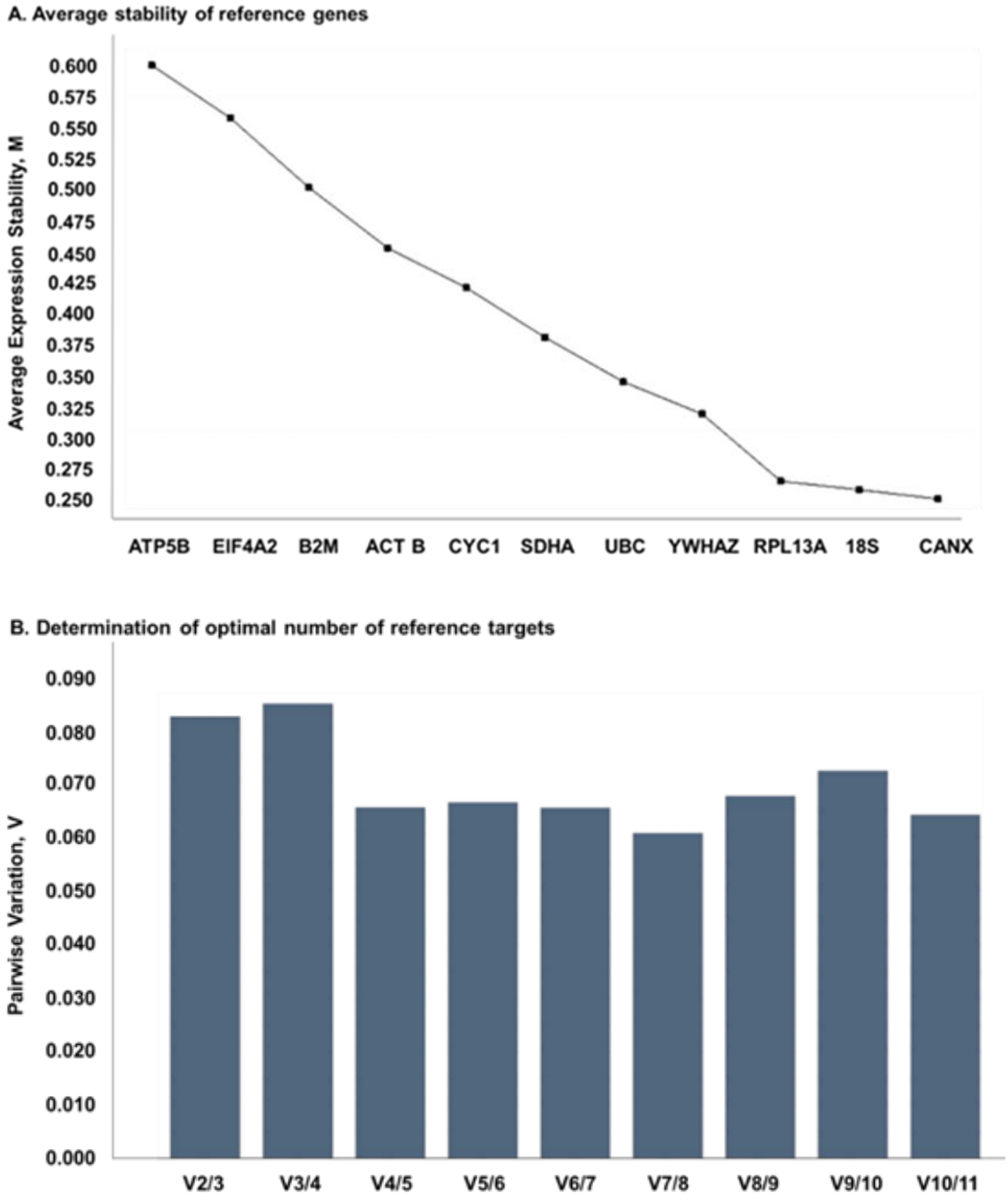

Figure 4.3 geNorm output for reference gene targets analysed for NPD and LPD mESC lines.

(A) geNorm analysis showing average gene expression stability M. M was calculated by comparing average pairwise variation of expression between 12 target reference genes (x-axis). M was calculated for each gene individually, and the least stable gene was excluded from the next round of calculations. Two genes with highest reference target stability (average geNorm, M ≤ 0.5) are shown on the right-most side on the x-axis (i.e. Canx and Rpl13a) and were selected for normalisation. (B) Shows optimal number of reference genes selected for normalisation. geNorm V is <0.10 when comparing a normalisation factor based on the 2 or 3 most stable targets and suggests that no more than 2 or 3 genes are required for accurate normalisation. In the present study, V< 0.15, therefore an optimal number of reference targets = 2.

4.2.6 Immunocytochemistry (ICC) staining

For pluripotent samples, mESCs (28,500 cells/cm^2) were cultured on sterile coverslips, pre-coated with inactivated MMC-MEFs (27,000 cells/well, on sterile coverslips) on 24-well plates. mESCs were cultured in mESC medium (Section 4.2.3) and samples were fixed at Day 4 of culturing. For NI samples, mESCs (28,500 cells/cm^2) were seeded on sterile coverslips coated with Matrigel on 24-well plates. Cells were cultured in NI medium (Section 4.2.4) that was replaced by fresh medium every day. Cell samples were fixed on Days 0, 2, 4, 7, 10 and 14 of neural induction. Plating density and number of days of culture were each fixed to make sure that any changes in cell proliferation between the groups were also recorded. At selected NI time points, the samples were fixed with 4% PFA and stored at 4°C until required. The fixation and staining procedures were as described in Section 2.2.8. The details for antibodies and dilutions used are provided in the Appendix C, Table 1.

4.2.7 Statistical Analysis

For reasons described earlier (Section 4.1), it was not possible to undertake a formal statistical analysis of the data generated in this chapter. Optimisation steps (for optimal density and NIM selection) were restricted to a single control NPD mESC line in different conditions. Differences between the NI efficiency of NPD and LPD mESC lines (cultured with and without serum) are presented (n=2 per group). Results are therefore divided into two parts. Part I presents NI optimisation procedures, whereas Part II presents a prelude to differences between NI efficiency of NPD and LPD mESC lines, expanded under serum (ES-FBS) and serum-free (KO/SR) conditions during pluripotent stage of culture (i.e. before NI). Hence, transcript data are reported as simple means. The immunocytochemistry image analysis is qualitative rather than quantitative in nature given the inability to process the multilayer 3D structures and extremely dense cultures.

4.3 Results

4.3.1 PART 1: Optimisation of neural induction (NI) protocol for NPD and LPD mESCs

4.3.1.1 Increasing proliferation of mESCs- Serum and serum-free mESC culture conditions

Mouse ESC lines were expanded as described in Section 4.2.1. Briefly, cells were cultured on MMC-MEFs, in mESC medium (DMEM/F-12, 15% KO/SR and 1000 U/ml LIF, Section 4.2.1). These culture conditions were established for derivation and growth of NPD and LPD mESCs in Southampton. However, using the same culture medium at Biotalentum Ltd in Hungary, the mESC lines (2 NPD, 2 LPD) showed reduced proliferation and cell numbers, even after 7-10 days of culturing and passaging (Figure 4.4 A and D). Given the slow growth rate and negligible number of colonies in both NPD and LPD mESCs, it was decided to discard the cells in culture at the time, and thaw fresh vials of the same cell lines, under standard pluripotent culture practices at Biotalentum Ltd (i.e. with serum, ES-FBS).

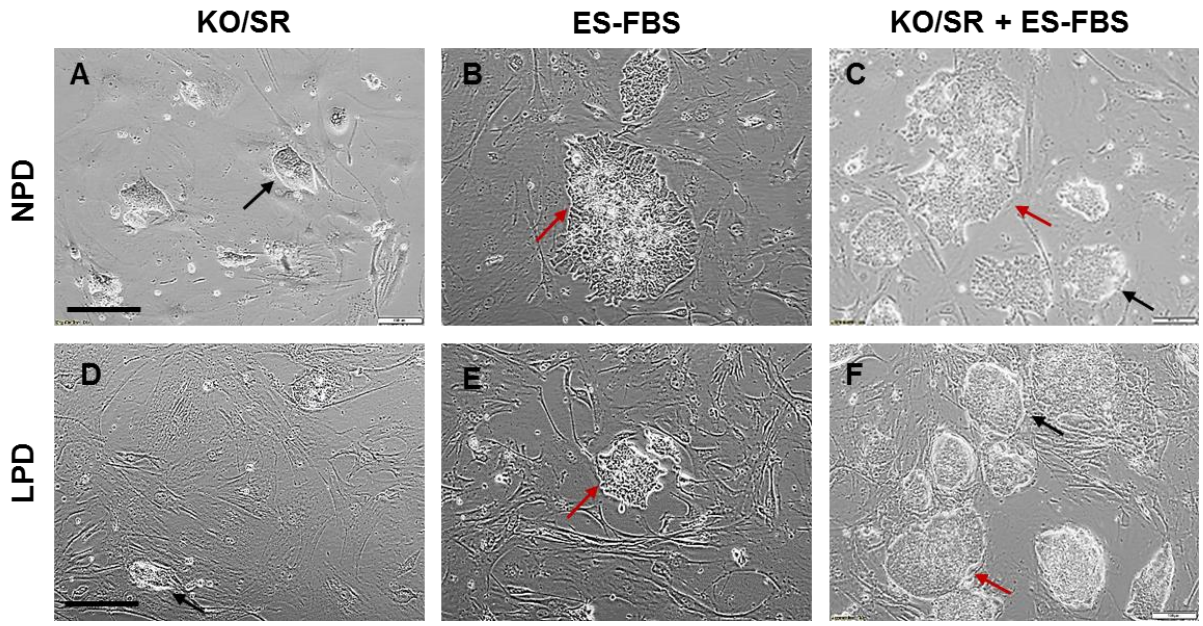

Figure 4.4 Representative images showing proliferation and morphological changes in mESC lines in pluripotent medium (with LIF) under three serum conditions.

A and D: KO/SR only, B and E: ES-FBS only and C and F: initially cultured in ES-FBS for 1 passage and then in KO/SR for 2 passages. Here A-C: NPD 8P11 and D-F: LPD 24P11 mESC lines. Arrows (A, B and C) point to key morphological features of KO/SR (spherical, tomb-like colonies, black arrow (A)), ES-FBS (flat colonies with edge boundaries, red arrow (B)) and KO/SR+ES-FBS (both spherical, tomb-like colonies (black arrow) and flat colonies with edge boundaries (red arrow) (C)). Scale bar = 100 µm.

The only difference between the two pluripotent culture protocols was the presence (Biotalentum) or absence (Southampton) of serum (ES-FBS). Both protocols included Knockout DMEM/F-12 and 1000 U/ml of LIF, and MMC-induced, mitotically inactivated MEFs as a cellular matrix.

Freshly thawed mESC lines (2 NPD, 2 LPD) were cultured in 15% ES-FBS to enhance growth and proliferation. Figure 4.4 B and E shows representative images of increased number of colonies and colony size under serum (ES-FBS) culture conditions, compared to KO/SR conditions (Figure 4.4 A and D) for the same cell lines. Although the replacement of KO/SR appeared to promote increased cell proliferation, it also led to excessive differentiation of the pluripotent mESCs. This is identified by the arrows pointing to the morphological changes in mESC colony shape from spherical, tomb-like colonies (Figure 4.4 A and D) to flat colonies with edge boundaries (Figure 4.4 B and E). Although ES-FBS culture medium improved the proliferation rate of the four mESC lines (2 NPD and 2 LPD), it also showed morphological signs of cellular differentiation in both treatment groups. For this reason, culture conditions were reverted to KO/SR and the four mESC lines were cultured and expanded according to pre-established, KO/SR culture conditions until the beginning of NI. Even though the culture conditions were reverted to original Southampton (KO/SR) conditions, the cells continued to reveal combination of ES-FBS- and KO/SR-induced colony morphologies (Figure 4.4 C and F).

It is known that partially differentiated mESCs have reduced potential for targeted differentiation (Sommer and Rao 2002). Therefore, the remaining four mESC lines (2 NPD and 2 LPD), were cultured 'exclusively' in KO/SR culture conditions, strictly restricted to protocols established in Southampton. Figure 4.5 shows the morphological differences between the eight NPD and LPD mESC lines used in this study, under both ES-FBS (Figure 4.5 A-D) and KO/SR (Figure 4.5 E-H) conditions. Irrespective of dietary group, ES-FBS treated mESC lines appeared bigger, more heterogeneous, and had flatter colonies with better defined boundaries compared to the smaller, more homogeneous and rounder colonies observed under KO/SR culture conditions; morphology more typical of mESCs.

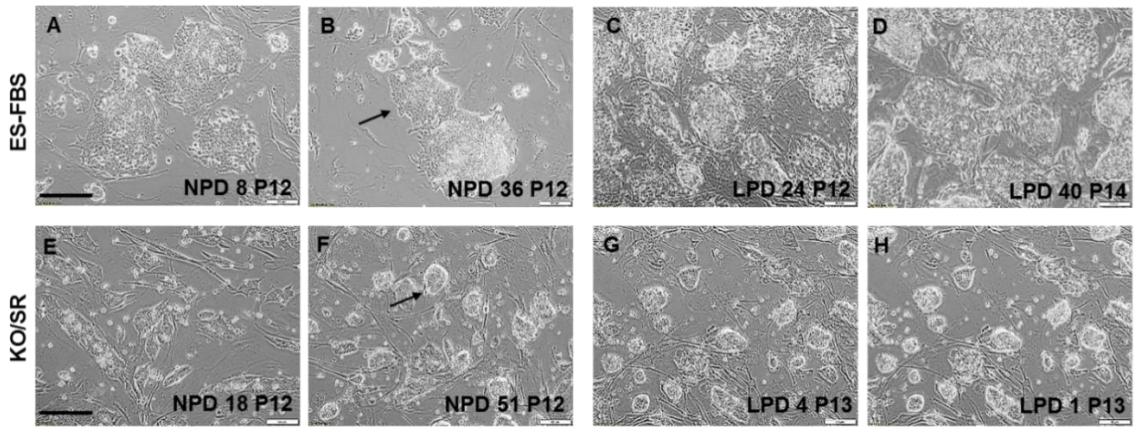

Figure 4.5 Brightfield images showing proliferation and morphological differences in NPD and LPD mESC lines in serum (ES-FBS) and serum-free (KO/SR) culture conditions.

A-D: ES-FBS and E-H: KO/SR conditions in (A, B, E, F) NPD and (C, D, G, H) LPD mESC lines cultured in mESC medium (DMEM/F-12 and LIF). Arrows (B and F) point to key morphological features of ES-FBS (flat colonies with edge boundaries (B)) and KO/SR (spherical, tomb-like colonies (F)). Scale bar= 100 µm.

Two NPD and two LPD mESC lines from both serum conditions (i.e. ES-FBS and KO/SR) were differentiated using the standard neural induction medium (S-NIM, Section 4.2.4.1) protocol, and differences between their NI efficiency were analysed. However, due to limited sample availability at the time, only one representative KO/SR-NPD mESC line was used in the following protocol optimisation steps (density and NI medium).

4.3.1.2 Optimal cell density for neural induction (NI) of NPD and LPD mESCs

Neural induction protocol established at Biotalentum, was originally designed for a commercial and robust, pluripotent mESC line HM1, which had been cultured and expanded exclusively under serum (ES-FBS) conditions. The established NI cell plating density for HM1 was 12,500 cells/cm^2, which when tested for Southampton derived NPD and LPD mESC lines (cultured with or without serum), resulted in excessive cell death and negligible rosette or neurite formation (data not presented), therefore indicating no NI in these lines. It is known that cell density influences survival and neural differentiation capacity of mESCs (Wongpaiboonwattana and Stavridis, 2015; Cha et al., 2017). Thus to verify if this was the case, a representative KO/SR-cultured NPD mESC line (36 P13), was expanded in pluripotent mESC medium (Section 4.2.3), trypsinized, cultured in S-NIM (Section 4.2.4.1) overnight, and plated in three different cell densities of low- 12,500 cells/cm^2, moderate- 25,000 cells/cm^2 and high- 35,000 cells/cm^2, from Day 0 to Day 7 of NI (Figure 4.6).

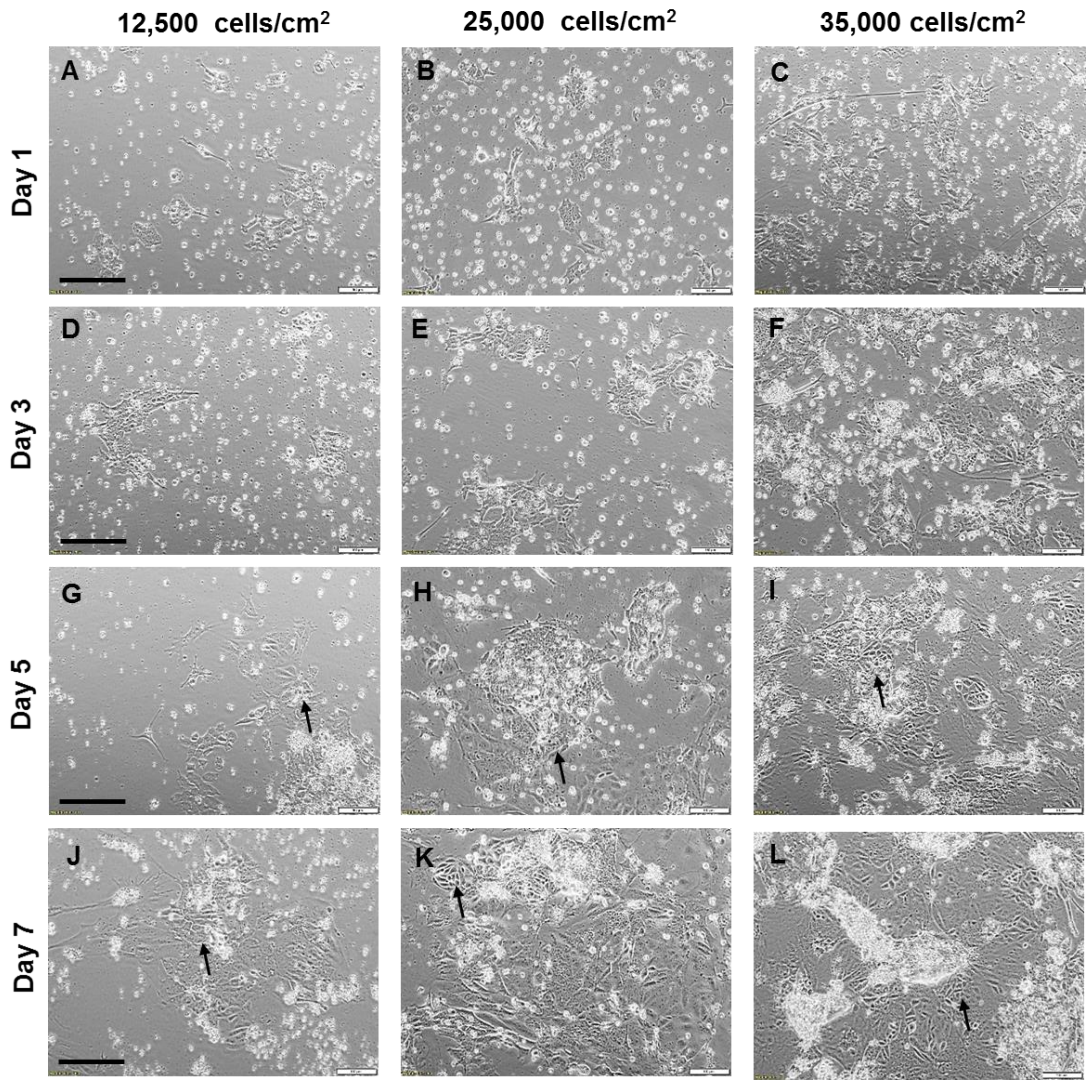

Figure 4.6 Selecting the most efficient cell density for neural induction protocol.

mESC line NPD 36 P13 (maintained in KO/SR+LIF+DMEM/F12) was plated at three different cell densities of (A, D, G, J) low 12,500 cells/cm^2, (B, E, H, K) moderate 25,000 cells/cm^2 and (C, F, I, L) high 35,000 cells/cm^2 in order to test the effect of cell density on neural induction from D1 to D7. Arrows point to (H) initiation of rosette formation at D5, (I) increased density of rosettes from D5 and D7 (K and L). Comparatively few rosettes were observed in (G) D5 and (J) D7 of the low density (12,500 cells/cm^2). Scale bar = 100 µm.

S-NIM was changed daily, and cells were observed under a bright-field microscope for structural changes every day during the first 7 days of induction. Morphological assessment revealed that while cells from all three-cell densities appeared to have radially arranged columnar cells by Day 5 of induction (Figure 4.6 G, H and I), the largest number of cell aggregates and neuronal rosettes were observed at the high cell density of 35,000 cells/cm^2 by Day 7 (Figure 4.6 L). Neural rosettes, or radially

arranged columnar cells, are known as the developmental signatures of neural progenitors in ESCs undergoing neuronal induction (Wilson and Stice, 2006).

For sample collection at Day 2, 4 and 7 (Section 4.2.4), cells from mESC NPD 36 P15 were seeded in duplicate, on Matrigel coated 6-well (for RT-PCR, Section 4.2.5) and sterile cover slips in 24-well (for immunocytochemistry, Section 4.2.6) culture dishes, in the given three different cell densities.

Relative gene expression was normalised to *Rpl13a* and *Canx* within geNorm (Section 4.2.5.4) and cells were analysed for pluripotent (*Oct4*, *Nanog* and *Sox2*), other lineage (*Gata4* and *Brachyury*) (Figure 4.7), early neural stem cell (*Sox1, Nestin* and *Pax6*) and mature neuron (*Beta III Tubulin* and *Map2*) markers (Figure 4.8) on Days 2, 4 and 7 of the NI protocol. While the low and high cell densities appeared to show consistent pluripotency expression from Day 2 to Day 7 (Figure 4.7 A-C), expression in the moderate density cells appeared to increase from Day 2 to Day 4, and decrease by Day 7. The differentiation markers appeared to have a similar trend of increasing expression from Day 2 to Day 4 (Figure 4.7 D and E), which decreased by Day 7 (Figure 4.7 F) for both moderate and high cell densities. However, the low density appeared to have a continuous rise in expression until Day 7 of induction. Consequently, in moderate density cells expression for both neural stem cells (also referred as neural progenitors) (Figure 4.8 A-C) and neuron (Figure 4.8 D-E) markers tended to be higher on Days 2, 4 and 7 compared to the low and high density groups. Similarly, protein expression for Beta III Tubulin appeared greater for the moderate and high-density groups compared to the low-density group (Figure 4.9 B, F and J). The high cell density group also showed the maximum expression (depicted by the number of cells or neurites) for the mature neuron marker, Map2 (Figure 4.9 K).

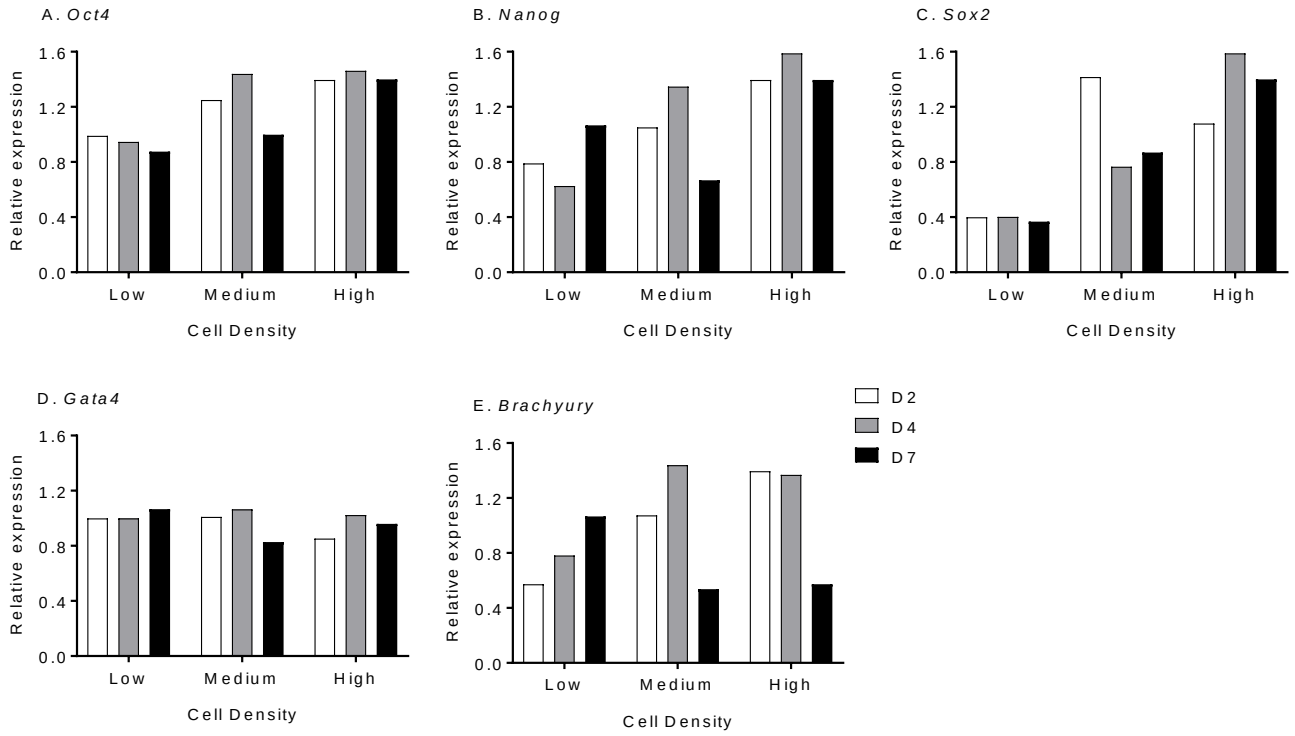

Figure 4.7 Effect of mESC density on relative gene expression of pluripotency and differentiation markers during standard neural induction.

mESC line NPD 36 P15 (maintained in KO/SR+LIF+DMEM/F12) was plated at three different cell densities of 12,500 cells/cm^2, 25,000 cells/cm^2 and 35,000 cells/cm^2 in order to test the effect of cell density on neural induction from D1 to D7. Genes of interest were normalized to *Rpl13a* and *Canx* within geNorm. The low (12,500 cells/cm^2) and high (35,000 cells/cm^2) cell densities showed consistent expression of pluripotency markers (*Oct4*, *Nanog* and *Sox2*) from D2-D7 (A-C). Expression for moderate density (25,000 cells/cm^2) increased from (A) D2 to (B) D4, but decreased by (C) D7. Differentiation marker(s) expression (*Gata4* and *Brachyury*) increased from D2-D4 (D, E), and decreased by D7 (F) for moderate and high cell densities, but continued to increase for the low density. n = 1 mESC line.

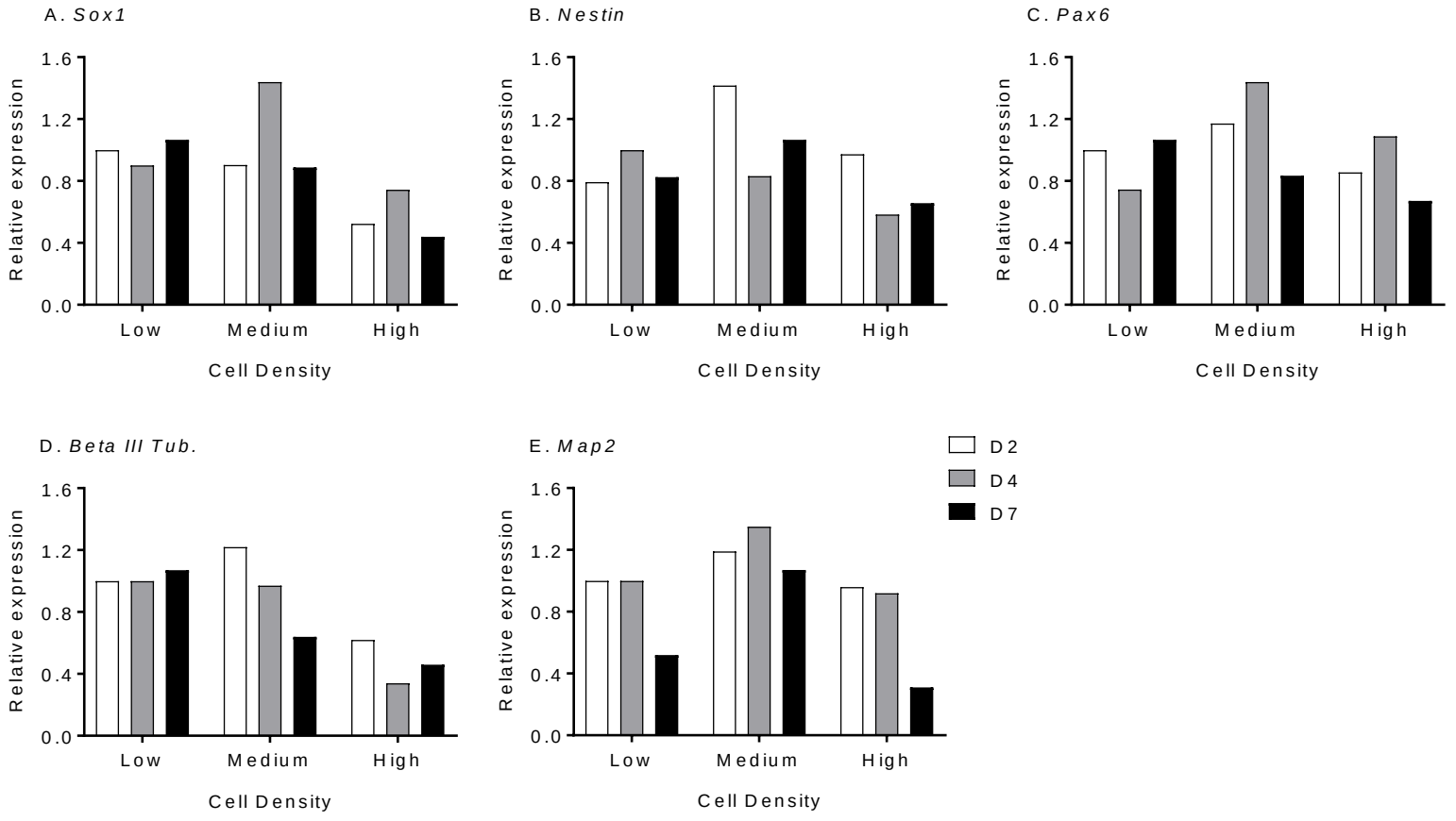

Figure 4.8 Effect of mESC density on relative gene expression of neural stem cell (NSC) and mature neuron markers during standard neural induction.

mESC line NPD 36 P15 (maintained in KO/SR+LIF+DMEM/F12) was plated at three different cell densities of 12,500 cells/cm^2, 25,000 cells/cm^2 and 35,000 cells/cm^2 in order to test the effect of cell density on neural induction from D1 to D7. Genes of interest were normalized to *Rpl13a* and *Canx* within geNorm. Moderate density cells showed high expression of NSC (*Sox1, Nestin* and *Pax6*) and mature neuron (*Beta III Tub* and *Map2*) markers on Day 2, 4 and 7, compared to cells from the low and high density groups. n = 1 mESC line.

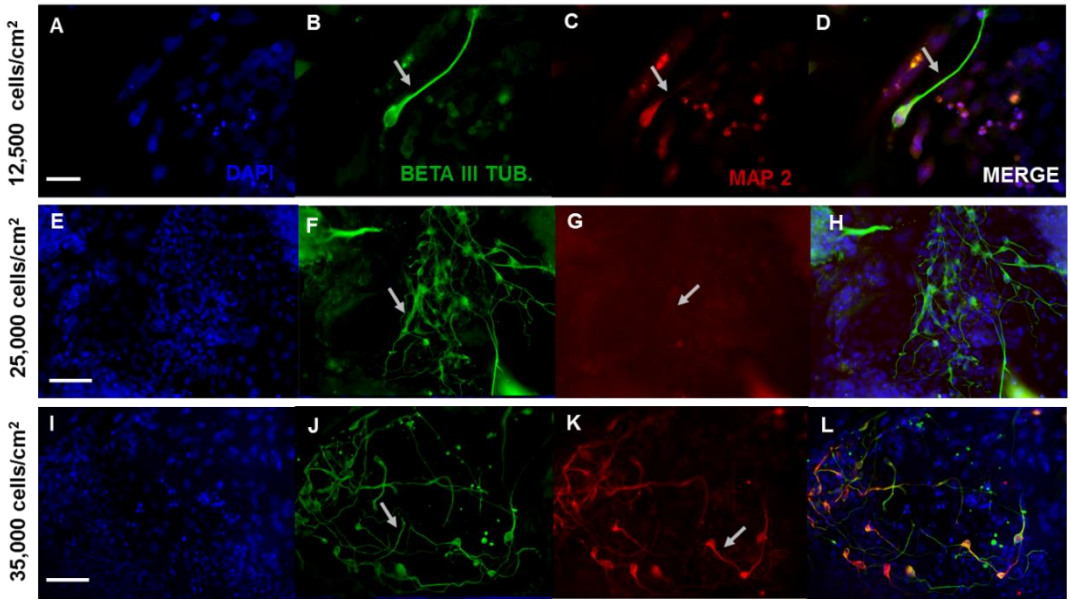

Figure 4.9 Immunocytochemistry of neuron marker(s) expression: Beta III Tubulin (Green), Map 2 (Red) and Nuclear marker Dapi (blue).

mESC line NPD 36 P15 (maintained in KO/SR+LIF+DMEM/F12) was plated at different cell densities of (A, B, C, D) low, 12,500 cells/cm^2, (E, F, G, H) moderate, 25,000 cells/cm^2 and (I, J, K, L) high, 35,000 cells/cm^2 in order to determine the most efficient cell density for neural induction at D7. Arrows point to (B, F, J) Beta III Tubulin positive and (C, G, K) Map 2 positive cells at the given densities. Maximum mature neurons appeared to develop at the high-density group of 35,000 cells/cm^2. Scale bar = 200 µm.

Based on cell morphology (i.e. appearance of neural rosettes) and gene and protein expression (i.e. loss of pluripotency, other lineage markers and gain of neuronal lineage markers), neural induction in mESCs derived and established in KO/SR culture was greatest for the moderate and high cell density groups. **Therefore, a cell density of 28,500 cells/cm^2, which is between the moderate and high densities, was chosen for further analysis.**

4.3.1.3 Characteristics of neural induction protocol

NPD and LPD mESC lines were directed towards neural induction (NI) under Standard-NI media (S-NIM) at the optimised cell density of 28,500 cells/cm^2 and the following common features were observed in the differentiating cell lines. Irrespective of maternal diet (NPD or LPD) and pluripotent culture (ES-FBS vs KO/SR) conditions, differentiating mESCs displayed (i) reduction in pluripotency expression (Oct4, Nanog and Sox2), (ii) changes in neural stem cell (Nestin and Pax6) markers and presence of other lineage (i.e. endodermal, Gata4 and mesodermal, Brachyury) markers with the progression of neural induction (S-NIM). Figure 4.10 shows changes in pluripotency expression from pluripotent state to Day

4 of induction. High expression (A-D) is observed when pluripotent mESCs were cultured on MEFs, in mESC medium (i.e. before starting neural induction).

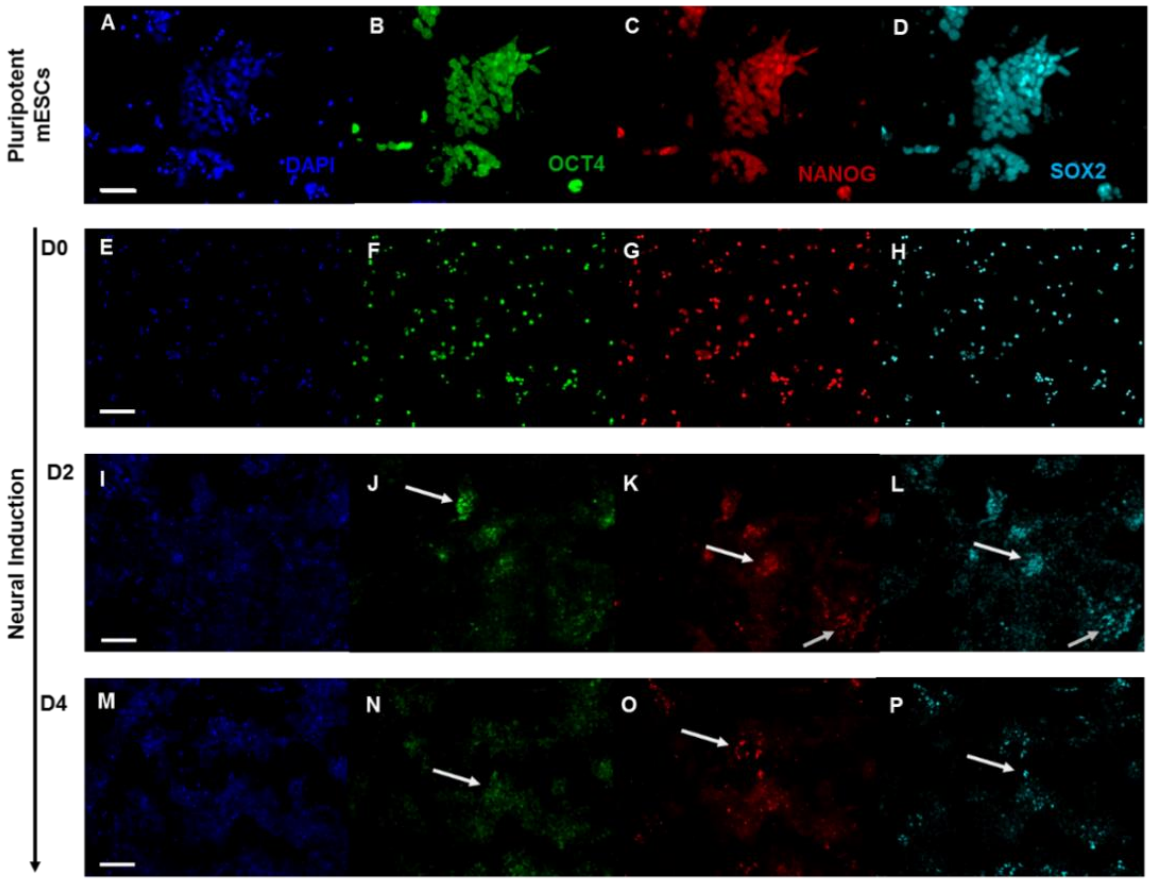

Figure 4.10 Representative images of a gradual decrease in pluripotency marker expression- Oct4 (green), Nanog (red) and Sox2 (light blue) from pluripotency to NI.

Pluripotent mESCs stained positively for all markers (A-D). Decrease in marker expression with increasing cell proliferation and progression into neural induction (E-P). As indicated by arrows, Nanog was the first marker to be down regulated (G, K, O), followed by Oct4 (F, J, N) and Sox2 (H, L, P) from D0-D4 of neural induction. Scale bar = 100 µm.

During induction however, pluripotency expression gradually decreased from Day 0 (E-H) to Day 2 (I-L), with minimal expression for all markers by Day 4 (M-P). Nanog (Figure 4.10 G, K, J) appeared to be the first marker to be downregulated, whereas Sox2 (Figure 4.10 P) was maintained until Day 4 of induction. As evidence of pluripotency diminished (Day 0 to Day 4), markers of neural stem cells (NSC) began to increase. Figure 4.11 shows the gradual increase in NSC markers Nestin (Figure 4.11 B, F, I) and Pax6 (Figure 4.11 O, R, U) from Day 0 to Day 4 of NI. Although expression for Nestin (Figure 4.11 L) was negligible by Day 7, though reduced, Pax6 (Figure 4.11 X) continued to be expressed.

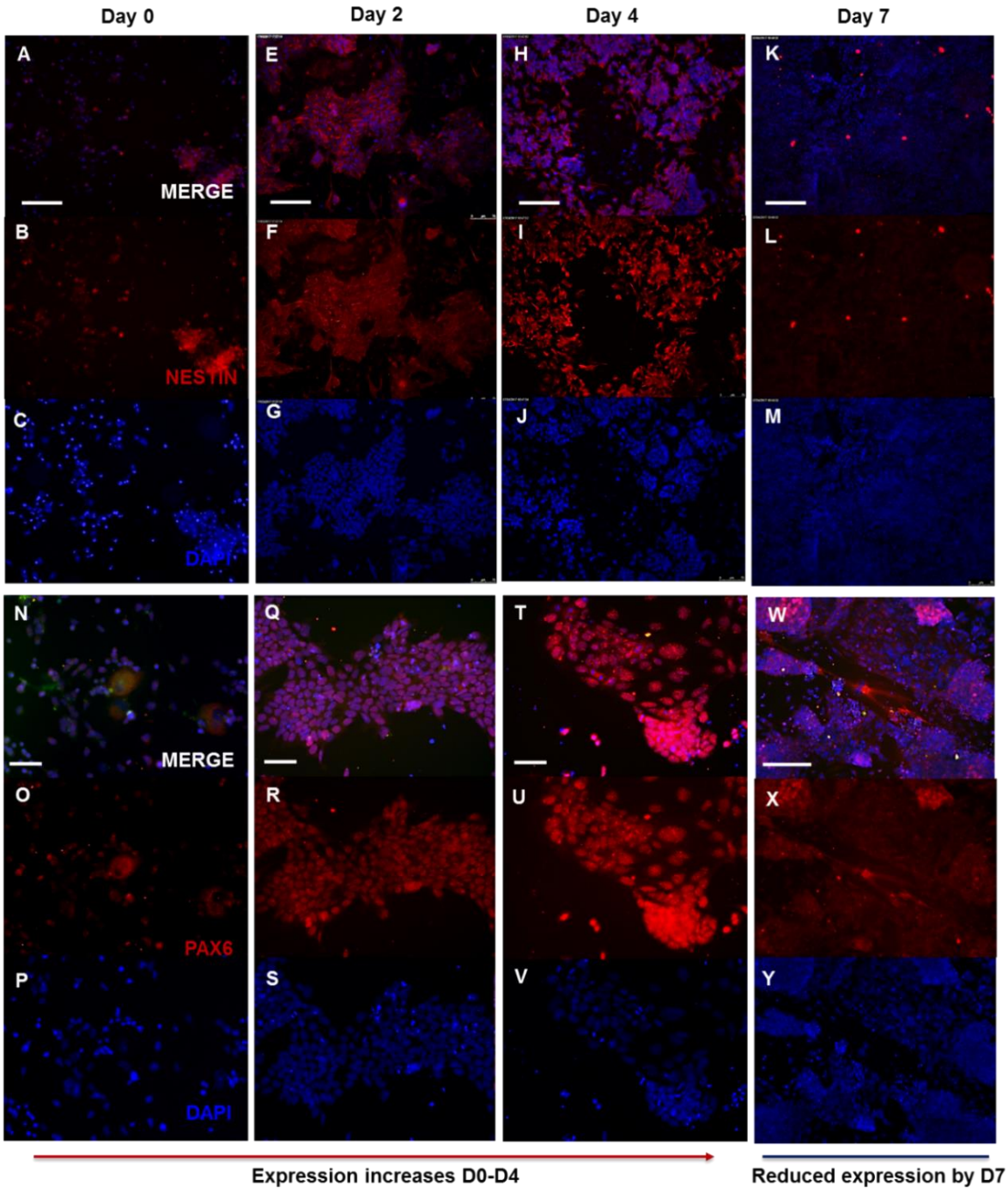

Figure 4.11 Changes in neural stem cell (NSC) marker(s) expression, Nestin and Pax6 (red), from D0 to D7 of neural induction (NI).

mESC lines stained for NSC markers Nestin (B, F, I, L) and Pax6 (O, R, U, X) on D0, D2, D4 and D7 of NI. The images show a progressive increase in Nestin and Pax6 expression from D0-D4, and negligible expression by D7 (L, X) of induction. Scale bar = 100 µm.

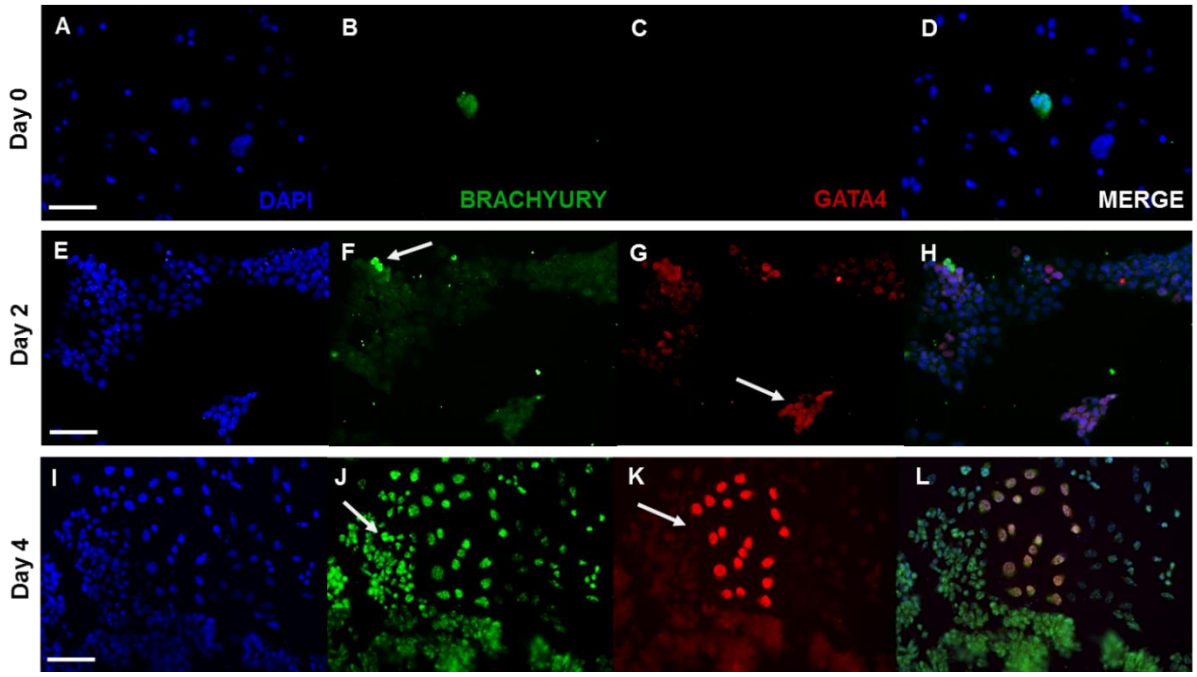

Figure 4.12 Presence of other lineage marker expression during Neural Induction (NI).

Representative images of mESCs stained for Brachyury (green, mesodermal marker) (B, F, J), Gata 4 (red, endodermal marker) (C, G, K) and Dapi (nuclear marker) (A, E, and I) for D0-D4 of NI. Negligible expression of both lineage markers on D0 (B, C). The expression for both markers increased from D2 to D4 of induction. Arrows point to cells positive for Brachyury (F, J) and Gata 4 (G, K) respectively. Scale bar = 200 µm.

Although the current S-NIM protocol induced neural induction, characterised by the increase of NSCs (Figure 4.11), it did not inhibit the emergence of cells from other lineages (i.e. mesoderm and endoderm). Figure 4.12 shows negligible expression of both markers at Day 0 (Brachyury, B and Gata4, C), but a gradual increase from Day 2 to Day 4 (Brachyury F, J and Gata4 G, K).

Mouse ESCs from NPD and LPD groups, directed towards NI under Standard NI media at an optimised cell density of 28,500 cells/cm^2 induced NI in both dietary groups, the characteristics of which were depicted by reduction in pluripotency (from Day 0- Day4) and a simultaneous increase in neural stem cell (NSC) markers (from Day 0-Day 4). No diet-based differences were observed between the NPD and LPD lines for these aspects. Moreover, both groups also showed presence of cells from other lineages, i.e. mesoderm and endoderm.

4.3.1.4 Neural induction of KO/SR cultured mESC lines in Standard or Advanced NIM

Overall, from the above data, the standard NIM (S-NIM) protocol induced gradual reduction in pluripotency (Nanog, Oct4 and Sox2; Day 0 to Day 4; Figure 4.10) and increase in early NSC (Nestin and

Pax6; Day 2 to Day 7; Figure 4.11) markers. This therefore demonstrates successful neural induction of pluripotent NPD and LPD mESCs (Section 4.2.4). However, in addition to NI, S-NIM also led to the development of other lineage (i.e. endodermal and mesodermal) cells (Figure 4.12). It is known that other lineage cells (often referred to as culture contaminants) release factors that reduce efficiency of targeted differentiation (Arkin and Wells, 2004). Therefore, to promote lineage-specific differentiation by inhibiting other lineages, and to enhance the efficiency of S-NIM in mESC lines, an advanced NIM (A-NIM, Section 4.2.4.2) protocol was designed using small-molecule inhibitors (SMI). The present study utilized dual-SMAD inhibitors, SB and LDN, which inhibit TGF-β/Activin/Nodal and BMP signalling pathway respectively (Section 4.2.4.2).

4.3.1.4.1 Morphological differences (Brightfield images)

A representative KO/SR NPD mESC line, 18 P12 maintained on MMC-MEFs, was incubated with S-NIM overnight. On the following day, cells were passaged and plated (28,500 cells/cm^2) on Matrigel-coated dishes (Section 4.2.4) in either S-NIM or A-NIM, for 8 days of NI (Figure 4.13). As small molecule inhibitors (SMIs) are known to induce increased cell death (Watanabe et al., 2007), A-NIM also contained ROCK (Rho-associated protein kinase) inhibitor from Day 0 to Day 1 of induction, which was discontinued from Day 1 to Day 8. Although cells mostly maintained a pluripotent colony morphology ('round and tomb-like') before and after induction with S-NIM (Figure 4.13 A and B), colony morphology changed to being 'elongated and flatter with sharp edges', as early as Day 1 of the neural induction (Figure 4.13 D and I). Despite using ROCK, A-NIM cultures appeared to display excessive cell death, which was observed throughout induction (i.e. Day 0 to Day 8, Figure 4.13 H-L), and became more prominent from Day 4 to Day 8 with increasing cell density. Although morphologically, A-NIM cultured cells did not display other lineage contaminants, and appeared to show initiation of rosette formation (Figure 4.13 K, L), the number of cells with the typical neurite morphology was evidently reduced in these cells compared to S-NIM cultures (Figure 4.13 F, G), which showed bigger, denser and more mature rosettes.

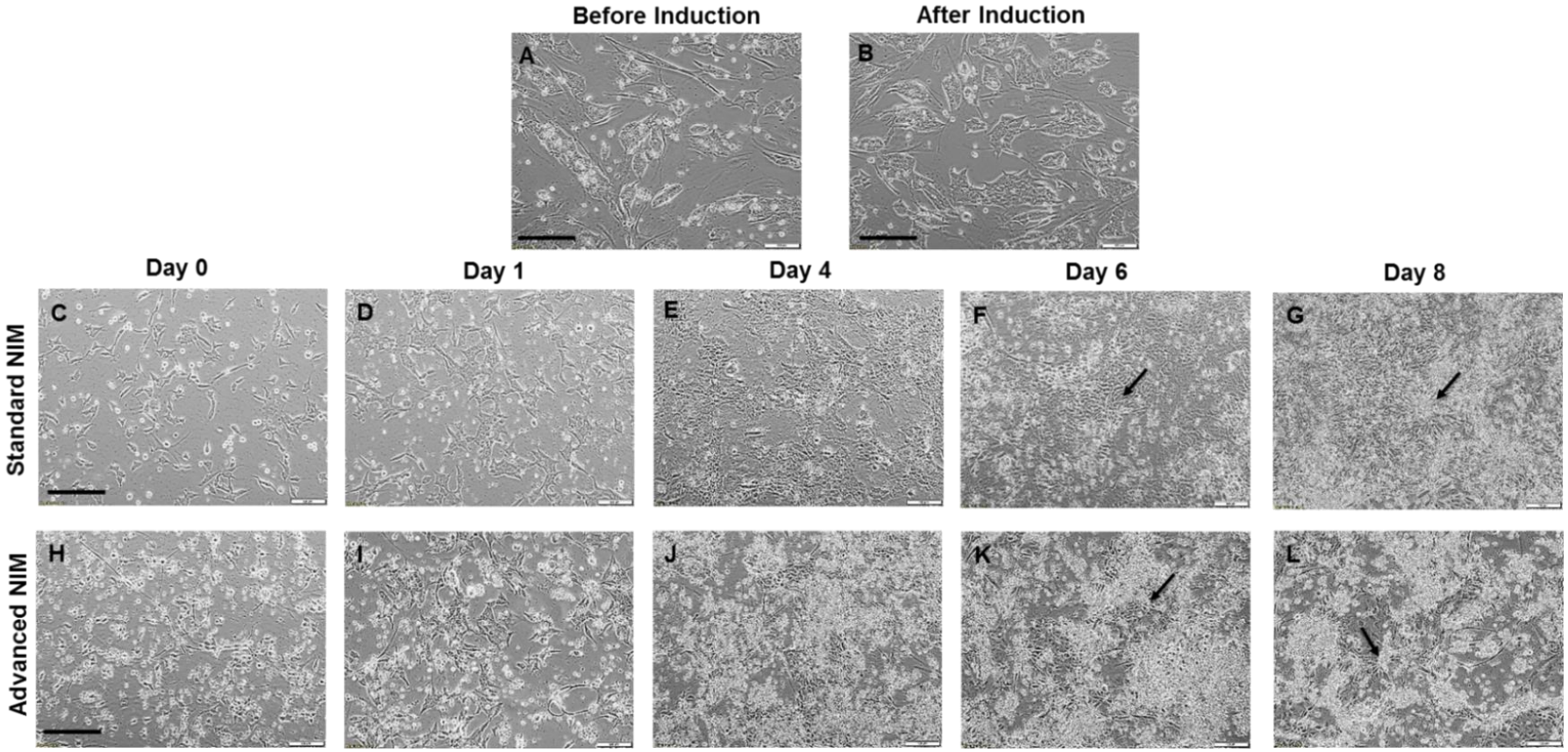

Figure 4.13 Comparison between neural induction under Standard (S-NIM) and Advanced (A-NIM) culture conditions.

mESC NPD 18P12 was maintained under similar pluripotency conditions (KO/SR) and was switched to different NI medium on D0 of induction. Cells maintained pluripotent morphology under KO/SR, LIF with MEF conditions (A), and after overnight treatment with S-NIM (B). Images display morphological changes in S-NIM (C- G) and A-NIM (H- L) culture conditions. Excessive cell death was observed under A-NIM (depicted by bright white cells, H- L). Arrows indicate the appearance of radial cells forming rosettes (F, G, K, and L). Bigger and denser rosettes were observed under S-NIM, than A-NIM culture conditions. Scale bar = 100 µm.

4.3.1.4.2 Relative gene expression of S-NIM and A-NIM cultured cells

S-NIM and A-NIM treated differentiating KO/SR-NPD 18 P14 cell line was analysed for pluripotency (*Oct4, Nanog* and *Sox2*), differentiation (*Gata4* and *Brachyury*), apoptosis (*Caspase3*), early neural stem cell (NSC) (*Sox1*, *Nestin* and *Pax6*) and mature neuron (*Beta III Tubulin* and *Map2*) markers (Figure 4.14 and 4.15). Genes of interest were normalized to *Rpl13a* and *Canx* within geNorm (Section 4.2.5.4).

S-NIM cultured cells showed increased pluripotency expression (Figure 4.14 A-C) at Day 0, which appeared to reduce thereafter and was similar to A-NIM cultured cells, with the possible exception of *Sox2* (Figure 4.14 C), which was slightly elevated in A-NIM from Day 2 to Day 10. A-NIM cultured cells showed low expression for endodermal *Gata4* (Figure 4.14 D) and mesodermal *Brachyury* (Figure 4.14 E) markers with no variation over time, whereas S-NIM cultured cells showed increased *Gata4* expression from Day 4 to Day 10 and decreased *Brachyury* expression from Day 0 to Day 10 (Figure 4.14 E). The apoptosis marker, *Caspase3,* showed a similar pattern of expression for A-NIM and S-NIM culture conditions across time points (Figure 4.14 F).

Consistent with negligible neuronal morphology (Figure 4.13), A-NIM cultured cells showed low expression for NSC *(Sox1, Nestin* and *Pax6*) markers, with no variation over time (Figure 4.15 A-C). S-NIM cells on the other hand, showed increased relative expression for NSC markers from Day 2 to Day 4, and a reduction thereafter. No consistent pattern was observed for neuron marker *Beta III Tubulin* (Figure 4.15 D). *Map2* expression appeared to remain low for both S-NIM and A-NIM cultured cells from Day 0 to Day 7, but increased from Day 7 to Day 10 for S-NIM conditions (Figure 4.15 E).

In addition to KO/SR-NPD 18P12, two LPD lines cultured under similar A-NIM conditions (images not presented), also failed to produce the expected neural morphology (i.e. formation of neurites and/or rosettes) during the ten days of NI. Given that SMIs used in A-NIM induce increased cell death and that cell density greatly influences neural differentiation efficiency, it was believed that the optimised plating density for S-NIM, may not be optimal for A-NIM cultures. To investigate this further, the pluripotent KO/SR-NPD 18P14 was cultured and expanded further, and plated in increased (double- 57,000 cells/cm^2, triple- 85,500 cells/cm^2, and higher- 111,111 cells/cm^2) cell densities. Cells were cultured under A-NIM for eight days of NI, but no morphological signs of neural induction were observed (images not presented). Thus, given the aforementioned constraints (Section 4.1), these samples were not processed for further analysis.

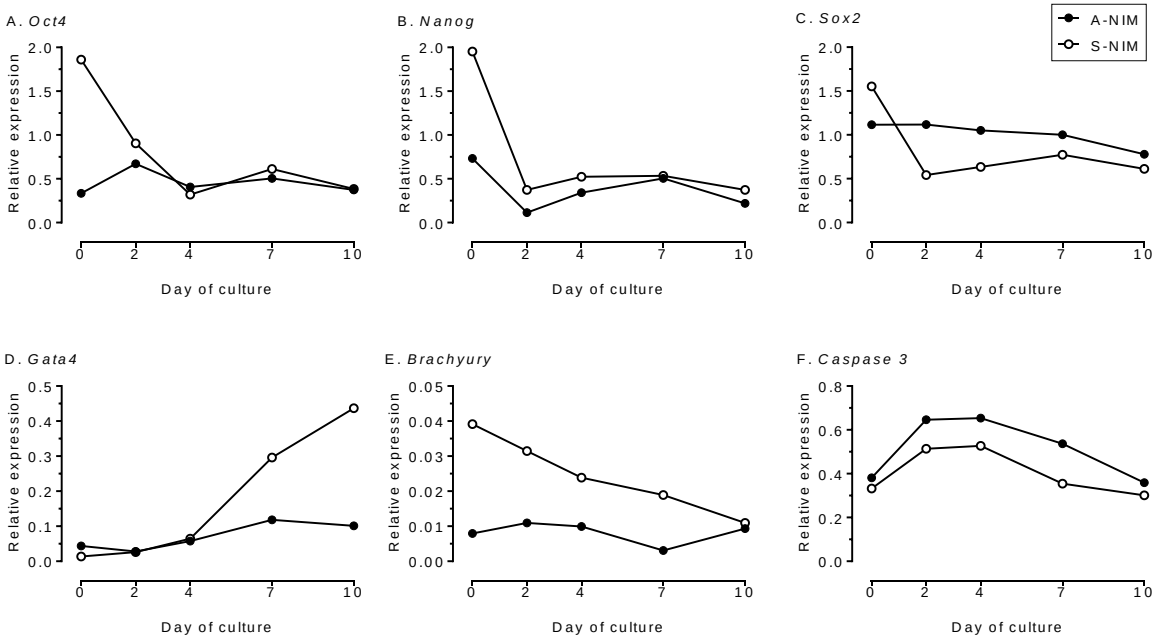

Figure 4.14 Comparison of relative gene expression for pluripotency, differentiation and apoptosis markers in mESCs undergoing NI under standard and advanced culture conditions.

KO/SR-NPD 18P12 was cultured in standard (S-NIM) or advanced (A-NIM) NI medium from D0-D10 of induction. Genes of interest were normalized to *Rpl13a* and *Canx* within geNorm. (A-C) Pluripotency (*Oct4*, *Nanog* and *Sox2*) marker(s) expression was reduced from D0- D2 (especially for cells cultured under S-NIM), and continued to remain low from D2-D10 in both culture conditions. Pluripotency Expression at D0 (A-C) was lower in A-NIM compared to S-NIM conditions, with the exception of (C) *Sox2*, which was slightly increased in A-NIM cultured cells from D2-D10. Additionally, differentiation marker(s) expression was observed to be comparatively low under A-NIM than S-NIM conditions from D0-D10 (D, E). For S-NIM, *Gata4* expression increased from D4-D10 (D), although *Brachyury* expression decreased consistently from D0-D10 (E). The apoptosis marker, *Caspase3,* showed a similar expression pattern for both conditions, although expression was slightly higher in A-NIM than in standard NI medium at all time points (F).

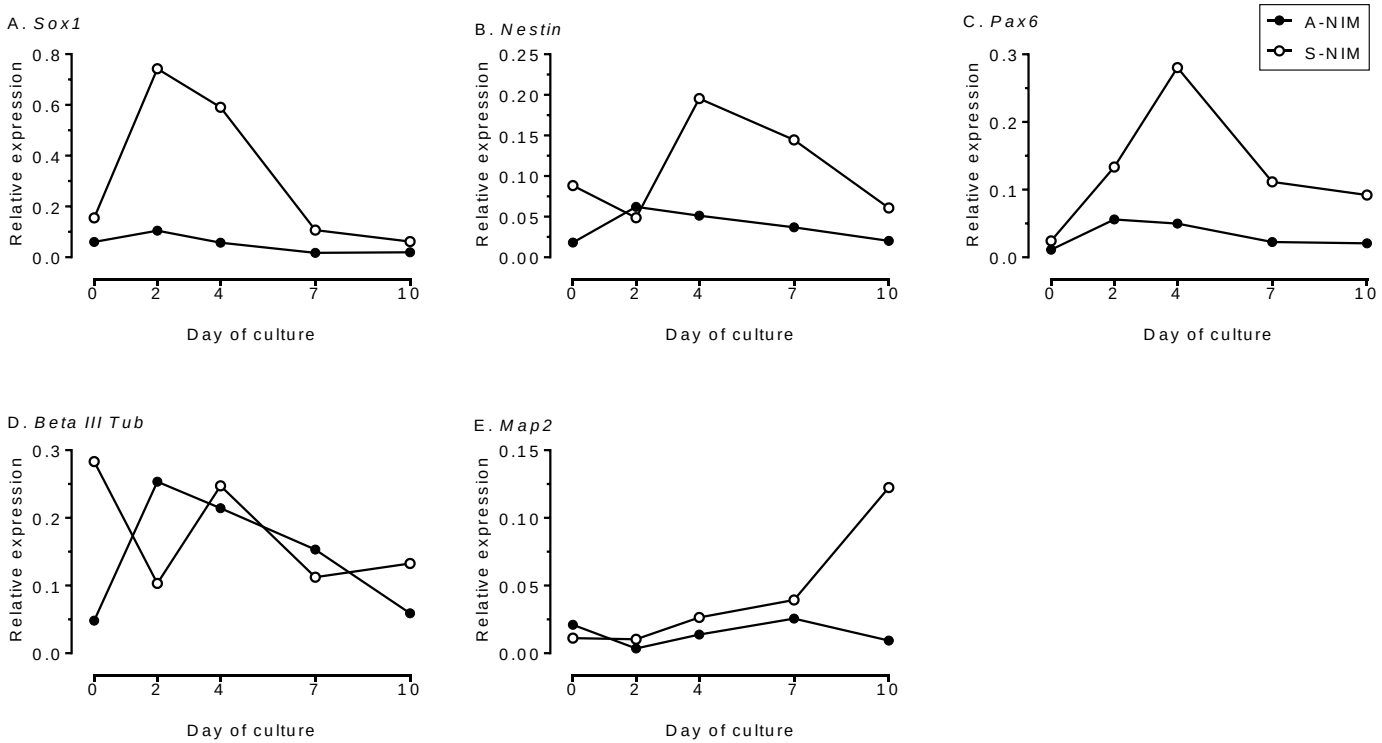

Figure 4.15 Comparison of relative gene expression for early neural stem cell (NSC) and mature neuron markers in mESCs undergoing NI under standard and advanced culture conditions.

KO/SR-NPD 18P12 was cultured in standard (S-NIM) or advanced (A-NIM) NI medium from D0-D10 of induction. Genes of interest were normalized to *Rpl13a* and *Canx* within geNorm. Early NSC markers (*Sox1, Nestin* and *Pax6*) showed increased expression under S-NIM than A-NIM conditions at all time points (A-C). Under S-NIM, expression increased from D0-D2 (A) and D0-D4 (B, C), but decreased consistently from D4-D10. Mature neuron marker *Beta III Tubb* decreased from D0-D2 and D4-D7 and increase thereafter for S-NIM whereas, for cells cultured in A-NIM, expression peaked at D2 and consistently decreased thereafter (D). *Map2* expression remained low for both conditions from D0-D7, but increased from D7-D10 for S-NIM (E).

Part 1 of this section focused on the optimisation of the original Biotalentum NI protocol based on three key factors including (i) culturing pluripotent NPD and LPD mESC lines (before NI) under serum (ES-FBS) or serum-free (KO/SR) conditions, (ii) choosing optimal cell plating density for NI (i.e. low 12,500 cells/cm^2, moderate 25,000 cells/cm^2 or high- 30,000 cells/cm^2), and (iii) selecting optimal NI medium (i.e. S-NIM or A-NIM). From the assessments made, it was concluded that mESCs must be cultured in the presence of KO/SR and not ES-FBS. For NI protocol, a higher cell density of 28,500 cells/cm^2 was selected as it displayed highest expression of NSC and neuron markers. Although the Advanced NI media (A-NIM) reduced other lineage differentiation, it also resulted in inhibition of neural differentiation. Therefore, the remaining experiments were be conducted using only Standard-NI media (S-NIM).

4.3.2 PART 2: Preliminary analysis of differences between NPD and LPD mESCs

The current section provides a preliminary assessment of NI efficiency for NPD and LPD mESCs cultured with or without serum. Following on from Part 1, mESC lines were plated at 28,500 cells/cm^2 under S-NIM conditions. Differences in NI efficiency were compared between 2 NPD and 2 LPD mESC lines from each serum group. However, due to the limited number of cells in the ES-FBS group (due to increased cell death), the comparison of the initial pluripotent status of NPD and LPD mESC lines (i.e. before the initiation of NI) was restricted to the 2 NPD and 2 LPD mESC lines cultured with KO/SR.

4.3.2.1 Pluripotency of KO/SR cultured NPD and LPD mESCs

As described in Section 4.2.1, NPD and LPD mESCs were cultured in pluripotent mESC culture conditions established in Southampton. Briefly, mESCs (500,000 cells/ 6-cm dish) were plated on MMC-MEFs (700,000 cells/ 6-cm dish) in mESC medium (Section 4.2.1, DMEM/ F-12, KO/SR and LIF). Cells were cultured and expanded for 2-3 passages and harvested for pluripotent RT-PCR (Section 4.2.5.1) the evening before the initiation of neural induction (Section 4.2.4). Pluripotent NPD and LPD mESC samples (n= 2 per group, P12-13) were normalized to *Rpl13a* and *Canx* within geNorm. The samples were analysed for pluripotent (*Oct4, Nanog* and *Sox2*), other lineage (*Gata4* and *Brachyury*), apoptotic (*Caspase3*), early neural stem cell (*Sox1*, *Nestin* and *Pax6*), and mature neuron (*Beta III Tub* and *Map2*) markers. Pluripotent LPD mESC lines appeared to show decreased expression for pluripotent (A-C), mesodermal (E) and apoptotic (F) markers, whereas the endodermal marker, *Gata4*, increased (D) (Figure 4.16).

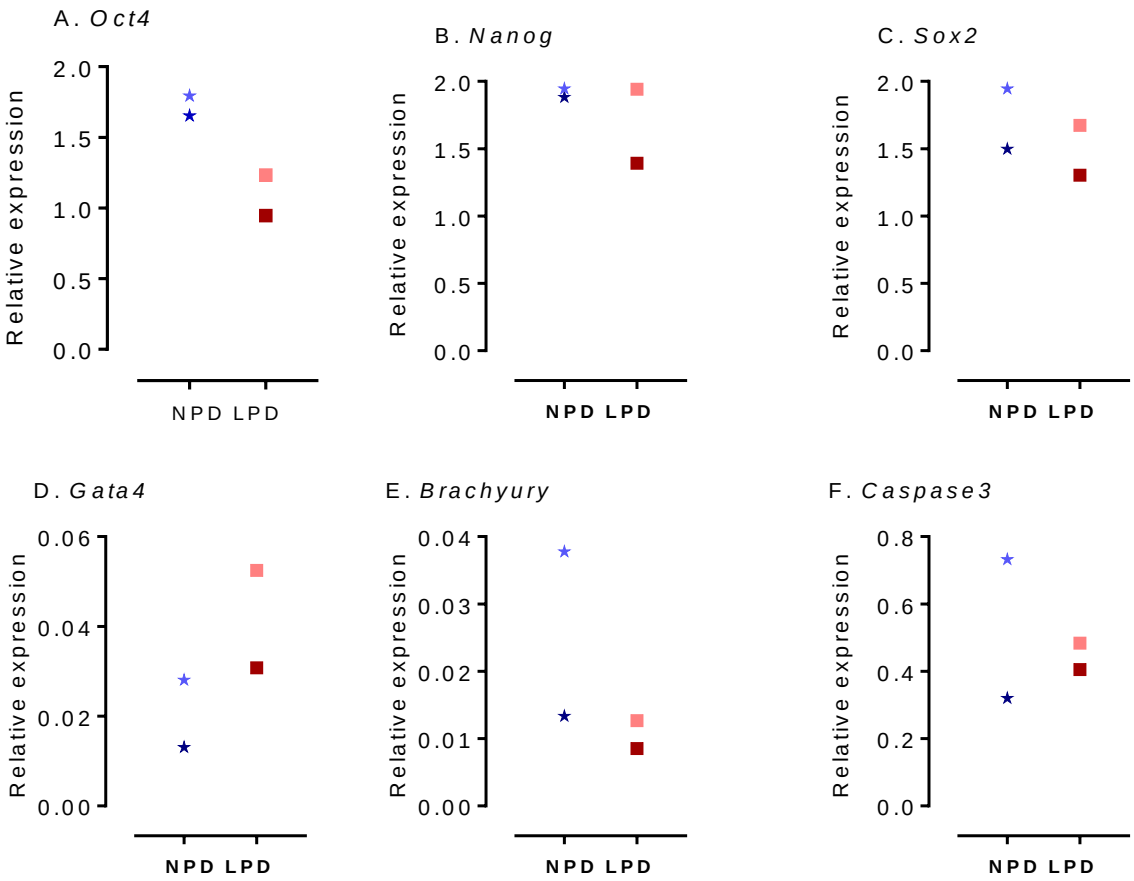

Figure 4.16 Comparison of relative gene expression for pluripotency, differentiation and apoptosis markers in pluripotent NPD and LPD mESCs cultured without serum.

mESCs (n=2 per group, P12-13) were cultured in KO/SR on MEFs. Genes of interest were normalized to *Rpl13a* and *Canx* within geNorm. Two KO/SR cultured NPD mESC lines (marked as light and dark shades of blue *) showed increased expression for pluripotency *Oct4* (A), *Nanog* (B) and *Sox2* (C), mesodermal *Brachyury* (E), and *apoptotic* (F) markers compared to LPD mESCs lines (marked as light and dark shades of red ▪). LPD mESCs lines showed increased endodermal marker *Gata4* (D) expression.

The expression of NSC (A-C) and neuron marker *Beta III Tub* (D) also appeared to decrease in LPD mESCs although *Map2* expression appeared to increase (Figure 4.17 E). On the other hand, pluripotent NPD and LPD mESC samples showed no obvious differences between the qualitative immunocytochemistry expression for pluripotency markers Oct4 (green), Nanog (red) and Sox2 (light blue) before NI (Figure 4.18).

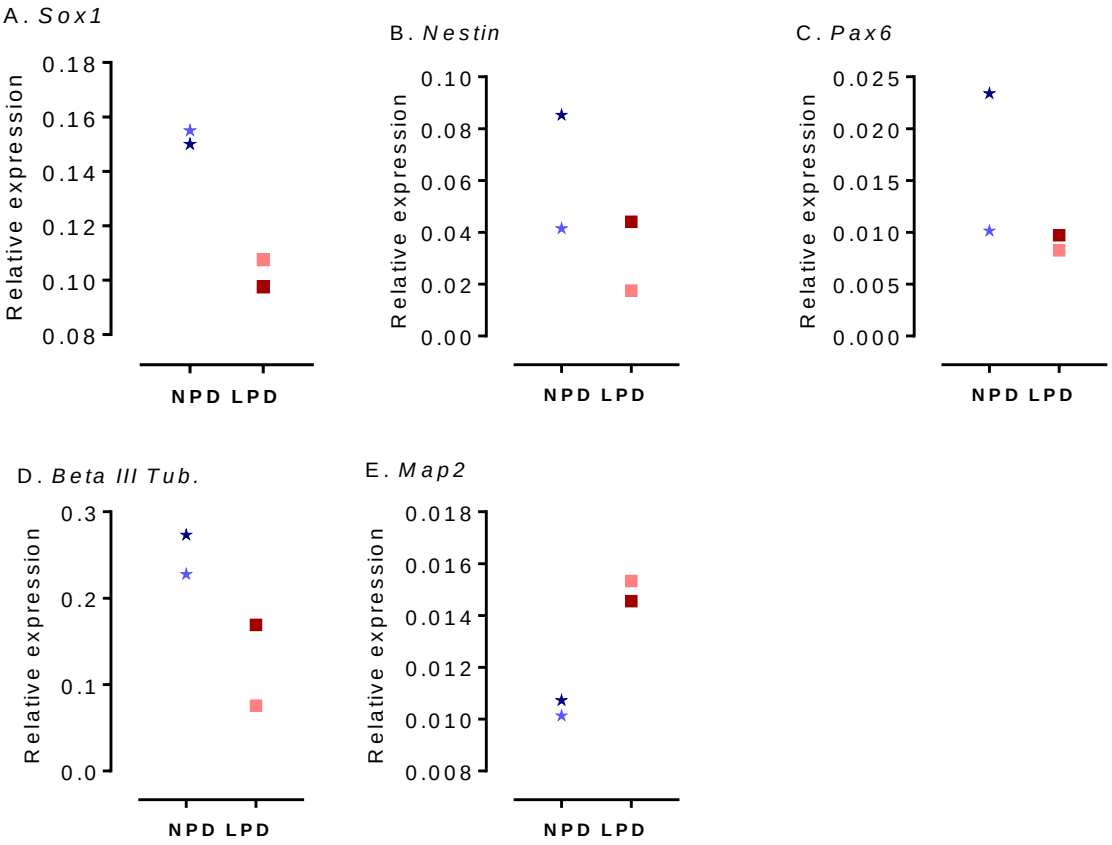

Figure 4.17 Comparison of relative gene expression for early neural stem cell (NSC) and mature neuron markers in pluripotent NPD and LPD mESCs cultured without serum.

mESCs (n=2, P12-13) were cultured in KO/SR on MEFs. Genes of interest were normalized to *Rpl13a* and *Canx* within geNorm. Two KO/SR cultured NPD mESC lines (marked as light and dark shades of blue *) showed increased expression for early NSC- *Sox1* (A), *Nestin* (B) and *Pax6* (C), and mature neuron- *Beta III Tub* (D) markers. However, LPD mESCs lines (marked as light and dark shades of red ▪) showed increased *Map2* (E) expression.

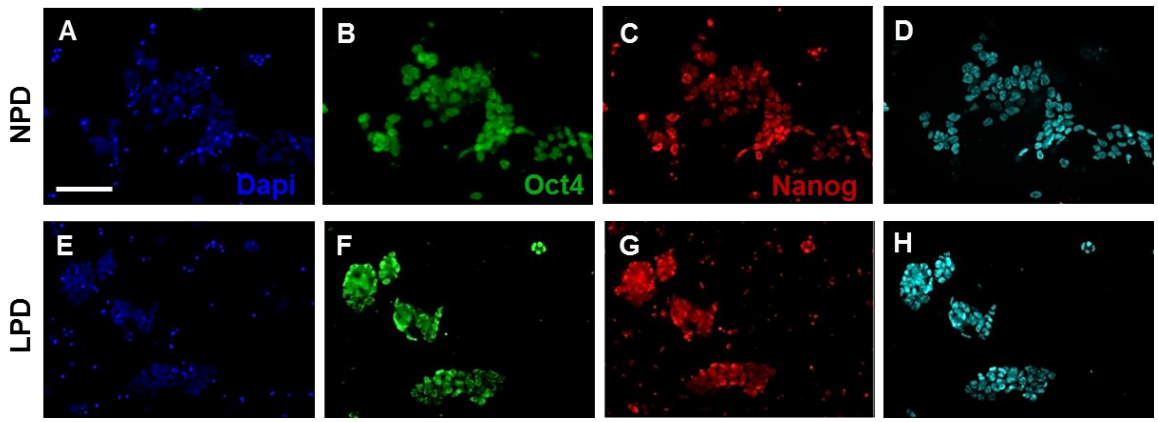

Figure 4.18 Figure 4.18. Representative images of pluripotency marker expression, Oct4 (green), Nanog (red) and Sox2 (light blue) in pluripotent NPD and LPD mESCs before NI.

Pluripotent mESCs stained positively for all markers (A-D) for both diet groups. Scale bar= 100 µm.

4.3.2.2 Neural induction of ES-FBS and KO/SR cultured NPD and LPD mESCs

As described in Section 4.2.3, NPD and LPD mESCs were cultured in either ES-FBS- or KO/SR-pluripotent mESC medium, on MMC-MEFs (Sections 2.2.2.1.1). Prior to induction, mESCs were washed with PBS (maintained on MMC-MEFs) and conditioned overnight with S-NIM (Section 4.2.4). On the following day, mESCs were split and plated on Matrigel-coated dishes at optimized cell density of 28,500 cells/cm^2 (Section 4.3.1.2) in S-NIM for a continuous period of 14 days, and samples were collected at the six defined time points i.e. Days 0, 2, 4, 7, 10 and 14 (Section 4.2.4) of NI. Medium were changed daily, and cell cultures were observed for morphological changes both before (to gauge cell death) and after media change.

4.3.2.2.1 Morphological differences (Brightfield images)

While rosette (neural tube-like columnar cells) clusters were visible as early as Day 3 in KO/SR NPD and LPD cell lines (Figure 4.19 G and H), ES-FBS LPD cell lines (Figure 4.19 F) only appeared to show rosette formation on Day 7, which was even more sparsely observed in NPD cell lines (Figure 4.19 E). Though mESCs were plated at the same density, cell number (and colony size) appeared to be higher in KO/SR cultured cell lines compared to ES-FBS cell lines at all time points. In both KO/SR and ES-FBS groups, LPD mESCs appeared to show increased cell density, earlier initiation of rosette formation, and consequently denser and more mature rosette clusters compared to NPD lines throughout NI. Given the increased density, LPD mESCs (Figure 4.19 L and Figure 4.20 K and L) also showed increased cell death, observed as bright white cells. Both groups also displayed the presence of other, non-neural lineage cells, around Day 5 of induction, with a flatter and bigger cell morphology (Figure 4.19 C, D and J).

Overall, cell lines from both serum groups appeared to maintain a pluripotent morphology from Day 0 to Day 1, and showed increased cell density by Day 2 (images not presented). Rosettes with interwoven networks of neurites continued to proliferate and gradually increase in density from Day 3 to Day 14 (initiation of rosettes was visible on Day 2 in LPD mESCs) of induction in KO/SR lines, and from Day 7 to Day 14 for ES-FBS lines. Based on cellular morphology (Figure 4.19 and 4.20), NPD lines seemed to proliferate and differentiate more slowly to neural rosettes and neurites. This was observed more in the presence of ES-FBS than in KO/SR compared to LPD lines in their respective groups.

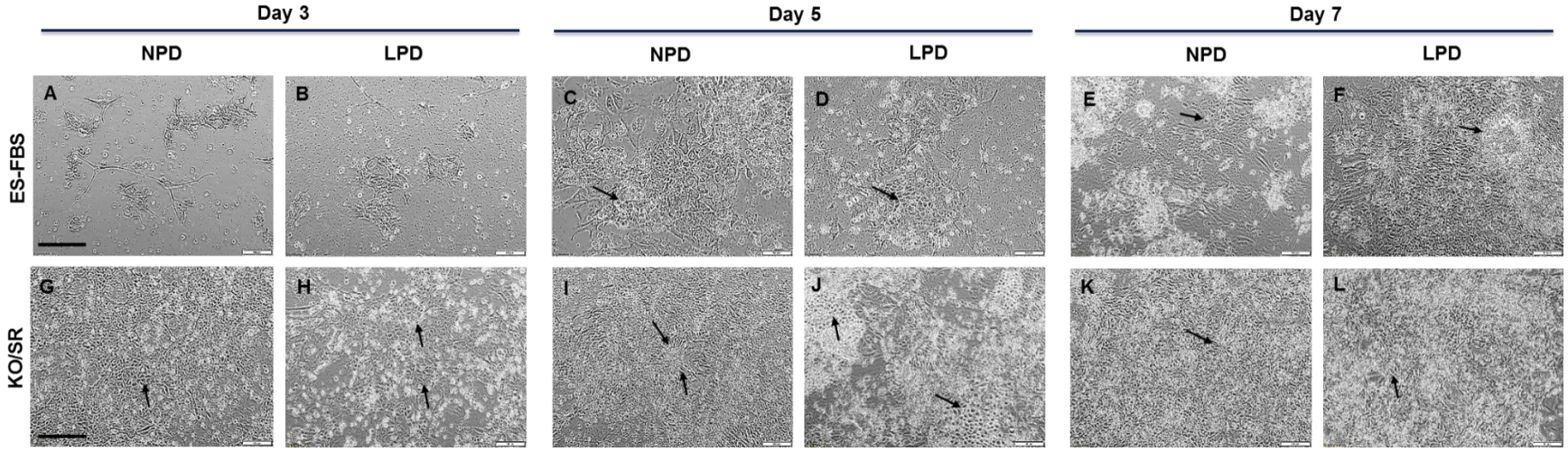

Figure 4.19 Neural induction (D3-D7) of NPD and LPD mESC lines cultured in ES-FBS and KO/SR.

Morphological changes in ES-FBS NPD (A, C, E) and LPD (B, D, F), KO/SR NPD (G, I, K) and LPD (H, J, L) mESC lines. KO/SR NPD and LPD have increased cell density on D3, D5, and D7 of induction (G-L), compared to ES-FBS NPD and LPD cell lines (A-F). Arrows point to little clusters of rosettes on D3 in KO/SR LPD and on D5 in NPDs cultured cells (G, H), which is absent in ES-FBS cells (A, B). Arrows point to gradual increase in rosette formation in D5 (I), and large, flat-cells which appear to be cells from other (non-neural) lineages (C, D, J). Arrows point to denser and bigger rosettes (F, K, L). Overall, cell density and rosette formation increases gradually from D3- D7 of induction in the KO/ SR mESC lines of both diet groups, unlike ES-FBS mESC lines, where the first appearance of rosettes is observed on D7, where LPDs (F) show much greater rosette formation compared to NPD (E) cells. Scale bar= 100 µm.

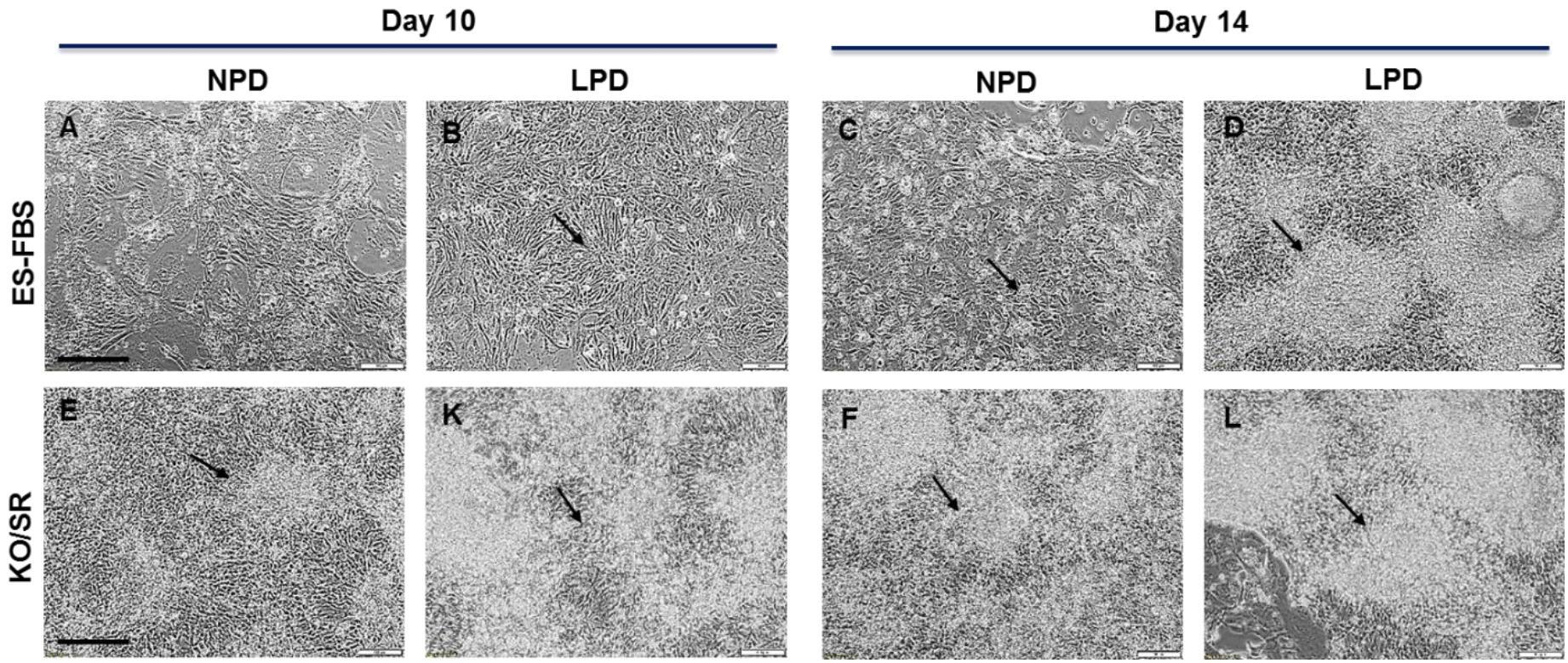

Figure 4.20 Neural induction (D10-D14) of NPD and LPD mESC lines cultured in ES-FBS and KO/SR.

Morphological changes in ES-FBS NPD (A, C) and LPD (B, D), KO/SR NPD (E, F) and LPD (K, L) mESC lines. KO/SR NPD and LPD displayed increased cell density on D10 and D14 of induction (E-L) compared to ES-FBS NPD and LPD cell lines (A-D). Arrows point to dense columnar cells forming rosettes on D10 and D14 in KO/SR NPD (E, K) and LPD (F, L) and ES-FBS LPD (B, D), which is observed sparsely in ES-FBS NPD cells (A, C). Overall, rosettes become denser and more mature from D10-D14 of induction in the ES-FBS and KO/SR mESC lines of both diet groups. Scale bar= 100 µm.

4.3.2.2.2 Differences in relative gene expression and immunocytochemistry

NPD and LPD mESC lines were cultured in pluripotent mESC medium (with or without serum, Section 4.2.3) and cultured on Matrigel at a density of 28,500 cells/cm^2 for 14 days of neural induction (S-NIM) (Section 4.2.4.1). Cells were harvested for RT-PCR on Days 0, 2, 4, 7, 10 and 14 of NI (Section 4.2.5). Differentiating NPD and LPD cell lines (n=2 per group, P14-16) were analysed for pluripotency (*Oct4, Nanog* and *Sox2*), other lineages (*Gata4* and *Brachyury*), apoptosis (*Caspase3*), early NSC (*Sox1*, *Nestin* and *Pax6*) and mature neuron (*Beta III Tubulin* and *Map2*) markers (Figure 4.21 and 4.22). Genes of interest were normalized to *Rpl13a* and *Canx* within geNorm (Section 4.2.5.4) and preliminary data is presented as simple means (Section 4.2.7).

As displayed in Figure 4.21, KO/SR cultured NPD and LPD cell lines appeared to show increased mean expression for the three pluripotency markers (A-C) at Day 0, while expression for *Sox2* continued to increase from Day 4 to Day 14 of induction compared to NPD and LPD cell lines cultured in ES-FBS. While mean expression of the endodermal marker, *Gata4* (Figure 4.21 D), continued to increase from Day 0 to Day 14 (irrespective of diet and serum conditions), the mesodermal marker, *Brachyury* (Figure 4.21 E), showed a relatively low and constant expression throughout induction (Day 0 to Day 14). However, ES-FBS NPD showed high peaks at the start (i.e. Day 0) and end (i.e. Day 14) of NI. The apoptosis marker *Caspase3* (Figure 4.21 F), on the other hand, showed a more variable expression pattern with diet, serum conditions and time; and displayed a continuously increasing expression in ES-FBS NPD mESCs, reaching the highest expression at Day 14 of induction.

While serum did not appear to have a direct effect on changes in pluripotent cells, other lineages or on apoptotic marker expression (Figure 4.21), KO/SR cultured NPD and LPD cell lines displayed a consistent tendency of increased neuronal lineage (Figure 4.22 A-E); i.e. NSC (Day 0 to Day 14) and mature neuron (Day 7 to Day 14) marker expression, compared to ES-FBS cultured cell lines. Although mean expression of NSC markers (Figure 4.22 A-C) peaked earlier for KO/SR NPDs, both NPDs and LPDs displayed similar patterns of increasing and decreasing expression.

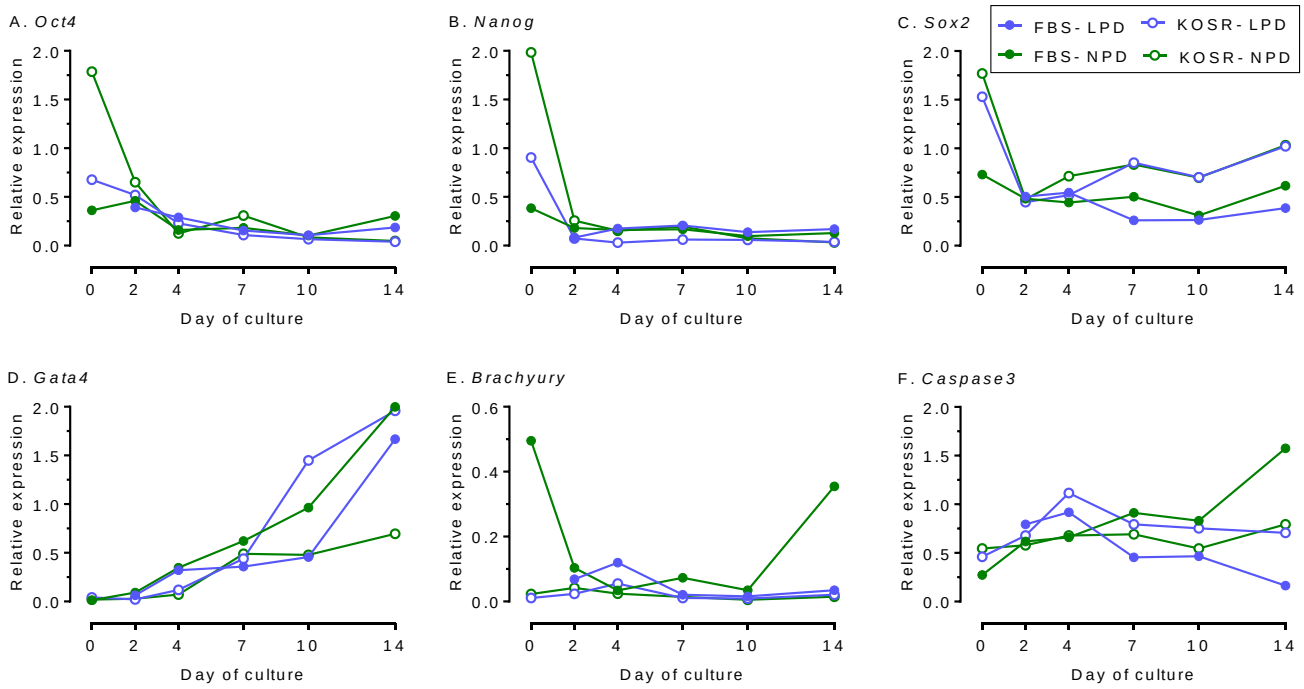

Figure 4.21 Comparison of relative gene expression for pluripotency, differentiation and apoptosis markers in mESCs cultured with or without serum, undergoing standard NI.

mESCs (n=2 per group, P14-16) were cultured in ES-FBS or KO/SR, and differentiated in standard NI medium from D0-D14. Genes of interest were normalized to Rpl13a and Canx within geNorm. KO/SR cultured mESC lines showed increased expression of pluripotency markers Oct4 (A) and Nanog (B) at D0, and Sox2 (C) at D0 and D4-D14, compared to the lines cultured in ES-FBS. Differentiation marker Gata4 (D) showed increased expression from D4 and D7-D14 in all groups. With the exception of ES-FBS NPD at D0 and D14, Brachyury (E) displayed reduced expression throughout the induction for all four groups. Apoptosis marker Caspase3 (F) showed an inconsistent expression pattern with time and culture treatment, and displayed highest expression in ES-FBS NPD at D14 of induction.

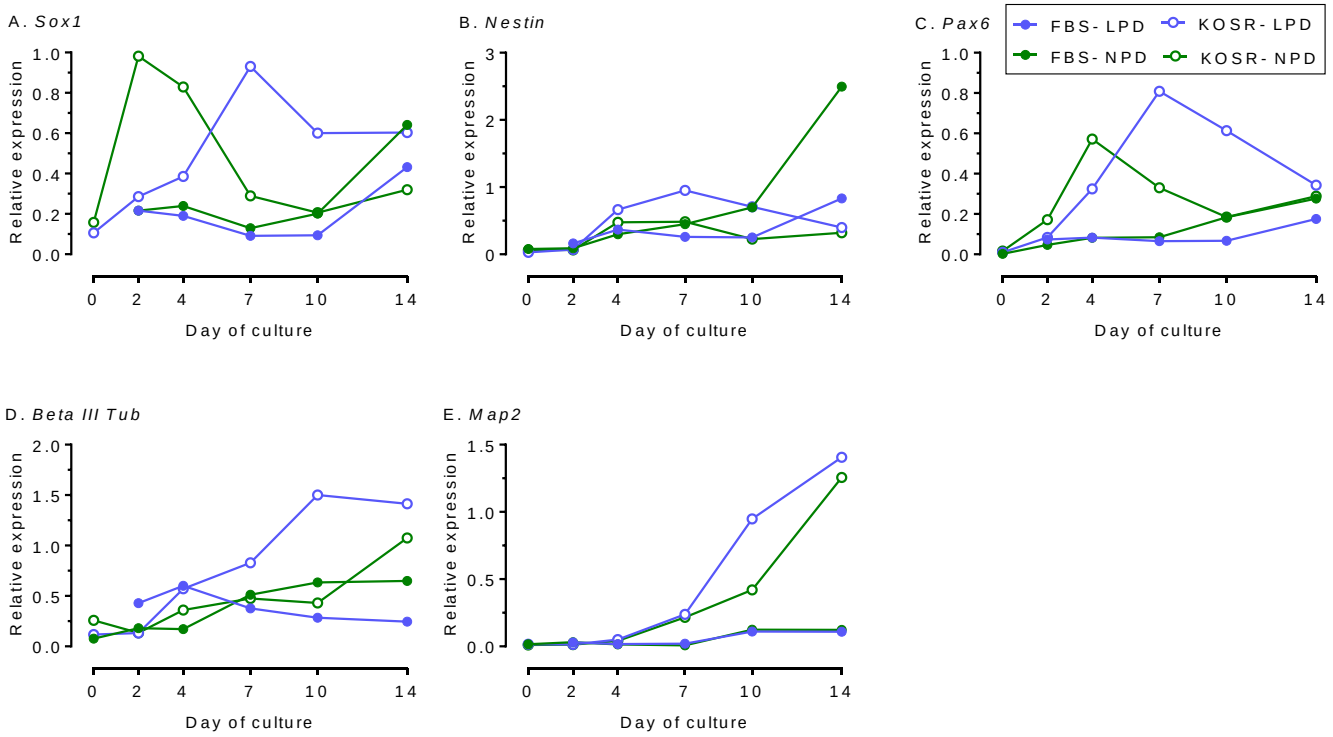

Figure 4.22 Comparison of relative gene expression for early neural stem cell (NSC) and mature neuron markers in mESCs cultured with or without serum, undergoing standard NI.

mESCs (n=2 per group, P14-16) were cultured in ES-FBS or KO/SR, and differentiated in standard NI medium from D0-D14 of induction. Genes of interest were normalized to *Rpl13a* and *Canx* within geNorm. KO/SR cultured mESC lines showed increased expression of early NSC (*Sox1, Nestin* and *Pax6*; D0-D10) (A-C) and mature neuron (*Beta III Tubb.* and *Map2*; D7-D14) (D, E) markers compared to the lines cultured in FBS. Within the KO/SR group, although NPDs expressed the NSC markers before LPD lines (A-C), mature neuron marker(s) expression was higher in LPDs for *Beta III Tubulin* between D4-D14 (D) and *Map2* between D7-D14 (E) compared to NPDs.

Mean expression of mature neuron markers *Beta III Tubulin* (Day 4 to Day 14) and *Map2* (Day 7 to Day 14) appeared to be slightly increased in KO/SR LPDs than NPDs (Figure 4.22 E, F).

Although no major changes were noticeable between pluripotent, NSC and other lineage protein expression (by immunocytochemistry), subtle differences were observed between the mature neuron marker(s) expression of KO/SR cultured NPD and LPD mESCs at Day 7, 10 and 14 of neural induction. As displayed in Figure 4.23, both NPD and LPD cell lines appeared to show gradual increase in Beta III Tubulin and Map2 marker expression from Day 7 (B, F, C, G) to Day 14 (R, V, S, W). However, LPD lines showed noticeable increase in the number of cells positive for both the markers across all time points (i.e. Day 7, 10 and 14). Additionally, in both NPD and LPD lines, Beta III Tubulin showed visibly greater expression compared to Map2, which although observed throughout induction, was most prominent at Day 7 (B, F and E, G).

Part 2 of this study utilised this optimised NI protocol from Part 1. Independent of diet, mESCs cultured under KO/SR during pluripotency showed superior NI compared to those cultured under ES-FBS. Within the KO/SR group, LPD displayed more efficient NI compared to NPD lines. This was characterised by faster appearance of rosette and neurites in the differentiating cells and a protracted period of neural marker expression.

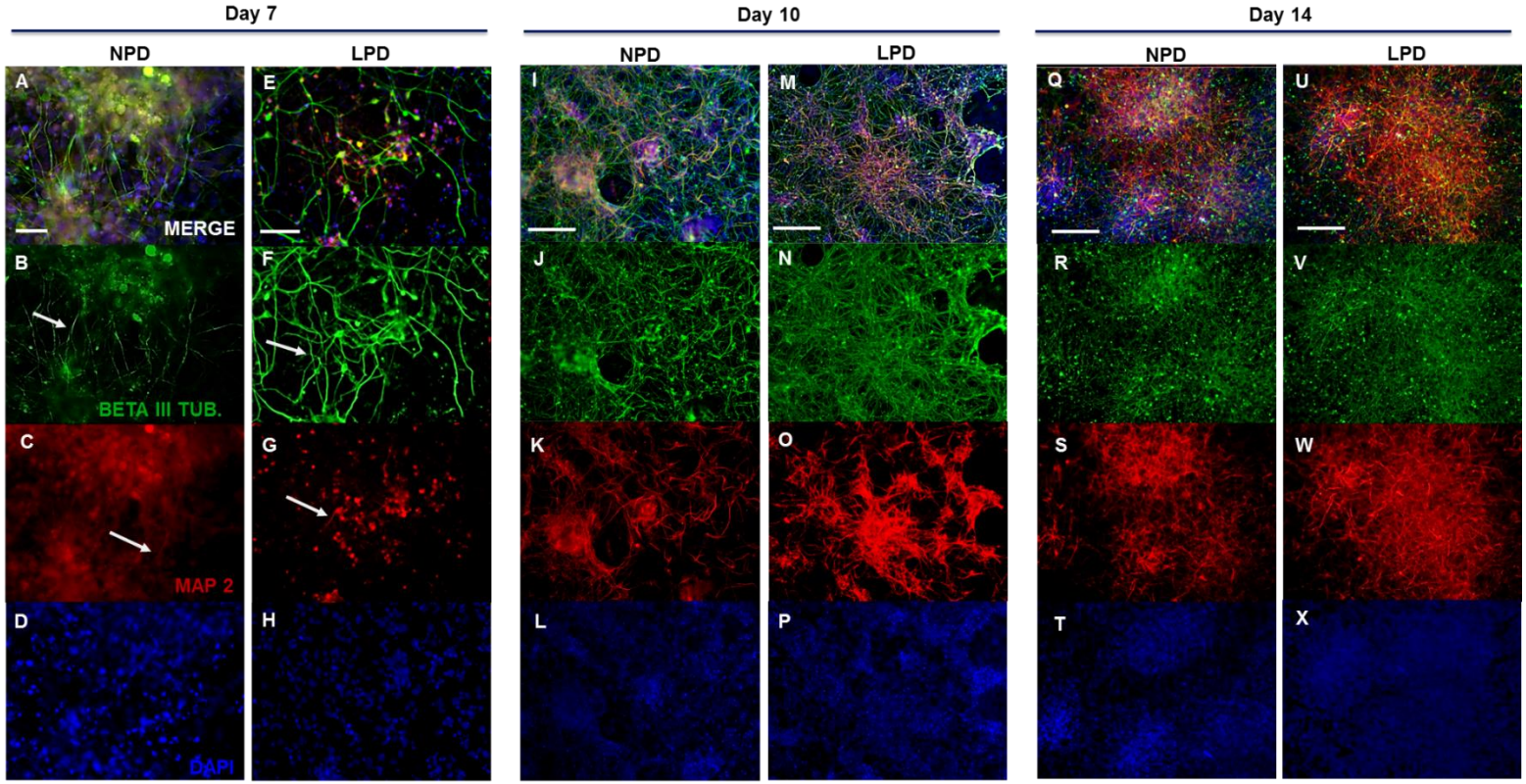

Figure 4.23 Representative images for mature neuron marker(s) expression: Beta III Tubulin (Green), Map 2 (Red) and Nuclear marker Dapi (Blue) at Day 7, 10 and 14 of NI.

NPD and LPD mESC lines (P16) were stained for Beta III Tub, Map 2 and Dapi under Standard NIM culture conditions. Arrows point to Beta III Tub (B, F) and Map 2 positive (C, G) cells at D7 of NI. Although an overall increase in expression was observed for both Beta III Tub and Map2 from D7 (B, F, C, G) to D14 (R, V, S, W) in both NPD and LPD cell lines, LPD lines showed increased number of cells positive for both markers at all time points. In addition, Beta III Tubulin had increased expression compared to Map2, most prominently at D7, but also observed on D10 and D14 of induction. Magnification for all images = 100 µm, except A-D, where magnification = 200 µm.

4.4 General Discussion

Part 1 of this study focussed on establishing a NI protocol for Southampton-derived NPD and LPD mESC lines. The NI protocol adopted initially was that established at Biotalentum Ltd (Klincumhom et al., 2012) which was optimised for the HM1 mESC line, that is cultured during the pluripotent phase in serum (ES-FBS). In contrast, the Southampton NPD and LPD mESC lines were derived and established under serum-free (KO/SR) conditions. Consequently, the established NI protocol at Biotalentum did not produce efficient NI results and thus required modification.

As cell density and cell-to-cell contact play a significant role in the growth, survival and NI of mESCs (Wongpaiboonwattana and Stavridis, 2015), the first aspect of optimisation focussed on finding an optimal cell density for efficient NI. From the three cell densities tested, i.e. low (12,500 cells/cm^2), moderate (25,000 cells/cm^2) and high (35,000 cells/cm^2), the low density showed least NI. Moderate and high densities on the other hand displayed (i) increased formation of rosettes and corresponding changes in gene expression including (ii) reduction of pluripotency and (iii) increase in both of NSC and mature-neuron markers. While changes in transcript expression were most prominent at moderate density, high-density culture showed maximum expression of protein neuron markers (established by immunocytochemistry). Consequently, an intermediate cell density of 28,500 cells/cm^2 was selected for subsequent experiments.

Density optimisation increased NI efficiency in both NPD and LPD mESC lines. However, it also initiated non-specific differentiation. As non-specific differentiation reduces NI (Marks et al., 2012), the second aspect of optimisation aimed at inhibiting the production of other-lineage cells by using small molecule inhibitors (SMIs) SB431542 and LDN193189 in advanced NI medium (A-NIM). Although the inclusion of SMIs reduced non-neural differentiation (i.e. decreased *Gata4* and *Brachyury* expression) they also suppressed NI (i.e. reduced rosettes and decreased NSC and mature neuron markers expression). Therefore, they were not adopted in the final NI protocol. Thus, NI protocol for NPD and LPD mESC lines was optimised with a plating cell density of 28,500 cells/cm^2 and standard NI medium without SMIs (S-NIM).

Part 2 of this study utilised this optimised NI protocol to perform a preliminary analysis of NI efficiency between NPD and LPD mESC lines. Given that the first aliquots from two mESC lines per treatment (initially cultured in KO/SR) did not thrive, the remaining two aliquots of same mESC lines were cultured in Biotalentum's ES-FBS conditions. Although ES-FBS increased cell proliferation, it also induced differentiation. For this reason, the remaining two NPD and LPD mESC lines were maintained exclusively in KO/SR conditions until NI. Figure 4.24 and 4.25 summarize the NPD-LPD mESC NI model, analysed characteristics and results presented in Chapter 4, in a schematic format.

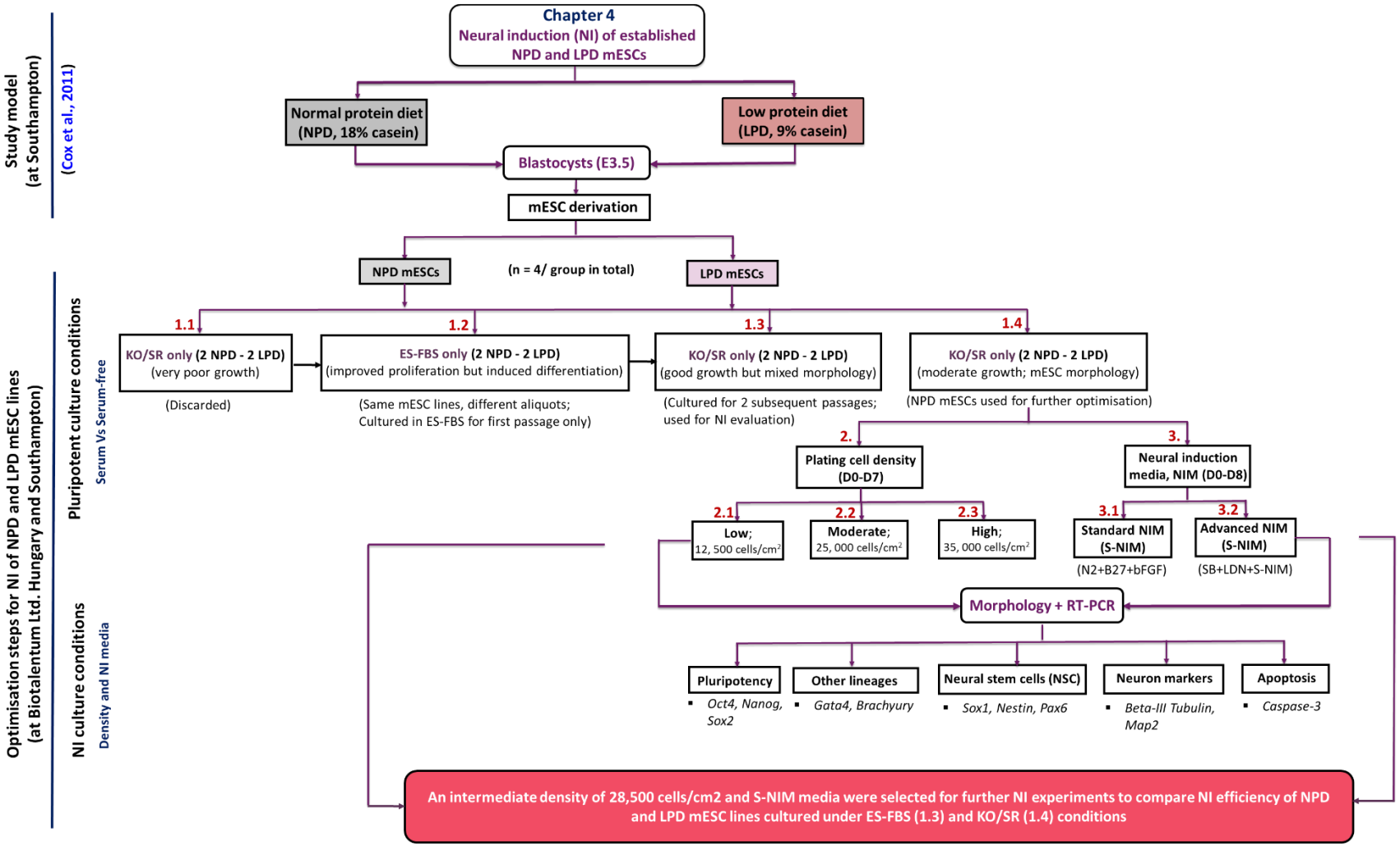

Figure 4.24 Flow diagram representing study layout and optimisation techniques from Chapter 4 of this thesis.

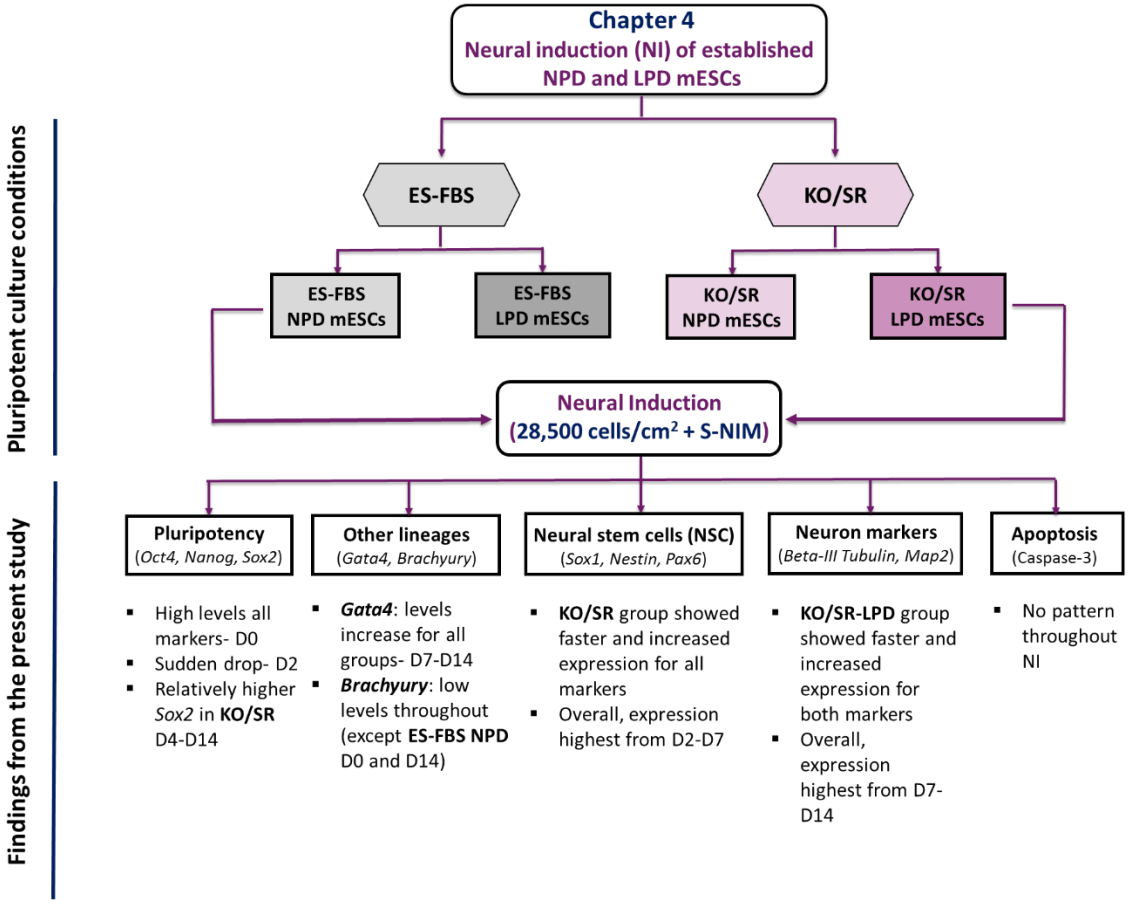

Figure 4.25 Flow diagram representing study findings from Chapter 4 of this thesis

4.4.1 Effect of serum on pluripotent mESCs

As an internal control, the HM1 mESC line was cultured alongside Southampton NPD and LPD mESC lines throughout the course of study. During culture, the two sets of pluripotent mESC lines (Southampton v HM1) displayed stark differences in cell survival after thawing, cell morphology and proliferation rate. While Southampton mESC lines showed increased cell death in the first passage after thawing, and round and tomb-like colony morphology, HM1 displayed better survival post thawing, a mix of round and flat colony morphology and increased cell proliferation compared to Southampton mESC lines (see Appendix B for representative HM1 images).

When Southampton NPD and LPD mESCs were cultured in ES-FBS, they underwent phenotypic changes and developed a flatter, sharp-edged colony morphology. Moreover, consistent with HM1's growth pattern, ES-FBS mESC lines also showed increased proliferation, compared to the KO/SR mESC lines. However, pluripotent mESC lines started differentiating just within 2 to 3 days under ES-FBS conditions. The differences between HM1 and Southampton ES-FBS and KO/SR mESC lines were not only limited to pluripotent phenotype, but also affected their NI efficiency. While HM1 mESC line showed optimal proliferation and NI efficiency with a low cell density (12,500

cells/cm^2), Southampton ES-FBS or KO/SR mESC lines could not cope and displayed increased cell death and very poor NI.

It is noteworthy, that Southampton mESC lines were transferred suddenly from KO/SR to ES-FBS conditions. In contrast, HM1 was continuously maintained in ES-FBS. Thus, the differentiation induced in ES-FBS NPD and LPD mESC lines could be a result of the sudden change in culture conditions. Moreover, it is known that undefined components in serum can not only influence plating efficiency, growth and induce spontaneous differentiation in pluripotent mESCs, but also limit their directed differentiation capacity, thereby reducing experimental reproducibility (Cheng et al., 2004; Silva and Smith, 2008; Tamm et al., 2013).

Although cellular heterogeneity is a hallmark of ESCs (Graf and Stadtfeld, 2008) and is constantly influenced by transcriptional noise and network fluctuation, heterogeneity plays a stochastic role in determining cellular fate (Chang et al., 2008). However, it has been shown that external culture systems can also affect cellular network variability (G. Guo et al., 2016). Single-cell RNA-seq and Chip-seq analyses revealed that undifferentiated mESCs cultured in the presence of serum showed a significant increase in heterogeneity with highly variable gene clusters and distinct chromatin states (i.e. bivalent genes), while serum-free cultures reduced heterogeneity and transcriptome variability. Serum-cultured mESCs were also observed to exit the naive ESC state and enter an intermediate primed state (G. Guo et al., 2016), thereby disrupting self-renewal and pluripotency mechanisms and cellular plasticity (Buecker and Geijsen, 2010). The fact that serum and serum-free cultured mESCs have distinct gene expression, and that serum cultures display more germ layer lineage-specific genes and less pluripotent genes compared to the serum-free cultures (Marks et al., 2012), further confirms that induction of lineage-specific genes in undifferentiated mESCs is enhanced by serum rather than by intrinsic factors.

4.4.2 Factors influencing NI efficiency

It is important to note that when mESCs are driven towards NI, two factors interplay, i.e. (i) cells experience a sudden withdrawal of LIF (a member of interleukin-6 cytokine family that maintains stemness in mESCs) and (ii) they are cultured with NI supplements. However, it is known that the pluripotent state of the cells can determine their differentiation fate (Marks et al., 2012; Wongpaiboonwattana and Stavridis, 2015). LIF removal alone induces rapid differentiation of serum-cultured mESCs to endoderm, mesoderm and to a lesser extent, to hematopoietic cell fate, whereas serum-free cultured mESCs do not form mesoderm and differentiate to neuroectoderm (Johansson and Wiles, 1995). This could be due to the heavy LIF dependence of serum cultures to maintain pluripotency and self-renewal that is not the case in serum-free cultures that inhibit MAPK

(Mitogen-activated protein kinases) and GSK3 (Glycogen synthase kinase-3), i.e. so called 2i media (Ohtsuka et al., 2015). In the current study, although LIF was immediately replaced by S-NIM to drive mESCs towards NI, it is possible that the ES-FBS mESC lines were already primed towards lineages other than neuroectoderm and thus showed poor NI efficiency compared to KO/SR mESC lines.

Secondly, the state of mESCs prior to induction can also determine their plating cell density, which in turn plays an important role in NI. In the current study, the HM1 and ES-FBS mESC lines displayed increased cell proliferation rate compared to KO/SR mESC lines, which then influenced their optimal plating density required for NI. Cell density is one of the most critical factors for neural induction, where very high density reduces differentiation efficiency and very low density induces excessive cell death (Wongpaiboonwattana and Stavridis, 2015), an observation also made in the current study. This could be due to the role of autocrine FGF4 (fibroblast growth factor 4) that stimulates MAPK signalling cascade and induces transition of pluripotent mESCs to lineage commitment (Kunath et al., 2007). Additionally, mESCs also secrete LIF, which activates STAT3 (Signal transducer and activator of transcription 3) to promote self-renewal (Niwa et al., 1998). NI supplements used in the current study, i.e. N2 and B27, although allowing survival of mESCs, are devoid of LIF and BMP4 that inhibit neural differentiation, and thus promote growth of neural cells (Ying et al., 2003). Thus, it is the critical balance between autocrine FGF4 and LIF that makes plating cell density a chief determinant of neural differentiation efficiency, where excessive cell density increases autocrine LIF and BMP4 inhibiting differentiation, whereas low cell density disrupts cell-cell contact and communication thereby impairing survival and differentiation (i.e. reduced FGF4) of mESCs.

Thirdly, based on the factors mentioned above, (i.e. state of mESCs before NI, cell survival rate and plating cell density), the timing of NI may also vary (Wongpaiboonwattana and Stavridis, 2015). In the current study, where NI was observed, rosette formation could be noticed as early as Day 2 of induction protocol. However, different mESC lines, even within the same treatment group, showed slight differences in the NSC and neuron marker expression, indicating a unique rate of NI in each cell line. Differences in functional and epigenetic states have also been observed across different colonies within the same ESC lines (Singh et al., 2007; Hayashi et al., 2008) arising due to heterogeneity existing within internal network of each unique mESC line. Therefore, if there are more naive mESCs within a cell line, it may take much longer to get primed and differentiate toward neural progenitors. On the other hand, if a cell line has mESCs that are already primed toward other lineages that would also influence the time it takes to achieve NI.

4.4.3 Alternative neural induction protocols

In the early years, protocols adopted aggregate cultures (i.e. embryoid body formation) in the presence of retinoic acid (RA) to differentiate mESCs to phenotypes associated with neurons (Bain et al., 1995) and glial cells (Fraichard et al., 1995). However, many of these protocols used serum, which limited their application (Stavridis and Smith, 2003). Protocols since have utilised serum-free, adherent-monolayer cultures with scalable and defined medium components, and focussed on generating pure populations of neural progenitors to increase differentiation efficiency in a short period of time (Ying et al., 2003; Ying and Smith, 2003). Given the beneficial role of RA in maintaining FGF signalling, and thus promoting neural differentiation, it is frequently used in 2D and 3D NI protocols. (Marios et al., 2010; Yang et al., 2017; Park et al., 2017). Other studies also utilize SMIs for more directed differentiation (Bian et al., 2016; Takayama et al., 2017), although the type, duration, combination and concentration of these molecules have a huge impact on differentiation efficiency. The current study used the combined effect of SB431542 and LDN193189 to promote NI, although when used alone, SB431542 inhibits differentiation and maintains pluripotency in mESCs (Du et al., 2014). Though biomolecules significantly influence neural differentiation ability of mESCs, external factors like local cell concentration and vessel type (of culture dish), also play an important role (Wongpaiboonwattana and Stavridis, 2015).

4.4.4 Effect of LPD on neural induction (NI)

It is noteworthy that analysis conducted in the current study is based on a limited number of replicates and therefore, observations could not be confirmed statistically. However, suggestive differences indicated that LPD lines appeared to undergo faster (appearance of rosettes) and increased NI compared to NPD lines. They displayed higher and protracted transcript and protein (by qualitative immunocytochemistry) expression for both immature (Beta III Tubulin) and mature neurons (Map2). The preliminary data appear to be congruent with our recent *in vivo* findings that maternal LPD (for E3.5 at 9% casein, i.e. similar to the current study) increased the number of late neural progenitors and early neurons in the ganglionic eminences and cortex of the fetal brain (Gould et al., 2018). Additionally, maternal LPD fetal brain samples showed increased apoptosis, a feature also observed in the undifferentiated LPD mESC lines (by a former PhD student) (Cox et al., 2011).

Interestingly in the present study, similar to differentiating LPD lines, mature neuron expression (*Map2*) was also observed to be higher in undifferentiated LPD mESC lines compared to NPD mESC lines. Moreover, LPD mESC lines also displayed reduced pluripotent transcript expression, which could suggest priming of undifferentiated LPD mESC lines towards neural lineage differentiation.

As a response to poor nutritional environment induced by maternal LPD, blastocysts show reduced mTOR signalling (Eckert et al., 2012b). This may be reflective of poor derivation of LPD mESC lines from LPD blastocysts, and decreased proliferation rates and increased phosphorylated ERK (endoplasmic reticulum kinase) signalling of the derived LPD mESC lines (Cox et al., 2011), findings consistent with less number of neurospheres and reduced proliferation (Ki67) derived from maternal LPD fetal brain samples (Gould et al., 2018).

Together, previous pluripotent LPD mESC data (Cox et al., 2011) and preliminary findings of the present study indicate that maternal LPD (E3.5) can have an impact on the derivation, pluripotency, proliferation, survival and neural lineage differentiation of derived mESCs. Whilst *in vivo* studies show a correlation between maternal LPD, increased rate of neural differentiation in fetal brains and behavioural defects in offspring (Watkins et al., 2008b; Gould et al., 2018), *in vitro* LPD mESC studies require increased replication to validate the findings from the current study and to perform in-depth analysis using electrophysiology, to test the neural activity and thus functionality of the derived neurons.

4.4.5 Conclusions

In the current study, the optimised NI protocol used a moderate cell density (28,500 cells/cm^2) under serum-free conditions using defined NI supplements N2, B27 and bFGF, in an adherent monolayer culture. The protocol induced efficient NI, developing neural rosettes and progenitors as early as Day 2-3 and neurons between Day 5 to Day 7. Interestingly, within KO/SR cultures, preliminary findings suggested faster, increased and protracted NI in LPD lines compared to NPD lines, while no differences were observed within ES-FBS NPD-LPD lines. However, as the current study was only replicated twice, it will be necessary to repeat these experiments with KO/SR cultures in order to validate these preliminary findings.

Although the optimised protocol with KO/SR increased NI efficiency, it also led to the development of other lineage cells. Whilst the use of SMIs successfully inhibited mesodermal and endodermal differentiation, they also compromised NI. Therefore, effects of alternative SMIs like noggin, dorsomorphin or LDN193189 alone, at different concentrations and combinations, and for different durations of exposure, should be evaluated.

The current NI protocol focussed on selective NSC and neuron markers. However, during NI of heterogeneous mESCs, additional neural cell populations, such as neural crests, more mature neurons (i.e. cortical or motor) and glial cells may also have developed. Therefore, increasing the range of neural markers could help determine the efficiency and specificity of NI protocol. In conclusion, the current study demonstrated that serum reduces efficiency of NI, highlighted the

importance of plating density on cell survival and NI, and identified putative differences in the rate of NI between NPD and LPD mESC lines.

Chapter 5 General discussion

Operating within the framework of the 'Developmental Origins of Health and Disease (DOHaD)' hypothesis, a number of human and animal studies have, in recent years, demonstrated that maternal factors, such as advanced reproductive age and malnutrition, can induce changes in the early embryo that have long-lasting consequences for the health and wellbeing of offspring (Watkins et al., 2008; Wadhwa et al., 2009; De Oliveira et al., 2012; Padmanabhan et al., 2016; Velazquez et al., 2016). Collectively, these studies indicate that the mammalian preimplantation period is perhaps the most critical stage of development. As preimplantation embryo consists of two distinct cell populations of pluripotent ICM and placenta forming-TE cells, programming events occurring at this stage have a direct and long lasting impact on cell lineage formation. It has therefore, been postulated that ESCs derived from the ICM could mediate developmental programming events experienced by the embryo from its initial formation as a zygote until blastocyst formation (i.e. E0.5-E3.5 in mice). Moreover, previous studies from Southampton found that mESCs and derived EBs propagated the effects of maternal-undernutrition (i.e. low protein diet, LPD) induced changes in the E3.5 embryo, even after a protracted period of *in vitro* culture.

5.1 Key findings emerging from this thesis

Based on aforementioned research, the current study investigated the impact of two maternal factors, that is advanced maternal age (AMA; Young, 7-8 weeks vs Old, 7-8 months) and normal or low protein diet (i.e. NPD, 18% casein vs LPD, 9% casein) on mESC lines derived from E3.5 blastocysts. Key findings from the AMA study indicated that advanced reproductive age impaired embryo development, and reduced the proliferative capacity and viability of derived ESCs, which also exhibited an increased incidence of aneuploidy. Glycolysis and fatty acid metabolism was altered in derived LPD mESC lines, and preliminary analyses indicated precocious onset of neural differentiation in these cells.

5.2 Preimplantation development

The programming effects observed may depend on the nature, extent and duration of maternal insult, and can vary between studies. For example, while AMA was associated with delayed embryonic development, the LPD induced greater alterations in cell number within the ICM and TE of E3.5 blastocysts in the current series of experiments. In contrast, Cox et al. (2011) found no diet-induced differences in embryo development. However, AMA is associated with fewer implantation sites and a higher number of resorption sites (Care et al.,

2015). Chromosomal abnormalities in oocytes and embryos are increased in embryos from older mothers (Eichenlaub-Ritter, 2002; Atala, 2012), and in humans, delayed implantation is linked to reduced levels of hCG (Jukic et al., 2011); a hormone secreted by trophoblast cells of the early embryo (Zeleznik and Pohl, 2006). Lower levels of this hormone are observed in ectopic pregnancies (Seeber et al., 2006) and pregnancy loss (Chung and Allen, 2008). Although blastocyst development was reduced in the current study, no differences were observed in the derivation efficiency of mESC lines between Young and Old dams. This is in line with a similar number of ICM cells in E3.5 blastocysts between age groups (M. A. Velazquez et al., 2016). Maternal LPD on the other hand, has been shown to enhance proliferation of TE cells in the pre- and post-implantation embryo; possibly as a compensatory response to increase nutrient supply and regulate fetal growth. A concomitant reduction in the number of ICM cells could explain the reduced derivation efficiency of LPD mESC lines compared to NPD mESC lines.

mESC lines derived from embryos of old dams displayed higher rates of aneuploidy compared to those of young dams. Chromosomal abnormalities were not observed in LPD mESC lines (Cox et al., 2011). Aneuploidy was higher in female than male mESC lines derived from embryos of old dams. This sex-related effect on aneuploidy could explain reduced viability in female mESC lines. A similar sex-bias in adverse offspring phenotype was also observed in the aged-dam study of Velazquez et al. (2016). In contrast, human studies suggest that the consequences of stress induced by increased maternal age are more apparent in male than female fetuses (Rueness et al., 2012).

5.3 Programmed cell death

One of the mechanisms associated with AMA-induced reduction in oocyte quality (Alikani et al., 1999), and increased rate of blastocyst fragmentation, is programmed cell death (PCD) or apoptosis (Jurisicova et al., 1998). Apoptosis is characterized by distinct morphological characteristics and energy-dependent mechanisms (Elmore, 2007) and is a vital component of processes such as normal cell turnover, development and functioning of the immune system, embryonic development and stress-induced cell death. While it is a normal and an essential process in cell development and survival, different stress stimuli determine if cells die by apoptosis or necrosis. In the course of development, PCD occurs in the ICM of a healthy blastocyst during the transition from early (when ICM has the potential to make trophectoderm) to late (when the ICM lacks the potential to make trophectoderm) blastocyst stage. It is thus postulated that PCD is designed to eliminate redundant ICM cells with trophectodermal potential and that the mechanism is mediated by epigenetic factors (Handyside and Hunter, 1986; Pierce et al., 1989). Hence

maintaining a regulated level of cell death is crucial for the survival and developmental potential of the blastocyst. However, the rate of apoptosis increases with maternal age (Igarashi et al., 2015).

In the present study, cell death and necrosis was greater in 'Old male' mESC lines, which were also less proliferative, compared to 'Young male' mESC lines. Within the old group, the proportion of apoptotic and necrotic cells was greater in Female than Male mESCs. Women carrying chromosomally abnormal embryos show a 2.5-fold increase in apoptosis compared to those with normal embryos (Kolialexi et al., 2001). This observation is consistent with the increased incidence of apoptosis in 'Old Female' mESC lines, which had a higher degree of aneuploidy than 'Old Male' mESC lines. These processes are coordinated and often energy-dependent, whereby they activate a group of cysteine proteases called caspases, although no differences were observed in the transcript levels of *Caspase 3* in 'Old vs Young' mESC lines in the current studies.

The current study with AMA mESC lines did not explore further the potential mechanisms that could have triggered PCD. However, increased levels of basal apoptosis in LPD mESC lines were associated with reduced signalling of phosphorylated ERK (Extracellular signal-regulated protein kinases 1 and 2) (Cox et al., 2011) which is a member of MAPK (mitogen-activated protein kinase) superfamily and mediates cell proliferation and apoptosis (Mebratu and Tesfaigzi, 2009). However, reduced ERK signalling observed in LPD mESC lines was independent of PI3K/ AKT, and JAK/ Stat survival pathways and stress-activated p38-MAPK signalling (Cox et al., 2011), which suggests a decrease in survival, rather than an increase in apoptosis, as the primary cause of increased cell death in the LPD mESC lines.

5.4 Cell metabolism

Metabolomic analysis in Chapter 3 hinted at altered glucose flux through glycolysis between LPD and NPD mESC lines. Deviations between the two treatment groups revolved around phosphofructokinase 1 and 2 (PFK1 and 2), key allosteric regulators of glycolysis and enzymes whose activity are determined by prevailing levels of ATP and ADP, down-stream metabolites, (i.e. phosphoenolpyruvic acid and citrate) (Berg et al., 2002) and, indirectly, by insulin and glucagon (Pilkis et al., 1982; Silva et al., 2004). A clear biological interpretation of glycolytic differences between NPD and LPD mESC lines, however, is difficult with the available data, but the findings may represent a legacy of differences in circulating glucose and insulin concentrations in embryo donors. Blood glucose concentrations in fed NPD and LPD dams differ at E3.5, and are typically around 11 and 13 mmol/l respectively (Eckert et al., 2012a). These levels are toward the upper limit of euglycaemia in this species. The elevation in blood glucose in LPD dams probably arises as a consequence of reduced blood BCAAs and insulin, and increased sucrose in LPDs (Appendix A,

Table1). Furthermore, maternal LPD disrupts insulin sensitivity in the mouse embryo, by altering the mTOR signalling (Eckert et al., 2012a).

Importantly, derivation, establishment and culture of mESCs requires pluripotent embryonic cells to adapt to considerably higher glucose concentrations (25 mmol/l) which are a feature of standard Knockout DMEM. However, mESCs cultured in the presence of physiological levels of glucose (~5 mmol/l) express similar Glut2 receptor activity as observed the in vivo blastocyst, whereas high glucose concentrations (25 mM) increase oxidative stress and inhibit *Pax3* expression (Jung et al., 2013). Furthermore, 25 mM glucose in culture medium induces cell senescence in rat mesenchymal stem cells, while its reduction (to around 1.4 mmol/l) enhances cell proliferation, decreases apoptosis and increases colony-forming units (Stolzing et al., 2006). The foregoing discussion is important, because these levels of glucose are not representative of those found in either LPD or NPD dams during gestation, so that the nature of metabolic adaptation of pluripotent ESCs reported in this thesis may differ from that experience by ICM cells within the blastocyst during implantation *in vivo*.

Similar to the discussion above, KnockOut DMEM and KO/SR each contain varying quantities of essential and non-essential amino acids (AAs), some of which are included at non-physiological levels (Appendix A). This could account for the fact that, apart from asparagine, AA levels in mESCs did not differ between treatment groups.

5.4.1 Fatty acids and neurogenesis

Chapter 3 demonstrated that fatty acid (FA) levels were generally greater in mESC lines derived from embryos of LPD fed dams. This was the case for medium to long chain saturated, monounsaturated and polyunsaturated FAs. It is not readily apparent why this should be the case. The primary source of FAs in blastocysts from which these lines were derived was maize oil present in maternal diet; and this was similar for both NPDs and LPDs. Similarly, the primary source of FAs during stem-cell derivation was KO/SR, which contains lipid-rich albumin, the FA composition of which is not disclosed. Again, this will have been similar for both dietary treatment groups. Given the importance of PUFAs (particularly n-3 PUFAs) in neurogenesis (Beltz et al., 2007; Vaca et al., 2008), however, these observations could have contributed to the findings reported in Chapter 4. Preliminary findings from that chapter showed LPD mESC lines to have increased neural induction (NI) efficiency compared to NPD mESC lines. Increased efficiency was demonstrated by faster rosette and neurite development in the LPD mESC lines, in addition to rapid and protracted NSC and neuron marker expression. It is well established that FAs have an important function in neural development. For example, eicosanoids, especially DHA (docosahexaenoic, C22:6, n-3) enhances

survival, proliferation and differentiation of neural stem cells (NSCs) (Beltz et al., 2007; Vaca et al., 2008). This is achieved by regulating Hes1 and/or Hes6 pathways (Katakura et al., 2009; 2013), and by promoting neuritogenesis (characterised by increased neurite length, neurite number and number of neurite branches) (Vaca et al., 2008); features observed and reported in Chapter 4 (although lacking statistical validation).

On first inspection, these findings seem to be at odds with previous reports on the effects of LPDs, FA metabolism and neurogenesis. For example, maternal LPD fed throughout gestation reduced levels of n-3 PUFAs (Torres et al., 2010) and induced neurodevelopmental abnormalities in offspring (Mathieu et al., 2008; Levant, 2013; Maekawa et al., 2017). Most recently, a maternal LPD (until E3.5, followed by NPD throughout the remainder of gestation) reduced the population of NSC in the fetal brain, which subsequently underwent enhanced neural differentiation, followed by signs of short-term memory loss in offspring (Gould et al., 2018). Accepting the preliminary nature of findings reported in Chapter 4, there are two important differences between the studies cited above and those reported in this thesis. Firstly, studies undertaken in Chapters 3 and 4 measured responses in pluripotent mESCs and mESCs undergoing neural induction (corresponding approximately to a developmental period spanning E3.5 to E12). Consequently, findings reported in the current thesis pertain to an earlier period of embryonic development than has been studied previously. Secondly, studies reported in the current thesis were undertaken entirely *in vitro*, using KO/SR supplemented DMEM, the non-declared metabolite composition of which will inevitably differ from that of the poorly defined *in utero* environment.

5.5 Future directions

Within the AMA studies, mESC lines derived from Old dams displayed sexual dimorphism, where Female mESC lines had adverse phenotype compared to Male mESC lines. As Young dams gave rise to only one Female mESC line, this restricted age-related comparison of the Female mESC lines, and thus requires derivation and establishment of additional mESC lines from Young dams. It is also necessary to repeat and confirm the findings of apoptotic mechanisms by other methods. As maternal reproductive ageing increases the incidence of oxidative stress, mitochondrial dysfunction and DNA-damage, Male and Female AMA mESC lines should be analysed for reactive oxygen species (ROS), mitochondrial membrane potential and DNA-fragmentation by (Poly (ADP-ribose) Polymerase (PARP) assays. Additionally, for mechanistic analysis, it is important to evaluate if mESC lines from Old dams exhibit increased cell death due to reduced survival ability or because of increased expression of pro-apoptotic factors. This could be determined by analysing ERK activity and real-time PCR for an array of apoptotic genes.

Given the indeterminate nature of outliers observed in the PFK activity assay of mESC lines derived from dams fed either NPD or LPD, it will be necessary to repeat the PFK and BCA assays with fresh lysate samples.

In order to compare differences between neural induction (NI) of NPD and LPD mESC lines efficiently, it is first required to characterise the *in vitro* process of NI, using at least three mESC lines from both dietary groups. While the heterogeneous nature of mESCs would inevitably produce cell populations that express different markers even within the same colony, characterising the process would provide a better estimate to gauge the degree of variation(s) of specific markers with the progression of NI protocol (i.e. Day 0 until Day 14), both within and between the dietary groups. Doing this may also assist in comparing *in vitro* NI to the initial stages of neurogenesis *in vivo*. The preliminary findings reported in the current study need to be validated statistically by repeating the experiments (following the optimised NI protocol) with an increased number of replicates. Given that the effects of LPD on neurodevelopmental programming of ICM cells is largely unknown; neural lineages other than neurons, such as glial, astrocytes and oligodendrocytes should also be investigated.

While AMA is strongly associated with increased risks of neurodevelopmental disorders in offspring, the biological mechanisms responsible are not clearly understood. In the present study, Old dams had delayed embryo development, and displayed increased aneuploidy and apoptosis in derived mESC lines. However, these outcomes do not address the factors leading to such disorders. Thus, a well-characterised NI system for NPD-LPD mESC lines could be tested and incorporated in an AMA study to assess the effects of maternal age on NI efficiency of derived Male and Female mESC lines.

In addition to dietary effects, increased levels of upstream glycolytic metabolites in NPD and LPD mESC lines could have also been influenced by the presence of high-glucose concentration in mESC medium (i.e. Knockout DMEM). Thus, to minimise confounding factors, NPD and LPD mESC lines need to be derived and established in culture medium containing metabolites (such as glucose, AAs, vitamins and PUFAs) at levels similar to their physiological concentrations *in vivo.* Culturing mESCs under these conditions would enhance similarity between metabolic environments of the *in vitro* mESC lines and the *in vivo* blastocyst. Furthermore, it would make the NI model of NPD-LPD mESC lines more comparable with *in vivo* neural differentiation studies (Gould et al., 2018).

The field of developmental biology is based on the intriguing abilities of genetically distinct cells, i.e. the male and female gametes, to combine and to form an embryo with pre-programmed characteristics and functions that determine its' developmental fate throughout conception and into adulthood (Tom P. Fleming et al., 2015). These remarkable events can

partly be explained by the instructive epigenetic marks possessed by these cells, which, during fertilization and early development are reprogrammed distinctively and passed on to the embryo for the acquisition of totipotency and zygotic genome activation (ZGA). Previous studies have demonstrated that germ cells and the preimplantation embryo undergo significant epigenetic remodelling (Santos et al., 2002), yet the limited number of cell material derived restricts the potential of such studies. Moreover, maternal environment such as undernutrition and advanced reproductive age during periconceptional programming, also influence the transcriptome and epigenome of the developing embryo, which have been associated with disease phenotypes in later life. To address the issues of limited cellular material and complying with the principles of 3Rs (i.e. Replacement, Reduction and Refinement) of research, the current study utilised the pluripotent ability of ICM of blastocysts from maternal reproductive ageing and protein restriction models to study their effects on mESCs.

Innate characteristics such as self-renewal, broad range of differentiation capacity, relatively homogeneous cultures with an ability to maintain uncommitted cell-population for an extended period, while sustaining a stable karyotype, indeed make *in vitro* ESC model a lucrative alternative to *in vivo* animal-based research. When reintroduced in early embryos, ESCs generate into embryogenesis and are present in the resulting differentiated cell types, thus making them an important tool for genetic engineering via homologous recombination. However, data generated from these highly potent cells require thorough validation to draw parallels between the two (i.e. *in vitro* and *in vivo*) model systems. One of the most revolutionising advances in the field of developmental biology has been the introduction of next generation sequencing for epigenetic profiling. Until recently, these techniques required millions of cells, which has now been drastically scaled down to 100-200 cells. Refinements in DNA methylation techniques such as 'bisulphite conversion followed by sequencing', and the development of post bisulphite-adaptor tagging (PBAT) and reduced representation bisulphite (RRBS) sequencing allow generation of high-resolution genomic maps and DNA methylation assessments even on a single-cell level (Smallwood and Kelsey, 2012). Such advances could assist direct comparisons of the epigenetic marks (or memory) induced by maternal environment (such as AMA or LPD) that is experienced by the individual ICM and TE cells of the blastocyst and thus the derived stem cells.

During implantation, the embryo undergoes widespread morphological and epigenetic programming. Lineage specification is accompanied by *de novo* acquisition of repressive DNA methylation and histone (H3K9me2 and H3K27me3) modification (Okano et al., 1999; Zylicz et al., 2015; Zheng et al., 2016), genetic ablation of which, cause developmental abnormalities

and lethality in mid-gestation mice (Tachibana et al., 2002). During differentiation, histone modifications (H2K27ac) regulate enhancer-promoter interactions inducing target genes, thus controlling cell fate transitions (Wang et al., 2016; Rubin et al., 2017). However, findings thus far, suggest that epigenetic modifications at this stage, 'reinforce' lineage commitment rather than 'direct' it, indicating an early programming of molecular hierarchy for gene regulation. These studies further highlight the importance of understanding the events occurring during the critical window of preimplantation period.

In vitro differentiation capacity of ESCs therefore provides a unique opportunity for evaluating gene regulation and its functional effect on early cell/ lineage commitment and differentiation during embryonic development, and its interaction with alterations (if any) due to maternal environment (Keller, 1995). Generation of embryo-like EBs (that are derivatives of three embryonic germ layers) in suspension cultures, is another example of the unique ability of ESCs to maintain transient cell populations *in vitro* (Rohwedel et al., 1996), providing a unique window to study gastrulation (pluripotent, multipotent and differentiating cells), similar to the *in vivo* embryo. Additionally, comparisons of epigenetic modifications of pluripotent mESC lines (for eg. from AMA and LPD models) and derived cell lineages would offer insights into the epigenetic basis of developmental programming. As pluripotent mESCs are derived from the post-global demethylation stage of blastocyst development, differentiated cell lines may be better candidates for such studies. Utilisation of stem cell technology not only gives a platform for advancement in developmental biology, but also serves as a robust model system for cell replacement strategies in disease management. Moreover, characteristics and differentiation potential of somatic stem cells derived from maternal/ offspring tissues could further add to the understanding of similarities and unique differences between the physiological and *in vitro* derived cell types, and the associated variations in their respective epigenetic and genetic profiles. Thus, further investigation of novel regulatory mechanisms would be very helpful in bridging the gaps between our understanding of epigenetic information transferred to the gametes, the early embryo, the derived mESCs, and their influence on pregnancy and health of the offspring in adulthood. However, it is imperative to appreciate that although mESCs are derived from the ICM of *in vivo* blastocyst, *in vitro* handling and culturing does induce significant alterations in their physiological and epigenetic profile, therefore making it essential to understand, not only the similarities, but also the acquired dissimilarities of the two model systems.

5.6 Conclusions

The current series of studies established mESC lines as *in vitro* model to analyse effects of AMA and maternal LPD. Observations represent alterations in embryo development beyond the preimplantation period and prior to post-implantation and lineage allocation stage, *in vivo*. Overall, advanced reproductive age delayed blastocyst development, and increased aneuploidy and cell death in derived mESC lines; whereas maternal LPD altered glucose and fatty acid metabolism, and appeared to induce faster and more efficient neural induction compared to the NPD group. These findings are indicative of the ability of derived mESC lines to propagate phenotypic and metabolic memories *in vitro.*

Appendix A Media and Diet Composition

Embryo Media 1: H6-BSA

Stock B (stored at 4-8C for up to 2 weeks)	
Deionised water, sterile	10 ml
Sodium hydrogen carbonate (NaHCO3)	0.2106 g
Stock E (stored at 4-8C for up to 3 months)	
Deionised water, sterile	50 ml
Hepes	2.9785 g
Stock F (stored at 4-8C for up to 3 months)	
Sodium chloride (NaCl)	4.720 g
Potassium Chloride (KCL)	0.110 g
Sodium dihydrogen orthophosphate (NaH2PO4.2H2O)	0.060 g
Magnesium chloride (MgCl2)	0.100 g
D-glucose	1.000 g
DL-lactic acid	3.4 ml
Deionised water	Made up to 100 ml
Stock G (stored at 4-8C for up to 2 weeks)	
Deionised water, sterile	10 ml
Pyruvic acid	0.030 g
Penicillin	0.060 g
Streptomycin	0.050 g
Stock H (stored at 4-8C for up to 3 months)	
Deionised water, sterile	10 ml
Calcium chloride dehydrate (CaCl2.2H2O)	0.260 g
20% Sodium Chloride	
Deionised water, sterile	10 ml
Sodium Chloride (NaCl)	2.0 g
To prepare 100 ml of H6-BSA:	
Deionised water, sterile	78 ml
Stock B	1.6 ml
Stock E	8.4 ml
Stock F	10 ml
Stock G	1.0 ml
Stock H	1.0 ml
20% NaCl	0.6 ml
BSA (Sigma, embryo culture tested, A3311)	0.4 g
pH adjusted to 7.4; osmolarity adjusted to 270-280 mOsm; sterile filtered (0.22 µM filter); aliquots stored at 4ºC.	

Embryo Media 2: KSOM culture medium

2x stock KSOM	
Sodium chloride (NaCl)	1.110 g
Potassium chloride (KCl)	0.0095 g
Magnesium sulphate7-hydrate (MgSO4.7H2O)	0.0099 g
Lactic acid	0.362 ml
Sodium pyruvate	0.0044 g
Glucose	0.0072 g
Sodium bicarbonate (NaHCO3)	0.420 g
Penicillin	0.01256 g
Streptomycin	1 ml
EDTA	4 ml
Tissue culturegrade water	Made up to 100 ml
5 ml aliquots stored at -80ºC for up to 2 months.	
1 x KSOM (10ml) **The following was added to 5 ml of thawed 2x KSOM stock:**	
Calcium chloride (CaCl2; 100x stock 25 mg/ml	100 µl
Non-essential amino acids (100x stock; 10 mM)	50 µl
Essential amino acids (50 x stock)	100 µl
L-glutamine (200 mM)	50 µl
Deionised water, sterile	4.75 ml
BSA	0.040 g
Sterile filtered (0.22 µm filter); osmolarity adjusted to 255 ± 5 mOsm with 20% NaCl; aliquots stored at 4ºC for up to 1 week.	

mESC culture media 1: KnockOut™ DMEM- 10829018, Gibco

KnockOut™ DMEM (with high glucose)	Concentration (g/L)
Inorganic Salts	
Calcium Chloride	0.2
Ferric Nitrate • $9H_2O$	0.0001
Magnesium Sulfate (anhydrous)	0.09767
Potassium Chloride	0.4
Sodium Bicarbonate	3.7
Sodium Chloride	6.4
Sodium Phosphate Monobasic (anhydrous)	0.109
Amino Acids	
L-Arginine • HCl	0.084
L-Cystine • 2HCl	—
Glycine	0.03
L-Histidine • HCl • H_2O	0.042
L-Isoleucine	0.105
L-Leucine	0.105
L-Lysine • HCl	1.46
L-Methionine	—
L-Phenylalanine	0.066
L-Serine	0.042
L-Threonine	0.095
L-Tryptophan	0.016
L-Tyrosine • 2Na •$2H_2O$	0.12037
L-Valine	0.094
Vitamins	
Choline Chloride	0.004
Folic Acid	0.004
myo-Inositol	0.0072
Niacinamide	0.004
D-Pantothenic Acid (hemicalcium)	0.004
Pyridoxal • HCl	—
Pyridoxine • HCl	0.004
Riboflavin	0.0004
Thiamine • HCl	0.004
Other	
D-Glucose	4.5
Phenol Red • Na	0.0159
Pyruvic Acid • Na	0.11

mESC culture media 2: KnockOut Serum Replacement

Amino Acids	Glycine, L-histidine, L-isoleucine, L-methionine, L-phenylalanine, L-proline, L-hydroxyproline, L-serine, L-threonine, L-tryptophan, L-tyrosine, L-valine
Vitamins/Antioxidants	Thiamine, reduced glutathione, ascorbic acid 2-PO4
Trace Elements	Ag^{+}, $Al3^{+}$, Ba^{2+}, Cd^{2+}, Co^{2+}, Cr^{3+}, Ge^{4+}, Se^{4+}, Br^{-}, I^{-}, F^{-}, Mn^{2+}, Si^{4+}, V^{5+}, Mo^{6+}, Ni^{2+}, Rb^{+}, Sn^{2+}, Zr^{4+}
Proteins	Transferrin (iron-saturated), insulin, **lipid-rich albumin (AlbuMAX**)

NPD and LPD Diet Composition

Appendix A. Table 1 Composition of isocaloric experimental (LPD) and control (NPD) diets

Diet Constituents	LPD (9% casein; g/kg)	NPD (18% casein; g/kg)
Casein	90	180
Starch Maize	485	425
Cellulose	50	50
Sucrose	243	213
Choline chloride	2	2
DL-Methionine	5	5
AIN-76 mineral mix1	20	20
AIN-76 vitamin mix2	5	5
Corn oil	100	100
Gross Energy, MJ/kg	18.27	18.39

Appendix B Supplementary Figures

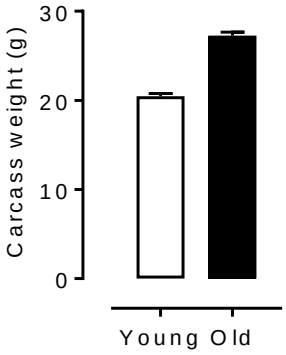

Appendix B. Figure 1 Carcass weight of Young (7-8 weeks) v Old (7-8 months) dams at E3.5

Carcasses were weighed after retrieving embryos at E3.5. Old dams weighed significantly more than Young dams ($P < 0.0001$). Data presented as means ± SEMs based on n = 18.

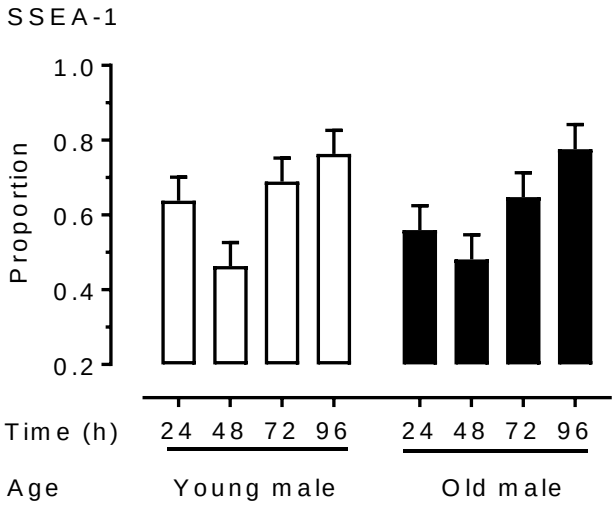

Appendix B. Figure 2 Effect of time on protein expression of pluripotency surface marker, SSEA-1, in undifferentiated male (young (7-8 weeks) vs old (7-8 months)) ES lines.

mESCs (100,000 cells/well) from AMA groups were cultured (in duplicates) on gelatin (0.01%) coated 6-well dishes, pre-seeded with 135,000 cells/well MMC-MEFs. ES cells were selected from a combined mESC and MEF population of cells using a pluripotency surface marker, SSEA-1. Adhered cells were trypsinized, centrifuged and divided into two categories, i.e., stained with SSEA-1 and unstained cells, at 24h intervals over a period of 96h. Samples were analysed by flow cytometry. Marker expressions were calculated using FlowJo software and are displayed as the proportion positive of total cells (stained and unstained cells). Both young and old ES lines showed differences in SSEA-1 expression with time ($P<0.001$), with a sudden drop in expression at 48h. Data presented as means ± SEMs based on n = 4.

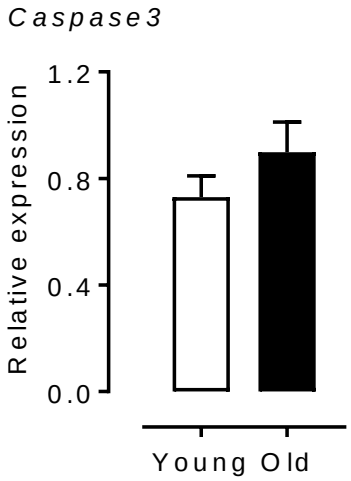

Appendix B. Figure 3 Relative gene expression for cell apoptosis marker in undifferentiated male (young (7-8 weeks) vs old (7-8 months)) mESC lines.

Real-time PCR analysis of cell apoptosis marker, *Caspase 3*. Gene of interest was normalized to *Ywhaz* and *Rpl13a* within geNorm. No difference was observed between AMA groups. Data presented as means ± SEMs based on n = 4.

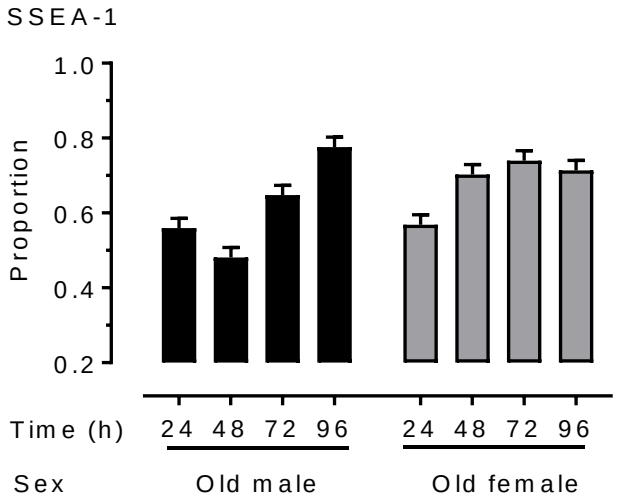

Appendix B. Figure 4 Effect of time on protein expression of pluripotency surface marker, SSEA-1, in undifferentiated old ((7-8 months) male vs female) ES lines.

mESCs were cultured in duplicate. Adhered cells were trypsinized, centrifuged and divided into two categories, i.e. stained with SSEA-1 and unstained cells. Old male ES lines showed differences in SSEA-1 expression ($P=0.02$) compared to Old Female ES lines. Both Old Male and Old Female ES lines showed differences in SSEA-1 expression over time ($P<0.001$). Changes in SSEA-1 expression were observed at 48h ($P<0.001$). Data presented as means ± SEMs based on n = 4.

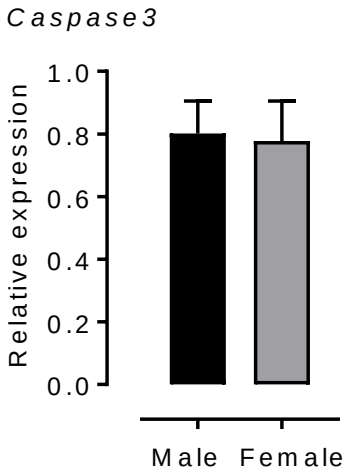

Appendix B. Figure 5 Relative gene expression for cell apoptosis marker in undifferentiated old ((7-8 months) male vs female) mESC lines.

Real-time PCR analysis of cell apoptosis marker, *Caspase 3*. Gene of interest was normalized to *Ywhaz* and *Rpl13a* within geNorm. No difference was observed between AMA groups. Data presented as means ± SEMs based on n = 4.

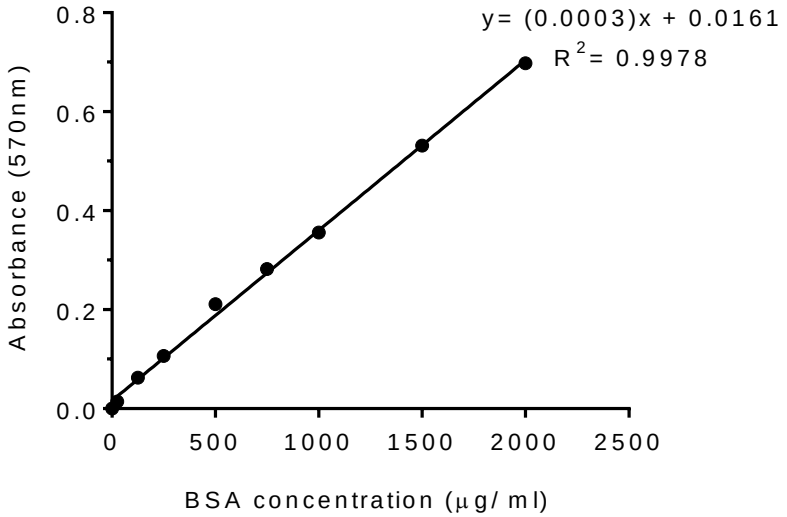

Appendix B. Figure 6 BSA Standard Curve at 570 nm absorbance.

Background corrected standards were plotted on a graph and the linear equation (y= (a) x (x)+b) was obtained. Sample values (in triplicate) were averaged and corrected for background. The resulting value was replaced for 'y' in the linear equation, i.e. x = (y-b)/ a, where x was the estimated protein (µg/ ml).

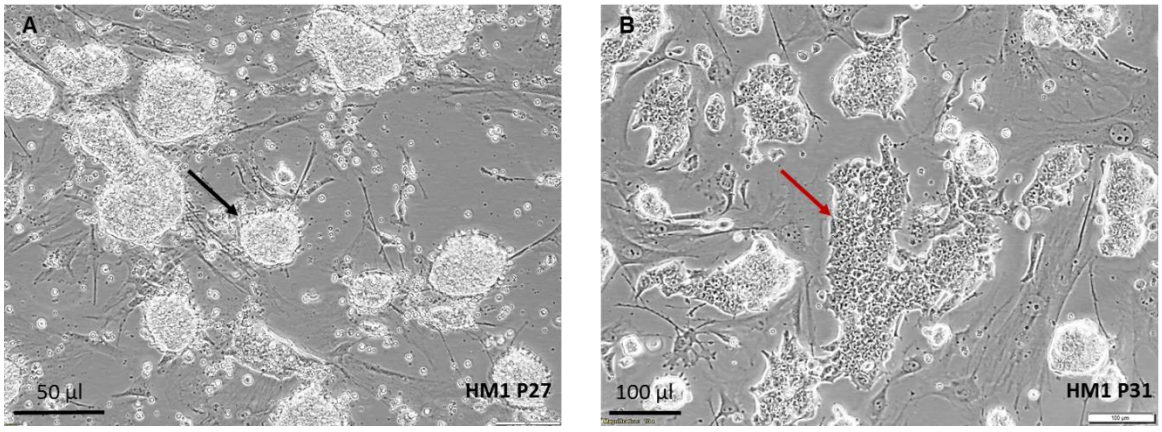

Appendix B. Figure 7 Brightfield images showing proliferation and morphological differences in control mESC line, HM1 in serum-free (KO/SR) and serum (ES-FBS) based pluripotent culture conditions.

(A) KO/SR and (B) ES-FBS culture conditions in HM1 line, cultured in mESC medium (DMEM/F-12 and LIF). Arrows point to key morphological features of KO/SR (spherical, tomb-like colonies (A)) and ES-FBS (flat colonies with edge boundaries (B)). Scale bar (A) = 50 µm and (B) = 100 µm.

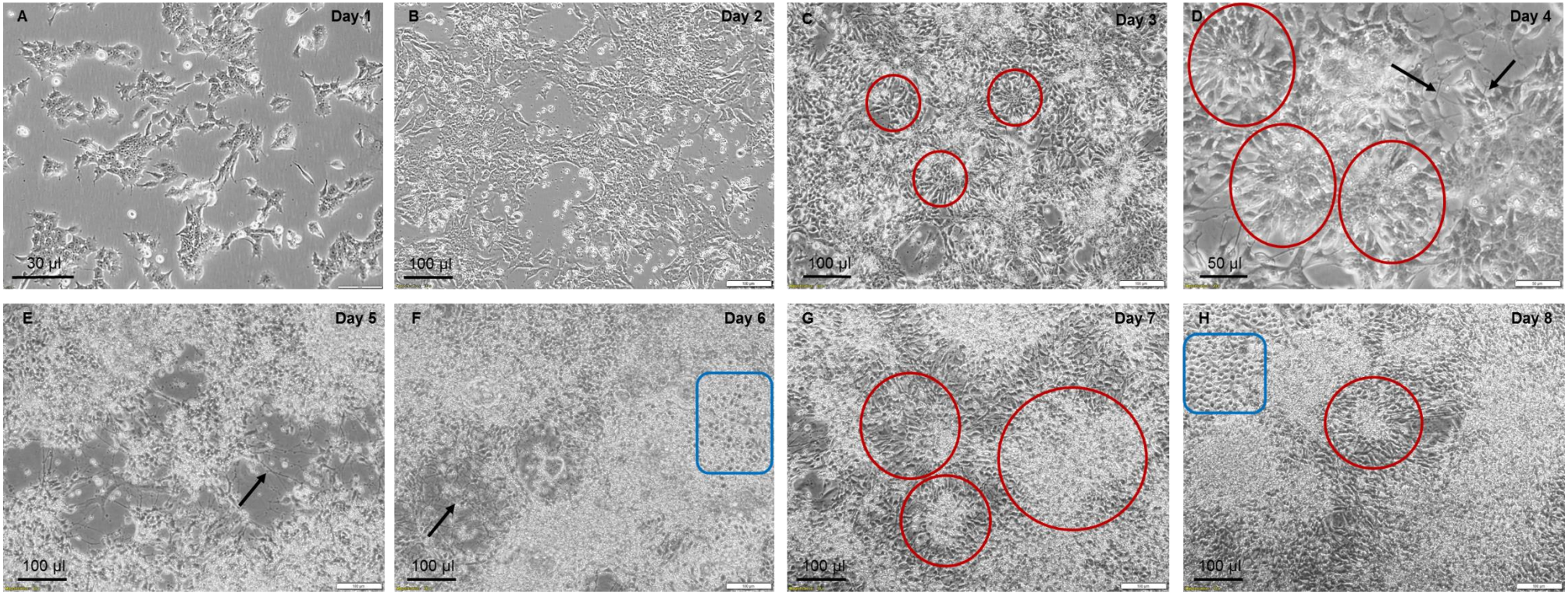

Appendix B. Figure 8 Neural induction (D1-D8) of HM1 control mESC line cultured in S-NIM.

Morphological changes in HM1 mESC line observed from D1 to D8 (A-H) during NI under S-NIM. HM1 cells maintain pluripotent morphology (characteristic to HM1 cultured under ES-FBS) on D1 and D2 of induction (A, B). Rosettes start appearing from D3 of NI, marked in red circles (C) and continue to appear and increase in size and density throughout induction up to D8 (C- H). Arrows point to neurites observed from D4 (D), D5 (E) and D6 (F), after which the cultures get much denser. Large, flat-cells which appear to be cells from other (non-neural) lineages (F, H) can be observed in blue boxes on D6 and D8. Scale bars vary between 30 µm (A), 50 µm (D) and 100 µm (B, C, E, F, G, H), as also indicated in individual images.

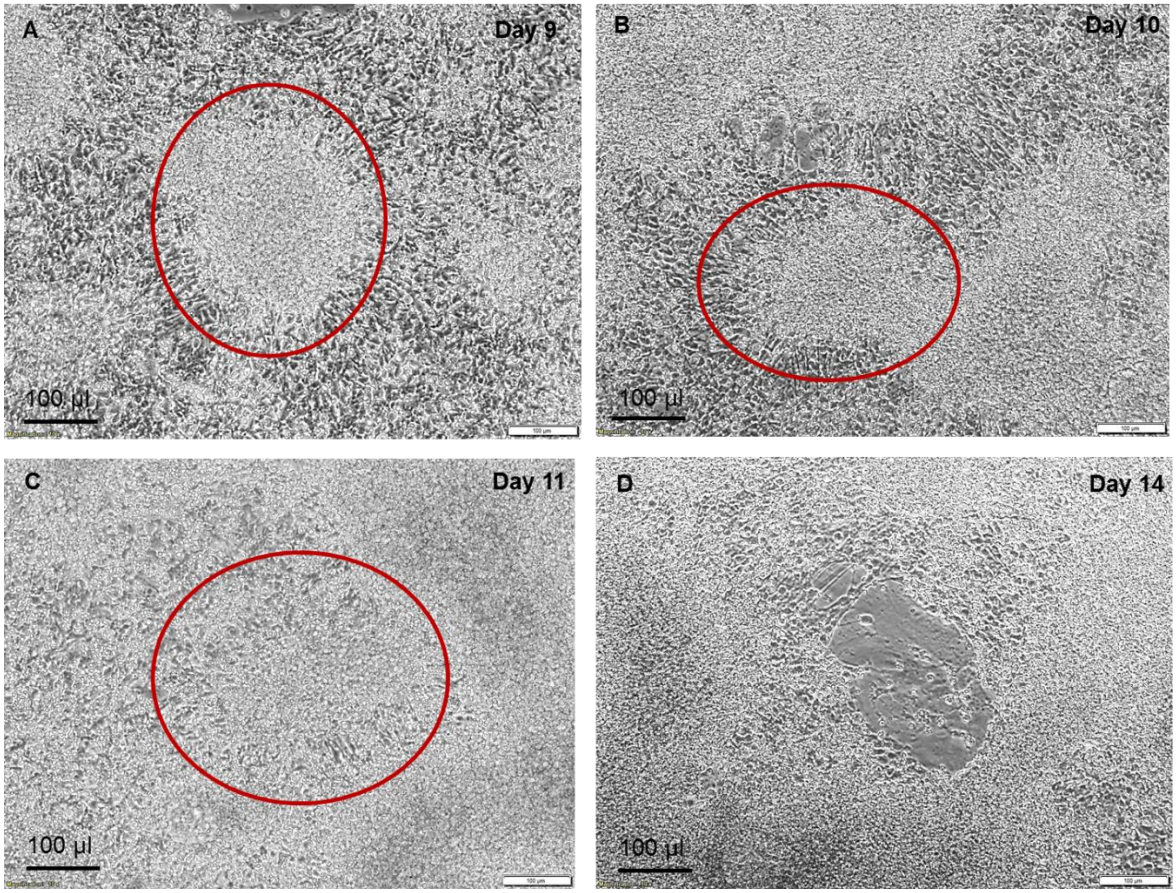

Appendix B. Figure 9 Neural induction (D9-D14) of HM1 control mESC line cultured in S-NIM.

Morphological changes in HM1 mESC line observed from D9 to D14 (A-D) during NI under S-NIM. Overall, rosettes become denser and more mature from D9 - D14 of induction in the HM1 mESC line, marked within red circles. Scale bar= 100 µm.

Appendix C List of Antibodies and Primers

Appendix C. Table 2 Antibodies used for Immunocytochemistry procedures

Antigen	Species	Company	Cat #	Working Dilution
Nestin	Rat	Merck Millipore	MAB353	1:200
Sox1	Goat	R&D System	AF3369	1:50
Pax6	Rabbit	Bioscience (Formerly Covance)	901301 PRB-278P	1:250
Tubulinβ-3	Rabbit	Bioscience (Formerly Covance)	802001 PRB-435P	1:1000
Map2	Mouse	Merck Millipore	MAB3418	1:1000
Nanog	Mouse	SantaCruz Biotechnology (SCBT)	293121	1:50
Oct-04	Mouse	SCBT	5279	1:50
Sox2	Mouse	SCBT	365823	1:50
Gata4	Mouse	SCBT	25310	1:50
Brachyury	Mouse	SCBT	166962	1:50
Alexa 488	Goat	Abcam	A11008	1:1000
Alexa 594	Donkey	Abcam	A21203	1:1000

Appendix C. Table 3 Antibodies used for Flow Cytometry

Coupled Antigen	Company	Catalog #	Working Dilution
Nanog- APC	Miltenyi Biotec	REA297	1:10
Oct 3/4 isoform A- APC	Miltenyi Biotec	REA622	1:10
Sox2- PE	Miltenyi Biotec	REA320	1:10
SSEA-1-APC	Miltenyi Biotec	REA321	1:10
Ki67-FITC	Miltenyi Biotec	REA183	1:10
AnnexinV-FITC Kit	eBioscience	BMS500FI	1:4 for Annexin-FITC 1:5 for PI

Appendix C. Table 4 Primers used for gene expression (RT PCR)

Gene name	Gene symbol	Forward sequence (5'- 3')	Reverse sequence (3'- 5')	Base pair sequence length
Octamer-binding transcription factor 4	*Oct4*	GTTGGAGAAGGTGGAACCAA	CTCCTTCTGCAGGGCTTTC	61
Homeobox protein Nanog	*Nanog*	TGCTTACAAGGGTCTGCTACTG	GAGGCAGGTCTTCAGAGGAA	76
Sex determining region Y-box 2	*Sox2*	TGGGCTCTGTGGTCAAGTC	TGATCATGTCCCGGAGGT	105
Transcription factor Gata-4	*Gata4*	GGAAGACACCCCAATCTCG	CATGGCCCCACAATTGAC	72
T box transcription factor T	*Brachyury (TBXT)*	GCTTCAAGGAGCTAACTAACGAG	CCAGCAAGAAAGAGTACATGGC	117
SRY-box containing gene 1	*Sox1*	GCCCAGGAAAACCCCAAGAT	CTCGGACATGACCTTCCACTC	75
Nestin	*Nes*	CCAAAGAGGTGTCCGATCATC	CTCCTTCTTCTTCATCAGCATCT	147
Paired box gene 6	*Pax6*	GAGAAGAGAAGAGAAACTGAGGAA	ATTGGCTGGTAGACACTGGTA	102
Tubulin beta 3	*Tubb3*	GGAGAACACAGACGAGACCTA	AGACACAAGGTGGTTGAGGT	112
Microtubule-associated protein 2	*Map2*	CAGGATAGGAAGATGTAGGAGTGTC	GACTGTCACATTGGTCATAATACTCAA	112
Caspase-3 precursor	*Casp3*	GACTCCACTTTCCACGCAAA	CCCACCCCCAATCATTCCT	97
DNA methyltransferase 1	*Dnmt 1*	GCTACCAGTGCACCTTTGGT	ATGATGGCCCTCCTTCGT	73
DNA methyltransferase 3a	*Dnmt 3a*	ACACAGGGCCCGTTACTTCT	TCACAGTGGATGCCAAAGG	65
DNA methyltransferase 3b	*Dnmt 3b*	GCCTGCAAGACTTCTTCACTACT	GGTACAACTTGGGTGGCTCA	63
DNA methyltransferase 3L	*Dnmt 3L*	AACCGACGGAGCATTGAA	CCGAGTGTACACCTGGAGACT	60
14-3-3 protein zeta/delta	*Ywhaz*	Proprietary information	Proprietary information	195
Ribosomal protein L13a	*Rpl13a*	Proprietary information	Proprietary information	180
Calnexin	*Canx*	Proprietary information	Proprietary information	127

Appendix D Supplementary details

geNorm analysis details (Section 2.2.5.6)

- **geNorm M-** This denotes average expression stability value (M) of reference gene at each step, during a stepwise exclusion of least stably expressed gene. Starting from the least stable gene at left (highest M value), genes are ranked according to increased expression stability, with the most stable genes on the right.
- **geNorm V-** This is a normalisation factor that determines the optimum number of reference genes required for normalisation. It depicts the variation in average stability of the reference genes starting with the most stable genes on the left, with the inclusion of 3, 4 or 5 etc. genes moving towards the right. This type of measure is known as 'pairwise variation, V (n/n+1)' which is obtained by averaging the C(t) values of the selected genes. The optimal number of reference genes is found when the average <0.15, so if a V2/3 score of 0.25 is achieved where n=2, and a V (3/4) score of 0.14 is achieved where n= 3, the optimal number of reference genes required is three for the given set of experiment.

Data analysis of RT-PCR details (Section 2.2.5.7)

Quantitative real time PCR analysis was stored in Opticon Monitior v3.1 software

In the data graph view of the software (under quantitation tab), the following parameters were changed before the raw data was copied to an excel file:

1. The graph was changed to log scale, removing the smooth option.
2. Baseline was subtracted and average over cycle range was selected at 13 (usually set between 3-15). This is the baseline fluorescence before the target is amplified over the background signal. Therefore, in highly abundant targets-such as 18S, a very low baseline of ~2-3 cycles may be set to record the amplified fluorescence.
3. The threshold was manually adjusted at the inflection of the curve (not more than halfway up the linear part, just over background noise/ signal). The signals were considered positive above 10.00 standard deviation over cycle.
4. In the melting curve tab, all occupied wells were highlighted and the data was copied from the quantitation tab. All sample wells for a particular primer pair, had a single melting peak, with similar (+/-1) melting temperature (Tm), which matched with the Tm of the amplicons. Tm of each primer pair was calculated using the following formula:

$$Tm = 64.9 + \left(0.41 * \left(\frac{G+C}{length} * 100\right)\right) - \left(\frac{500}{length}\right)$$

5. After fixing the above mentioned parameters, the raw C(t) values were copied into an excel file and the duplicate values were averaged and their standard deviation calculated.
6. Next, delta C(t) was calculated using the formula:
   dCt = mean Ct-$ (column with mean Ct values) $ the earliest Ct
7. The relative expression was calculated using the formula =2^- dCt (where 2 represents 100% efficiency of the primers).

Flow cytometry details (Section 2.2.7)

Cell doublets were avoided using area-height gate of forward scatter. To format fluorescence parameters for dual-colour analysis, singly stained, along with unstained samples were used and appropriate compensation levels were set in order to eliminate spectral overlap and bleed-through between fluorophores. This was achieved by adjusting median fluorescence of the positive population so that it was parallel with median fluorescence of the negative population. ES cell populations were further analyzed by generating dot plots to examine levels of fluorescently labelled markers.

List of References

Abranches, E., Silva, M., Pradier, L., Schulz, H., Hummel, O., Henrique, D., & Bekman, E. (2009a). Neural differentiation of embryonic stem cells in vitro: A road map to neurogenesis in the embryo. *PLoS ONE*. https://doi.org/10.1371/journal.pone.0006286

Abranches, E., Silva, M., Pradier, L., Schulz, H., Hummel, O., Henrique, D., & Bekman, E. (2009b). Neural differentiation of embryonic stem cells in vitro: A road map to neurogenesis in the embryo. *PLoS ONE*, *4*(7). https://doi.org/10.1371/journal.pone.0006286

Adams Waldorf, K. M., & McAdams, R. M. (2013). Influence of infection during pregnancy on fetal development. *Reproduction (Cambridge, England)*, *146*(5), R151-62. https://doi.org/10.1530/REP-13-0232

Afonso, C., & Henrique, D. (2006). PAR3 acts as a molecular organizer to define the apical domain of chick neuroepithelial cells. *Journal of Cell Science*. https://doi.org/10.1242/jcs.03170

Aihie Sayer, a, Dunn, R., Langley-Evans, S., & Cooper, C. (2001). Prenatal exposure to a maternal low protein diet shortens life span in rats. *Gerontology*, *47*(1), 9–14. https://doi.org/52764

Alamy, M., & Bengelloun, W. A. (2012). Malnutrition and brain development: An analysis of the effects of inadequate diet during different stages of life in rat. *Neuroscience and Biobehavioral Reviews*. https://doi.org/10.1016/j.neubiorev.2012.03.009

Aldous, M. B., & Edmonson, M. B. (1993). Maternal age at first childbirth and risk of low birth weight and preterm delivery in Washington State. *JAMA*, *270*(21), 2574–2577. https://doi.org/10.1001/jama.270.21.2574

Alikani, M., Cohen, J., Tomkin, G., Garrisi, G. J., Mack, C., & Scott, R. T. (1999). Human embryo fragmentation in vitro and its implications for pregnancy and implantation. *Fertility and Sterility*, *71*(5), 836–842. https://doi.org/10.1016/S0015-0282(99)00092-8

Almeida, S. S., Tonkiss, J., & Galler, J. R. (1996). Prenatal protein malnutrition affects the social interactions of juvenile rats. *Physiology and Behavior*, *60*(1), 197–201. https://doi.org/10.1016/0031-9384(95)02236-8

Alrefaei, G. I., Al-Karim, S., Ayuob, N. N., & Ali, S. S. (2015). Does the maternal age affect the mesenchymal stem cell markers and gene expression in the human placenta? What is the evidence? *Tissue & Cell*, *47*(4), 406–419. https://doi.org/10.1016/j.tice.2015.05.005

Alviggi, C., Conforti, A., Carbone, I. F., Borrelli, R., de Placido, G., & Guerriero, S. (2018). Influence of cryopreservation on perinatal outcome after blastocyst- vs cleavage-stage embryo transfer: systematic review and meta-analysis. *Ultrasound in Obstetrics & Gynecology*, *51*(1), 54–63. https://doi.org/10.1002/uog.18942

Alviggi, C., Humaidan, P., Howles, C. M., Tredway, D., & Hillier, S. G. (2009). Biological versus chronological ovarian age: Implications for assisted reproductive technology. *Reproductive Biology and Endocrinology*. https://doi.org/10.1186/1477-7827-7-101

Ambrosetti, D. C., Basilico, C., & Dailey, L. (1997). Synergistic activation of the fibroblast growth factor 4 enhancer by Sox2 and Oct-3 depends on protein-protein interactions facilitated by a specific spatial arrangement of factor binding sites. *Molecular and Cellular Biology*, *17*(11), 6321–6329. https://doi.org/10.1128/MCB.17.11.6321

Angulo-Colmenares, A. G., Vaughan, D. W., & Hinds, J. W. (1979). Rehabilitation following early

malnutrition in the rat: body weight, brain size, and cerebral cortex development. *Brain Res*, *169*(1), 121–138.

Annette, M., Gerhard, A., Sauer, M. V., Hamilton, C. J. C. M., & Paulson, R. J. (1997). The impact of the woman's age on the success of standard and donor in vitro fertilization. *Fertility and Sterility*, *67*(4), 702–710. https://doi.org/10.1016/S0015-0282(97)81370-2

Antinori, S., Versaci, C., Panci, C., Caffa, B., & Gholami, G. H. (1995). Fetal and maternal morbidity and mortality in menopausal women aged 45-63 years. *Hum Reprod*, *10*(2), 464–469. https://doi.org/10.1093/oxfordjournals.humrep.a135963

Antonov, A. N. (1947). Children born during The Siege of Leningrad in 1942. *The Journal of Pediatrics*, *30*(3), 250–259. https://doi.org/10.1016/S0022-3476(47)80160-X

Arkin, M. R., & Wells, J. a. (2004). Small-molecule inhibitors of protein-protein interactions: progressing towards the dream. *Nature Reviews. Drug Discovery*, *3*(4), 301–317. https://doi.org/10.1038/nrd1343

Armstrong, D. T. (2001). Effects of maternal age on oocyte developmental competence. *Theriogenology*. https://doi.org/10.1016/S0093-691X(01)00484-8

Atala, A. (2012). Re: Prevention of maternal aging-associated oocyte aneuploidy and meiotic spindle defects in mice by dietary and genetic strategies. *Journal of Urology*. https://doi.org/10.1016/j.juro.2012.01.042

Aubert, J., Dunstan, H., Chambers, I., & Smith, A. (2002). Functional gene screening in embryonic stem cells implicates Wnt antagonism in neural differentiation. *Nature Biotechnology*, *20*(12), 1240–1245. https://doi.org/10.1038/nbt763

Avilion, A. A., Nicolis, S. K., Pevny, L. H., Perez, L., Vivian, N., & Lovell-Badge, R. (2003). Multipotent cell lineages in early mouse development depend on SOX2 function. *Genes and Development*, *17*(1), 126–140. https://doi.org/10.1101/gad.224503

Azuara, V., Perry, P., Sauer, S., Spivakov, M., Jørgensen, H. F., John, R. M., … Fisher, A. G. (2006). Chromatin signatures of pluripotent cell lines. *Nature Cell Biology*, *8*(5), 532–538. https://doi.org/10.1038/ncb1403

Baart, E. B., Martini, E., Eijkemans, M. J., Van Opstal, D., Beckers, N. G. M., Verhoeff, A., … Fauser, B. C. J. M. (2007). Milder ovarian stimulation for in-vitro fertilization reduces aneuploidy in the human preimplantation embryo: A randomized controlled trial. *Human Reproduction*, *22*(4), 980–988. https://doi.org/10.1093/humrep/del484

Baharvand, H., & Matthaei, K. I. (2004). Culture condition difference for establishment of new embryonic stem cell lines from the C57BL/6 and BALB/c mouse strains. *In Vitro Cellular & Developmental Biology. Animal*, *40*, 76–81. https://doi.org/10.1290/1543-706X(2004)040<0076:CCDFEO>2.0.CO;2

Bain, G., Kitchens, D., Yao, M., Huettner, J. E., & Gottlieb, D. I. (1995). Embryonic stem cells express neuronal properties in vitro. *Developmental Biology*, *168*(2), 342–357. https://doi.org/10.1006/dbio.1995.1085

Bain, G., Kitchens, D., Yao, M., Huettner, J. E., & Gottlieb, D. I. (1995). Embryonic stem cells express neuronal properties in vitro. *Dev Biol*. https://doi.org/10.1006/dbio.1995.1085\rS0012-1606(85)71085-8 [pii]

Baird, D. D. (2013). Women's Fecundability and Factors Affecting It. In *Women and Health* (pp. 193–207). https://doi.org/10.1016/B978-0-12-384978-6.00014-5

Baker, D. E. C., Harrison, N. J., Maltby, E., Smith, K., Moore, H. D., Shaw, P. J., … Andrews, P. W. (2007). Adaptation to culture of human embryonic stem cells and oncogenesis in vivo. *Nature Biotechnology*, *25*(2), 207–215. https://doi.org/10.1038/nbt1285

Balasch, J., & Gratacós, E. (2012). Delayed childbearing: Effects on fertility and the outcome of pregnancy. *Current Opinion in Obstetrics and Gynecology*. https://doi.org/10.1097/GCO.0b013e3283517908

Banik, A., Kandilya, D., Ramya, S., Stünkel, W., Chong, Y. S., & Thameem Dheen, S. (2017). Maternal factors that induce epigenetic changes contribute to neurological disorders in offspring. *Genes*. https://doi.org/10.3390/genes8060150

Barbehenn, E. K., Wales, R. G., & Lowry, O. H. (1978). Measurement of metabolites in single preimplantation embryos; a new means to study metabolic control in early embryos. *Journal of Embryology and Experimental Morphology*, *43*, 29–46.

Barkan, S. E., & Bracken, M. B. (1987). Delayed childbearing: no evidence for increased risk of low birth weight and preterm delivery. *American Journal of Epidemiology*, *125*, 101–109.

Barker, D., Eriksson, J., Forsen, T., & Osmond, C. (2002). Fetal origins of adult disease: strength of effects and biological basis. *Int J Epidemiol*, *31*, 1235–1239. https://doi.org/10.1093/ije/31.6.1235

Barker, D. J., Bull, A. R., Osmond, C., & Simmonds, S. J. (1990). Fetal and placental size and risk of hypertension in adult life. *BMJ (Clinical Research Ed.)*, *301*, 259–262. https://doi.org/10.1136/bmj.301.6751.552

Barker, D. J., Gluckman, P. D., Godfrey, K. M., Harding, J. E., Owens, J. A., & Robinson, J. S. (1993). Fetal nutrition and cardiovascular disease in adult life. *Lancet*, *341*(8850), 938–941. https://doi.org/10.1016/0140-6736(93)91224-A

Barker, D. J., Martyn, C. N., Osmond, C., Hales, C. N., & Fall, C. H. (1993). Growth in utero and serum cholesterol concentrations in adult life. *BMJ (Clinical Research Ed.)*, *307*(6918), 1524–1527. https://doi.org/10.1136/bmj.307.6918.1524

Barker, D. J. P. (1997). Maternal nutrition, fetal nutrition, and disease in later life. *Nutrition*, *13*, 807–813. https://doi.org/10.1016/S0899-9007(97)00193-7

Barker, D. J. P. (2007). The origins of the developmental origins theory. In *Journal of Internal Medicine* (Vol. 261, pp. 412–417). https://doi.org/10.1111/j.1365-2796.2007.01809.x

Barker, D. J. P., Osmond, C., Kajantie, E., & Eriksson, J. G. (2009). Growth and chronic disease: Findings in the Helsinki Birth Cohort. *Annals of Human Biology*, *36*(5), 444–458. https://doi.org/10.1080/03014460902980295

BARKER, D. J. P., & THORNBURG, K. L. (2013). The Obstetric Origins of Health for a Lifetime. *Clinical Obstetrics and Gynecology*, *56*(3), 511–519. https://doi.org/10.1097/GRF.0b013e31829cb9ca

Barker, D., & Osmond, C. (1986). Infant Mortality, Childhood Nutrition, and Ischaemic Heart Disease in England and Wales. *The Lancet*, *327*(8489), 1077–1081. https://doi.org/10.1016/S0140-6736(86)91340-1

Barnett, D. K., & Bavister, B. D. (1996). What is the relationship between the metabolism of preimplantation embryos and their developmental competence? *Molecular Reproduction and Development*. https://doi.org/10.1002/(SICI)1098-2795(199601)43:1<105::AID-MRD13>3.0.CO;2-4

Barnhart, K. T. (2013). Assisted reproductive technologies and perinatal morbidity: Interrogating the association. *Fertility and Sterility*, *99*(2), 299–302. https://doi.org/10.1016/j.fertnstert.2012.12.032

Barry, J. S., Rozance, P. J., & Anthony, R. V. (2008). An Animal Model of Placental Insufficiency-Induced Intrauterine Growth Restriction. *Seminars in Perinatology*. https://doi.org/10.1053/j.semperi.2007.11.004

Bayrampour, H., & Heaman, M. (2010). Advanced maternal age and the risk of cesarean birth: a systematic review. *Birth (Berkeley, Calif.)*, *37*(3), 219–226. https://doi.org/10.1111/j.1523-536X.2010.00409.x

Bell, C. E., Calder, M. D., & Watson, A. J. (2008). Genomic RNA profiling and the programme controlling preimplantation mammalian development. *Molecular Human Reproduction*, *14*(12), 691–701. https://doi.org/10.1093/molehr/gan063

Belluscio, L. M., Berardino, B. G., Ferroni, N. M., Ceruti, J. M., & Cánepa, E. T. (2014). Early protein malnutrition negatively impacts physical growth and neurological reflexes and evokes anxiety and depressive-like behaviors. *Physiology and Behavior*, *129*, 237–254. https://doi.org/10.1016/j.physbeh.2014.02.051

Beltz, B. S., Tlusty, M. F., Benton, J. L., & Sandeman, D. C. (2007). Omega-3 fatty acids upregulate adult neurogenesis. *Neuroscience Letters*, *415*(2), 154–158. https://doi.org/10.1016/j.neulet.2007.01.010

Bennis-Taleb, N., Remacle, C., Hoet, J. J., & Reusens, B. (1999). A low-protein isocaloric diet during gestation affects brain development and alters permanently cerebral cortex blood vessels in rat offspring. *J Nutr*, *129*(8), 1613–1619. https://doi.org/10.1093/jn/129.8.1613

Benshushan, A., & Schenker, J. G. (1993). Age limitation in human reproduction: Is it justified? *Journal of Assisted Reproduction and Genetics*, *10*(5).

Berg, J. M., Tymoczko, J. L., & Stryer, L. (2002). The Glycolytic Pathway Is Tightly Controlled. In *Biochemistry*.

Beringue, F., Blondeau, B., Castellotti, M. C., Breant, B., Czernichow, P., & Polak, M. (2002). Endocrine pancreas development in growth-retarded human fetuses. *Diabetes*, *51*(2), 385–391. https://doi.org/10.2337/diabetes.51.2.385

Berry, C. L., Gosling, R. G., Laogun, A. A., & Bryan, E. (1976). Anomalous iliac compliance in children with a single umbilical artery. *British Heart Journal*, *38*(5), 510–515. https://doi.org/10.1136/hrt.38.5.510

Besson, A. a, Lagisz, M., Senior, A. M., Hector, K. L., & Nakagawa, S. (2015). Effect of maternal diet on offspring coping styles in rodents: a systematic review and meta-analysis. *Biological Reviews*, *64*(November). https://doi.org/10.1111/brv.12210

Beydoun, H. A., Sicignano, N., Beydoun, M. A., Matson, D. O., Bocca, S., Stadtmauer, L., & Oehninger, S. (2010). A cross-sectional evaluation of the first cohort of young adults conceived by in vitro fertilization in the United States. *Fertility and Sterility*, *94*(6), 2043–2049. https://doi.org/10.1016/j.fertnstert.2009.12.023

Bian, J., Zheng, J., Li, S., Luo, L., & Ding, F. (2016). Sequential differentiation of embryonic stem cells into neural epithelial-like stem cells and oligodendrocyte progenitor cells. *PLoS ONE*, *11*(5). https://doi.org/10.1371/journal.pone.0155227

Biggers, J. D., & Summers, M. C. (2008). Choosing a culture medium: making informed choices.

Fertility and Sterility. https://doi.org/10.1016/j.fertnstert.2008.08.010

Biro, M. A., Davey, M. A., Carolan, M., & Kealy, M. (2012). Advanced maternal age and obstetric morbidity for women giving birth in Victoria, Australia: A population-based study. *Australian and New Zealand Journal of Obstetrics and Gynaecology*, *52*(3), 229–234. https://doi.org/10.1111/j.1479-828X.2012.01427.x

Boer, B., Kopp, J., Mallanna, S., Desler, M., Chakravarthy, H., Wilder, P. J., … Rizzino, A. (2007). Elevating the levels of Sox2 in embryonal carcinoma cells and embryonic stem cells inhibits the expression of Sox2:Oct-3/4 target genes. *Nucleic Acids Research*, *35*(6), 1773–1786. https://doi.org/10.1093/nar/gkm059

Bonatto, F., Polydoro, M., Andrades, M. É., Conte Da Frota, M. L., Dal-Pizzol, F., Rotta, L. N., … Fonseca Moreira, J. C. (2005). Effect of protein malnutrition on redox state of the hippocampus of rat. *Brain Research*, *1042*(1), 17–22. https://doi.org/10.1016/j.brainres.2005.02.002

Bongso, A., & Tan, S. (2005). Human blastocyst culture and derivation of embryonic stem cell lines. *Stem Cell Reviews*, *1*(2), 87–98. https://doi.org/10.1385/SCR:1:2:087

Bottenstein, J. E. (1985). Growth and Differentiation of Neural Cells in Defined Media BT - Cell Culture in the Neurosciences. In J. E. Bottenstein & G. Sato (Eds.) (pp. 3–43). Boston, MA: Springer US. https://doi.org/10.1007/978-1-4613-2473-7_1

Braude, P., Bolton, V., & Moore, S. (1988). Human gene expression first occurs between the four- and eight-cell stages of preimplantation development. *Nature*, *332*, 459–461. https://doi.org/10.1038/332459a0

Brevini, T. A. L., Antonini, S., Cillo, F., Crestan, M., & Gandolfi, F. (2007). Porcine embryonic stem cells: Facts, challenges and hopes. *Theriogenology*, *68*. https://doi.org/10.1016/j.theriogenology.2007.05.043

Brickman, J. M., & Serup, P. (2017). Properties of embryoid bodies. *WIREs Dev Biol*, *6*. https://doi.org/10.1002/wdev.259

Brinster, R. L. (1974). Embryo Development. *J Anim Sci*, *38*(5), 1003–1012.

Brinster, R. L., & April, R. (1966). PROTEIN CONTENT OF THE MOUSE EMBRYO DURING THE FIRST FIVE DAYS OF DEVELOPMENT King Ranch Laboratory of Reproductive Physiology , School of Veterinary Medicine , University of Pennsylvania , Philadelphia , Pennsylvania Obtaining embryos.

Brinster, R. L., & Troike, D. E. (1979). Requirements for blastocyst development in vitro. *Journal of Animal Science*. https://doi.org/10.1093/ansci/49.Supplement_II.26

Broekmans, F. J., Soules, M. R., & Fauser, B. C. (2009). Ovarian aging: Mechanisms and clinical consequences. *Endocrine Reviews*. https://doi.org/10.1210/er.2009-0006

Brons, I. G. M., Smithers, L. E., Trotter, M. W. B., Rugg-Gunn, P., Sun, B., Chuva De Sousa Lopes, S. M., … Vallier, L. (2007). Derivation of pluripotent epiblast stem cells from mammalian embryos. *Nature*, *448*(7150), 191–195. https://doi.org/10.1038/nature05950

Broughton, D. E., & Moley, K. H. (2017). Obesity and female infertility: potential mediators of obesity's impact. *Fertility and Sterility*. https://doi.org/10.1016/j.fertnstert.2017.01.017

Brown, A. S., Susser, E. S., Lin, S. P., Neugebauer, R., & Gorman, J. M. (1995a). Increased risk of affective disorders in males after second trimester prenatal exposure to the Dutch hunger

winter of 1944-45. *The British Journal of Psychiatry*, *166*(5), 601 LP-606.

Brown, A. S., Susser, E. S., Lin, S. P., Neugebauer, R., & Gorman, J. M. (1995b). Increased risk of affective disorders in males after second trimester prenatal exposure to the Dutch hunger winter of 1944-45. *British Journal of Psychiatry*, *166*(MAY), 601–606. https://doi.org/10.1192/BJP.166.5.601

Buck, C., & Simpson, H. (1982). Infant diarrhoea and subsequent mortality from heart disease and cancer. *Journal of Epidemiology and Community Health*, *36*, 27–30. https://doi.org/10.1136/jech.36.1.27

Buecker, C., & Geijsen, N. (2010). Different flavors of pluripotency, molecular mechanisms, and practical implications. *Cell Stem Cell*. https://doi.org/10.1016/j.stem.2010.10.007

Buehr, M., Meek, S., Blair, K., Yang, J., Ure, J., Silva, J., … Smith, A. (2008). Capture of Authentic Embryonic Stem Cells from Rat Blastocysts. *Cell*, *135*(7), 1287–1298. https://doi.org/10.1016/j.cell.2008.12.007

Bühler, K., Czeromin, U., Krüssel, J. S., Blumenauer, V., Fiedler, K., Gnoth, C., … Tandler-Schneider, A. (2014). D·I·R - Annual 2012. *Journal Fur Reproduktionsmedizin Und Endokrinologie*. https://doi.org/10.1783/147118910791749425

Burdge, G. C., Dunn, R. L., Wootton, S. A., & Jackson, A. A. (2002). Effect of reduced dietary protein intake on hepatic and plasma essential fatty acid concentrations in the adult female rat: effect of pregnancy and consequences for accumulation of arachidonic and docosahexaenoic acids in fetal liver and brain. *British Journal of Nutrition*, *88*(4), 379–387. https://doi.org/DOI: 10.1079/BJN2002664

Burdick, J. A., & Vunjak-Novakovic, G. (2009). Engineered Microenvironments for Controlled Stem Cell Differentiation. *Tissue Engineering Part A*, *15*(2), 205–219. https://doi.org/10.1089/ten.tea.2008.0131

Burdon, T., Smith, A., & Savatier, P. (2002). Signalling, cell cycle and pluripotency in embryonic stem cells. *Trends in Cell Biology*. https://doi.org/10.1016/S0962-8924(02)02352-8

Bustin, S. A. (2000). Absolute quantification of mrna using real-time reverse transcription polymerase chain reaction assays. *Journal of Molecular Endocrinology*. https://doi.org/JME00927 [pii]

Cagnol, S., & Chambard, J. C. (2010). ERK and cell death: Mechanisms of ERK-induced cell death - Apoptosis, autophagy and senescence. *FEBS Journal*. https://doi.org/10.1111/j.1742-4658.2009.07366.x

Calle, A., Fernandez-Gonzalez, R., Ramos-Ibeas, P., Laguna-Barraza, R., Perez-Cerezales, S., Bermejo-Alvarez, P., … Gutierrez-Adan, A. (2012). Long-term and transgenerational effects of in vitro culture on mouse embryos. *Theriogenology*. https://doi.org/10.1016/j.theriogenology.2011.07.016

Cannon, D., Corrigan, A. M., Miermont, A., McDonel, P., & Chubb, J. R. (2015). Multiple cell and population-level interactions with mouse embryonic stem cell heterogeneity. *Development*, *142*(16), 2840–2849. https://doi.org/10.1242/dev.120741

Caperton, L., Murphey, P., Yamazaki, Y., McMahan, C. A., Walter, C. A., Yanagimachi, R., & McCarrey, J. R. (2007). Assisted reproductive technologies do not alter mutation frequency or spectrum. *Proceedings of the National Academy of Sciences of the United States of America*, *104*(12), 5085–5090. https://doi.org/10.1073/pnas.0611642104

Care, A. S., Bourque, S. L., Morton, J. S., Hjartarson, E. P., & Davidge, S. T. (2015). Effect of Advanced Maternal Age on Pregnancy Outcomes and Vascular Function in the Rat. *Hypertension*, *65*(6), 1324–1330. https://doi.org/10.1161/HYPERTENSIONAHA.115.05167

Carolan, M. (2013). Maternal age ≥45 years and maternal and perinatal outcomes: A review of the evidence. *Midwifery*, *29*(5), 479–489. https://doi.org/10.1016/j.midw.2012.04.001

Carolan, M., & Frankowska, D. (2011a). Advanced maternal age and adverse perinatal outcome: A review of the evidence. *Midwifery*, *27*(6), 793–801. https://doi.org/10.1016/j.midw.2010.07.006

Carolan, M., & Frankowska, D. (2011b). Advanced maternal age and adverse perinatal outcome: A review of the evidence. *Midwifery*, *27*, 793–801. https://doi.org/10.1016/j.midw.2010.07.006

Carolan, M., & Nelson, S. (2007). First mothering over 35 years: Questioning the association of maternal age and pregnancy risk. *Health Care for Women International*, *28*(6), 534–555. https://doi.org/10.1080/07399330701334356

Ceelen, M., Van Weissenbruch, M. M., Vermeiden, J. P. W., Van Leeuwen, F. E., & Delemarre-Van De Waal, H. A. (2008a). Cardiometabolic differences in children born after in vitro fertilization: Follow-up study. *Journal of Clinical Endocrinology and Metabolism*, *93*(5), 1682–1688. https://doi.org/10.1210/jc.2007-2432

Ceelen, M., Van Weissenbruch, M. M., Vermeiden, J. P. W., Van Leeuwen, F. E., & Delemarre-Van De Waal, H. A. (2008b). Pubertal development in children and adolescents born after IVF and spontaneous conception. *Human Reproduction*, *23*(12), 2791–2798. https://doi.org/10.1093/humrep/den309

Cha, K. J., Kong, S. Y., Lee, J. S., Kim, H. W., Shin, J. Y., La, M., … Kim, H. J. (2017). Cell density-dependent differential proliferation of neural stem cells on omnidirectional nanopore-arrayed surface. *Scientific Reports*, *7*(1). https://doi.org/10.1038/s41598-017-13372-6

Chan, B. C., & Lao, T. T. (1999). Influence of parity on the obstetric performance of mothers aged 40 years and above. *Human Reproduction (Oxford, England)*, *14*(3), 833–837.

Chan, B. C. P., & Lao, T. T. H. (2008). Effect of parity and advanced maternal age on obstetric outcome. *International Journal of Gynecology and Obstetrics*, *102*(3), 237–241. https://doi.org/10.1016/j.ijgo.2008.05.004

Chang, A. S., Moley, K. H., Wangler, M., Feinberg, A. P., & DeBaun, M. R. (2005). Association between Beckwith-Wiedemann syndrome and assisted reproductive technology: A case series of 19 patients. *Fertility and Sterility*, *83*(2), 349–354. https://doi.org/10.1016/j.fertnstert.2004.07.964

Chang, H. H., Hemberg, M., Barahona, M., Ingber, D. E., & Huang, S. (2008). Transcriptome-wide noise controls lineage choice in mammalian progenitor cells. *Nature*, *453*(7194), 544–547. https://doi.org/10.1038/nature06965

Chapkin, R. S., Kim, W., Lupton, J. R., & McMurray, D. N. (2009). Dietary docosahexaenoic and eicosapentaenoic acid: Emerging mediators of inflammation. *Prostaglandins Leukotrienes and Essential Fatty Acids*, *81*(2–3), 187–191. https://doi.org/10.1016/j.plefa.2009.05.010

Charlotte, V., Jean-Marc, K., Stefan, G., Kaatje, T., & Bruno, L. (2016). Maternal age at childbirth is associated with glucose metabolism in adult men. *Acta Clinica Belgica: International Journal of Clinical and Laboratory Medicine*, *71*, 5.

Chavatte-Palmer, P., Tarrade, A., & Rousseau-Ralliard, D. (2016). Diet before and during pregnancy and offspring health: The importance of animal models and what can be learned from them. *International Journal of Environmental Research and Public Health*, *13*(6), 1–14. https://doi.org/10.3390/ijerph13060586

Chen, J. C., Turiak, G., Galler, J., & Volicer, L. (1997). Postnatal changes of brain monoamine levels in prenatally malnourished and control rats. *International Journal of Developmental Neuroscience*, *15*(2), 257–263. https://doi.org/10.1016/S0736-5748(96)00121-9

Chen, X., Xu, H., Yuan, P., Fang, F., Huss, M., Vega, V. B., … Ng, H. H. (2008). Integration of External Signaling Pathways with the Core Transcriptional Network in Embryonic Stem Cells. *Cell*, *133*(6), 1106–1117. https://doi.org/10.1016/j.cell.2008.04.043

Cheng, J., Dutra, A., Takesono, A., Garrett-Beal, L., & Schwartzberg, P. L. (2004). Improved generation of C57BL/6J mouse embryonic stem cells in a defined serum-free media. *Genesis*, *39*(2), 100–104. https://doi.org/10.1002/gene.20031

Chertoff, M. (2015). Protein Malnutrition and Brain Development. *Brain Disorders & Therapy*, *04*(03). https://doi.org/10.4172/2168-975X.1000171

Chiang, T., Schultz, R. M., & Lampson, M. A. (2012). Meiotic Origins of Maternal Age-Related Aneuploidy1. *Biology of Reproduction*, *86*(1). https://doi.org/10.1095/biolreprod.111.094367

Chiavaroli, V., Cutfield, W. S., Derraik, J. G. B., Pan, Z., Ngo, S., Sheppard, A., … Ahlsson, F. (2015). Infants born large-for-gestational-age display slower growth in early infancy, but no epigenetic changes at birth. *Scientific Reports*, *5*. https://doi.org/10.1038/srep14540

Chiba, H., Hiura, H., Okae, H., Miyauchi, N., Sato, F., Sato, A., & Arima, T. (2013). DNA methylation errors in imprinting disorders and assisted reproductive technology. *Pediatrics International*. https://doi.org/10.1111/ped.12185

Chung, K., & Allen, R. (2008). The use of serial human chorionic gonadotropin levels to establish a viable or a nonviable pregnancy. *Seminars in Reproductive Medicine*. https://doi.org/10.1055/s-0028-1087104

Claeyssens, S., Lavoinne, A., Vaillant, C., Rakotomanga, J. A., Bois-Joyeux, B., & Peret, J. (1992). Metabolic changes during early starvation in rats fed a low-protein diet in the postweaning growth period. *Metabolism*, *41*(7), 722–727. https://doi.org/10.1016/0026-0495(92)90311-W

Cockburn, K., & Rossant, J. (2010). Making the blastocyst: Lessons from the mouse. *Journal of Clinical Investigation*. https://doi.org/10.1172/JCI41229

Cohen, M. A., Itsykson, P., & Reubinoff, B. E. (2010). The role of FGF-signaling in early neural specification of human embryonic stem cells. *Developmental Biology*, *340*(2), 450–458. https://doi.org/10.1016/j.ydbio.2010.01.030

Cohen, M. A., Lindheim, S. R., & Sauer, M. V. (1999). Donor age is paramount to success in oocyte donation. *Human Reproduction*, *14*(11), 2755–2758. https://doi.org/10.1093/humrep/14.11.2755

Comstock, I. A., Kim, S., Behr, B., & Lathi, R. B. (2015). Increased body mass index negatively impacts blastocyst formation rate in normal responders undergoing in vitro fertilization. *Journal of Assisted Reproduction and Genetics*, *32*(9), 1299–1304. https://doi.org/10.1007/s10815-015-0515-1

Conaghan, J., Handyside, A. H., Winston, R. M., & Leese, H. J. (1993). Effects of pyruvate and glucose on the development of human preimplantation embryos in vitro. *J Reprod Fertil*, *99*(1), 87–95. https://doi.org/10.1530/jrf.0.0990087

Condic, M. L. (2014). Totipotency: What It Is and What It Is Not. *Stem Cells and Development*, *23*(8), 796–812. https://doi.org/10.1089/scd.2013.0364

Conner, D. A. (2001). Mouse Embryo Fibroblast (MEF) Feeder Cell Preparation. In *Current Protocols in Molecular Biology*. https://doi.org/10.1002/0471142727.mb2302s51

Coutu, D. L., & Galipeau, J. (2011). Roles of FGF signaling in stem cell self-renewal, senescence and aging. *Aging*, *3*(10), 920–933. https://doi.org/100369 [pii]

Crossland, R. F., Balasa, A., Ramakrishnan, R., Mahadevan, S. K., Fiorotto, M. L., & Van Den Veyver, I. B. (2017). Chronic maternal low-protein diet in mice affects anxiety, night-time energy expenditure and sleep patterns, but not circadian rhythm in male offspring. *PLoS ONE*, *12*(1). https://doi.org/10.1371/journal.pone.0170127

Czechanski, A., Byers, C., Greenstein, I., Schrode, N., Donahue, L. R., Hadjantonakis, A. K., & Reinholdt, L. G. (2014). Derivation and characterization of mouse embryonic stem cells from permissive and nonpermissive strains. *Nature Protocols*, *9*(3), 559–574. https://doi.org/10.1038/nprot.2014.030

Czeizel, A. E., & Dudás, I. (1993). Prevention of the first occurrence of neural-tube defects by periconceptional vitamin supplementation. *Obstetrical and Gynecological Survey*, *48*(6), 395–397. https://doi.org/10.1097/00006254-199306000-00005

Das, U. G., & Sysyn, G. D. (2004). Abnormal fetal growth: Intrauterine growth retardation, small for gestational age, large for gestational age. *Pediatric Clinics of North America*. https://doi.org/10.1016/j.pcl.2004.01.004

de Bruin, J. P., Dorland, M., Spek, E. R., Posthuma, G., van Haaften, M., Looman, C. W. N., & te Velde, E. R. (2004). Age-Related Changes in the Ultrastructure of the Resting Follicle Pool in Human Ovaries1. *Biology of Reproduction*, *70*(2), 419–424. https://doi.org/10.1095/biolreprod.103.015784

De Carvalho, B. R., Rosa E Silva, A. C. J. D. S., Rosa E Silva, J. C., Dos Reis, R. M., Ferriani, R. A., & Silva De Sá, M. F. (2008). Ovarian reserve evaluation: State of the art. *Journal of Assisted Reproduction and Genetics*. https://doi.org/10.1007/s10815-008-9241-2

De Oliveira, J. C., Grassiolli, S., Gravena, C., & De Mathias, P. C. F. (2012). Early postnatal low-protein nutrition, metabolic programming and the autonomic nervous system in adult life. *Nutrition and Metabolism*. https://doi.org/10.1186/1743-7075-9-80

DeBaun, M. R., Niemitz, E. L., & Feinberg, A. P. (2003). Association of In Vitro Fertilization with Beckwith-Wiedemann Syndrome and Epigenetic Alterations of LIT1 and H19. *The American Journal of Human Genetics*, *72*(1), 156–160. https://doi.org/10.1086/346031

Declercq, E., Luke, B., Belanoff, C., Cabral, H., Diop, H., Gopal, D., … Hornstein, M. D. (2015). Perinatal outcomes associated with assisted reproductive technology: The Massachusetts Outcomes Study of Assisted Reproductive Technologies (MOSART). *Fertility and Sterility*, *103*(4), 888–895. https://doi.org/10.1016/j.fertnstert.2014.12.119

Del Corral, R. D., & Storey, K. G. (2004). Opposing FGF and retinoid pathways: A signalling switch that controls differentiation and patterning onset in the extending vertebrate body axis. *BioEssays*. https://doi.org/10.1002/bies.20080

Delaune, E., Lemaire, P., & Kodjabachian, L. (2005). Neural induction in Xenopus requires early FGF signalling in addition to BMP inhibition. *Development*, *132*(2), 299–310. https://doi.org/10.1242/dev.01582

Delbaere, I., Verstraelen, H., Goetgeluk, S., Martens, G., De Backer, G., & Temmerman, M. (2007). Pregnancy outcome in primiparae of advanced maternal age. *European Journal of Obstetrics Gynecology and Reproductive Biology*, *135*(1), 41–46. https://doi.org/10.1016/j.ejogrb.2006.10.030

Denisenko, O., Lucas, E. S., Sun, C., Watkins, A. J., Mar, D., Bomsztyk, K., & Fleming, T. P. (2016). Regulation of ribosomal RNA expression across the lifespan is fine-tuned by maternal diet before implantation. *Biochimica et Biophysica Acta - Gene Regulatory Mechanisms*, *1859*(7), 906–913. https://doi.org/10.1016/j.bbagrm.2016.04.001

Dhana, K., Haines, J., Liu, G., Zhang, C., Wang, X., Field, A. E., … Sun, Q. (2018). Association between maternal adherence to healthy lifestyle practices and risk of obesity in offspring: results from two prospective cohort studies of mother-child pairs in the United States. *BMJ*, *362*.

Di-Gregorio, A., Sancho, M., Stuckey, D. W., Crompton, L. A., Godwin, J., Mishina, Y., & Rodriguez, T. A. (2007). BMP signalling inhibits premature neural differentiation in the mouse embryo. *Development*, *134*(18), 3359–3369. https://doi.org/10.1242/dev.005967

Diaz-Cintra, S., Cintra, L., Ortega, A., Kemper, T., & Morgane, P. J. (1990). Effects of protein deprivation on pyramidal cells of the visual cortex in rats of three age groups. *J Comp Neurol*, *292*(1), 117–126. https://doi.org/10.1002/cne.902920108

Díaz-Cintra, S., González-Maciel, A., Morales, M. Á., Aguilar, A., Cintra, L., & Prado-Alcalá, R. A. (2007). Protein malnutrition differentially alters the number of glutamic acid decarboxylase-67 interneurons in dentate gyrus and CA1-3 subfields of the dorsal hippocampus. *Experimental Neurology*, *208*(1), 47–53. https://doi.org/10.1016/j.expneurol.2007.07.003

Dietz, W. H. (2004). Overweight in Childhood and Adolescence. *New England Journal of Medicine*, *350*(9), 855–857. https://doi.org/10.1056/NEJMp048008

Dobson, A. T., Raja, R., Abeyta, M. J., Taylor, T., Shen, S., Haqq, C., & Reijo Pera, R. A. (2004). The unique transcriptome through day 3 of human preimplantation development. *Human Molecular Genetics*, *13*(14), 1461–1470. https://doi.org/10.1093/hmg/ddh157

Du, J., Wu, Y., Ai, Z., Shi, X., Chen, L., & Guo, Z. (2014). Mechanism of SB431542 in inhibiting mouse embryonic stem cell differentiation. *Cellular Signalling*, *26*(10). https://doi.org/10.1016/j.cellsig.2014.06.002

Dulioust, E., Toyama, K., Busnel, M. C., Moutier, R., Carlier, M., Marchaland, C., … Auroux, M. (1995). Long-term effects of embryo freezing in mice. *Proceedings of the National Academy of Sciences of the United States of America*, *92*(2), 589–593. https://doi.org/10.1073/pnas.92.2.589

Duranthon, V., Watson, A. J., & Lonergan, P. (2008). Preimplantation embryo programming: Transcription epigenetics, and culture environment. In *Reproduction* (Vol. 135, pp. 141–150). https://doi.org/10.1530/REP-07-0324

Dvash, T., Lavon, N., & Fan, G. (2010). Variations of X chromosome inactivation occur in early passages of female human embryonic stem cells. *PLoS ONE*, *5*(6). https://doi.org/10.1371/journal.pone.0011330

E. Michalska, A. (2007). Isolation and Propagation of Mouse Embryonic Fibroblasts and

Preparation of Mouse Embryonic Feeder Layer Cells. In *Current Protocols in Stem Cell Biology*. https://doi.org/10.1002/9780470151808.sc01c03s3

E. Zambrano1, C. J. B., & H. Ledesma1, J. M. (2006). A low maternal protein diet during pregnancyand lactation has sex- and window of exposure-specificeffects on offspring growth and food intake, glucosemetabolism and serum leptin in the rat. *JOURNAL OF PHYSIOLOGY*, *571.1*.

Ebrahim, S., & Smith, G. D. (1997). Systematic review of randomised controlled trials of multiple risk factor interventions for preventing coronary heart disease. *BMJ*, *314*(7095), 1666–1674. https://doi.org/10.1136/bmj.314.7095.1666

Eckert, J. J., Porter, R., Watkins, A. J., Burt, E., Brooks, S., Leese, H. J., … Fleming, T. P. (2012a). Metabolic induction and early responses of mouse blastocyst developmental programming following maternal low protein diet affecting life-long health. *PloS One*, *7*, e52791. https://doi.org/10.1371/journal.pone.0052791

Eckert, J. J., Porter, R., Watkins, A. J., Burt, E., Brooks, S., Leese, H. J., … Fleming, T. P. (2012b). Metabolic Induction and Early Responses of Mouse Blastocyst Developmental Programming following Maternal Low Protein Diet Affecting Life-Long Health. *PLoS ONE*, *7*(12). https://doi.org/10.1371/journal.pone.0052791

Edwards, R. G., Purdy, J. M., Steptoe, P. C., & Walters, D. E. (1981). The growth of human preimplantation embryos in vitro. *American Journal of Obstetrics and Gynecology*, *141*(4), 408–416. https://doi.org/10.1016/0002-9378(81)90603-7

Edwards, R. G., Steptoe, P. C., & Purdy, J. M. (1980). ESTABLISHING FULL-TERM HUMAN PREGNANCIES USING CLEAVING EMBRYOS GROWN IN VITRO. *BJOG: An International Journal of Obstetrics & Gynaecology*, *87*(9), 737–756. https://doi.org/10.1111/j.1471-0528.1980.tb04610.x

Eichenlaub-Ritter, U. (2002). Ageing and Aneuploidy in Oocytes BT - The Future of the Oocyte. In J. Eppig, C. Hegele-Hartung, & M. Lessl (Eds.) (pp. 111–136). Berlin, Heidelberg: Springer Berlin Heidelberg.

Eiselleova, L., Peterkova, I., Neradil, J., Slaninova, I., Hampl, A., & Dvorak, P. (2008). Comparative study of mouse and human feeder cells for human embryonic stem cells. *The International Journal of Developmental Biology*, *52*(4), 353–363. https://doi.org/10.1387/ijdb.082590le

Elbling, L., & Colot, M. (1985). Abnormal development and transport and increased sister-chromatid exchange in preimplantation embryos following superovulation in mice. *Mutation Research/Environmental Mutagenesis and Related Subjects*, *147*(4), 189–195. https://doi.org/10.1016/0165-1161(85)90057-3

Elmore, S. (2007). Apoptosis: A Review of Programmed Cell Death. *Toxicologic Pathology*. https://doi.org/10.1080/01926230701320337

Endl, E., Steinbach, P., Knüchel, R., & Hofstädter, F. (1997). Analysis of cell cycle-related Ki-67 and p120 expression by flow cytometric BrdUrd-Hoechst/7AAD and immunolabeling technique. *Cytometry*, *29*(3), 233–241. https://doi.org/10.1002/(SICI)1097-0320(19971101)29:3<233::AID-CYTO6>3.0.CO;2-C

Erhuma, A., Salter, A. M., Sculley, D. V, Langley-Evans, S. C., & Bennett, A. J. (2007). Prenatal exposure to a low protein diet programmes disordered regulation of lipid metabolism in the ageing rat. *Am J Physiol Endocrinol Metab*, *292*(6), In Press. https://doi.org/10.1152/ajpendo.00605.2006

Eriksson, J., Forsén, T., Tuomilehto, J., Osmond, C., & Barker, D. (2000). Fetal and childhood growth and hypertension in adult life. *Hypertension*, *36*, 790–794. https://doi.org/10.1161/01.HYP.36.5.790

Eriksson, J. G., Forsén, T., Tuomilehto, J., Osmond, C., & Barker, D. J. (2001). Early growth and coronary heart disease in later life: longitudinal study. *BMJ (Clinical Research Ed.)*, *322*(7292), 949–953. https://doi.org/10.1136/bmj.322.7292.949

Eriksson, J. G., Forsén, T., Tuomilehto, J., Osmond, C., & Barker, D. J. P. (2003). Early adiposity rebound in childhood and risk of Type 2 diabetes in adult life. *Diabetologia*, *46*(2), 190–194. https://doi.org/10.1007/s00125-002-1012-5

Ertzeid, G., & Storeng, R. (1992). Adverse effects of gonadotrophin treatment on pre- and postimplantation development in mice. *Journal of Reproduction and Fertility*, *96*(2), 649–655. https://doi.org/10.1530/jrf.0.0960649

Evans, M. J., & Kaufman, M. H. (1981). Establishment in culture of pluripotential cells from mouse embryos. *Nature*, *292*(5819), 154–156. https://doi.org/10.1038/292154a0

Fanchin, R., Schonäuer, L. M., Righini, C., Guibourdenche, J., Frydman, R., & Taieb, J. (2003). Serum anti-Müllerian hormone is more strongly related to ovarian follicular status than serum inhibin B, estradiol, FSH and LH on day 3. *Human Reproduction*, *18*(2), 323–327. https://doi.org/10.1093/humrep/deg042

Farmer, G., Russell, G., Hamilton-Nicol, D. R., Ogenbede, H. O., Ross, I. S., Pearson, D. W. M., … Sutherland, H. W. (1988). The influence of maternal glucose metabolism on fetal growth, development and morbidity in 917 singleton pregnancies in nondiabetic women. *Diabetologia*, *31*(3), 134–141. https://doi.org/10.1007/BF00276845

Fauque, P., Jouannet, P., Lesaffre, C., Ripoche, M. A., Dandolo, L., Vaiman, D., & Jammes, H. (2007). Assisted reproductive technology affects developmental kinetics, H19 imprinting control region methylation and H19 gene expression in individual mouse embryos. *BMC Developmental Biology*, *7*. https://doi.org/10.1186/1471-213X-7-116

Feoli, A. M., Siqueira, I. R., Almeida, L., Tramontina, A. C., Vanzella, C., Sbaraini, S., … Gonçalves, C. A. (2006). Effects of protein malnutrition on oxidative status in rat brain. *Nutrition*, *22*(2), 160–165. https://doi.org/10.1016/j.nut.2005.06.007

Ferré, C., Callaghan, W., Olson, C., Sharma, A., & Barfield, W. (2016). Effects of Maternal Age and Age-Specific Preterm Birth Rates on Overall Preterm Birth Rates — United States, 2007 and 2014. *MMWR. Morbidity and Mortality Weekly Report*, *65*(43), 1181–1184. https://doi.org/10.15585/mmwr.mm6543a1

Ferro, J., Martínez, M. C., Lara, C., Pellicer, A., Remohí, J., & Serra, V. (2003). Improved accuracy of hysteroembryoscopic biopsies for karyotyping early missed abortions. *Fertility and Sterility*, *80*(5), 1260–1264. https://doi.org/10.1016/S0015-0282(03)02195-2

Fiacco, T. A., Rosene, D. L., Galler, J. R., & Blatt, G. J. (2003). Increased density of hippocampal kainate receptors but normal density of NMDA and AMPA receptors in a rat model of prenatal protein malnutrition. *Journal of Comparative Neurology*, *456*(4), 350–360. https://doi.org/10.1002/cne.10531

FILOSA, S., FICO, A., PAGLIALUNGA, F., BALESTRIERI, M., CROOKE, A., VERDE, P., … MARTINI, G. (2003). Failure to increase glucose consumption through the pentose-phosphate pathway results in the death of glucose-6-phosphate dehydrogenase gene-deleted mouse embryonic stem cells subjected to oxidative stress. *Biochemical Journal*, *370*(3), 935–943. https://doi.org/10.1042/bj20021614

Finlay, B., & Darlington, R. (1995). Linked regularities in the development and evolution of mammalian brains. *Science*, *268*(5217), 1578–1584. https://doi.org/10.1126/science.7777856

Fleming, T. P., Ghassemifar, M. R., & Sheth, B. (2000). Junctional complexes in the early mammalian embryo. *Seminars in Reproductive Medicine*. https://doi.org/10.1055/s-2000-12557

Fleming, T. P., Kwong, W. Y., Porter, R., Ursell, E., Fesenko, I., Wilkins, A., … Eckert, J. J. (2004). The embryo and its future. *Biology of Reproduction*, *71*(4), 1046–1054. https://doi.org/10.1095/biolreprod.104.030957

Fleming, T. P., Lucas, E. S., Watkins, A. J., & Eckert, J. J. (2012). Adaptive responses of the embryo to maternal diet and consequences for post-implantation development, 35–44.

Fleming, T. P., Velazquez, M. A., Eckert, J. J., Lucas, E. S., & Watkins, A. J. (2012). Nutrition of females during the peri-conceptional period and effects on foetal programming and health of offspring. *Animal Reproduction Science*, *130*(3–4), 193–197. https://doi.org/10.1016/j.anireprosci.2012.01.015

Fleming, T. P., Watkins, A. J., Sun, C., Velazquez, M. A., Smyth, N. R., & Eckert, J. J. (2015). Do little embryos make big decisions? How maternal dietary protein restriction can permanently change an embryo's potential, affecting adult health. *Reproduction, Fertility and Development*, *27*(4), 684–692. https://doi.org/10.1071/RD14455

Fleming, T. P., Watkins, A. J., Velazquez, M. A., Mathers, J. C., Prentice, A. M., Stephenson, J., … Godfrey, K. M. (2018). Origins of lifetime health around the time of conception: causes and consequences. *The Lancet*. https://doi.org/10.1016/S0140-6736(18)30312-X

Ford, J. H. (2013). Reduced quality and accelerated follicle loss with female reproductive aging - Does decline in theca dehydroepiandrosterone (DHEA) underlie the problem? *Journal of Biomedical Science*. https://doi.org/10.1186/1423-0127-20-93

Forsdahl, A. (1977). Are poor living conditions in childhood and adolescence an important risk factor for arteriosclerotic heart disease? *British Journal of Preventive & Social Medicine*, *31*(2), 91–95. https://doi.org/10.1136/jech.31.2.91

Fraichard, A., Chassande, O., Bilbaut, G., Dehay, C., Savatier, P., & Samarut, J. (1995). In vitro differentiation of embryonic stem cells into glial cells and functional neurons. *Journal of Cell Science*, *108 (Pt 1*, 3181–3188. https://doi.org/7593279

Frankel, S., Elwood, P., Sweetnam, P., Yarnell, J., & Smith, G. D. (1996). Birthweight, body-mass index in middle age, and incident coronary heart disease. *Lancet*, *348*(9040), 1478–1480. https://doi.org/10.1016/S0140-6736(96)03482-4

Gabrielsen, A., Bhatnager, P. R., Petersen, K., & Lindenberg, S. (2000). Influence of zona pellucida thickness of human embryos on clinical pregnancy outcome following in vitro fertilization treatment. *Journal of Assisted Reproduction and Genetics*, *17*(6), 323–328. https://doi.org/10.1023/A:1009453011321

Gallagher, E. a L., Newman, J. P., Green, L. R., & Hanson, M. a. (2005). The effect of low protein diet in pregnancy on the development of brain metabolism in rat offspring. *The Journal of Physiology*, *568*(2005), 553–558. https://doi.org/10.1113/jphysiol.2005.092825

García-Palomares, S., Navarro, S., Pertusa, J. F., Hermenegildo, C., García-Pérez, M. A., Rausell, F., … Tarín, J. J. (2009). Delayed Fatherhood in Mice Decreases Reproductive Fitness and Longevity of Offspring1. *Biology of Reproduction*, *80*(2), 343–349.

https://doi.org/10.1095/biolreprod.108.073395

Gardner, R. L., & Beddington, R. S. (1988). Multi-lineage “stem” cells in the mammalian embryo. *Journal of Cell Science. Supplement*, *10*, 11–27.

Gaspar-Maia, A., Alajem, A., Meshorer, E., & Ramalho-Santos, M. (2011). Open chromatin in pluripotency and reprogramming. *Nature Reviews Molecular Cell Biology*. https://doi.org/10.1038/nrm3036

Gavrilov, L. A., & Gavrilova, N. S. (1997). Parental age at conception and offspring longevity. *Reviews in Clinical Gerontology*. https://doi.org/10.1017/S0959259897000026

Gaztelumendi, N., & Nogués, C. (2014). Chromosome Instability in mouse Embryonic Stem Cells. *Scientific Reports*, *4*. https://doi.org/10.1038/srep05324

Gilbert, W. M., Nesbitt, T. S., & Danielsen, B. (1999). Childbearing beyond age 40: Pregnancy outcome in 24,032 cases. *Obstetrics and Gynecology*, *93*, 9–14. https://doi.org/10.1016/S0029-7844(98)00382-2

Gillespie, D. O. S., Russell, A. F., & Lummaa, V. (2013). The Effect Of Maternal Age And Reproductive History On Offspring Survival And Lifetime Reproduction In Preindustrial Humans. *Evolution*, *67*(7), 1964–1974. https://doi.org/10.1111/evo.12078

Gluckman, P. D., Cutfield, W., Hofman, P., & Hanson, M. A. (2005). The fetal, neonatal, and infant environments-the long-term consequences for disease risk. In *Early Human Development* (Vol. 81, pp. 51–59). https://doi.org/10.1016/j.earlhumdev.2004.10.003

Gluckman, P. D., & Hanson, M. A. (2004). Maternal constraint of fetal growth and its consequences. *Seminars in Fetal and Neonatal Medicine*. https://doi.org/10.1016/j.siny.2004.03.001

Gluckman, P. D., Hanson, M. A., & Beedle, A. S. (2007). Early life events and their consequences for later disease: A life history and evolutionary perspective. *American Journal of Human Biology*, *19*(1), 1–19. https://doi.org/10.1002/ajhb.20590

Gluckman, P. D., Hanson, M. A., & Spencer, H. G. (2005). Predictive adaptive responses and human evolution. *Trends in Ecology & Evolution*, *20*(10), 527–533. https://doi.org/10.1016/j.tree.2005.08.001

Gluckman, P. D., Hanson, M. A., Spencer, H. G., & Bateson, P. (2005). Environmental influences during development and their later consequences for health and disease: implications for the interpretation of empirical studies. *Proceedings of the Royal Society Biological Sciences Series B*, *272*(1564), 671–677. https://doi.org/10.1098/rspb.2004.3001

Godfrey, K. M., & Barker, D. J. P. (1995). Maternal nutrition in relation to fetal and placental growth. *European Journal of Obstetrics and Gynecology and Reproductive Biology*, *61*(1), 15–22. https://doi.org/10.1016/0028-2243(95)02148-L

Godfrey, K. M., & Barker, D. J. P. (2000). Fetal nutrition and adult disease. In *American Journal of Clinical Nutrition* (Vol. 71).

Godfrey, K. M., Reynolds, R. M., Prescott, S. L., Nyirenda, M., Jaddoe, V. W., Eriksson, J. G., & Broekman, B. F. (2017). Influence of maternal obesity on the long-term health of offspring. *The Lancet*, *5*, 53–64.

Goisis, A., Remes, H., Barclay, K., Martikainen, P., & Myrskylä, M. (2017). Advanced Maternal Age and the Risk of Low Birth Weight and Preterm Delivery: A Within-Family Analysis Using

Finnish Population Registers. *American Journal of Epidemiology*, *186*(11), 1219–1226. https://doi.org/10.1093/aje/kwx177

Gould, J. M., Smith, P. J., Airey, C. J., Mort, E. J., Airey, L. E., Warricker, F. D. M., … Willaime-Morawek, S. (2018). Mouse maternal protein restriction during preimplantation alone permanently alters brain neuron proportion and adult short-term memory. *Proceedings of the National Academy of Sciences*.

Graf, T., & Stadtfeld, M. (2008). Heterogeneity of Embryonic and Adult Stem Cells. *Cell Stem Cell*. https://doi.org/10.1016/j.stem.2008.10.007

Graham, S. J. L., Wicher, K. B., Jedrusik, A., Guo, G., Herath, W., Robson, P., & Zernicka-Goetz, M. (2014). BMP signalling regulates the pre-implantation development of extra-embryonic cell lineages in the mouse embryo. *Nature Communications*, *5*. https://doi.org/10.1038/ncomms6667

Greber, B., Wu, G., Bernemann, C., Joo, J. Y., Han, D. W., Ko, K., … Scholer, H. R. (2010). Conserved and divergent roles of FGF signaling in mouse epiblast stem cells and human embryonic stem cells. *Cell Stem Cell*, *6*, 215–226. https://doi.org/10.1016/j.stem.2010.01.003

Gstraunthaler, G., Lindl, T., & Van Der Valk, J. (2013). A plea to reduce or replace fetal bovine serum in cell culture media. *Cytotechnology*. https://doi.org/10.1007/s10616-013-9633-8

Guglielmino, M. R., Santonocito, M., Vento, M., Ragusa, M., Barbagallo, D., Borzì, P., … Di Pietro, C. (2011). TAp73 is downregulated in oocytes from women of advanced reproductive age. *Cell Cycle*. https://doi.org/10.4161/cc.10.19.17585

Guo, G., Pinello, L., Han, X., Lai, S., Shen, L., Lin, T. W., … Orkin, S. H. (2016). Serum-Based Culture Conditions Provoke Gene Expression Variability in Mouse Embryonic Stem Cells as Revealed by Single-Cell Analysis. *Cell Reports*, *14*(4), 956–965. https://doi.org/10.1016/j.celrep.2015.12.089

Guo, X. Y., Liu, X. M., Jin, L., Wang, T. T., Ullah, K., Sheng, J. Z., & Huang, H. F. (2017). Cardiovascular and metabolic profiles of offspring conceived by assisted reproductive technologies: a systematic review and meta-analysis. *Fertil Steril*, *107*(3), 622–631.e5. https://doi.org/10.1016/j.fertnstert.2016.12.007

Hack, M., Klein, N. K., & Taylor, H. G. (1995). Long-term developmental outcomes of low birth weight infants. *The Future of Children / Center for the Future of Children, the David and Lucile Packard Foundation*.

Hadjantonakis, a, & Papaioannou, V. (2001). The stem cells of early embryos. *Differentiation; Research in Biological Diversity*, *68*(4–5), 159–166.

Hamatani, T., Carter, M. G., Sharov, A. A., & Ko, M. S. (2004). Dynamics of global gene expression changes during mouse preimplantation development. *Dev Cell*, *6*(1), 117–131. https://doi.org/10.1016/S1534-5807(03)00373-3

Hamatani, T., Falco, G., Carter, M. G., Akutsu, H., Stagg, C. A., Sharov, A. A., … Ko, M. S. H. (2004). Age-associated alteration of gene expression patterns in mouse oocytes. *Human Molecular Genetics*, *13*(19), 2263–2278. https://doi.org/10.1093/hmg/ddh241

Handyside, A. H., & Hunter, S. (1986). Cell division and death in the mouse blastocyst before implantation. *Roux's Archives of Developmental Biology*, *195*(8), 519–526. https://doi.org/10.1007/BF00375893

Hanna, J., Saha, K., Pando, B., Van Zon, J., Lengner, C. J., Creyghton, M. P., … Jaenisch, R. (2009).

Direct cell reprogramming is a stochastic process amenable to acceleration. *Nature*, *462*(7273), 595–601. https://doi.org/10.1038/nature08592

Hansen, J. P. (1986). Older maternal age and pregnancy outcome: a review of the literature. *Obstetrical & Gynecological Survey*, *41*(11), 726–742. https://doi.org/10.1097/00006254-198611000-00024

Hanson, M. A., & Gluckman, P. D. (2008). Developmental Origins of Health and Disease: New Insights. *Basic & Clinical Pharmacology & Toxicology*, *102*(2), 90–93. https://doi.org/10.1111/j.1742-7843.2007.00186.x

Hansson, J., Rafiee, M. R., Reiland, S., Polo, J. M., Gehring, J., Okawa, S., … Krijgsveld, J. (2012). Highly Coordinated Proteome Dynamics during Reprogramming of Somatic Cells to Pluripotency. *Cell Reports*, *2*(6), 1579–1592. https://doi.org/10.1016/j.celrep.2012.10.014

Hao, J., Li, T. G., Qi, X., Zhao, D. F., & Zhao, G. Q. (2006). WNT/β-catenin pathway up-regulates Stat3 and converges on LIF to prevent differentiation of mouse embryonic stem cells. *Developmental Biology*, *290*(1), 81–91. https://doi.org/10.1016/j.ydbio.2005.11.011

Harlow, G. M., & Quinn, P. (1982). Development of preimplantation mouse embryos in vivo and in vitro. *Australian Journal of Biological Sciences*, *35*(2), 187–193. https://doi.org/10.1071/BI9820187

Harman, S. M., & Talbert, G. B. (1970). The effect of maternal age on ovulation, corpora lutea of pregnancy, and implantation failure in mice. *Journal of Reproduction and Fertility*, *23*, 33–39. https://doi.org/10.1530/jrf.0.0230033

Hart, R., & Norman, R. J. (2013). The longer-term health outcomes for children born as a result of ivf treatment: Part i-general health outcomes. *Human Reproduction Update*, *19*(3), 232–243. https://doi.org/10.1093/humupd/dms062

Harton, G. L., Munné, S., Surrey, M., Grifo, J., Kaplan, B., McCulloh, D. H., … Wells, D. (2013). Diminished effect of maternal age on implantation after preimplantation genetic diagnosis with array comparative genomic hybridization. *Fertility and Sterility*, *100*(6), 1695–1703. https://doi.org/10.1016/j.fertnstert.2013.07.2002

Hassold, T., Abruzzo, M., Adkins, K., Griffin, D., Merrill, M., Millie, E., … Zaragoza, M. (1996). Human aneuploidy: Incidence, origin and etiology. In *Environmental and Molecular Mutagenesis* (Vol. 28, pp. 167–175). https://doi.org/10.1002/(SICI)1098-2280(1996)28:3<167::AID-EM2>3.0.CO;2-B

Hayashi, K., Lopes, S. M. C. de S., Tang, F., & Surani, M. A. (2008). Dynamic Equilibrium and Heterogeneity of Mouse Pluripotent Stem Cells with Distinct Functional and Epigenetic States. *Cell Stem Cell*, *3*(4), 391–401. https://doi.org/10.1016/j.stem.2008.07.027

Herculano-Houzel, S., Collins, C. E., Wong, P., & Kaas, J. H. (2007). Cellular scaling rules for primate brains. *Proceedings of the National Academy of Sciences*, *104*(9), 3562–3567. https://doi.org/10.1073/pnas.0611396104

Hers, H. G., Hue, L., & Van Schaftingen, E. (1982). Fructose 2,6-bisphosphate. *Trends in Biochemical Sciences*, *7*(9), 329–331. https://doi.org/10.1016/0968-0004(82)90265-1

Herskind, A. M., McGue, M., Holm, N. V., Sørensen, T. I. A., Harvald, B., & Vaupel, J. W. (1996). The heritability of human longevity: A population-based study of 2872 Danish twin pairs born 1870-1900. *Human Genetics*, *97*(3), 319–323. https://doi.org/10.1007/s004390050042

Hillman, D. E., & Chen, S. (1981). Vulnerability of cerebellar development in malnutrition-I.

Quantitation of layer volume and neuron numbers. *Neuroscience*, *6*(7), 1249–1262. https://doi.org/10.1016/0306-4522(81)90185-8

Hochberg, Z. (2011). Developmental plasticity in child growth and maturation. *Frontiers in Endocrinology*. https://doi.org/10.3389/fendo.2011.00041

Hodges, C.A.; Ilagan, A; Jennings, D.; Keri, R,; Nilson, J.; Hunt, P. A. (2002). Experimental evidence that changes in oocyte growth influence meiotic chromosome segregation. *Human Reproduction*, *17*(5), 1171–1180. https://doi.org/10.1093/humrep/17.5.1171

Homayoun, H., Zahiri, S., Hemayatkhah Jahromi, V., & Hassanpour Dehnavi, A. (2016). Morphological and morphometric study of early-cleavage mice embryos resulting from in vitro fertilization at different cleavage stages after vitrification. *Iranian Journal of Veterinary Research*, *17*(1), 55–58.

Hovatta, O., Mikkola, M., Gertow, K., Strömberg, A. M., Inzunza, J., Hreinsson, J., … Ährlund-Richter, L. (2003). A culture system using human foreskin fibroblasts as feeder cells allows production of human embryonic stem cells. *Human Reproduction*, *18*, 1404–1409. https://doi.org/10.1093/humrep/deg290

Huang, J., Okuka, M., Wang, F., Zuo, B., Liang, P., Kalmbach, K., … Keefe, D. L. (2010). Generation of pluripotent stem cells from eggs of aging mice. *Aging Cell*, *9*(2), 113–125. https://doi.org/10.1111/j.1474-9726.2009.00539.x

Huang, L., Sauve, R., Birkett, N., Fergusson, D., & van Walraven, C. (2008). Maternal age and risk of stillbirth: a systematic review. *CMAJ : Canadian Medical Association Journal = Journal de l'Association Medicale Canadienne*, *178*(2), 165–172. https://doi.org/10.1503/cmaj.070150

Huang, Z., Hankinson, S. E., Colditz, G. A., Stampfer, M. J., Hunter, D. J., Manson, J. E., … Willett, W. C. (1997). Dual effects of weight and weight gain on breast cancer risk. *JAMA*, *278*(17), 1407–1411. https://doi.org/10.1001/jama.1997.03550170037029

Huynh, K. O., & Lee, J. T. (2003). Inheritance of a pre-inactivated paternal X chromosome in early mouse embryos. *Nature*, *426*(6968), 857–862. https://doi.org/10.1038/nature02222

Hyrapetian, M., Loucaides, E. M., & Sutcliffe, A. G. (2014). Health and disease in children born after assistive reproductive therapies (ART). *Journal of Reproductive Immunology*. https://doi.org/10.1016/j.jri.2014.08.001

Igarashi, H., Takahashi, T., & Nagase, S. (2015). Oocyte aging underlies female reproductive aging: biological mechanisms and therapeutic strategies. *Reproductive Medicine and Biology*, *14*(4), 159–169. https://doi.org/10.1007/s12522-015-0209-5

Inman, G. J. (2002). SB-431542 Is a Potent and Specific Inhibitor of Transforming Growth Factor-beta Superfamily Type I Activin Receptor-Like Kinase (ALK) Receptors ALK4, ALK5, and ALK7. *Molecular Pharmacology*, *62*(1), 65–74. https://doi.org/10.1124/mol.62.1.65

Innis, S. M. (2008). Dietary omega 3 fatty acids and the developing brain. *Brain Res*, *1237*, 35–43. https://doi.org/10.1016/j.brainres.2008.08.078

Ivanova, N., Dobrin, R., Lu, R., Kotenko, I., Levorse, J., DeCoste, C., … Lemischka, I. R. (2006). Dissecting self-renewal in stem cells with RNA interference. *Nature*, *442*(7102), 533–538. https://doi.org/10.1038/nature04915

Iwahashi, H., Takeshita, a, & Hanazawa, S. (2000). Prostaglandin E2 stimulates AP-1-mediated CD14 expression in mouse macrophages via cyclic AMP-dependent protein kinase A. *Journal of Immunology (Baltimore, Md. : 1950)*, *164*, 5403–5408.

https://doi.org/10.4049/jimmunol.164.10.5403

J.R., T., & C.J., W. (2005). Genomic imprinting and assisted reproductive technology: Connections and potential risks. *Seminars in Reproductive Medicine*, *23*(3), 285–295.

Jacobsson, B., Ladfors, L., & Milsom, I. (2004). Advanced maternal age and adverse perinatal outcome. *Obstetrics and Gynecology*, *104*(4), 727–733. https://doi.org/10.1097/01.AOG.0000140682.63746.be

Jahangiri, M., Shahhoseini, M., & Movaghar, B. (2014). H19 and MEST gene expression and histone modification in blastocysts cultured from vitrified and fresh two-cell mouse embryos. *Reproductive BioMedicine Online*, *29*(5), 559–566. https://doi.org/10.1016/j.rbmo.2014.07.006

Jahangiri, M., Shahhoseini, M., & Movaghar, B. (2018). The effect of vitrification on expression and histone marks of Igf2 and Oct4 in blastocysts cultured from two-cell mouse embryos. *Cell Journal*, *19*(4), 607–613. https://doi.org/10.22074/cellj.2018.3959

Janny, L., & Menezo, Y. J. (1996). Maternal age effect on early human embryonic development and blastocyst formation. *Molecular Reproduction and Development*, *45*(1), 31–37. https://doi.org/10.1002/(SICI)1098-2795(199609)45:1<31::AID-MRD4>3.0.CO;2-T

Jochems, C. E. A., Van der Valk, J. B. F., Stafleu, F. R., & Baumans, V. (2002). The use of fetal bovine serum: Ethical or scientific problem? *ATLA Alternatives to Laboratory Animals*, *30*(2), 219–227.

Johansson, B. M., & Wiles, M. V. (1995). Evidence for involvement of activin A and bone morphogenetic protein 4 in mammalian mesoderm and hematopoietic development. *Molecular and Cellular Biology*, *15*(1), 141–151. https://doi.org/10.1128/MCB.15.1.141

Johnson, F. B., Sinclair, D. A., & Guarente, L. (1999). Molecular biology of aging. *Cell*, *96*(2), 291–302. https://doi.org/S0092-8674(00)80567-X [pii]

Johnson, M. H., & McConnell, J. M. L. (2004). Lineage allocation and cell polarity during mouse embryogenesis. *Seminars in Cell and Developmental Biology*. https://doi.org/10.1016/j.semcdb.2004.04.002

Johnson, M. T., Mahmood, S., Hyatt, S. L., Yang, H. S., Soloway, P. D., Hanson, R. W., & Patel, M. S. (2001). Inactivation of the murine pyruvate dehydrogenase (Pdha1) gene and its effect on early embryonic development. *Molecular Genetics and Metabolism*, *74*, 293–302. https://doi.org/10.1006/mgme.2001.3249\rS1096-7192(01)93249-4 [pii]

Johnson, M. T., Mahmood, S., & Patel, M. S. (2003). Intermediary metabolism and energetics during murine early embryogenesis. *Journal of Biological Chemistry*. https://doi.org/10.1074/jbc.R300002200

Johnson, M. T., Yang, H. S., Magnuson, T., & Patel, M. S. (1997). Targeted disruption of the murine dihydrolipoamide dehydrogenase gene (Dld) results in perigastrulation lethality. *Proceedings of the National Academy of Sciences of the United States of America*, *94*(26), 14512–14517. https://doi.org/10.1073/pnas.94.26.14512

Jolly, M., Sebire, N., Harris, J., Robinson, S., & Regan, L. (2000). The risks associated with pregnancy in women aged 35 years or older. *Human Reproduction (Oxford, England)*, *15*, 2433–2437. https://doi.org/10.1093/humrep/15.11.2433

Joseph, K. S., Allen, A. C., Dodds, L., Turner, L. A., Scott, H., & Liston, R. (2005). The perinatal effects of delayed childbearing. *Obstetrics and Gynecology*, *105*(6), 1410–1418.

https://doi.org/10.1097/01.AOG.0000163256.83313.36

Jukic, A. M. Z., Weinberg, C. R., Baird, D. D., & Wilcox, A. J. (2011). The association of maternal factors with delayed implantation and the initial rise of urinary human chorionic gonadotrophin. *Human Reproduction*, *26*(4), 920–926. https://doi.org/10.1093/humrep/der009

Juliandi, B., Abematsu, M., & Nakashima, K. (2010). Epigenetic regulation in neural stem cell differentiation. *Development, Growth & Differentiation*, *52*(6), 493–504. https://doi.org/10.1111/j.1440-169X.2010.01175.x

Jung, J. H., Wang, X. D., & Loeken, M. R. (2013). Mouse embryonic stem cells established in physiological-glucose media express the high KM Glut2 glucose transporter expressed by normal embryos. *Stem Cells Transl Med*, *2*(12), 929–934. https://doi.org/10.5966/sctm.2013-0093

Jurdak, N., & Kanarek, R. B. (2009). Sucrose-induced obesity impairs novel object recognition learning in young rats. *Physiology & Behavior*, *96*, 1–5. https://doi.org/10.1016/j.physbeh.2008.07.023

Jurisicova, a, Rogers, I., Fasciani, a, Casper, R. F., & Varmuza, S. (1998). Effect of maternal age and conditions of fertilization on programmed cell death during murine preimplantation embryo development. *Molecular Human Reproduction*, *4*(2), 139–145. https://doi.org/10.1093/molehr/4.2.139

Jurisicova, A., Varmuza, S., & Casper, R. F. (1996). Programmed cell death and human embryo fragmentation. *Molecular Human Reproduction*, *2*(2), 93–98. https://doi.org/10.1093/molehr/2.2.93

Kader, A., Agarwal, A., Abdelrazik, H., Sharma, R. K., Ahmady, A., & Falcone, T. (2009). Evaluation of post-thaw DNA integrity of mouse blastocysts after ultrarapid and slow freezing. *Fertility and Sterility*, *91*(5 SUPPL.), 2087–2094. https://doi.org/10.1016/j.fertnstert.2008.04.049

KalantarMotamedi, Y., Peymani, M., Baharvand, H., Nasr-Esfahani, M. H., Bender, A., Zhu, S., … Karbalaei, K. (2016). Systematic selection of small molecules to promote differentiation of embryonic stem cells and experimental validation for generating cardiomyocytes. *Cell Death Discovery*, *2*, 16007. https://doi.org/10.1038/cddiscovery.2016.7

Källén, B., Finnström, O., Lindam, A., Nilsson, E., Nygren, K. G., & Otterblad, P. O. (2010a). Congenital malformations in infants born after in vitro fertilization in Sweden. *Birth Defects Research Part A - Clinical and Molecular Teratology*, *88*, 137–143. https://doi.org/10.1002/bdra.20645

Källén, B., Finnström, O., Lindam, A., Nilsson, E., Nygren, K. G., & Otterblad, P. O. (2010b). Congenital malformations in infants born after in vitro fertilization in Sweden. *Birth Defects Research Part A - Clinical and Molecular Teratology*, *88*(3), 137–143. https://doi.org/10.1002/bdra.20645

Källén, B., Finnström, O., Nygren, K. G., & Olausson, P. O. (2005). In vitro fertilization (IVF) in Sweden: Infant outcome after different IVF fertilization methods. *Fertility and Sterility*, *84*(3), 611–617. https://doi.org/10.1016/j.fertnstert.2005.02.038

Kalra, S. K., & Molinaro, T. A. (2008). The association of in vitro fertilization and perinatal morbidity. *Seminars in Reproductive Medicine*. https://doi.org/10.1055/s-0028-1087108

Kang, M.-H., Das, J., Gurunathan, S., Park, H.-W., Song, H., Park, C., & Kim, J.-H. (2017). The cytotoxic effects of dimethyl sulfoxide in mouse preimplantation embryos: a mechanistic

study. *Theranostics*, *7*(19), 4735–4752. https://doi.org/10.7150/thno.21662

Kang, W., Lee, M. S., & Baik, M. (2011). Dietary protein restriction alters lipid metabolism and insulin sensitivity in rats. *Asian-Australasian Journal of Animal Sciences*, *24*(9).

Katakura, M., Hashimoto, M., Okui, T., Shahdat, H. M., Matsuzaki, K., & Shido, O. (2013). Omega-3 polyunsaturated fatty acids enhance neuronal differentiation in cultured rat neural stem cells. *Stem Cells International*. https://doi.org/10.1155/2013/490476

Katakura, M., Hashimoto, M., Shahdat, H. M., Gamoh, S., Okui, T., Matsuzaki, K., & Shido, O. (2009). Docosahexaenoic acid promotes neuronal differentiation by regulating basic helix-loop-helix transcription factors and cell cycle in neural stem cells. *Neuroscience*, *160*(3), 651–660. https://doi.org/10.1016/j.neuroscience.2009.02.057

Kawasaki, H., Mizuseki, K., Nishikawa, S., Kaneko, S., Kuwana, Y., Nakanishi, S., … Sasai, Y. (2000). Induction of midbrain dopaminergic neurons from ES cells by stromal cell-derived inducing activity. *Neuron*, *28*(1), 31–40. https://doi.org/10.1016/S0896-6273(00)00083-0

Kawase, E., Suemori, H., Takahashi, N., Okazaki, K., Hashimoto, K., & Nakatsuji, N. (1994). Strain difference in establishment of mouse embryonic stem (ES) cell lines. *International Journal of Developmental Biology*, *38*(2), 385–390.

Keefer, C. L., Pant, D., Blomberg, L., & Talbot, N. C. (2007). Challenges and prospects for the establishment of embryonic stem cell lines of domesticated ungulates. *Animal Reproduction Science*, *98*(1–2), 147–168. https://doi.org/10.1016/j.anireprosci.2006.10.009

Kehoe, P., Mallinson, K., Bronzino, J., & McCormick, C. M. (2001). Effects of prenatal protein malnutrition and neonatal stress on CNS responsiveness. *Developmental Brain Research*, *132*(1), 23–31. https://doi.org/10.1016/S0165-3806(01)00292-9

Keller, G. M. (1995). In vitro differentiation of embryonic stem cells. *Current Opinion in Cell Biology*. https://doi.org/10.1016/0955-0674(95)80071-9

Kelly, Y. J., Nazroo, J. Y., McMunn, A., Boreham, R., & Marmot, M. (2001). Birthweight and behavioural problems in children: a modifiable effect? *International Journal of Epidemiology*, *30*(1), 88–94. https://doi.org/10.1093/ije/30.1.88

Kemkes-Grottenthaler, A. (2004). Parental effects on offspring longevity - Evidence from 17th to 19th century reproductive histories. *Annals of Human Biology*, *31*(2), 139–158. https://doi.org/10.1080/03014460410001663407

Khashan, A. S., Abel, K. M., McNamee, R., Pedersen, M. G., Webb, R. T., Baker, P. N., … Mortensen, P. B. (2008). Higher risk of offspring schizophrenia following antenatal maternal exposure to severe adverse life events. *Archives of General Psychiatry*, *65*(2), 146–152. https://doi.org/10.1001/archgenpsychiatry.2007.20

Khosla, S., Dean, W., Brown, D., Reik, W., & Feil, R. (2001). Culture of preimplantation mouse embryos affects fetal development and the expression of imprinted genes. *Biology of Reproduction*, *64*(3), 918–926. https://doi.org/10.1095/biolreprod64.3.918

Kim, Y. J., Lee, J. E., Kim, S. H., Shim, S. S., & Cha, D. H. (2013). Maternal age-specific rates of fetal chromosomal abnormalities in Korean pregnant women of advanced maternal age. *Obstetrics & Gynecology Science*, *56*(3), 160–166. https://doi.org/10.5468/ogs.2013.56.3.160

Kirz, D. S., Dorchester, W., & Freeman, R. K. (1985). Advanced maternal age: The mature gravida. *American Journal of Obstetrics and Gynecology*, *152*(1), 7–12.

https://doi.org/10.1016/S0002-9378(85)80166-6

Klincumhom, N., Pirity, M. K., Berzsenyi, S., Ujhelly, O., Muenthaisong, S., Rungarunlert, S., … Dinnyes, A. (2012). Generation of neuronal progenitor cells and neurons from mouse sleeping beauty transposon-generated induced pluripotent stem cells. *Cellular Reprogramming*, *14*(5), 390–397. https://doi.org/10.1089/cell.2012.0010

Knauff, E. a H., Eijkemans, M. J. C., Lambalk, C. B., ten Kate-Booij, M. J., Hoek, A., Beerendonk, C. C. M., … Fauser, B. C. J. M. (2009). Anti-Mullerian hormone, inhibin B, and antral follicle count in young women with ovarian failure. *The Journal of Clinical Endocrinology and Metabolism*, *94*(3), 786–792. https://doi.org/10.1210/jc.2008-1818

Knight, M., Kurinczuk, J. J., Spark, P., & Brocklehurst, P. (2009). Inequalities in maternal health: national cohort study of ethnic variation in severe maternal morbidities. *BMJ (Clinical Research Ed.)*, *338*, b542. https://doi.org/10.1136/bmj.b542

Kolialexi, A., Tsangaris, G. T., Antsaklis, A., Tzortzatou, F., Amentas, C., Koratzis, A., & Mavrou, A. (2001). Apoptosis in maternal peripheral blood during pregnancy. *Fetal Diagnosis and Therapy*, *16*(1), 32–37. https://doi.org/10.1159/000053877

Kondoh, H., Lleonart, M. E., Nakashima, Y., Yokode, M., Tanaka, M., Bernard, D., … Beach, D. (2006). A High Glycolytic Flux Supports the Proliferative Potential of Murine Embryonic Stem Cells. *Antioxidants & Redox Signaling*, *0*(0), 061221112325011. https://doi.org/10.1089/ars.2007.9.ft-14

Kopp, J. L., Ormsbee, B. D., Desler, M., & Rizzino, A. (2008). Small Increases in the Level of Sox2 Trigger the Differentiation of Mouse Embryonic Stem Cells. *Stem Cells*, *26*(4), 903–911. https://doi.org/10.1634/stemcells.2007-0951

Kovac, J. R., Addai, J., Smith, R. P., Coward, R. M., Lamb, D. J., & Lipshultz, L. I. (2013). The effects of advanced paternal age on fertility. *Asian Journal of Andrology*. https://doi.org/10.1038/aja.2013.92

Kramer, M. S., & Joseph, K. S. (1996). Enigma of fetal/infant-origins hypothesis. *Lancet*. https://doi.org/10.1016/S0140-6736(05)65750-9

Kumbak, B., Oral, E., & Bukulmez, O. (2012). Female obesity and assisted reproductive technologies. *Seminars in Reproductive Medicine*, *30*(6), 507–516. https://doi.org/10.1055/s-0032-1328879

Kunath, T., Saba-El-Leil, M. K., Almousailleakh, M., Wray, J., Meloche, S., & Smith, A. (2007). FGF stimulation of the Erk1/2 signalling cascade triggers transition of pluripotent embryonic stem cells from self-renewal to lineage commitment. *Development*, *134*(16), 2895–2902. https://doi.org/10.1242/dev.02880

Kushnir, V. A., Ludaway, T., Russ, R. B., Fields, E. J., Koczor, C., & Lewis, W. (2012). Reproductive aging is associated with decreased mitochondrial abundance and altered structure in murine oocytes. *Journal of Assisted Reproduction and Genetics*, *29*(7), 637–642. https://doi.org/10.1007/s10815-012-9771-5

Kwong, W. Y., Wild, a E., Roberts, P., Willis, a C., & Fleming, T. P. (2000). Maternal undernutrition during the preimplantation period of rat development causes blastocyst abnormalities and programming of postnatal hypertension. *Development*, *127*(19), 4195–4202. https://doi.org/10.1016/s0093-691x(99)00264-2

Laas, E., Lelong, N., Thieulin, A.-C., Houyel, L., Bonnet, D., Ancel, P.-Y., … Khoshnood, B. (2012). Preterm birth and congenital heart defects: a population-based study. *Pediatrics*, *130*(4),

e829-37. https://doi.org/10.1542/peds.2011-3279

Lands, B. (2012). Consequences of essential fatty acids. *Nutrients*. https://doi.org/10.3390/nu4091338

Lane, M., & Gardner, D. K. (1996). Selection of viable mouse blastocysts prior to transfer using a metabolic criterion. *Human Reproduction (Oxford, England)*, *11*(9), 1975–1978.

Langley-Evans, S. C. (2013). Fetal programming of CVD and renal disease: animal models and mechanistic considerations. *The Proceedings of the Nutrition Society*, *72*(3), 317–325. https://doi.org/10.1017/S0029665112003035

Langley-Evans, S. C. (2015). Nutrition in early life and the programming of adult disease: A review. *Journal of Human Nutrition and Dietetics*. https://doi.org/10.1111/jhn.12212

Langley-Evans, S. C., Gardner, D. S., & Jackson, A. A. (1996). Maternal protein restriction influences the programming of the rat hypothalamic-pituitary-adrenal axis. *The Journal of Nutrition*, *126*(6), 1578–1585.

Langley-Evans, S. C., Welham, S. J. M., & Jackson, A. A. (1999). Fetal exposure to a maternal low protein diet impairs nephrogenesis and promotes hypertension in the rat. *Life Sciences*, *64*(11), 965–974. https://doi.org/10.1016/S0024-3205(99)00022-3

Langley, M. T., Marek, D. M., Gardner, D. K., Doody, K. M., & Doody, K. J. (2001). Extended embryo culture in human assisted reproduction treatments. *Human Reproduction*, *16*(5), 902–908. https://doi.org/10.1093/humrep/16.5.902

Langley, S. C., & Jackson, a a. (1994). Increased systolic blood pressure in adult rats induced by fetal exposure to maternal low protein diets. *Clinical Science (London, England : 1979)*, *86*(2), 217–222; discussion 121. https://doi.org/10.1042/cs0860217

LANSING, A. I. (1947). A transmissible, cumulative, and reversible factor in aging. *Journal of Gerontology*, *2*(3), 228–239. https://doi.org/10.1093/geronj/2.3.228

Laopaiboon, M., Lumbiganon, P., Intarut, N., Mori, R., Ganchimeg, T., Vogel, J. P., … WHO Multicountry Survey on Maternal Newborn Health Research Network. (2014). Advanced maternal age and pregnancy outcomes: a multicountry assessment. *BJOG : An International Journal of Obstetrics and Gynaecology*, *121 Suppl*, 49–56. https://doi.org/10.1111/1471-0528.12659

Larman, M. G., Katz-Jaffe, M. G., McCallie, B., Filipovits, J. a, & Gardner, D. K. (2011). Analysis of global gene expression following mouse blastocyst cryopreservation. *Human Reproduction (Oxford, England)*, *26*(10), 2672–2680. https://doi.org/10.1093/humrep/der238

Latham, K. E. (2001). Embryonic genome activation. *Frontiers in Bioscience*, *6*(3), A639. https://doi.org/10.2741/A639

Lazaraviciute, G., Kauser, M., Bhattacharya, S., Haggarty, P., & Bhattacharya, S. (2014). A systematic review and meta-analysis of DNA methylation levels and imprinting disorders in children conceived by IVF/ICSI compared with children conceived spontaneously. *Human Reproduction Update*, *20*(6), 840–852. https://doi.org/10.1093/humupd/dmu033

Lee, G., Papapetrou, E. P., Kim, H., Chambers, S. M., Tomishima, M. J., Fasano, C. A., … Studer, L. (2009). Modelling pathogenesis and treatment of familial dysautonomia using patient-specific iPSCs. *Nature*, *461*(7262), 402–406. https://doi.org/10.1038/nature08320

Lee, K.-H., Chuang, C.-K., Guo, S.-F., & Tu, C.-F. (2012). Simple and Efficient Derivation of Mouse

Embryonic Stem Cell Lines Using Differentiation Inhibitors or Proliferation Stimulators. *Stem Cells and Development*. https://doi.org/10.1089/scd.2011.0021

Lee, K.-H., Li, M., Michalowski, A. M., Zhang, X., Liao, H., Chen, L., … Huang, J. (2010). A genomewide study identifies the Wnt signaling pathway as a major target of p53 in murine embryonic stem cells. *Proc Natl Acad Sci U S A*, *107*(1), 69–74. https://doi.org/10.1073/pnas.0909734107

Lee, K. sun, Ferguson, R. M., Corpuz, M., & Gartner, L. M. (1988). Maternal age and incidence of low birth weight at term: A population study. *American Journal of Obstetrics and Gynecology*, *158*(1), 84–89. https://doi.org/10.1016/0002-9378(88)90783-1

Lee, M. Y., Ryu, J. M., Lee, S. H., Park, J. H., & Han, H. J. (2010). Lipid rafts play an important role for maintenance of embryonic stem cell self-renewal. *Journal of Lipid Research*, *51*(8), 2082–2089. https://doi.org/10.1194/jlr.M001545

Lee, S. H., Lumelsky, N., Studer, L., Auerbach, J. M., & McKay, R. D. (2000). Efficient generation of midbrain and hindbrain neurons from mouse embryonic stem cells. *Nature Biotechnology*, *18*(6), 675–679. https://doi.org/10.1038/76536

Leese, H. J. (1995). Metabolic control during preimplantation mammalian development. *Human Reproduction Update*, *1*(1), 63–72. https://doi.org/10.1093/humupd/1.1.63

Leese, H. J., & Barton, A. M. (1984). Pyruvate and glucose uptake by mouse ova and preimplantation embryos. *Reproduction*, *72*(1), 9–13. https://doi.org/10.1530/jrf.0.0720009

Lerch, S., Brandwein, C., Dormann, C., Gass, P., & Chourbaji, S. (2015). Mice age - Does the age of the mother predict offspring behaviour? *Physiology and Behavior*, *147*, 157–162. https://doi.org/10.1016/j.physbeh.2015.04.041

Levant, B. (2013). N-3 (omega-3) polyunsaturated Fatty acids in the pathophysiology and treatment of depression: pre-clinical evidence. *CNS & Neurological Disorders Drug Targets*, *12*(4), 450–459. https://doi.org/10.2174/18715273113120400003

Li, J., Liu, S., Li, S., Feng, R., Na, L., Chu, X., … Sun, C. (2017). Prenatal exposure to famine and the development of hyperglycemia and type 2 diabetes in adulthood across consecutive generations: A population-based cohort study of families in Suihua, China. *American Journal of Clinical Nutrition*, *105*(1), 221–227. https://doi.org/10.3945/ajcn.116.138792

Li, M., Ma, W., Hou, Y., Sun, X.-F., Sun, Q.-Y., & Wang, W.-H. (2004). Improved isolation and culture of embryonic stem cells from Chinese miniature pig. *The Journal of Reproduction and Development*, *50*(2), 237–244. https://doi.org/10.1262/jrd.50.237

Li, M., Pevny, L., Lovell-Badge, R., & Smith, A. (1998). Generation of purified neural precursors from embryonic stem cells by lineage selection. *Current Biology*, *8*(17), 971-S2. https://doi.org/10.1016/S0960-9822(98)70399-9

Li, V. C., & Kirschner, M. W. (2014). Molecular ties between the cell cycle and differentiation in embryonic stem cells. *Proceedings of the National Academy of Sciences of the United States of America*, *111*(26), 9503–9508. https://doi.org/10.1073/pnas.1408638111

Li, W., & Ding, S. (2010). Small molecules that modulate embryonic stem cell fate and somatic cell reprogramming. *Trends in Pharmacological Sciences*. https://doi.org/10.1016/j.tips.2009.10.002

Li, X.-Y., Di, K.-Q., & Wei, W. (2005). Effects of Genetic Background on Establishment of Mouse Embryonic Stem Cells. *Zoological Research*, *26*, 250–254.

Li, Y., Jaddoe, V. W., Qi, L., He, Y., Lai, J., Wang, J., … Ma, G. (2011). Exposure to the Chinese famine in early life and the risk of hypertension in adulthood. *Journal of Hypertension*, *29*(6), 1085–1092. https://doi.org/10.1097/HJH.0b013e328345d969

Li, Y., Jaddoe, V. W., Qi, L., He, Y., Wang, D., Lai, J., … Hu, F. B. (2011). Exposure to the Chinese famine in early life and the risk of metabolic syndrome in adulthood. *Diabetes Care*, *34*(4), 1014–1018. https://doi.org/10.2337/dc10-2039

Lialios, G., Kaponis, A., & Adonakis, G. (1999). Maternal age as an independent risk factor for cesarean delivery. *International Journal of Gynecology and Obstetrics*. https://doi.org/10.1016/S0020-7292(99)00112-5

Lind, M. I., Berg, E. C., Alavioon, G., & Maklakov, A. A. (2015). Evolution of differential maternal age effects on male and female offspring development and longevity. *Functional Ecology*, *29*(1), 104–110. https://doi.org/10.1111/1365-2435.12308

Lipman, T., & Tiedje, L. B. (2006). Epigenetic Differences Arise During the Lifetime of Monozygotic Twins. *MCN, The American Journal of Maternal/Child Nursing*. https://doi.org/10.1097/00005721-200605000-00016

Lister, J. P., Blatt, G. J., DeBassio, W. A., Kemper, T. L., Tonkiss, J., Galler, J. R., & Rosene, D. L. (2005). Effect of prenatal protein malnutrition on numbers of neurons in the principal cell layers of the adult rat hippocampal formation. *Hippocampus*, *15*(3), 393–403. https://doi.org/10.1002/hipo.20065

Liu, K., Case, A., Cheung, A. P., Sierra, S., AlAsiri, S., Carranza-Mamane, B., … Wong, B. C. M. (2011). Advanced Reproductive Age and Fertility. *Journal of Obstetrics and Gynaecology Canada*, *33*(11), 1165–1175. https://doi.org/10.1016/S1701-2163(16)35087-3

Liu, N., Lu, M., Tian, X., & Han, Z. (2007). Molecular mechanisms involved in self-renewal and pluripotency of embryonic stem cells. *Journal of Cellular Physiology*. https://doi.org/10.1002/jcp.20978

Liu, X., Wei, Q., Zhang, J., Yang, W., Zhao, X., & Ma, B. (2015). Derivation of embryonic stem cells from Kunming mice IVF blastocyst in feeder- and serum-free condition. *In Vitro Cellular and Developmental Biology - Animal*, *51*(6), 541–545. https://doi.org/10.1007/s11626-014-9863-x

Lopes, F. L., Fortier, A. L., Darricarrère, N., Chan, D., Arnold, D. R., & Trasler, J. M. (2009). Reproductive and epigenetic outcomes associated with aging mouse oocytes. *Human Molecular Genetics*, *18*(11), 2032–2044. https://doi.org/10.1093/hmg/ddp127

Lopez-Cardona, A. P., Fernandez-Gonzalez, R., Perez-Crespo, M., Alen, F., de Fonseca, F. R., Orio, L., & Gutierrez-Adan, A. (2015). Effects of Synchronous and Asynchronous Embryo Transfer on Postnatal Development, Adult Health, and Behavior in Mice. *Biology of Reproduction*, *93*(4), 85–85. https://doi.org/10.1095/biolreprod.115.130385

Lossos, I. S., Czerwinski, D. K., Wechser, M. A., & Levy, R. (2003). Optimization of quantitative real-time RT-PCR parameters for the study of lymphoid malignancies. *Leukemia*, *17*(4), 789–795. https://doi.org/10.1038/sj.leu.2402880

Ludwig, M., Katalinic, A., Groß, S., Sutcliffe, A., Varon, R., & Horsthemke, B. (2005). Increased prevalence of imprinting defects in patients with Angelman syndrome born to subfertile couples. *Journal of Medical Genetics*. https://doi.org/10.1136/jmg.2004.026930

Luke, B., Gopal, D., Cabral, H., Stern, J. E., & Diop, H. (2017). Pregnancy, birth, and infant outcomes by maternal fertility status: the Massachusetts Outcomes Study of Assisted

Reproductive Technology. *American Journal of Obstetrics and Gynecology*, *217*(3), 327.e1-327.e14. https://doi.org/10.1016/j.ajog.2017.04.006

Luzzo, K. M., Wang, Q., Purcell, S. H., Chi, M., Jimenez, P. T., Grindler, N., … Moley, K. H. (2012). High Fat Diet Induced Developmental Defects in the Mouse: Oocyte Meiotic Aneuploidy and Fetal Growth Retardation/Brain Defects. *PLoS ONE*, *7*(11). https://doi.org/10.1371/journal.pone.0049217

Maekawa, M., Watanabe, A., Iwayama, Y., Kimura, T., Hamazaki, K., Balan, S., … Yoshikawa, T. (2017). Polyunsaturated fatty acid deficiency during neurodevelopment in mice models the prodromal state of schizophrenia through epigenetic changes in nuclear receptor genes. *Translational Psychiatry*, *7*(9). https://doi.org/10.1038/tp.2017.182

Maher, E., Brueton, L., Bowdin, S., Luharia, A., Cooper, W., Cole, T., … Hawkins, M. (2003). Beckwith-Wiedemann syndrome and assisted reproduction technology (ART). *Journal of Medical Genetics*, *40*(1), 62–64. https://doi.org/10.1136/jmg.40.1.62

Maher, E. R., Afnan, M., & Barratt, C. L. (2003). Epigenetic risks related to assited reproductive technologies: Epigenetics, imprinting, ART and icebergs? *Human Reproduction*. https://doi.org/10.1093/humrep/deg486

Mamo, S., Bodo, S., Kobolak, J., Polgar, Z., Tolgyesi, G., & Dinnyes, A. (2006). Gene expression profiles of vitrified in vivo derived 8-cell stage mouse embryos detected by high density oligonucleotide microarrays. *Molecular Reproduction and Development*, *73*(11), 1380–1392. https://doi.org/10.1002/mrd.20588

Mann, M. A., Kinsley, C., Broida, J., & Svare, B. (1983). Infanticide exhibited by female mice: Genetic, developmental and hormonal influences. *Physiology and Behavior*, *30*(5), 697–702. https://doi.org/10.1016/0031-9384(83)90165-8

Marks, H., Kalkan, T., Menafra, R., Denissov, S., Jones, K., Hofemeister, H., … Stunnenberg, H. G. (2012). The transcriptional and epigenomic foundations of ground state pluripotency. *Cell*, *149*(3), 590–604. https://doi.org/10.1016/j.cell.2012.03.026

Markunas, C. A., Wilcox, A. J., Xu, Z., Joubert, B. R., Harlid, S., Panduri, V., … Taylor, J. A. (2016). Maternal age at delivery is associated with an epigenetic signature in both newborns and adults. *PLoS ONE*, *11*(7). https://doi.org/10.1371/journal.pone.0156361

Martin, G. R. (1981). Isolation of a pluripotent cell line from early mouse embryos cultured in medium conditioned by teratocarcinoma stem cells. *Proceedings of the National Academy of Sciences of the United States of America*, *78*, 7634–7638. https://doi.org/10.1073/pnas.78.12.7634

Martin, G. R., & Evans, M. J. (1974). The morphology and growth of a pluripotent teratocarcinoma cell line and its derivatives in tissue culture. *Cell*, *2*(3), 163–172. https://doi.org/10.1016/0092-8674(74)90090-7

Martin, J. A., Hamilton, B. E., D, P., Sutton, P. D., Ventura, S. J., Menacker, F., … Statistics, V. (2015). National Vital Statistics Reports Births : Final Data for 2013. *Statistics*, *64*(1), 1–104. https://doi.org/May 8, 2013

Martin, J. A., Hamilton, B. E., Osterman, M. J. K., Driscoll, A. K., & Mathews, T. J. (2017). Births: Final Data for 2015. *National Vital Statistics Reports : From the Centers for Disease Control and Prevention, National Center for Health Statistics, National Vital Statistics System*, *66*(1), 1. https://doi.org/May 8, 2013

Martin, R. H. (2008). Meiotic errors in human oogenesis and spermatogenesis. *Reproductive*

BioMedicine Online, *16*(4), 523–531. https://doi.org/10.1016/S1472-6483(10)60459-2

Martinez, Y., Béna, F., Gimelli, S., Tirefort, D., Dubois-Dauphin, M., Krause, K. H., & Preynat-Seauve, O. (2012). Cellular diversity within embryonic stem cells: Pluripotent clonal sublines show distinct differentiation potential. *Journal of Cellular and Molecular Medicine*, *16*(3), 456–467. https://doi.org/10.1111/j.1582-4934.2011.01334.x

Martyn, C. N., Barker, D. J., Jespersen, S., Greenwald, S., Osmond, C., & Berry, C. (1995). Growth in utero, adult blood pressure, and arterial compliance. *British Heart Journal*, *73*(2), 116–121. https://doi.org/10.1136/hrt.73.2.116

Martyn, C. N., Barker, D. J. P., & Osmond, C. (1996). Mothers' pelvic size, fetal growth, and death from stroke and coronary heart disease in men in the UK. *Lancet*, *348*(9037), 1264–1268. https://doi.org/10.1016/S0140-6736(96)04257-2

Marwarha, G., Claycombe-Larson, K., Schommer, J., & Ghribi, O. (2017). Maternal low-protein diet decreases brain-derived neurotrophic factor expression in the brains of the neonatal rat offspring. *The Journal of Nutritional Biochemistry*, *45*, 54–66. https://doi.org/10.1016/j.jnutbio.2017.03.005

Massip, A., Van Der Zwalmen, P., & Leroy, F. (1984). Effect of stage of development on survival of mouse embryos frozen-thawed rapidly. *Cryobiology*, *21*(5), 574–577. https://doi.org/10.1016/0011-2240(84)90057-9

Master, J. S., Thouas, G. A., Harvey, A. J., Sheedy, J. R., Hannan, N. J., Gardner, D. K., & Wlodek, M. E. (2015). Low female birth weight and advanced maternal age programme alterations in next-generation blastocyst development. *Reproduction*, *149*(5), 497–510. https://doi.org/10.1530/REP-14-0619

Masui, S., Nakatake, Y., Toyooka, Y., Shimosato, D., Yagi, R., Takahashi, K., … Niwa, H. (2007). Pluripotency governed by Sox2 via regulation of Oct3/4 expression in mouse embryonic stem cells. *Nature Cell Biology*, *9*(6), 625–635. https://doi.org/10.1038/ncb1589

Mathieu, G., Denis, S., Lavialle, M., & Vancassel, S. (2008). Synergistic effects of stress and omega-3 fatty acid deprivation on emotional response and brain lipid composition in adult rats. *Prostaglandins Leukot Essent Fatty Acids*, *78*(6), 391–401. https://doi.org/10.1016/j.plefa.2008.05.003

Matsuda, T., Nakamura, T., Nakao, K., Arai, T., Katsuki, M., Heike, T., & Yokota, T. (1999). STAT3 activation is sufficient to maintain an undifferentiated state of mouse embryonic stem cells. *EMBO Journal*, *18*(15), 4261–4269. https://doi.org/10.1093/emboj/18.15.4261

McCall, S. J., Nair, M., & Knight, M. (2016). Factors associated with maternal mortality at advanced maternal age: a population-based case-control study. *BJOG : An International Journal of Obstetrics and Gynaecology*, Published Online. https://doi.org/10.1111/1471-0528.14216

Mccance, D. R., Pettitt, D. J., Hanson, R. L., Jacobsson, L. T. H., Knowler, W. C., & Bennett, P. H. (1994). Birth weight and non-insulin dependent diabetes: Thrifty genotype, thrifty phenotype, or surviving small baby genotype? *BMJ*, *308*(6934), 942. https://doi.org/10.1136/bmj.308.6934.942

McCauley, B. S., & Dang, W. (2014). Histone methylation and aging: Lessons learned from model systems. *Biochimica et Biophysica Acta - Gene Regulatory Mechanisms*. https://doi.org/10.1016/j.bbagrm.2014.05.008

McDonald, S. D., Han, Z., Mulla, S., Murphy, K. E., Beyene, J., & Ohlsson, A. (2009). Preterm birth

and low birth weight among in vitro fertilization singletons: A systematic review and meta-analyses. *European Journal of Obstetrics Gynecology and Reproductive Biology*. https://doi.org/10.1016/j.ejogrb.2009.05.035

McMahon, J. A., Takada, S., Zimmerman, L. B., Fan, C. M., Harland, R. M., & McMahon, A. P. (1998). Noggin-mediated antagonism of BMP signaling is required for growth and patterning of the neural tube and somite. *Genes and Development*, *12*(10), 1438–1452. https://doi.org/10.1101/gad.12.10.1438

Mcmillen, I. C. (2005). Developmental Origins of the Metabolic Syndrome: Prediction, Plasticity, and Programming. *Physiological Reviews*, *85*(2), 571–633. https://doi.org/10.1152/physrev.00053.2003

McMillen, & Robinson. (2005). Developmental origins of the metabolic syndrome: prediction, plasticity, and programming. *Physiological Reviews*, *85*, 571–633. https://doi.org/10.1152/physrev.00053.2003

McNamara, R. K., & Carlson, S. E. (2006). Role of omega-3 fatty acids in brain development and function: potential implications for the pathogenesis and prevention of psychopathology. *Prostaglandins Leukot Essent Fatty Acids*, *75*(4–5), 329–349. https://doi.org/10.1016/j.plefa.2006.07.010

Mebratu, Y., & Tesfaigzi, Y. (2009). How ERK1/2 activation controls cell proliferation and cell death is subcellular localization the answer? *Cell Cycle*. https://doi.org/10.4161/cc.8.8.8147

Meden-Vrtovec, H. (2004). Ovarian aging and infertility. *Clinical and Experimental Obstetrics and Gynecology*. https://doi.org/10.17772/gp/1580

Mercader, A., Valbuena, D., & Simon, C. (2006). Human embryo culture. *Methods Enzymol*, *420*, 3–18. https://doi.org/10.1016/S0076-6879(06)20001-6

Mitalipov, S., & Wolf, D. (2009). Totipotency, pluripotency and nuclear reprogramming. *Advances in Biochemical Engineering/Biotechnology*, *114*, 185–199. https://doi.org/10.1007/10_2008_45

Mitchell, B. D., Hsueh, W. C., King, T. M., Pollin, T. I., Sorkin, J., Agarwala, R., … Shuldiner, A. R. (2001). Heritability of life span in the old order amish. *American Journal of Medical Genetics*, *102*(4), 346–352. https://doi.org/10.1002/ajmg.1483

Mitchell, M., Schulz, S. L., Armstrong, D. T., & Lane, M. (2009). Metabolic and mitochondrial dysfunction in early mouse embryos following maternal dietary protein intervention. *Biology of Reproduction*, *80*(4), 622–630. https://doi.org/10.1095/biolreprod.108.072595

Mitsui, K., Tokuzawa, Y., Itoh, H., Segawa, K., Murakami, M., Takahashi, K., … Yamanaka, S. (2003). The homeoprotein nanog is required for maintenance of pluripotency in mouse epiblast and ES cells. *Cell*, *113*(5), 631–642. https://doi.org/10.1016/S0092-8674(03)00393-3

Moaddab, A., Chervenak, F. A., Mccullough, L. B., Sangi-Haghpeykar, H., Shamshirsaz, A. A., Schutt, A., … Shamshirsaz, A. A. (2017). Effect of advanced maternal age on maternal and neonatal outcomes in assisted reproductive technology pregnancies. *European Journal of Obstetrics Gynecology and Reproductive Biology*, *216*, 178–183. https://doi.org/10.1016/j.ejogrb.2017.07.029

Mohammadzadeh, M., Fesahat, F., Khoradmehr, A., & Khalili, M. A. (2018). Influential effect of age on oocyte morphometry, fertilization rate and embryo development following IVF in mice. *Middle East Fertility Society Journal*, *23*(2), 117–120. https://doi.org/10.1016/j.mefs.2017.09.006

Mohan, C. (1974). Age-Dependent in a Colony, 83–84.

Monk, M., & Harper, M. I. (1979). Sequential X chromosome inactivation coupled with cellular differentiation in early mouse embryos. *Nature*, *281*, 311.

Morgan, H. D., Santos, F., Green, K., Dean, W., & Reik, W. (2005). Epigenetic reprogramming in mammals. *Human Molecular Genetics*. https://doi.org/10.1093/hmg/ddi114

Morgane, P. J., Austin-LaFrance, R., Bronzino, J., Tonkiss, J., Díaz-Cintra, S., Cintra, L., … Galler, J. R. (1993). Prenatal malnutrition and development of the brain. *Neuroscience and Biobehavioral Reviews*, *17*(1), 91–128. https://doi.org/10.1016/S0149-7634(05)80234-9

Morris, S. A., & Zernicka-Goetz, M. (2012). Formation of distinct cell types in the mouse blastocyst. *Results Probl Cell Differ*, *55*, 203–217. https://doi.org/10.1007/978-3-642-30406-4_11

Morrison, J. L., & Regnault, T. R. H. (2016). Nutrition in pregnancy: Optimising maternal diet and fetal adaptations to altered nutrient supply. *Nutrients*, *8*(6). https://doi.org/10.3390/nu8060342

Mukhopadhaya, N., & Arulkumaran, S. (2007). Reproductive outcomes after in-vitro fertilization. *Current Opinion in Obstetrics & Gynecology*, *19*(2), 113–119. https://doi.org/10.1097/GCO.0b013e32807fb199

Mumm, H., Kamper-Jørgensen, M., Nybo Andersen, A. M., Glintborg, D., & Andersen, M. (2013). Birth weight and polycystic ovary syndrome in adult life: A register-based study on 523,757 Danish women born 1973-1991. *Fertility and Sterility*, *99*(3), 777–782. https://doi.org/10.1016/j.fertnstert.2012.11.004

Munné, S. (2006). Chromosome abnormalities and their relationship to morphology and development of human embryos. *Reproductive BioMedicine Online*. https://doi.org/10.1016/S1472-6483(10)60866-8

Muñoz-Sanjuán, I., & Brivanlou, A. H. (2002). Neural induction, the default model and embryonic stem cells. *Nature Reviews Neuroscience*. https://doi.org/10.1038/nrn786

Murray, P., & Edgar, D. (2001). The regulation of embryonic stem cell differentiation by leukaemia inhibitory factor (LIF). *Differentiation*, *68*(4–5), 227–234. https://doi.org/10.1046/j.1432-0436.2001.680410.x

Nagy, A., Rossant, J., Nagy, R., Abramow-Newerly, W., & Roder, J. C. (1993). Derivation of completely cell culture-derived mice from early-passage embryonic stem cells. *Proceedings of the National Academy of Sciences of the United States of America*, *90*(18), 8424–8428. https://doi.org/10.1073/pnas.90.18.8424

Nathanielsz, P. W. (2006). Animal models that elucidate basic principles of the developmental origins of adult diseases. *ILAR Journal*. https://doi.org/10.1093/ilar.47.1.73

Niakan, K. K., Han, J., Pedersen, R. A., Simon, C., & Pera, R. A. R. (2012). Human pre-implantation embryo development. *Development (Cambridge, England)*, *139*(5), 829–841. https://doi.org/10.1242/dev.060426

Nicholas, L. M., Morrison, J. L., Rattanatray, L., Zhang, S., Ozanne, S. E., & McMillen, I. C. (2016). The early origins of obesity and insulin resistance: Timing, programming and mechanisms. *International Journal of Obesity*, *40*(2), 229–238. https://doi.org/10.1038/ijo.2015.178

Nichols, J., & Ying, Q.-L. (2006). Derivation and propagation of embryonic stem cells in serum- and

feeder-free culture. *Methods in Molecular Biology (Clifton, N.J.)*, *329*, 91–98. https://doi.org/10.1385/1-59745-037-5:91

Niemann, H., & Wrenzycki, C. (2000). Alterations of expression of developmentally important genes in preimplantation bovine embryos by in vitro culture conditions: Implications for subsequent development. In *Theriogenology* (Vol. 53, pp. 21–34). https://doi.org/10.1016/S0093-691X(99)00237-X

Niemitz, E. L., & Feinberg, A. P. (2004). Epigenetics and Assisted Reproductive Technology: A Call for Investigation. *The American Journal of Human Genetics*, *74*(4), 599–609. https://doi.org/10.1086/382897

Niwa, H., Burdon, T., Chambers, I., & Smith, A. (1998). Self-renewal of pluripotent embryonic stem cells is mediated via activation of STAT3. *Genes & Development*, *12*(13), 2048–2060. https://doi.org/10.1101/gad.12.13.2048

Niwa, H., Ogawa, K., Shimosato, D., & Adachi, K. (2009). A parallel circuit of LIF signalling pathways maintains pluripotency of mouse ES cells. *Nature*, *460*(7251), 118–122. https://doi.org/10.1038/nature08113

Noback, C. R., & Eisenman, L. M. (1981). Some effects of protein-calorie undernutrition on the developing central nervous system of the rat. *The Anatomical Record*, *201*(1), 67–73. https://doi.org/10.1002/ar.1092010109

Notkola, V. J., & Husman, K. R. (1988). Mortality among female farmers in Finland in 1979-1985. *Scandinavian Journal of Social Medicine*, *16*(3), 187–191. https://doi.org/10.1177/140349488801600312

Odibo, A. O., Nelson, D., Stamilio, D. M., Sehdev, H. M., & Macones, G. A. (2006). Advanced maternal age is an independent risk factor for intrauterine growth restriction. *American Journal of Perinatology*, *23*(5), 325–328. https://doi.org/10.1055/s-2006-947164

Office for National Statistics. (2016). Births in England and Wales, *2011*(November), 1–10.

Ohtsuka, S., Nakai-Futatsugi, Y., & Niwa, H. (2015). LIF signal in mouse embryonic stem cells. *JAK-STAT*. https://doi.org/10.1080/21623996.2015.1086520

Ohtsuka, T., Ishibashi, M., Gradwohl, G., Nakanishi, S., & Kageyama, R. (1999). Hes1 and Hes5 as Notch effectors in mammalian neuronal differentiation. *The EMBO Journal*. https://doi.org/10.1093/emboj/18.8.2196

Okano, M., Bell, D. W., Haber, D. A., & Li, E. (1999). DNA methyltransferases Dnmt3a and Dnmt3b are essential for de novo methylation and mammalian development. *Cell*, *99*(3), 247–257. https://doi.org/10.1016/S0092-8674(00)81656-6

Okun, N., Sierra, S., Douglas Wilson, R., Audibert, F., Brock, J. A., Campagnolo, C., … Robson, H. (2014). Pregnancy Outcomes After Assisted Human Reproduction. *Journal of Obstetrics and Gynaecology Canada*, *36*(1), 64–83. https://doi.org/10.1016/S1701-2163(15)30685-X

Ombelet, W., Martens, G., De Sutter, P., Gerris, J., Bosmans, E., Ruyssinck, G., … Gyselaers, W. (2006). Perinatal outcome of 12 021 singleton and 3108 twin births after non-IVF-assisted reproduction: A cohort study. *Human Reproduction*, *21*(4), 1025–1032. https://doi.org/10.1093/humrep/dei419

Ornoy, A., & Ergaz, Z. (2010). Alcohol abuse in pregnant women: Effects on the fetus and newborn, mode of action and maternal treatment. *International Journal of Environmental Research and Public Health*. https://doi.org/10.3390/ijerph7020364

Osmond, C., Barker, D. J., Winter, P. D., Fall, C. H., & Simmonds, S. J. (1993). Early growth and death from cardiovascular disease in women. *BMJ (Clinical Research Ed.)*, *307*(6918), 1519–1524. https://doi.org/10.1136/bmj.307.6918.1519

Ota, E., Haruna, M., Suzuki, M., Anh, D. D., Tho, L. H., Tam, N. T. T., … Yanai, H. (2011). Maternal body mass index and gestational weight gain and their association with perinatal outcomes in Viet Nam. *Bulletin of the World Health Organization*, *89*(2), 127–136. https://doi.org/10.2471/BLT.10.077982

Paczkowski, M., Schoolcraft, W. B., & Krisher, R. L. (2015). Dysregulation of methylation and expression of imprinted genes in oocytes and reproductive tissues in mice of advanced maternal age. *Journal of Assisted Reproduction and Genetics*, *32*(5), 713–723. https://doi.org/10.1007/s10815-015-0463-9

Padmanabhan, V., Cardoso, R. C., & Puttabyatappa, M. (2016). Developmental programming, a pathway to disease. *Endocrinology*. https://doi.org/10.1210/en.2016-1003

Painter, R. C., De Rooij, S. R., Bossuyt, P. M., Simmers, T. A., Osmond, C., Barker, D. J., … Roseboom, T. J. (2006). Early onset of coronary artery disease after prenatal exposure to the Dutch famine. *American Journal of Clinical Nutrition*, *84*(2), 322–327. https://doi.org/84/2/322 [pii]

Pan, H., Ma, P., Zhu, W., & Schultz, R. M. (2008). Age-associated increase in aneuploidy and changes in gene expression in mouse eggs. *Developmental Biology*, *316*(2), 397–407. https://doi.org/10.1016/j.ydbio.2008.01.048

Pandey, S., Shetty, A., Hamilton, M., Bhattacharya, S., & Maheshwari, A. (2012). Obstetric and perinatal outcomes in singleton pregnancies resulting from ivf/icsi: A systematic review and meta-analysis. *Human Reproduction Update*. https://doi.org/10.1093/humupd/dms018

Pantaleon, M., & Kaye, P. L. (1998). Glucose transporters in preimplantation development. *Reviews of Reproduction*, *3*, 77–81. https://doi.org/10.1530/ROR.0.0030077

Pantos, K., Meimeti-Damianaki, T., Vaxevanoglou, T., & Kapetanakis, E. (1993). Oocyte donation in menopausal women aged over 40 years. *Human Reproduction Oxford England*, *8*(3), 488–491.

Park, S.-J., Kim, S., Kim, S.-Y., Jeon, N. L., Song, J. M., Won, C., & Min, D.-H. (2017). Highly Efficient and Rapid Neural Differentiation of Mouse Embryonic Stem Cells Based on Retinoic Acid Encapsulated Porous Nanoparticle. *ACS Applied Materials and Interfaces*, *9*(40). https://doi.org/10.1021/acsami.7b09760

Park, Y.-G., Lee, S.-E., Kim, E.-Y., Hyun, H., Shin, M.-Y., Son, Y.-J., … Park, S.-P. (2015). Effects of Feeder Cell Types on Culture of Mouse Embryonic Stem Cell In Vitro. *Development & Reproduction*, *19*(3), 119–126. https://doi.org/10.12717/DR.2015.19.3.119

Pasupathy, D., Wood, A. M., Pell, J. P., Fleming, M., & Smith, G. C. S. (2011). Advanced maternal age and the risk of perinatal death due to intrapartum anoxia at term. *Journal of Epidemiology and Community Health*, *65*(3), 241–245. https://doi.org/10.1136/jech.2009.097170

Paulson, R. J., Boostanfar, R., Saadat, P., Mor, E., Tourgeman, D. E., Slater, C. C., … Jain, J. K. (2002). Pregnancy in the sixth decade of life: obstetric outcomes in women of advanced reproductive age. *JAMA : The Journal of the American Medical Association*, *288*(18), 2320–2323. https://doi.org/10.1097/01.OGX.0000058691.18516.26

Paulson, R. J., Hatch, I. E., Lobo, R. A., & Sauer, M. V. (1997). Cumulative conception and live birth

rates after oocyte donation: Implications regarding endometrial receptivity. *Human Reproduction*, *12*(4), 835–839. https://doi.org/10.1093/humrep/12.4.835

Pellicer, A., Simón, C., & Remohí, J. (1995). Effects of aging on the female reproductive system. *Human Reproduction (Oxford, England)*, *10 Suppl 2*, 77–83. https://doi.org/10.1007/s10815-016-0663-y

Pfaffl, M. W., & Hageleit, M. (2001). Validities of mRNA quantification using recombinant RNA and recombinant DNA external calibration curves in real-time RT-PCR. *Biotechnology Letters*, *23*(4), 275–282. https://doi.org/10.1023/A:1005658330108

Philipp, T., Philipp, K., Reiner, A., Beer, F., & Kalousek, D. K. (2003). Embryoscopic and cytogenetic analysis of 233 missed abortions: Factors involved in the pathogenesis of developmental defects of early failed pregnancies. *Human Reproduction*, *18*(8), 1724–1732. https://doi.org/10.1093/humrep/deg309

Phillips, D. I. W., Barker, D. J. P., Hales, C. N., Hirst, S., & Osmond, C. (1994). Thinness at birth and insulin resistance in adult life. *Diabetologia*, *37*, 150–154. https://doi.org/10.1007/s001250050086

Phipps, K., Barker, D. J., Hales, C. N., Fall, C. H., Osmond, C., & Clark, P. M. (1993). Fetal growth and impaired glucose tolerance in men and women. *Diabetologia*, *36*(3), 225–228.

Pierce, G. B., Lewellyn, A. L., & Parchment, R. E. (1989). Mechanism of programmed cell death in the blastocyst. *Proc Natl Acad Sci U S A*, *86*(10), 3654–3658. https://doi.org/10.1073/pnas.86.10.3654

Pilkis, S. J., El-Maghrabi, M. R., McGrane, M., Pilkis, J., & Claus, T. H. (1982). Regulation by glucagon of hepatic pyruvate kinase, 6-phosphofructo 1-kinase, and fructose-1,6-bisphosphatase. *Federation Proceedings*, *41*(10), 2623–2628.

Pinborg, A., Lidegaard, O., & Andersen, A. N. (2006). The vanishing twin: a major determinant of infant outcome in IVF singleton births. *Br J Hosp Med (Lond)*, *67*(8), 417–420. https://doi.org/10.12968/hmed.2006.67.8.21976

Pinborg, A., Loft, A., Romundstad, L. B., Wennerholm, U.-B., Söderström-Anttila, V., Bergh, C., & Aittomäki, K. (2016). Epigenetics and assisted reproductive technologies. *Acta Obstetricia et Gynecologica Scandinavica*, *95*(1), 10–15. https://doi.org/10.1111/aogs.12799

Ponchio, L., Duma, L., Oliviero, B., Gibelli, N., Pedrazzoli, P., & Della Cuna, G. R. (2000). Mitomycin C as an alternative to irradiation to inhibit the feeder layer growth in long-term culture assays. *Cytotherapy*, *2*(4), 281–286. https://doi.org/10.1080/146532400539215

Powell, B., Steelman, L. C., & Carini, R. M. (2006). Advancing Age, Advantaged Youth: Parental Age and the Transmission of Resources to Children. *Social Forces*, *84*, 1359–1390. https://doi.org/10.1353/sof.2006.0064

Pozarowski, P., & Darzynkiewicz, Z. (2004). Analysis of cell cycle by flow cytometry. *Methods in Molecular Biology (Clifton, N.J.)*, *281*, 301–311. https://doi.org/10.1385/1-59259-811-0:301

Prentice, A. M., Whitehead, R. G., Roberts, S. B., & Paul, A. A. (1981). Long-term energy balance in child-bearing Gambian women. *The American Journal of Clinical Nutrition*, *34*(12), 2790–2799.

Preusser, M., Heinzl, H., Gelpi, E., Höftberger, R., Fischer, I., Pipp, I., … Hainfellner, J. A. (2008). Ki67 index in intracranial ependymoma: A promising histopathological candidate biomarker. *Histopathology*, *53*(1), 39–47. https://doi.org/10.1111/j.1365-2559.2008.03065.x

Probst, A. V., Dunleavy, E., & Almouzni, G. (2009). Epigenetic inheritance during the cell cycle. *Nature Reviews Molecular Cell Biology*. https://doi.org/10.1038/nrm2640

Qi, X., Li, T.-G., Hao, J., Hu, J., Wang, J., Simmons, H., … Zhao, G.-Q. (2004). BMP4 supports self-renewal of embryonic stem cells by inhibiting mitogen-activated protein kinase pathways. *Proceedings of the National Academy of Sciences*, *101*(16), 6027–6032. https://doi.org/10.1073/pnas.0401367101

Qi, Y., Zhang, X. J., Renier, N., Wu, Z., Atkin, T., Sun, Z., … Studer, L. (2017). Combined small-molecule inhibition accelerates the derivation of functional cortical neurons from human pluripotent stem cells. *Nature Biotechnology*, *35*(2), 154–163. https://doi.org/10.1038/nbt.3777

Qian, X., Shen, Q., Goderie, S. K., He, W., Capela, A., Davis, A. A., & Temple, S. (2000). Timing of CNS cell generation: A programmed sequence of neuron and glial cell production from isolated murine cortical stem cells. *Neuron*. https://doi.org/10.1016/S0896-6273(00)00086-6

Quinn, P., Moinipanah, R., Steinberg, J. M., & Weathersbee, P. S. (1995). Successful human in vitro fertilization using a modified human tubal fluid medium lacking glucose and phosphate ions. *Fertility and Sterility*, *63*(4), 922–924. https://doi.org/10.1016/S0015-0282(16)57504-9

Quinn, P., & Wales, R. G. (1971). Adenosine triphosphate content of preimplantation mouse embryos. *Journal of Reproduction and Fertility*, *25*(1), 133–135. https://doi.org/10.1530/jrf.0.0250133

Radonić, A., Thulke, S., Mackay, I. M., Landt, O., Siegert, W., & Nitsche, A. (2004). Guideline to reference gene selection for quantitative real-time PCR. *Biochemical and Biophysical Research Communications*, *313*(4), 856–862. https://doi.org/10.1016/j.bbrc.2003.11.177

Rajasingh, J., & Bright, J. J. (2006). 15-Deoxy-delta12,14-prostaglandin J2 regulates leukemia inhibitory factor signaling through JAK-STAT pathway in mouse embryonic stem cells. *Experimental Cell Research*, *312*(13), 2538–2546. https://doi.org/10.1016/j.yexcr.2006.04.010

Ramírez-Solis, R., Rivera-Pérez, J., Wallace, J. D., Wims, M., Zheng, H., & Bradley, A. (1992). Genomic DNA microextraction: A method to screen numerous samples. *Analytical Biochemistry*, *201*(2), 331–335. https://doi.org/10.1016/0003-2697(92)90347-A

Ranade, S. C., Sarfaraz Nawaz, M., Kumar Rambtla, P., Rose, A. J., Gressens, P., & Mani, S. (2012). Early protein malnutrition disrupts cerebellar development and impairs motor coordination. *The British Journal of Nutrition*, *107*(8), 1167–1175. https://doi.org/10.1017/S0007114511004119

Rasool, S., & Shah, D. (2017). Fertility with early reduction of ovarian reserve: the last straw that breaks the Camel's back. *Fertility Research and Practice*, *3*(1), 15. https://doi.org/10.1186/s40738-017-0041-1

Rastan, S., & Robertson, E. J. (1985). X-chromosome deletions in embryo-derived (EK) cell lines associated with lack of X-chromosome inactivation. *Journal of Embryology and Experimental Morphology*, *90*(1), 379–388.

Rayasam, G. V., Tulasi, V. K., Sodhi, R., Davis, J. A., & Ray, A. (2009). Glycogen synthase kinase 3: More than a namesake. *British Journal of Pharmacology*. https://doi.org/10.1111/j.1476-5381.2008.00085.x

Reamon-Buettner, S. M., & Borlak, J. (2007). A new paradigm in toxicology and teratology: Altering gene activity in the absence of DNA sequence variation. *Reproductive Toxicology*.

https://doi.org/10.1016/j.reprotox.2007.05.002

Rebuzzini, P., Neri, T., Mazzini, G., Zuccotti, M., Redi, C. A., & Garagna, S. (2008). Karyotype analysis of the euploid cell population of a mouse embryonic stem cell line revealed a high incidence of chromosome abnormalities that varied during culture. *Cytogenet Genome Res*, *121*(1), 18–24. https://doi.org/000124377 [pii]\r10.1159/000124377

Reik, W., Dean, W., & Walter, J. (2001). Epigenetic reprogramming in mammalian development. *Science (New York, N.Y.)*, *293*, 1089–1093. https://doi.org/10.1126/science.1063443

Resnick, O., & Morgane, P. J. (1984). Ontogeny of the levels of serotonin in various parts of the brain in severely protein malnourished rats. *Brain Research*, *303*(1), 163–170. https://doi.org/10.1016/0006-8993(84)90224-5

Resta, R. G. (2005). Changing demographics of Advanced Maternal Age (AMA) and the impact on the predicted incidence of down syndrome in the United States: Implications for prenatal screening and genetic counseling. *American Journal of Medical Genetics*, *133 A*(1), 31–36. https://doi.org/10.1002/ajmg.a.30553

Rexhaj, E., Paoloni-Giacobino, A., Rimoldi, S. F., Fuster, D. G., Anderegg, M., Somm, E., … Scherrer, U. (2013). Mice generated by in vitro fertilization exhibit vascular dysfunction and shortened life span. *Journal of Clinical Investigation*, *123*(12), 5052–5060. https://doi.org/10.1172/JCI68943

Reyes-Castro, L. A., Rodriguez, J. S., Rodríguez-González, G. L., Chavira, R., Bautista, C. J., McDonald, T. J., … Zambrano, E. (2012). Pre- and/or postnatal protein restriction developmentally programs affect and risk assessment behaviors in adult male rats. *Behavioural Brain Research*, *227*(2), 324–329. https://doi.org/10.1016/j.bbr.2011.06.008

Reyes-Castro, L. A., Rodriguez, J. S., Rodríguez-González, G. L., Wimmer, R. D., McDonald, T. J., Larrea, F., … Zambrano, E. (2011). Pre- and/or postnatal protein restriction in rats impairs learning and motivation in male offspring. *International Journal of Developmental Neuroscience*, *29*(2), 177–182. https://doi.org/10.1016/j.ijdevneu.2010.11.002

Rich-Edwards, J. W., Stampfer, M. J., Manson, J. E., Rosner, B., Hankinson, S. E., Colditz, G. A., … Hennekens, C. H. (1997). Birth weight and risk of cardiovascular disease in a cohort of women followed up since 1976. *BMJ (Clinical Research Ed.)*, *315*(7105), 396–400. https://doi.org/10.1136/bmj.315.7105.396

Roberts, R., Iatropoulou, A., Ciantar, D., Stark, J., Becker, D. L., Franks, S., & Hardy, K. (2005). Follicle-Stimulating Hormone Affects Metaphase I Chromosome Alignment and Increases Aneuploidy in Mouse Oocytes Matured in Vitro1. *Biology of Reproduction*, *72*(1), 107–118. https://doi.org/10.1095/biolreprod.104.032003

Robertson, K. D., & Wolffe, A. P. (2000). DNA methylation in health and disease. *Nature Reviews Genetics*. https://doi.org/10.1038/35049533

Robinson, J. J., Sinclair, K. D., & McEvoy, T. G. (1999). Nutritional effects on foetal growth. *Animal Science*, *68*, 315–331.

Rohwedel, J., Sehlmeyer, U., Shan, J., Meister, A., & Wobus, A. M. (1996). Primordial germ cell-derived mouse embryonic germ (EG) cells in vitro resemble undifferentiated stem cells with respect to differentiation capacity and cell cycle distribution. *Cell Biology International*. https://doi.org/10.1006/cbir.1996.0076

Ron-El, R., Raziel, A., Strassburger, D., Schachter, M., Kasterstein, E., & Friedler, S. (2000). Outcome of assisted reproductive technology in women over the age of 41. *Fertility and*

Sterility, *74*(3), 471–475. https://doi.org/10.1016/S0015-0282(00)00697-X

Roos, N., Sahlin, L., Ekman-Ordeberg, G., Kieler, H., & Stephansson, O. (2010). Maternal risk factors for postterm pregnancy and cesarean delivery following labor induction. *Acta Obstetricia et Gynecologica Scandinavica*, *89*(8), 1003–1010. https://doi.org/10.3109/00016349.2010.500009

Roseboom, T. J., Painter, R. C., Van Abeelen, A. F. M., Veenendaal, M. V. E., & De Rooij, S. R. (2011). Hungry in the womb: What are the consequences? Lessons from the Dutch famine. *Maturitas*. https://doi.org/10.1016/j.maturitas.2011.06.017

Rossant, J. (2004). Lineage development and polar asymmetries in the peri-implantation mouse blastocyst. *Seminars in Cell and Developmental Biology*. https://doi.org/10.1016/j.semcdb.2004.04.003

Rossant, J., & Cross, J. C. (2001). Placental development: lessons from mouse mutants. *Nature Reviews. Genetics*, *2*(7), 538–548. https://doi.org/10.1038/35080570

Rossant, J., & Tam, P. P. L. (2009). Blastocyst lineage formation, early embryonic asymmetries and axis patterning in the mouse. *Development*, *136*(5), 701–713. https://doi.org/10.1242/dev.017178

Rotta, L. N., Leszczinski, D. N., Brusque, A. M., Pereira, P., Brum, L. F. S., Nogueira, C. W., … Souza, D. O. (2008). Effects of undernutrition on glutamatergic parameters in the cerebral cortex of young rats. *Physiology and Behavior*, *94*(4), 580–585. https://doi.org/10.1016/j.physbeh.2008.03.018

Rubin, A. J., Barajas, B. C., Furlan-Magaril, M., Lopez-Pajares, V., Mumbach, M. R., Howard, I., … Khavari, P. A. (2017). Lineage-specific dynamic and pre-established enhancer-promoter contacts cooperate in terminal differentiation. *Nature Genetics*. https://doi.org/10.1038/ng.3935

Rueness, J., Vatten, L., & Eskild, A. (2012). The human sex ratio: effects of maternal age. *Human Reproduction*, *27*(1), 283–287. https://doi.org/10.1093/humrep/der347

Russell, R. B., Petrini, J. R., Damus, K., Mattison, D. R., & Schwarz, R. H. (2003). The changing epidemiology of multiple births in the United States. *Obstetrics and Gynecology*, *101*(1), 129–135. https://doi.org/10.1016/S0029-7844(02)02316-5

Sampino, S., Stankiewicz, A. M., Zacchini, F., Goscik, J., Szostak, A., Swiergiel, A. H., … Ptak, G. E. (2017). Pregnancy at Advanced Maternal Age Affects Behavior and Hippocampal Gene Expression in Mouse Offspring. *The Journals of Gerontology. Series A, Biological Sciences and Medical Sciences*, *72*(11), 1465–1473. https://doi.org/10.1093/gerona/glx016

Sandhu, K. S. (2010). Systems properties of proteins encoded by imprinted genes. *Epigenetics*, *5*(7), 627–636. https://doi.org/10.4161/epi.5.7.12883

Santos, F., Hendrich, B., Reik, W., & Dean, W. (2002). Dynamic reprogramming of DNA methylation in the early mouse embryo. *Developmental Biology*. https://doi.org/10.1006/dbio.2001.0501

Santos, N. C., Figueira-Coelho, J., Martins-Silva, J., & Saldanha, C. (2003). Multidisciplinary utilization of dimethyl sulfoxide: Pharmacological, cellular, and molecular aspects. *Biochemical Pharmacology*. https://doi.org/10.1016/S0006-2952(03)00002-9

Sapkota, G., Alarcón, C., Spagnoli, F. M., Brivanlou, A. H., & Massagué, J. (2007). Balancing BMP Signaling through Integrated Inputs into the Smad1 Linker. *Molecular Cell*.

https://doi.org/10.1016/j.molcel.2007.01.006

Sasaki, A., Nakagawa, I., & Kajimoto, M. (1982). Effect of protein nutrition throughout gestation and lactation on growth, morbidity and life span of rat progeny. *Journal of Nutritional Science and Vitaminology*, *28*(5), 543–555. https://doi.org/10.3177/jnsv.28.543

Sato, A., Otsu, E., Negishi, H., Utsunomiya, T., & Arima, T. (2007). Aberrant DNA methylation of imprinted loci in superovulated oocytes. *Human Reproduction*, *22*(1), 26–35. https://doi.org/10.1093/humrep/del316

Sato, E., Xian, M., Valdivia, R. P. A., & Toyoda, Y. (1995). Sex-linked differences in developmental potential of single blastomeres from in vitro-fertilized 2-cell stage mouse embryos. *Hormone Research in Paediatrics*, *44*, 4–8. https://doi.org/10.1159/000184653

Sauer, M. V., Paulson, R. J., & Lobo, R. A. (1990). A Preliminary Report on Oocyte Donation Extending Reproductive Potential to Women over 40. *New England Journal of Medicine*, *323*(17), 1157–1160. https://doi.org/10.1056/NEJM199010253231702

Sauer, M. V., Paulson, R. J., & Lobo, R. A. (1992). Reversing the Natural Decline in Human Fertility: An Extended Clinical Trial of Oocyte Donation to Women of Advanced Reproductive Age. *JAMA: The Journal of the American Medical Association*, *268*(10), 1275–1279. https://doi.org/10.1001/jama.1992.03490100073030

Sauer, M. V., Paulson, R. J., & Lobo, R. A. (1993). Pregnancy after age 50: application of oocyte donation to women after natural menopause. *The Lancet*, *341*(8841), 321–323. https://doi.org/10.1016/0140-6736(93)90132-Z

Savage, T., Derraik, J. G. B., Miles, H. L., Mouat, F., Hofman, P. L., & Cutfield, W. S. (2013). Increasing Maternal Age Is Associated with Taller Stature and Reduced Abdominal Fat in Their Children. *PLoS ONE*, *8*(3). https://doi.org/10.1371/journal.pone.0058869

Schachter, M., Raziel, A., Friedler, S., Strassburger, D., Bern, O., & Ron-El, R. (2001). Monozygotic twinning after assisted reproductive techniques: a phenomenon independent of micromanipulation. *Human Reproduction (Oxford, England)*, *16*(6), 1264–1269. https://doi.org/10.1093/humrep/16.6.1264

Scherrer, U., Rimoldi, S. F., Rexhaj, E., Stuber, T., Duplain, H., Garcin, S., … Sartori, C. (2012). Systemic and pulmonary vascular dysfunction in children conceived by assisted reproductive technologies. *Circulation*, *125*(15), 1890–1896. https://doi.org/10.1161/circulationaha.111.071183

Schieke, S. M., Ma, M., Cao, L., McCoy, J. P., Liu, C., Hensel, N. F., … Finkel, T. (2008). Mitochondrial metabolism modulates differentiation and teratoma formation capacity in mouse embryonic stem cells. *Journal of Biological Chemistry*, *283*(42), 28506–28512. https://doi.org/10.1074/jbc.M802763200

Schieve, L. a, Meikle, S. F., Ferre, C., Peterson, H. B., Jeng, G., & Wilcox, L. S. (2002). Low and very low birth weight in infants conceived with use of assisted reproductive technology. *The New England Journal of Medicine*, *346*(10), 731–737. https://doi.org/10.1056/NEJMoa010806

Schimmel, M. S., Bromiker, R., Hammerman, C., Chertman, L., Ioscovich, A., Granovsky-Grisaru, S., … Elstein, D. (2015). The effects of maternal age and parity on maternal and neonatal outcome. *Archives of Gynecology and Obstetrics*, *291*(4), 793–798. https://doi.org/10.1007/s00404-014-3469-0

Scholzen, T., & Gerdes, J. (2000). The Ki-67 protein: From the known and the unknown. *Journal of Cellular Physiology*. https://doi.org/10.1002/(SICI)1097-4652(200003)182:3<311::AID-

JCP1>3.0.CO;2-9

Schulkey, C. E., Regmi, S. D., Magnan, R. A., Danzo, M. T., Luther, H., Hutchinson, A. K., … Jay, P. Y. (2015). The maternal-age-associated risk of congenital heart disease is modifiable. *Nature*, *520*(7546), 230–233. https://doi.org/10.1038/nature14361

Schultz, R. M. (2005). From egg to embryo: A peripatetic journey. *Reproduction*. https://doi.org/10.1530/rep.1.00902

Seeber, B. E., Sammel, M. D., Guo, W., Zhou, L., Hummel, A., & Barnhart, K. T. (2006). Application of redefined human chorionic gonadotropin curves for the diagnosis of women at risk for ectopic pregnancy. *Fertility and Sterility*, *86*(2), 454–459. https://doi.org/10.1016/j.fertnstert.2005.12.056

Segall, J. (1981). Strategy of prevention: Lessons from cardiovascular disease. *British Medical Journal (Clinical Research Ed.)*. https://doi.org/10.1136/bmj.282.6282.2136

Seong, K. H., Maekawa, T., & Ishii, S. (2012). Inheritance and memory of stress-induced epigenome change: Roles played by the ATF-2 family of transcription factors. *Genes to Cells*. https://doi.org/10.1111/j.1365-2443.2012.01587.x

Severinski, N. S., Mamula, O., & Vlastelić, I. (2006). Adverse perinatal outcome after assisted reproductive technology. *Gynaecologia et Perinatologia, Supplement*, *15*(1), 73–76.

Sharma, D., Shastri, S., & Sharma, P. (2016). Intrauterine Growth Restriction: Antenatal and Postnatal Aspects. *Clinical Medicine Insights: Pediatrics*, *10*, CMPed.S40070. https://doi.org/10.4137/CMPed.S40070

Shen, Q., Wang, Y., Dimos, J. T., Fasano, C. A., Phoenix, T. N., Lemischka, I. R., … Temple, S. (2006). The timing of cortical neurogenesis is encoded within lineages of individual progenitor cells. *Nature Neuroscience*. https://doi.org/10.1038/nn1694

Shi, W., & Haaf, T. (2002). Aberrant methylation patterns at the two-cell stage as an indicator of early developmental failure. *Molecular Reproduction and Development*, *63*(3), 329–334. https://doi.org/10.1002/mrd.90016

Shirasuna, K., & Iwata, H. (2017). Effect of aging on the female reproductive function. *Contraception and Reproductive Medicine*, *2*, 23. https://doi.org/10.1186/s40834-017-0050-9

Shors, T. J., Miesegaes, G., Beylin, A., Zhao, M., Rydel, T., & Gould, E. (2001). Neurogenesis in the adult is involved in the formation of trace memories. *Nature*, *410*(6826), 372–376. https://doi.org/10.1038/35066584

Shyh-Chang, N., Daley, G. Q., & Cantley, L. C. (2013). Stem cell metabolism in tissue development and aging. *Development*, *140*(12), 2535–2547. https://doi.org/10.1242/dev.091777

Shyh-Chang, N., Locasale, J. W., Lyssiotis, C. A., Zheng, Y., Teo, R. Y., Ratanasirintrawoot, S., … Cantley, L. C. (2013). Influence of threonine metabolism on S-adenosylmethionine and histone methylation. *Science*, *339*(6116), 222–226. https://doi.org/10.1126/science.1226603

Shyh-chang, N., & Ng, H. (2017). The metabolic programming of stem cells. *Genes & Development*, *31*, 336–346. https://doi.org/10.1101/gad.293167.116.336

Shyh-Chang, N., Zheng, Y., Locasale, J. W., & Cantley, L. C. (2011). Human pluripotent stem cells decouple respiration from energy production. *The EMBO Journal*, *30*(24), 4851–4852. https://doi.org/10.1038/emboj.2011.436

Silva, A. P. P., Alves, G. G., Araújo, A. H. B., & Sola-Penna, M. (2004). Effects of insulin and actin on phosphofructokinase activity and cellular distribution in skeletal muscle. *Anais Da Academia Brasileira de Ciencias*, *76*(3), 541–548. https://doi.org/10.1590/S0001-37652004000300008

Silva, J., & Smith, A. (2008). Capturing Pluripotency. *Cell*. https://doi.org/10.1016/j.cell.2008.02.006

Simbolo, M., Gottardi, M., Corbo, V., Fassan, M., Mafficini, A., Malpeli, G., … Scarpa, A. (2013). DNA Qualification Workflow for Next Generation Sequencing of Histopathological Samples. *PLoS ONE*, *8*(6). https://doi.org/10.1371/journal.pone.0062692

Singh, A. M., Hamazaki, T., Hankowski, K. E., & Terada, N. (2007). A Heterogeneous Expression Pattern for Nanog in Embryonic Stem Cells. *Stem Cells*, *25*(10), 2534–2542. https://doi.org/10.1634/stemcells.2007-0126

Singh, S. J., Turner, W., Glaser, D. E., McCloskey, K. E., & Filipp, F. V. (2017). Metabolic shift in density-dependent stem cell differentiation. *Cell Communication and Signaling*, *15*(1). https://doi.org/10.1186/s12964-017-0173-2

Sinha, S., & Chen, J. K. (2006). Purmorphamine activates the Hedgehog pathway by targeting Smoothened. *Nature Chemical Biology*, *2*(1), 29–30. https://doi.org/10.1038/nchembio753

Smallwood, S. A., & Kelsey, G. (2012). Genome-wide analysis of DNA methylation in low cell numbers by reduced representation bisulfite sequencing. *Methods in Molecular Biology*. https://doi.org/10.1007/978-1-62703-011-3-12

Smith, A. G. (2001). Embryo-derived stem cells: of mice and men. *Annual Review of Cell and Developmental Biology*, *17*, 435–462. https://doi.org/10.1146/annurev.cellbio.17.1.435

Smith, A. G., Heath, J. K., Donaldson, D. D., Wong, G. G., Moreau, J., Stahl, M., & Rogers, D. (1988). Inhibition of pluripotential embryonic stem cell differentiation by purified polypeptides. *Nature*, *336*(6200), 688–690. https://doi.org/10.1038/336688a0

Smith, P. K., Krohn, R. I., Hermanson, G. T., Mallia, A. K., Gartner, F. H., Provenzano, M. D., … Klenk, D. C. (1985). Measurement of protein using bicinchoninic acid. *Analytical Biochemistry*, *150*(1), 76–85. https://doi.org/10.1016/0003-2697(85)90442-7

Sommer, L., & Rao, M. (2002). Neural stem cells and regulation of cell number. *Prog Neurobiol*, *66*(1), 1–18. https://doi.org/S0301008201000223 [pii]

Soto, N., Iñiguez, G., López, P., Larenas, G., Mujica, V., Rey, R. A., & Codner, E. (2009). Anti-Müllerian hormone and inhibin B levels as markers of premature ovarian aging and transition to menopause in type 1 diabetes mellitus. *Human Reproduction*, *24*(11), 2838–2844. https://doi.org/10.1093/humrep/dep276

Souza, D. de F. I., Ignacio-Souza, L. M., Reis, S. R. de L., Reis, M. A. de B., Stoppiglia, L. F., Carneiro, E. M., … Latorraca, M. Q. (2012). A low-protein diet during pregnancy alters glucose metabolism and insulin secretion. *Cell Biochemistry and Function*, *30*(2), 114–121. https://doi.org/10.1002/cbf.1824

Spijkers, S., Lens, J. W., Schats, R., & Lambalk, C. B. (2017). Fresh and Frozen-Thawed Embryo Transfer Compared to Natural Conception: Differences in Perinatal Outcome. *Gynecologic and Obstetric Investigation*, *82*(6), 538–546. https://doi.org/10.1159/000468935

St Clair, D., Xu, M., Wang, P., Yu, Y., Fang, Y., Zhang, F., … He, L. (2005). Rates of adult schizophrenia following prenatal exposure to the Chinese famine of 1959-1961. *Journal of the American Medical Association*, *294*(5), 557–562. https://doi.org/10.1001/jama.294.5.557

Ståhlberg, A., Aman, P., Ridell, B., Mostad, P., & Kubista, M. (2003). Quantitative real-time PCR method for detection of B-lymphocyte monoclonality by comparison of kappa and lambda immunoglobulin light chain expression. *Clinical Chemistry*, *49*(1), 51–59. https://doi.org/10.1373/49.1.51

Stanner, S. A., Bulmer, K., Andrès, C., Lantseva, O. E., Borodina, V., Poteen, V. V., & Yudkin, J. S. (1997). Does malnutrition in utero determine diabetes and coronary heart disease in adulthood? Results from the Leningrad siege study, a cross sectional study. *BMJ*, *315*(7119), 1342–1348. https://doi.org/10.1136/bmj.315.7119.1342

Stansfield, B. K., Fain, M. E., Bhatia, J., Gutin, B., Nguyen, J. T., & Pollock, N. K. (2016). Nonlinear Relationship between Birth Weight and Visceral Fat in Adolescents. *Journal of Pediatrics*, *174*, 185–192. https://doi.org/10.1016/j.jpeds.2016.04.012

Stavridis, M. P., Collins, B. J., & Storey, K. G. (2010). Retinoic acid orchestrates fibroblast growth factor signalling to drive embryonic stem cell differentiation. *Development (Cambridge, England)*, *137*(6), 881–890. https://doi.org/10.1242/dev.043117

Stavridis, M. P., Lunn, J. S., Collins, B. J., & Storey, K. G. (2007). A discrete period of FGF-induced Erk1/2 signalling is required for vertebrate neural specification. *Development*. https://doi.org/10.1242/dev.02858

Stavridis, M. P., & Smith, A. G. (2003). Neural differentiation of mouse embryonic stem cells. *Biochem Soc Trans*, *31*(Pt 1), 45–49. https://doi.org/10.1042/

Stefan Barakat, T., & Gribnau, J. (2010). X chromosome inactivation and embryonic stem cells. *Advances in Experimental Medicine and Biology*, *695*, 132–154. https://doi.org/10.1007/978-1-4419-7037-4_10

Steiger, J. L., Alexander, M. J., Galler, J. R., Farb, D. H., & Russek, S. J. (2003). Effects of prenatal malnutrition on GABAA receptor alpha1, alpha3 and beta2 mRNA levels. *Neuroreport*, *14*(13), 1731–1735. https://doi.org/10.1097/01.wnr.0000087730.58565.60

Stein, Z., & Susser, M. (1975). The Dutch Famine, 1944–1945, and the Reproductive Process. II. Interrelations of Caloric Rations and Six Indices at Birth. *Pediatric Research*, *9*(2), 76–83. https://doi.org/10.1203/00006450-197502000-00004

Stettler, N., Zemel, B. S., Kumanyika, S., & Stallings, V. A. (2002). Infant weight gain and childhood overweight status in a multicenter, cohort study. *Pediatrics*, *109*, 194–199. https://doi.org/10.1542/peds.109.2.194

Steuerwald, N. M., Bermúdez, M. G., Wells, D., Munné, S., & Cohen, J. (2007). Maternal age-related differential global expression profiles observed in human oocytes. *Reproductive BioMedicine Online*, *14*(6), 700–708. https://doi.org/10.1016/S1472-6483(10)60671-2

Stolzing, A., Coleman, N., & Scutt, A. (2006). Glucose-Induced Replicative Senescence in Mesenchymal Stem Cells. *Rejuvenation Research*, *9*(1), 31–35. https://doi.org/10.1089/rej.2006.9.31

Stothard, K. J., Tennant, P. W. G., Bell, R., & Rankin, J. (2009). Maternal overweight and obesity and the risk of congenital anomalies: a systematic review and meta-analysis. *JAMA : The Journal of the American Medical Association*, *301*(6), 636–650. https://doi.org/10.1001/jama.2009.113

Stuppia, L. (2013). Origins of oocyte aneuploidy. In *Oogenesis* (pp. 219–227). https://doi.org/10.1007/978-0-85729-826-3_16

Su, Y., Jiang, X., Li, Y., Li, F., Cheng, Y., Peng, Y., … Wang, W. (2016). Maternal low protein isocaloric diet suppresses pancreatic β-cell proliferation in mouse offspring via miR-15b. *Endocrinology*, *157*(12), 4782–4793. https://doi.org/10.1210/en.2016-1167

Sun, C., Denisenko, O., Sheth, B., Cox, A., Lucas, E. S., Smyth, N. R., & Fleming, T. P. (2015). Epigenetic regulation of histone modifications and Gata6 gene expression induced by maternal diet in mouse embryoid bodies in a model of developmental programming. *BMC Developmental Biology*, *15*, 3. https://doi.org/10.1186/s12861-015-0053-1

Sun, C., Denisenko, O., Sheth, B., Cox, A., Lucas, E. S., Smyth, N. R., & Fleming, T. P. (2015). Epigenetic regulation of histone modifications and Gata6 gene expression induced by maternal diet in mouse embryoid bodies in a model of developmental programming. *BMC Dev Biol*, *15*, 3. https://doi.org/10.1186/s12861-015-0053-1

Sun, C., Velazquez, M. A., & Fleming, T. P. (2015). DOHaD and the Periconceptional Period, a Critical Window in Time. In *The Epigenome and Developmental Origins of Health and Disease* (pp. 33–47). https://doi.org/10.1016/B978-0-12-801383-0.00003-7

Sun, C., Velazquez, M. A., Marfy-Smith, S., Sheth, B., Cox, A., Johnston, D. A., … Fleming, T. P. (2014). Mouse early extra-embryonic lineages activate compensatory endocytosis in response to poor maternal nutrition. *Development*, *141*(5), 1140–1150. https://doi.org/10.1242/dev.103952

Sun, C., Velazquez, M. a, Marfy-Smith, S., Sheth, B., Cox, A., Johnston, D. a, … Fleming, T. P. (2014). Mouse early extra-embryonic lineages activate compensatory endocytosis in response to poor maternal nutrition. *Development (Cambridge, England)*, *141*, 1140–1150. https://doi.org/10.1242/dev.103952

Susser, E., Neugebauer, R., Hoek, H. W., Brown, A. S., Lin, S., Labovitz, D., & Gorman, J. M. (1996). Schizophrenia after prenatal famine. Further evidence. *Archives of General Psychiatry*, *53*(1), 25–31. https://doi.org/10.1001/archpsyc.1996.01830010027005

Susser, E. S., & Lin, S. P. (1992). Schizophrenia After Prenatal Exposure to the Dutch Hunger Winter of 1944-1945. *Archives of General Psychiatry*, *49*(12), 983–988. https://doi.org/10.1001/archpsyc.1992.01820120071010

Susser, E. S., Neugebauer, R., Hoek, H. W., Brown, A. S., Lin, S. P., Labovitz, D., & Gorman, J. M. (1997). Schizophrenia After Prenatal Famine-Reply. *Archives of General Psychiatry*. https://doi.org/10.1001/archpsyc.1997.01830180096016

Sutcliffe, A. G., Barnes, J., Belsky, J., Gardiner, J., & Melhuish, E. (2012). The health and development of children born to older mothers in the United Kingdom: observational study using longitudinal cohort data. *BMJ (Clinical Research Ed.)*, *345*(aug21_1), e5116. https://doi.org/10.1136/bmj.e5116

Sutcliffe, A. G., Peters, C. J., Bowdin, S., Temple, K., Reardon, W., Wilson, L., … Maher, E. R. (2006). Assisted reproductive therapies and imprinting disorders - A preliminary British survey. *Human Reproduction*, *21*(4), 1009–1011. https://doi.org/10.1093/humrep/dei405

Tachibana, M., Sugimoto, K., Nozaki, M., Ueda, J., Ohta, T., Ohki, M., … Shinkai, Y. (2002). G9a histone methyltransferase plays a dominant role in euchromatic histone H3 lysine 9 methylation and is essential for early embryogenesis. *Genes and Development*. https://doi.org/10.1101/gad.989402

Tadokoro, Y., Ema, H., Okano, M., Li, E., & Nakauchi, H. (2007). De novo DNA methyltransferase is essential for self-renewal, but not for differentiation, in hematopoietic stem cells. *The Journal of Experimental Medicine*, *204*(4), 715–722. https://doi.org/10.1084/jem.20060750

Takagi, N., & Sasaki, M. (1975). Preferential inactivation of the paternally derived X chromosome in the extraembryonic membranes of the mouse. *Nature*, *256*(5519), 640–642. https://doi.org/10.1038/256640a0

Takahashi, T., Goto, T., Miyama, S., Nowakowski, R. S., & Caviness, V. S. (1999). Sequence of neuron origin and neocortical laminar fate: relation to cell cycle of origin in the developing murine cerebral wall. *The Journal of Neuroscience : The Official Journal of the Society for Neuroscience*, *19*(23), 10357–10371.

Takayama, Y., Wakabayashi, T., Kushige, H., Saito, Y., Shibuya, Y., Shibata, S., … Kida, Y. S. (2017). Brief exposure to small molecules allows induction of mouse embryonic fibroblasts into neural crest-like precursors. *FEBS Letters*. https://doi.org/10.1002/1873-3468.12572

Tamm, C., Galitó, S. P., & Annerén, C. (2013). A comparative study of protocols for mouse embryonic stem cell culturing. *PLoS ONE*, *8*(12). https://doi.org/10.1371/journal.pone.0081156

Tarín, J. J., Gómez-Piquer, V., Rausell, F., Navarro, S., Hermenegildo, C., & Cano, A. (2005). Delayed Motherhood Decreases Life Expectancy of Mouse Offspring1. *Biology of Reproduction*, *72*(6), 1336–1343. https://doi.org/10.1095/biolreprod.104.038919

Te Velde, E. R., & Pearson, P. L. (2002). The variability of female reproductive ageing. *Human Reproduction Update*. https://doi.org/10.1093/humupd/8.2.141

Tearne, J. E. (2015). Older maternal age and child behavioral and cognitive outcomes: A review of the literature. *Fertility and Sterility*, *103*(6), 1381–1391. https://doi.org/10.1016/j.fertnstert.2015.04.027

Tearne, J. E., Robinson, M., Jacoby, P., Allen, K. L., Cunningham, N. K., Li, J., & McLean, N. J. (2016). Older maternal age is associated with depression, anxiety, and stress symptoms in young adult female offspring. *Journal of Abnormal Psychology*, *125*(1), 1–10. https://doi.org/10.1037/abn0000119

Thomson, M., Liu, S. J., Zou, L. N., Smith, Z., Meissner, A., & Ramanathan, S. (2011). Pluripotency factors in embryonic stem cells regulate differentiation into germ layers. *Cell*, *145*(6), 875–889. https://doi.org/10.1016/j.cell.2011.05.017

Tonkiss, J., Galler, J. R., Formica, R. N., Shukitt-Hale, B., & Timm, R. R. (1990). Fetal protein malnutrition impairs acquisition of a DRL task in adult rats. *Physiology and Behavior*, *48*(1), 73–77. https://doi.org/10.1016/0031-9384(90)90263-4

Torres, N., Bautista, C. J., Tovar, A. R., Ordaz, G., Rodriguez-Cruz, M., Ortiz, V., … Zambrano, E. (2010). Protein restriction during pregnancy affects maternal liver lipid metabolism and fetal brain lipid composition in the rat. *AJP: Endocrinology and Metabolism*, *298*(2), E270–E277. https://doi.org/10.1152/ajpendo.00437.2009

Trasler, J. M. (2006). Gamete imprinting: Setting epigenetic patterns for the next generation. *Reproduction, Fertility and Development*. https://doi.org/10.1071/RD05118

Tropepe, V., Hitoshi, S., Sirard, C., Mak, T. W., Rossant, J., & Van Der Kooy, D. (2001). Direct neural fate specification from embryonic stem cells: A primitive mammalian neural stem cell stage acquired through a default mechanism. *Neuron*, *30*(1), 65–78. https://doi.org/10.1016/S0896-6273(01)00263-X

Trounson, A., Mohr, L. R., Wood, C., & Leeton, J. F. (1982). Effect of delayed insemination on in-vitro fertilization, culture and transfer of human embryos. *Journal of Reproduction and Fertility*, *64*(2), 285–294. https://doi.org/10.1530/jrf.0.0640285

Tsuge, H., Hotta, N., & Hayakawa, T. (2000). Effects of vitamin B-6 on (n-3) polyunsaturated fatty acid metabolism. *Journal of Nutrition*, *130*(2), 333S–334S.

Tsumura, A., Hayakawa, T., Kumaki, Y., Takebayashi, S. I., Sakaue, M., Matsuoka, C., … Okano, M. (2006). Maintenance of self-renewal ability of mouse embryonic stem cells in the absence of DNA methyltransferases Dnmt1, Dnmt3a and Dnmt3b. *Genes to Cells*, *11*(7), 805–814. https://doi.org/10.1111/j.1365-2443.2006.00984.x

Uechi, H., Tsutsumi, O., Morita, Y., Takai, Y., & Taketani, Y. (1999). Comparison of the effects of controlled-rate cryopreservation and vitrification on 2-cell mouse embryos and their subsequent development. *Human Reproduction*, *14*(11), 2827–2832.

Uyar, A., & Seli, E. (2014). The impact of assisted reproductive technologies on genomic imprinting and imprinting disorders. *Current Opinion in Obstetrics and Gynecology*. https://doi.org/10.1097/GCO.0000000000000071

Uyeda, K., Furuya, E., & Sherry, A. D. (1981). The structure of "activation factor" for phosphofructokinase. *Journal of Biological Chemistry*, *256*(16), 8679–8684.

Vaca, P., Berná, G., Araujo, R., Carneiro, E. M., Bedoya, F. J., Soria, B., & Martín, F. (2008). Nicotinamide induces differentiation of embryonic stem cells into insulin-secreting cells. *Experimental Cell Research*, *314*(5), 969–974. https://doi.org/10.1016/j.yexcr.2007.11.019

Valdez, R., Athens, M. A., Thompson, G. H., Bradshaw, B. S., & Stern, M. P. (1994). Birthweight and adult health outcomes in a biethnic population in the USA. *Diabetologia*, *37*, 624–631. https://doi.org/10.1007/BF00403383

Valenzuela-Alcaraz, B., Crispi, F., Bijnens, B., Cruz-Lemini, M., Creus, M., Sitges, M., … Gratacós, E. (2013). Assisted reproductive technologies are associated with cardiovascular remodeling in utero that persists postnatally. *Circulation*, *128*(13), 1442–1450. https://doi.org/10.1161/CIRCULATIONAHA.113.002428

Vallier, L., Touboul, T., Chng, Z., Brimpari, M., Hannan, N., Millan, E., … Pedersen, R. A. (2009). Early cell fate decisions of human embryonic stem cells and mouse epiblast stem cells are controlled by the same signalling pathways. *PloS One*, *4*(6), e6082. https://doi.org/10.1371/journal.pone.0006082

Van Blerkom, J. (2009). Mitochondria in early mammalian development. *Seminars in Cell and Developmental Biology*. https://doi.org/10.1016/j.semcdb.2008.12.005

Van Blerkom, J., Davis, P. W., & Lee, J. (1995). ATP content of human oocytes and developmental potential and outcome after in-vitro fertilization and embryo transfer. *Human Reproduction (Oxford, England)*, *10*(2), 415–424.

Van Calsteren, K., & Amant, F. (2011). Chemotherapy during pregnancy: pharmacokinetics and impact on foetal neurological development. *Verhandelingen - Koninklijke Academie Voor Geneeskunde van België*.

Van der Auwera, I., & D'Hooghe, T. (2001). Superovulation of female mice delays embryonic and fetal development. *Human Reproduction (Oxford, England)*, *16*(6), 1237–1243. https://doi.org/10.1093/humrep/16.6.1237

Van os, J. (1997). Schizophrenia After Prenatal Famine. *Archives of General Psychiatry*. https://doi.org/10.1001/archpsyc.1997.01830180095015

Vandesompele, J., De Preter, K., Pattyn, ilip, Poppe, B., Van Roy, N., De Paepe, A., & Speleman, rank. (2002). Accurate normalization of real-time quantitative RT-PCR data by geometric

averaging of multiple internal control genes. *Genome Biology*, *3*(711), 34–1. https://doi.org/10.1186/gb-2002-3-7-research0034

Vanneste, E., Voet, T., Le Caignec, C., Ampe, M., Konings, P., Melotte, C., … Vermeesch, J. R. (2009). Chromosome instability is common in human cleavage-stage embryos. *Nature Medicine*, *15*(5), 577–583. https://doi.org/10.1038/nm.1924

Vanroose, G., Van Soom, A., De Kruif, A., & Goff, A. K. (2001). From Co-culture to defined medium: State of the art and practical considerations. In *Reproduction in Domestic Animals* (Vol. 36, pp. 25–28). https://doi.org/10.1046/j.1439-0531.2001.00264.x

Varvarigou, A. a. (2010). Intrauterine growth restriction as a potential risk factor for disease onset in adulthood. *Journal of Pediatric Endocrinology & Metabolism : JPEM*, *23*(3), 215–224. https://doi.org/10.1515/JPEM.2010.23.3.215

Veening, M. A., van Weissenbruch, M. M., Heine, R. J., & Delemarre-van de Waal, H. A. (2003). Beta-cell capacity and insulin sensitivity in prepubertal children born small for gestational age: influence of body size during childhood. *Diabetes*, *52*, 1756–1760.

Velazquez, M. A., Sheth, B., Smith, S. J., Eckert, J. J., Osmond, C., & Fleming, T. P. (2018). Insulin and branched-chain amino acid depletion during mouse preimplantation embryo culture programmes body weight gain and raised blood pressure during early postnatal life. *Biochimica et Biophysica Acta - Molecular Basis of Disease*, *1864*(2), 590–600. https://doi.org/10.1016/j.bbadis.2017.11.020

Velazquez, M. A., Smith, C. G. C., Smyth, N. R., Osmond, C., & Fleming, T. P. (2016). Advanced maternal age causes adverse programming of mouse blastocysts leading to altered growth and impaired cardiometabolic health in post-natal life. *Human Reproduction*, *31*(9), 1970–1980. https://doi.org/10.1093/humrep/dew177

Veleva, Z., Tiitinen, A., Vilska, S., Hydén-Granskog, C., Tomás, C., Martikainen, H., & Tapanainen, J. S. (2008). High and low BMI increase the risk of miscarriage after IVF/ICSI and FET. *Human Reproduction (Oxford, England)*, *23*(4), 878–884. https://doi.org/10.1093/humrep/den017

Ventura-Juncï¿½, P., Irarrï¿½zaval, I., Rolle, A. J., Gutiï¿½rrez, J. I., Moreno, R. D., & Santos, M. J. (2015). In vitro fertilization (IVF) in mammals: Epigenetic and developmental alterations. Scientific and bioethical implications for IVF in humans. *Biological Research*. https://doi.org/10.1186/s40659-015-0059-y

Verberg, M. F. G., Macklon, N. S., Nargund, G., Frydman, R., Devroey, P., Broekmans, F. J., & Fauser, B. C. J. M. (2009). Mild ovarian stimulation for IVF. *Human Reproduction Update*, *15*(1), 13–29. https://doi.org/10.1093/humupd/dmn056

Vergani, L., Grattarola, M., & Nicolini, C. (2004). Modifications of chromatin structure and gene expression following induced alterations of cellular shape. *The International Journal of Biochemistry & Cell Biology*, *36*(8), 1447–1461. https://doi.org/10.1016/j.biocel.2003.11.015

Verroken, C., Zmierczak, H. G., Goemaere, S., Kaufman, J. M., & Lapauw, B. (2017). Maternal age at childbirth is associated with offspring insulin sensitivity: a cross-sectional study in adult male siblings. *Clinical Endocrinology*, *86*(1), 52–59. https://doi.org/10.1111/cen.13253

Visan, A., Hayess, K., Sittner, D., Pohl, E. E., Riebeling, C., Slawik, B., … Seiler, A. E. M. (2012). Neural differentiation of mouse embryonic stem cells as a tool to assess developmental neurotoxicity in vitro. *NeuroToxicology*, *33*(5), 1135–1146. https://doi.org/10.1016/j.neuro.2012.06.006

Visser, J. A., de Jong, F. H., Laven, J. S., & Themmen, A. P. (2006). Anti-Mullerian hormone: a new

marker for ovarian function. *Reproduction*, *131*(1), 1–9. https://doi.org/131/1/1 [pii]\r10.1530/rep.1.00529

Vogel, R., & Spielmann, H. (1992). Genotoxic and embryotoxic effects of gonadotropin-hyperstimulated ovulation of murine oocytes, preimplantation embryos, and term fetuses. *Reproductive Toxicology*, *6*(4), 329–333. https://doi.org/10.1016/0890-6238(92)90196-Z

Vogt, J., Traynor, R., & Sapkota, G. P. (2011). The specificities of small molecule inhibitors of the TGF?? and BMP pathways. *Cellular Signalling*, *23*(11), 1831–1842. https://doi.org/10.1016/j.cellsig.2011.06.019

Vulliemoz NR1, McVeigh E, K. J. (2012). In vitro fertilisation: Perinatal risks and early childhood outcomes. *Human Fertility*. https://doi.org/10.3109/14647273.2012.663571

Waal, E. De, & Mccarrey, J. R. (2010). Effects of exogenous endocrine stimulation on epigenetic programming of the female germline genome. *Reproductive Technologies*, 154–164.

Wadhwa, P. D., Buss, C., Entringer, S., & Swanson, J. M. (2009). Developmental origins of health and disease: Brief history of the approach and current focus on epigenetic mechanisms. *Seminars in Reproductive Medicine*. https://doi.org/10.1055/s-0029-1237424

Wakefield, S. L., Lane, M., & Mitchell, M. (2011). Impaired mitochondrial function in the preimplantation embryo perturbs fetal and placental development in the mouse. *Biology of Reproduction*, *84*(3), 572–580. https://doi.org/10.1095/biolreprod.110.087262

Wang, C., Lee, J.-E., Lai, B., Macfarlan, T. S., Xu, S., Zhuang, L., … Ge, K. (2016). Enhancer priming by H3K4 methyltransferase MLL4 controls cell fate transition. *Proceedings of the National Academy of Sciences*. https://doi.org/10.1073/pnas.1606857113

Wang, J., Alexander, P., Wu, L., Hammer, R., Cleaver, O., & McKnight, S. L. (2009). Dependence of Mouse Embryonic Stem Cells on Threonine Catabolism. *Science*, *325*(5939), 435–439. https://doi.org/10.1126/science.1173288

Wang, J., & Sauer, M. V. (2006). In vitro fertilization (IVF): A review of 3 decades of clinical innovation and technological advancement. *Therapeutics and Clinical Risk Management*. https://doi.org/10.2147/tcrm.2006.2.4.355

Wang, Y. A., Farquhar, C., & Sullivan, E. A. (2012). Donor age is a major determinant of success of oocyte donation/recipient programme. *Human Reproduction*, *27*(1), 118–125. https://doi.org/10.1093/humrep/der359

Wang, Y. A., Sullivan, E. A., Black, D., Dean, J., Bryant, J., & Chapman, M. (2005). Preterm birth and low birth weight after assisted reproductive technology-related pregnancy in Australia between 1996 and 2000. *Fertility and Sterility*, *83*(6), 1650–1658. https://doi.org/10.1016/j.fertnstert.2004.12.033

Wang, Y., Wang, F., Sun, T., Trostinskaia, A., Wygle, D., Puscheck, E., & Rappolee, D. A. (2004). Entire mitogen activated protein kinase (MAPK) pathway is present in preimplantation mouse embryos. *Developmental Dynamics : An Official Publication of the American Association of Anatomists*, *231*, 72–87. https://doi.org/10.1002/dvdy.20114

Wang, Z., Li, C., Yang, Z., Zou, Z., & Ma, J. (2016). Infant exposure to Chinese famine increased the risk of hypertension in adulthood: results from the China Health and Retirement Longitudinal Study. *BMC Public Health*, *16*(1), 435. https://doi.org/10.1186/s12889-016-3122-x

Wankhade, U. D., Thakali, K. M., & Shankar, K. (2016). Persistent influence of maternal obesity on

offspring health: Mechanisms from animal models and clinical studies. *Molecular and Cellular Endocrinology*, *435*, 7–19. https://doi.org/10.1016/j.mce.2016.07.001

Watanabe, K., Ueno, M., Kamiya, D., Nishiyama, A., Matsumura, M., Wataya, T., … Sasai, Y. (2007). A ROCK inhibitor permits survival of dissociated human embryonic stem cells. *Nature Biotechnology*, *25*(6), 681–686. https://doi.org/10.1038/nbt1310

Watkins, A. J., Lucas, E. S., Marfy-Smith, S., Bates, N., Kimber, S. J., & Fleming, T. P. (2015). Maternal nutrition modifies trophoblast giant cell phenotype and fetal growth in mice. *Reproduction*, *149*(6), 563–575. https://doi.org/10.1530/REP-14-0667

Watkins, A. J., Lucas, E. S., Wilkins, A., Cagampang, F. R. A., & Fleming, T. P. (2011). Maternal periconceptional and gestational low protein diet affects mouse offspring growth, cardiovascular and adipose phenotype at 1 year of age. *PLoS ONE*, *6*(12). https://doi.org/10.1371/journal.pone.0028745

Watkins, A. J., Papenbrock, T., & Fleming, T. P. (2008). The preimplantation embryo: Handle with care. *Seminars in Reproductive Medicine*. https://doi.org/10.1055/s-2008-1042956

Watkins, A. J., Platt, D., Papenbrock, T., Wilkins, A., Eckert, J. J., Kwong, W. Y., … Fleming, T. P. (2007). Mouse embryo culture induces changes in postnatal phenotype including raised systolic blood pressure. *Proceedings of the National Academy of Sciences*, *104*(13), 5449–5454. https://doi.org/10.1073/pnas.0610317104

Watkins, A. J., Ursell, E., Panton, R., Papenbrock, T., Hollis, L., Cunningham, C., … Fleming, T. P. (2008). Adaptive responses by mouse early embryos to maternal diet protect fetal growth but predispose to adult onset disease. *Biol Reprod*, *78*(2), 299–306. https://doi.org/10.1095/biolreprod.107.064220

Watkins, A. J., Ursell, E., Panton, R., Papenbrock, T., Hollis, L., Cunningham, C., … Fleming, T. P. (2008). Adaptive Responses by Mouse Early Embryos to Maternal Diet Protect Fetal Growth but Predispose to Adult Onset Disease1. *Biology of Reproduction*, *78*(2), 299–306. https://doi.org/10.1095/biolreprod.107.064220

Watkins, A. J., Wilkins, A., Cunningham, C., Perry, V. H., Seet, M. J., Osmond, C., … Fleming, T. P. (2008). Low protein diet fed exclusively during mouse oocyte maturation leads to behavioural and cardiovascular abnormalities in offspring. *J Physiol*, *586*(8), 2231–2244. https://doi.org/10.1113/jphysiol.2007.149229

Watkins, A. J., Wilkins, A., Cunningham, C., Perry, V. H., Seet, M. J., Osmond, C., … Fleming, T. P. (2008). Low protein diet fed exclusively during mouse oocyte maturation leads to behavioural and cardiovascular abnormalities in offspring. *Journal of Physiology*, *586*(8), 2231–2244. https://doi.org/10.1113/jphysiol.2007.149229

Watson, A. J. (1992). The cell biology of blastocyst development. *Molecular Reproduction and Development*, *33*(4), 492–504. https://doi.org/10.1002/mrd.1080330417

Watson, A. J., Natale, D. R., & Barcroft, L. C. (2004). Molecular regulation of blastocyst formation. In *Animal Reproduction Science* (Vol. 82–83, pp. 583–592). https://doi.org/10.1016/j.anireprosci.2004.04.004

Weissman, I. L., Anderson, D. J., & Gage, F. (2001). Stem and Progenitor Cells: Origins, Phenotypes, Lineage Commitments, and Transdifferentiations. *Annual Review of Cell and Developmental Biology*, *17*(1), 387–403. https://doi.org/10.1146/annurev.cellbio.17.1.387

Wennberg, A. L., Opdahl, S., Bergh, C., Aaris Henningsen, A.-K., Gissler, M., Romundstad, L. B., … Wennerholm, U.-B. (2016). Effect of maternal age on maternal and neonatal outcomes after

assisted reproductive technology. *Fertility and Sterility*, *106*(5), 1142–1149.e14. https://doi.org/10.1016/j.fertnstert.2016.06.021

Wichterle, H., Lieberam, I., Porter, J. A., & Jessell, T. M. (2002). Directed differentiation of embryonic stem cells into motor neurons. *Cell*, *110*(3), 385–397. https://doi.org/10.1023/B:JOGC.0000027959.37096.78

Wiechelman, K. J., Braun, R. D., & Fitzpatrick, J. D. (1988). Investigation of the bicinchoninic acid protein assay: Identification of the groups responsible for color formation. *Analytical Biochemistry*, *175*(1), 231–237. https://doi.org/10.1016/0003-2697(88)90383-1

Williams, D. R. R., Roberts, S. J., & Davies, T. W. (1979). Deaths from ischaemic heart disease and infant mortality in England and Wales, (1964), 199–202.

Williams, M. A., & Mittendorf, R. (1993). Increasing Maternal Age as a Determinant of Placenta Previa More Important Than Increasing Parity. *The Journal of Reproductive Medicine*, *38*(6), 425–428.

Williams, R. L., Hilton, D. J., Pease, S., Willson, T. A., Stewart, C. L., Gearing, D. P., … Gough, N. M. (1988). Myeloid leukaemia inhibitory factor maintains the developmental potential of embryonic stem cells. *Nature*, *336*, 684–687. https://doi.org/10.1038/336684a0

Wilson, P. G., & Stice, S. S. (2006). Development and differentiation of neural rosettes derived from human embryonic stem cells. *Stem Cell Reviews*, *2*(1), 67–77. https://doi.org/10.1385/SCR:2:1:67

Wilson, V., & Jones, P. (1983). DNA methylation decreases in aging but not in immortal cells. *Science*, *220*(4601), 1055–1057. https://doi.org/10.1126/science.6844925

Winter, R. M. (1993). The Atlas of Mouse Development. *Journal of Medical Genetics*. https://doi.org/10.1136/jmg.30.4.350-c

Wiweko, B., Prawesti, D. M. P., Hestiantoro, A., Sumapraja, K., Natadisastra, M., & Baziad, A. (2013). Chronological age vs biological age: An age-related normogram for antral follicle count, FSH and anti-Mullerian hormone. *Journal of Assisted Reproduction and Genetics*, *30*(12), 1563–1567. https://doi.org/10.1007/s10815-013-0083-1

Wongpaiboonwattana, W., & Stavridis, M. P. (2015). Neural Differentiation of Mouse Embryonic Stem Cells in Serum-free Monolayer Culture. *Journal of Visualized Experiments*, (99). https://doi.org/10.3791/52823

Wood, H. B., & Episkopou, V. (1999). Comparative expression of the mouse Sox1, Sox2 and Sox3 genes from pre-gastrulation to early somite stages. *Mechanisms of Development*. https://doi.org/10.1016/S0925-4773(99)00116-1

Wu, B., Tong, J., & Leibo, S. P. (1999). Effects of cooling germinal vesicle-stage bovine oocytes on meiotic spindle formation following in vitro maturation. *Molecular Reproduction and Development*, *54*(4), 388–395. https://doi.org/10.1002/(SICI)1098-2795(199912)54:4<388::AID-MRD9>3.0.CO;2-7

Wu, G., Bazer, F. W., Cudd, T. A., Meininger, C. J., & Spencer, T. E. (2004). Maternal nutrition and fetal development. *The Journal of Nutrition*, *134*(9), 2169–2172. https://doi.org/134/9/2169 [pii]

Wu, H.-W., Ren, L.-F., Zhou, X., & Han, D.-W. (2015). A high-fructose diet induces hippocampal insulin resistance and exacerbates memory deficits in male Sprague-Dawley rats. *Nutritional Neuroscience*, *18*(7), 323–328. https://doi.org/10.1179/1476830514Y.0000000133

Xie, P., Ouyang, Q., Leng, L., Hu, L., Cheng, D., Tan, Y., … Lin, G. (2016). The dynamic changes of X chromosome inactivation during early culture of human embryonic stem cells. *Stem Cell Research*, *17*(1), 84–92. https://doi.org/10.1016/j.scr.2016.05.011

Xin, X., Wang, W., Xu, H., Li, Z., & Zhang, D. (2018). Exposure to Chinese famine in early life and the risk of dyslipidemia in adulthood. *European Journal of Nutrition*. https://doi.org/10.1007/s00394-017-1603-z

Xu, M. Q., Sun, W. S., Liu, B. X., Feng, G. Y., Yu, L., Yang, L., … He, L. (2009). Prenatal malnutrition and adult Schizophrenia: Further evidence from the 1959-1961 chinese famine. *Schizophrenia Bulletin*, *35*(3), 568–576. https://doi.org/10.1093/schbul/sbn168

Yajnik, C. S., Fall, C. H. D., Coyaji, K. J., Hirve, S. S., Rao, S., Barker, D. J. P., … Kellingray, S. (2003). Neonatal anthropometry: The thin-fat Indian baby. The Pune maternal nutrition study. *International Journal of Obesity*, *27*(2), 173–180. https://doi.org/10.1038/sj.ijo.802219

Yamazaki, S., Iwama, A., Takayanagi, S. I., Morita, Y., Eto, K., Ema, H., & Nakauchi, H. (2006). Cytokine signals modulated via lipid rafts mimic niche signals and induce hibernation in hematopoietic stem cells. *EMBO Journal*, *25*(15), 3515–3523. https://doi.org/10.1038/sj.emboj.7601236

Yang, J., Wu, C., Stefanescu, I., & Horowitz, A. (2017). Analysis of Retinoic Acid-induced Neural Differentiation of Mouse Embryonic Stem Cells in Two and Three-dimensional Embryoid Bodies. *Journal of Visualized Experiments*, (122). https://doi.org/10.3791/55621

Yang, Y. P., & Klingensmith, J. (2006). Roles of organizer factors and BMP antagonism in mammalian forebrain establishment. *Developmental Biology*, *296*(2), 458–475. https://doi.org/10.1016/j.ydbio.2006.06.014

Yaron, Y., Botchan, A., Amit, A., Kogosowski, A., Yovel, I., & Lessing, J. B. (1993). Endometrial receptivity: The age-related decline in pregnancy rates and the effect of ovarian function. *Fertility and Sterility*, *60*(2), 314–318. https://doi.org/10.1016/S0015-0282(16)56104-4

Yeung, W. S. B., Lee, C. K. F., & Xu, J. S. (2002). The oviduct and development of the preimplantation embryo. *Reproductive Medicine Review*. https://doi.org/10.1017/S0962279902000121

Ying, Q.-L., Wray, J., Nichols, J., Batlle-Morera, L., Doble, B., Woodgett, J., … Smith, A. (2008a). The ground state of embryonic stem cell self-renewal. *Nature*, *453*(May), 519–523. https://doi.org/10.1038/nature06968

Ying, Q.-L., Wray, J., Nichols, J., Batlle-Morera, L., Doble, B., Woodgett, J., … Smith, A. (2008b). The ground state of embryonic stem cell self-renewal. *Nature*, *453*(7194), 519–523. https://doi.org/10.1038/nature06968

Ying, Q. L., Nichols, J., Chambers, I., & Smith, A. (2003). BMP induction of Id proteins suppresses differentiation and sustains embryonic stem cell self-renewal in collaboration with STAT3. *Cell*, *115*(3), 281–292. https://doi.org/10.1016/S0092-8674(03)00847-X

Ying, Q. L., & Smith, A. G. (2003). Defined Conditions for Neural Commitment and Differentiation. *Methods in Enzymology*. https://doi.org/10.1016/S0076-6879(03)65023-8

Ying, Q. L., Stavridis, M., Griffiths, D., Li, M., & Smith, A. (2003). Conversion of embryonic stem cells into neuroectodermal precursors in adherent monoculture. *Nature Biotechnology*, *21*(2), 183–186. https://doi.org/10.1038/nbt780

Yoon, K., & Gaiano, N. (2005). Notch signaling in the mammalian central nervous system: Insights

from mouse mutants. *Nature Neuroscience*. https://doi.org/10.1038/nn1475

Yoon, P. W., Freeman, S. B., Sherman, S. L., Taft, L. F., Gu, Y., Pettay, D., … Hassold, T. J. (1996). Advanced maternal age and the risk of Down syndrome characterized by the meiotic stage of chromosomal error: a population-based study. *American Journal of Human Genetics*, *58*(3), 628–633.

Yoshida, K., Chambers, I., Nichols, J., Smith, A., Saito, M., Yasukawa, K., … Kishimoto, T. (1994). Maintenance of the pluripotential phenotype of embryonic stem cells through direct activation of gp130 signalling pathways. *Mechanisms of Development*, *45*(2), 163–171. https://doi.org/10.1016/0925-4773(94)90030-2

Young, L. (1998). Large offspring syndrome in cattle and sheep. *Reviews of Reproduction*, *3*(3), 155–163. https://doi.org/10.1530/ror.0.0030155

Yue, M. X., Fu, X. W., Zhou, G. Bin, Hou, Y. P., Du, M., Wang, L., & Zhu, S. E. (2012). Abnormal DNA methylation in oocytes could be associated with a decrease in reproductive potential in old mice. *Journal of Assisted Reproduction and Genetics*, *29*(7), 643–650. https://doi.org/10.1007/s10815-012-9780-4

Yun, Y., Holt, J. E., Lane, S. I. R., McLaughlin, E. A., Merriman, J. A., & Jones, K. T. (2014). Reduced ability to recover from spindle disruption and loss of kinetochore spindle assembly checkpoint proteins in oocytes from aged mice. *Cell Cycle*, *13*(12), 1938–1947. https://doi.org/10.4161/cc.28897

Zander-Fox, D., Lane, M., & Hamilton, H. (2013). Slow freezing and vitrification of mouse morula and early blastocysts. *Journal of Assisted Reproduction and Genetics*, *30*, 1091–1098. https://doi.org/10.1007/s10815-013-0056-4

Zeleznik, A. J., & Pohl, C. R. (2006). Control of follicular development, corpus luteum function, the maternal recognition of pregnancy, and the neuroendocrine regulation of the menstrual cycle in higher primates. In *Knobil and Neill's Physiology of Reproduction* (pp. 2449–2510). https://doi.org/10.1016/B978-012515400-0/50050-6

Zeng, F., Baldwin, D. A., & Schultz, R. M. (2004). Transcript profiling during preimplantation mouse development. *Dev Biol*, *272*(2), 483–496. https://doi.org/10.1016/j.ydbio.2004.05.018

Zhang, J., Khvorostov, I., Hong, J. S., Oktay, Y., Vergnes, L., Nuebel, E., … Teitell, M. A. (2011). UCP2 regulates energy metabolism and differentiation potential of human pluripotent stem cells. *The EMBO Journal*, *30*(24), 4860–4873. https://doi.org/10.1038/emboj.2011.401

Zhang, Y., Li, W., Laurent, T., & Ding, S. (2012). Small molecules, big roles - the chemical manipulation of stem cell fate and somatic cell reprogramming. *Journal of Cell Science*, *125*(Pt 23), 5609–5620. https://doi.org/10.1242/jcs.096032

Zhao, J., & Li, Y. (2012). Adenosine triphosphate content in Human unfertilized oocytes, Undivided Zygotes and Embryos Unsuitable for Transfer or cryopreservation. *Journal of International Medical Research*, *40*(2), 734–739. https://doi.org/10.1177/147323001204000238

Zheng, H., Huang, B., Zhang, B., Xiang, Y., Du, Z., Xu, Q., … Xie, W. (2016). Resetting Epigenetic Memory by Reprogramming of Histone Modifications in Mammals. *Molecular Cell*. https://doi.org/10.1016/j.molcel.2016.08.032

Zheng, J., Xiao, X., Zhang, Q., Wang, T., Yu, M., & Xu, J. (2017). Maternal low-protein diet modulates glucose metabolism and hepatic microRNAs expression in the early life of offspring. *Nutrients*, *9*(3). https://doi.org/10.3390/nu9030205

Zheng, J., Xiao, X., Zhang, Q., Yu, M., Xu, J., & Wang, Z. (2015). Maternal protein restriction induces early-onset glucose intolerance and alters hepatic genes expression in the peroxisome proliferator-activated receptor pathway in offspring. *Journal of Diabetes Investigation*, *6*(3), 269–279. https://doi.org/10.1111/jdi.12303

Zhou, C. K., Sutcliffe, S., Welsh, J., Mackinnon, K., Kuh, D., Hardy, R., & Cook, M. B. (2016). Is birthweight associated with total and aggressive/lethal prostate cancer risks A systematic review and meta-analysis. *British Journal of Cancer*. https://doi.org/10.1038/bjc.2016.38

Zhou, D., Shen, X., Gu, Y., Zhang, N., Li, T., Wu, X., & Lei, L. (2014). Effects of dimethyl sulfoxide on asymmetric division and cytokinesis in mouse oocytes. *BMC Developmental Biology*, *14*(1). https://doi.org/10.1186/1471-213X-14-28

Zhu, Z., & Huangfu, D. (2013). Human pluripotent stem cells: an emerging model in developmental biology. *Development (Cambridge, England)*, *140*(4), 705–717. https://doi.org/10.1242/dev.086165

Zvetkova, I., Apedaile, A., Ramsahoye, B., Mermoud, J. E., Crompton, L. A., John, R., … Brockdorff, N. (2005). Global hypomethylation of the genome in XX embryonic stem cells. *Nature Genetics*, *37*(11), 1274–1279. https://doi.org/10.1038/ng1663

Zylicz, J. J., Dietmann, S., Günesdogan, U., Hackett, J. A., Cougot, D., Lee, C., & Surani, M. A. (2015). Chromatin dynamics and the role of G9a in gene regulation and enhancer silencing during early mouse development. *ELife*. https://doi.org/10.7554/eLife.09571